EXPLORATION OF BENZIMIDAZOLE CHEMISTRY

by

ROBERT TIMOTHY STIBRANY

A Dissertation submitted to the

Graduate School-New Brunswick

Rutgers, The State University of New Jersey

in partial fulfillment of the requirements

for the degree of

Doctor of Philosophy

Graduate Program in Chemistry

written under the direction of

Professor Joseph A. Potenza

and approved by

_____

_____

_____

_____

New Brunswick, New Jersey

January, 2008

ABSTRACT OF THE DISSERTATION

Exploration of Benzimidazole Chemistry

By Robert T. Stibrany

Dissertation Director:
Professor Joseph A. Potenza

Benzimidazoles have far reaching applications in the field of chemistry and beyond. The major focus of this work is on the synthesis of benzimidazoles and bis(benzimidazoles) and subsequent complexation chemistry which has been further applied to areas such as constrained geometry and catalysis. A number of new techniques, such as the facile oxidation of methylene bridged benzimidazoles, have been elucidated in this study. Many improvements in experimental conditions have also been found in the syntheses of members of this class of compounds. We report here the preparation and characterization of two systems with constrained coordination geometries. The first consists of tetrahedrally constrained complexes using bis[*rac*-2,2′-bis[2-(1-alkylbenzimidazol-2-yl)]biphenyl] characterized with several transition metal ions. The second consists of chiral, square-bipyramidally constrained complexes using chiral bis[1,2-bis(1-alkylbenzimidazol-2-yl)-1′,2′-bis(alkoxy)ethane] with first and second row transition metal ions. The copper complexes of selected bis(benzimidazoles) have been found to catalyze the oxidative carbonylation of methanol to form dimethyl carbonate. Such complexes have also been found to be remarkable polymerization catalysts with the ability to homopolymerize and copolymerize olefins and acrylates.

Dedication

Geraldine H. Stibrany

My Mother

And

Harvey J. Schugar

My Friend and Colleague

Whose Support Made This Work Possible

Table of Contents

List of Tables

List of Figures

ellipsoids are drawn at the 25% probability level.

8.0 mM in **2-13**.

List of Schemes

Cuprous Chloride Catalyst in the Liquid phase.

Introduction

Imidazoles and benzimidazoles (Figure 1) have far reaching applications in the field of chemistry and beyond. The major focus of this work is on the synthesis of benzimidazoles and bis(benzimidazoles) and the subsequent complexation chemistry which has been further applied to areas such as catalysis, charge-transfer, constrained geometry, and energy conversion. While not the main topic of this work, some of the many, wide-reaching areas of chemistry that this research has touched upon will be noted in this introduction.

Imidazole   **Benzimidazole**
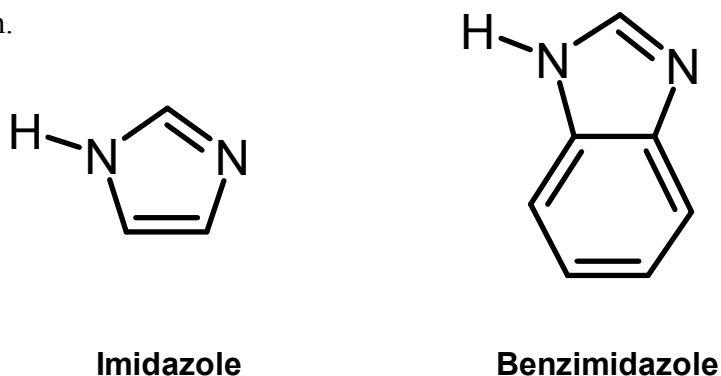
Figure 1. Molecular structure of imidazole and benzimidazole.

We begin with bidentate ligands. There are many prerequisite conditions that need to be considered when designing any new bidentate ligands. Our research has been focused on bis(benzimidazole) containing ligands specifically designed for use in the preparation of late transition metal complexes. Some of these conditions include, but are not limited to, electronics, steric considerations, chirality, stability, lability (binding constant), solubility, functionality, yield, cost, processability, recoverability, as well as

patentability. There has been a number of reviews and compilations containing the synthesis of hundreds of imidazole and benzimidazole compounds.[1] With the considerations noted above in mind, many new synthetic building blocks and final bidentate products have been designed, synthesized and characterized. New and improved synthetic techniques have also been developed. The synthesis of these organic moieties will be discussed and illustrated in the following chapter. Finally, these ligands have been chelated to transition metal ions to enforce geometric constraints with consequent spectroscopic, chemical, catalytic, and energy conversion properties.

Reported syntheses of benzimidazoles can be found in the literature as far back as 1862 with the synthesis of (1-*H*-benzimidazole)-2-carboxylic acid.[2] There may even have been earlier reports of these compounds. In addition there have been hundreds of patents covering the composition of imidazoles and benzimidazoles. They have been patented primarily for their pharmacological properties. With the recent explosive growth in the area of combinatorial chemistry, many pharmaceutical companies have been developing imidazole and benzimidazole libraries for drug high-throughput screening.[3] The benzimidazole libraries have received most of the early attention in combinatorial libraries due to their putative ease of synthesis.[3a] Some areas of chemistry have not found these syntheses to be quite so facile.[4] Imidazole and benzimidazole constituents are commonly found in pharmaceutical, veterinary and agrochemical products such as cimetidine (Tagamet®), azomycin, metronidazole, ketoconazole (Nizoral®) misonidazole, chlortrimazole, thiabendazole, benomyl, and astemizole[5] to name but a few. Representative chemical structures are depicted in Figure 2. Astemizole, which has been patented as a non-sedating antihistamine and has very recently been identified as a

antimalarial agent through drug-library screenings.[6] To underline the ubiquity of their medicinal applications, over one third of the pages of the compilation of the *Drug Compendium* in Volume 6 of *Comprehensive Medicinal Chemistry*[7] contain imidazole or benzimidazole fragments.
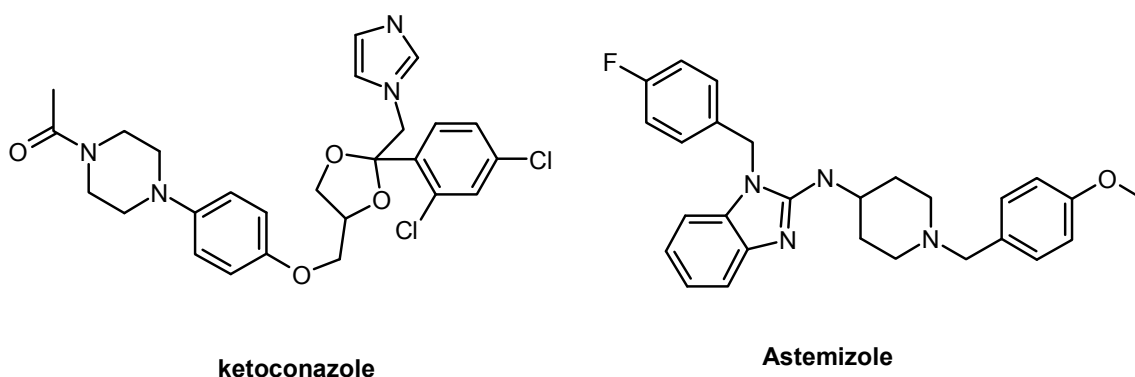
Figure 2. Chemical structures of ketoconazole and tecastemizole.

Bis(benzimidazoles) have been identified as potent zinc-mediated serine protease inhibitors.[8] These ligands have also been found to act as inhibitors of Botulinum Neurotoxin Type B Protease; in the latter instance, they utilize a different type mechanism than do the serine proteases.[9] Serine proteases have been linked to several disease states, which include thrombosis, inflammation, and bronchoconstriction.[10] Of the various human proteases tested, which include, trypsin, tryptase, thrombin, chymotrypsin, chymase, and Factor Xa, the bis(benzimidazoles) are particularly effective for trypsin.[8] The crystal structure of the protease reveals that at the trypsin active site, a Zn(II) atom is bound tetrahedrally by the bis(benzimidazole) ligand.[8] In a recent study, the bis(benzimidazoles) that were tested had no inhibition of trypsin in the absence of any

metal ion.[11] The study also showed that only first-row transition metals, which prefer tetrahedral coordination, showed any inhibition of protease. Metals which disfavor tetrahedral coordination, such as Cu(II) and Ni(II), showed no inhibition of trypsin. Of the various bis(benzimidazole) ligands tested in the study, BABIM (Figure 3) was shown to be the most effective. The BABIM ligand does not specifically enforce tetrahedral coordination. The amidine functionalities on the benzimidazole rings are thought to be important because of their interaction with an aspartic acid residue near the active site as shown in the crystal structure. An interesting extension of this research would be to utilize functionalized versions of the ligand BBIL (Figure 3) which we have synthesized and shown to enforce distorted-tetrahedral coordination of many of the transition metals.[12] An amidine functionality such as ABBIL (Figure 3) would be a logical compound with which to start such a study.
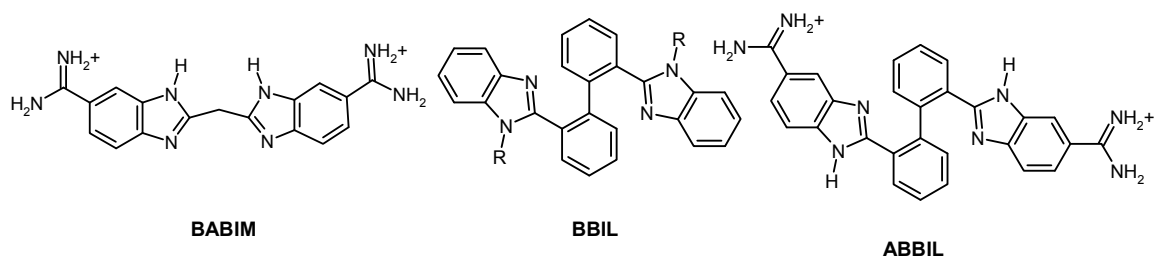
Figure 3. Molecular structures of BABIM, BBIL, and ABBIL.

With the realization of a worldwide HIV epidemic, vast amounts of research have poured into the discovery of inhibitors for the virus. Subsequent research has identified the reverse transcriptase enzyme of the virus as the most suitable target of inhibition. A number of studies have evaluated a select number of benzimidazole compounds as inhibitors of HIV-1 reverse transcriptase (RT); they showed various levels of efficacy.[13]

In the course of this research, approximately forty newly synthesized benzimidazole compounds were submitted for initial screening as HIV inhibitors. While many of these compounds were shown to be efficacious, sufficient advancement over current drugs were not forthcoming.[14] Future studies may produce more promising results.

Natrural products, which range from very-high-value antibiotics and cancer treatments to more broadly isolated terpenoids such as estragole and linalool which are used in perfumes and cosmetics, are important commercial compounds.[15] Terpenoids, which are found most concentrated in essential oils, are materials that are obtained by steam distillation of a specific plant material. For example, the oil obtained from the steam distillation of lavender is known as the essential oil of lavender. These oils generally contain a large number of chemical components which are very difficult to separate, especially on a commercial scale, by conventional means, such as distillation and chromatography. Many essential oils contain compounds that are known to have antimicrobial or antifungal properties; some have even been used in treatments for cancer. A well-known resin that is derived from the shrub *Commiphora abyssinica*, myrrh, contains a number of antibacterial, antifungal, and antimicrobial compounds.[16] Another well known example is paclitaxel (Taxol®), which is isolated from the Pacific Yew in a multi-step biomass extraction process, followed by HPLC.[17] The cost of such a process can make the isolation of many compounds uneconomical. A simple method of isolation would permit commercialization of many more of these compounds.

Another commonality to many of the compounds found in essential oils is that they contain olefinic bonds. Copper(I) compounds have been examined as separation agents in the removal of olefinic molecules from petroleum-based chemical streams.[18]

Chiral recognition of olefins with high stereoselectivity has been demonstrated using chiral diamines with Cu(I)[19] and Ag(I)[20]. It is conceivable that Cu(I) bis(benzimidazole) complexes can be designed to extract specific olefinic compounds catalytically from essential oils, because of their high affinity for olefins. Constraining the geometry of the open pocket of the Cu(I) site could lead to selective binding of the olefin of interest, thus making the isolation of specific compounds commercially viable.

Crystallography has been an invaluable technique for the characterization of many of the products synthesized in this research. Our single-crystal structure determinations have revealed polymorphs of some of the synthetic segments, monodentate building blocks, bidentate benzimidazoles, and metal complex products. A polymorph is a solid crystalline phase of a given compound resulting from the existence of at least two different arrangements of the molecules of that compound in two different crystals of the compound.[21] While polymorphism has been known for over a century, its importance has only gained widespread recognition in approximately the last two decades. Most notably, polymorphism has become most important in pharmacology from the standpoints of drug performance and intellectual property. As an example, sertraline hydrochloride, the active drug in Zoloft®, has been found to have 17 different polymorphic forms.[22] In this study, we have identified polymorphs of organic monodentate building blocks, bidentate bis(benzimidazoles), and, far less commonly found, metal-organic complexes. Recently, we published a manuscript describing two polymorphs of the mondentate building block 4,5-diphenyl-1*H*-imidazole (Figure 4-I).[23] Substituted versions of this compound are known to be pharmacologically active.[24] We have thus far discovered four polymorphs of the bidentate ligand, 1,1′-bis(1-methylbenzimidazol-2-yl)ketone (Figure 4-II).[25] These

polymorphs were induced by altering the solvent of crystallization, which is by far the best known method for preparing polymorphs. We have also discovered polymorphs of the geometrically constrained metal complex *rac*-bis-[2,2'-bis[2-(1-propylbenzimidazol-2-yl)]biphenyl)]]metal(II)] bis(perchlorate) (Figure 4-III), where the metals are cobalt, nickel, and copper. In this case an acetonitrile solution of the metal complex is crystallized by vapor diffusion of an ether solvent. When diethyl ether is utilized, the complex crystallizes in the orthorhombic space group *Pnn2*, and when tetrahydrofuran is utilized, the complex crystallizes in the monoclinic space group *Cc*.[26]
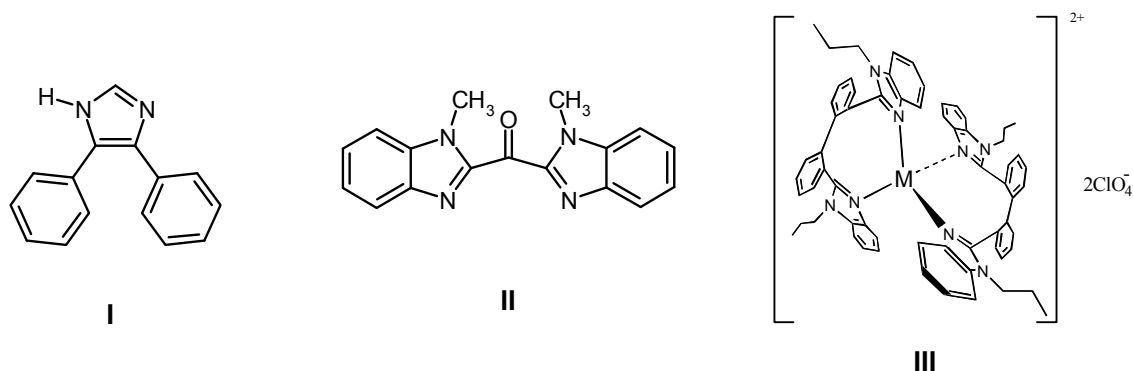
Figure 4. Polymorphic compounds.

We have found that proximally labile bidentate biphenylbis(benzimidazoles) (**BBIL**) (Figure 5) can behave as classical "proton sponges".[27] The term "proton sponge" is used for a class of compounds which combine unusual high basicity and low nucleophilicity. The best known "proton sponge", 1,8-bis(dimethylamino)naphthalene (**PS**) has been characterized structurally with many counter ions. The structure of one of

these salts, $\kappa^2 N,N'$-1,8-bis(dimethylamino)naphthalene trifluoromethanesulfonate ($\mathbf{PS^+}$)[28] is depicted in (Figure 6) along with the proximally labile analogue $\kappa^2 N^{13},N^{13'}$-hydro-*rac*-2,2′-bis[2-(1-propylbenzimidazol-2-yl)]biphenyl trifluoromethanesulfonate[27a], ($\mathbf{BBIL^+}$).
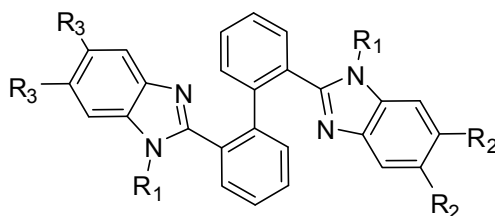
Figure 5. Structural diagram of substituted **BBIL**.
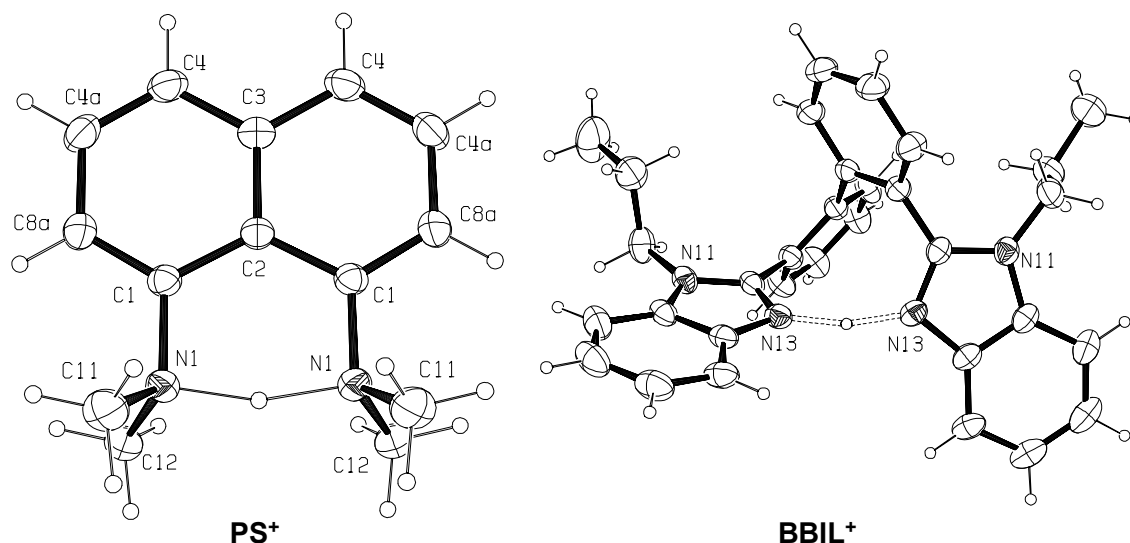
Figure 6. ORTEP[29] diagram of the cation of $\mathbf{PS^+}$ and of the cation $\mathbf{BBIL^+}$. The thermal ellipsoids are drawn at the 25% probability level.

To estimate the base strength of the substituted **BBIL** species, competitive NMR experiments were performed. In deuterated acetonitrile and using the

trifluoromethanesulfonate (triflate) anion, **BBIL** (R_1 = *n*-propyl, R_2 = R_3 = methyl) deprotonates $\textbf{PS}^+$ while **BBIL** (R_1 = *n*-propyl, R_2 = R_3 = chloro) does not. This suggests that, in deuterated acetonitrile, **BBIL** and **PS** have comparable pK_a values.[26] The pK_a of **PS** in deuterated acetonitrile correlates well with the chemical shift of the bound proton. The pK_a of **PS** in acetonitrile has been determined to be 18.2.[30]

An important consideration in homogeneous systems is the binding constant of the ligands used for chelating the active metal sites. For example, the π-bound (metal – C) ligands that are found in early transition-metal polymerization catalysts are very stable and are extremely difficult to remove once formed. These π-bound ligands are completely inapplicable for later transition-metal systems, owing to their instability. When considering metal-chelating moieties for the late tranisition metals, only a few potential donor atoms remain, namely, nitrogen, phosphorus, arsenic, oxygen, and sulfur. In particular, when considering either copper or nickel as the metals of interest, this leaves only nitrogen as a feasible donor atom. The other potential donor atoms are either too weakly coordinating or introduce redox instability to the metal center. The next consideration is to determine which nitrogen-containing ligands exhibit the highest binding constant for the target metals of first-row, late-transition metals. An appropriate starting point of this investigation is to look at how nature has been utilizing these metals for catalysis in metalloenzymes for millions of years.

It is well known that numerous metalloenzymes containing copper utilize imidazoles in the form of histidine. A review of binding constants for imidazoles and benzimidazoles with first-row transition metals indicates that imidazoles and benzimidazoles have much greater binding affinities for these metals over those of

ammonia and pyridine.[31] This observation can not simply be predicted on the basis of basicity or π-donation ability. In the view of the fact that ammonia is an order of magnitude more basic than benzimidazole and pyridine should have similar π-donating ability as benzimidazole, additional factors seem likely to account for the higher binding affinities of benzimidazoles. Copper is at the pinnacle of binding constants for benzimidazoles with first row transition metals.[31,32] All other first row transition metals monotonically approach the binding constant of copper as they approach its atomic number. The preferential binding ability of benzimidazole over that of pyridine is further demonstrated in the crystal structure of Co(BBBP)Cl$_2$, (Figure 7), where Co(II) forms a four-coordinate complex, utilizing a single 6,6'-bis[2-(1-hydrobenzimidazol-2-yl)]2,2'-bipyridine (BBBP), a ligand very similar to BBIL. The bidentate ligand structure utilizes the bisbenzimidazole binding site instead of the available bipyridine site.[33]
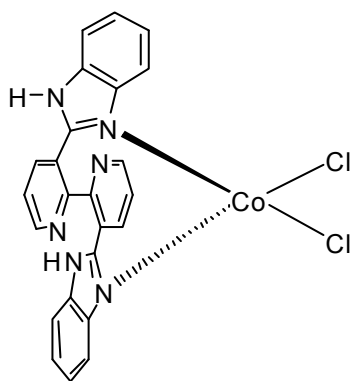
Figure 7. The molecular structure of [6,6'-bis[2-(1-hydrobenzimidazol-2-yl)]2,2'-bipyridine]Cobalt(II) dichloride, Co(BBBP)Cl$_2$.

A previous work designed to study electron self-exchange for a Cu(I)/Cu(II) pair constrained to a pseudotetrahedral geometry utilized a bidentate imidazole ligand.[34] The ligand, *rac*-2,2'-bis(2-imidazolyl)biphenyl (**BIL**) (Figure 8), was a member of the first

generation of biphenyl ligands designed to constrain complexes to distorted- tetrahedral coordination geometries. In that study, an NMR experiment, which was designed to determine the extent of ligand exchange between M(**BIL**)$_2$ and free **BIL** in solution, was conducted. The variable temperature experiment, which was conducted over the -30 to 50 °C range, led to the conclusion that complete ligand exchange occurred at ca. 5-10 °C. In this study, the same experiment was conducted using the analogous **BBIL** metal complex; in that instance, complete ligand exchange did not occur until ca. 70 °C. These findings indicate a significant increase in binding constant of benzimidazole over that of the analogous imidazole.
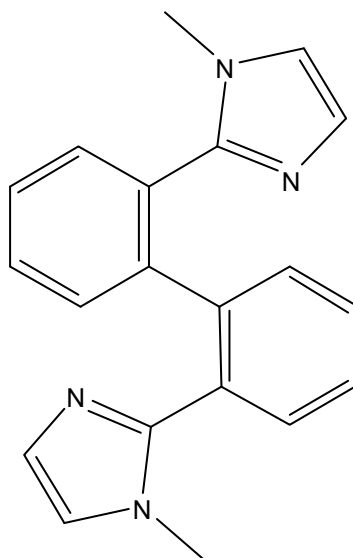
Figure 8. Molecular structure of **BIL**.

This report will focus on the synthesis of benzimidazoles and more specifically bis(benzimidazoles). The most studied naturally occurring benzimidazole is found in the coenzyme B$_{12}$, cobalamin, which partakes in many different rearrangement reactions in biological systems. In the coenzyme, a 5,6-dimethylbenzimidazole acts as an apical fifth

ligand linked to a cobalt ion via the imine nitrogen atom (Figure 9). It is thought that the benzimidazole acts to control the reactivity of the cobalt metal center. This is one of the very few "biologically occurring" organometallic systems where a metal-alkyl bond can be formed. The coenzyme catalyzes three general types of reactions. The first is called the *isomerase reaction*, in which two substituents on adjacent carbon atoms are interchanged. In the second type, methylcobalamin (Figure 9) methylates a substrate. The best known example of this is *methionine synthetase*, in which homocysteine ($HSCH_2CH_2CH(CO_2H)NH_2$) is methylated to give methionine ($CH_3CH_2CH_2CH(CO_2H)NH_2$). Finally, the coenzyme is used in the conversion of the ribose rings of RNA to deoxyribose rings of DNA.
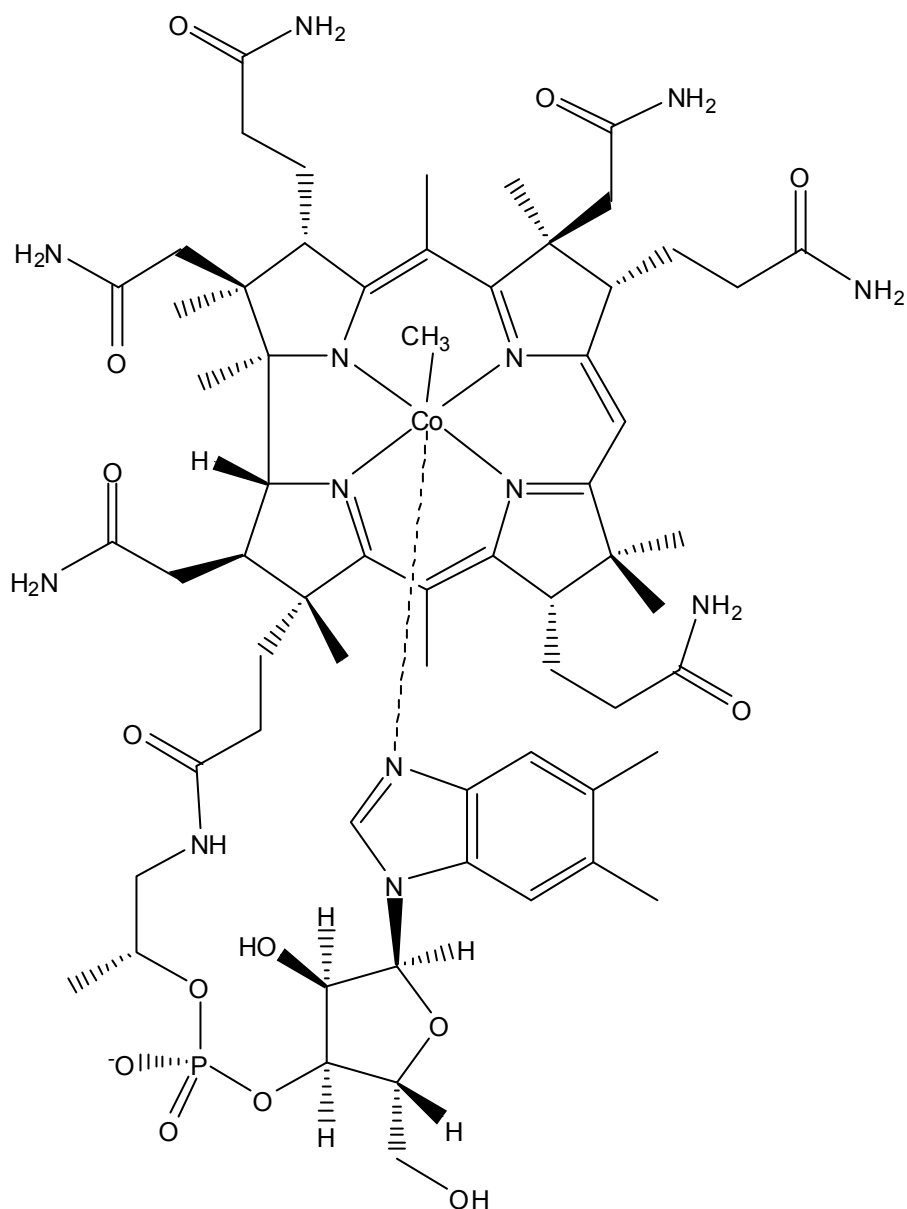
Figure 9. Molecular structure of the coenzyme methylcobalamin.

Further reflection on the Cobalamin coenzyme makes one question why nature has chosen 5,6-dimethylbenzimidazole to act as the likely regulating apical ligand on cobalt, when many more readily available nitrogen donor ligands in biological systems, such as imidazole, could have been utilized. A recent study designed to examine the affinity of cobalt for the apical nitrogen ligand donor was conducted by varying the

nitrogen donor moiety in Cobalamin.[35] The binding affinity was assessed based on the crystallographic bond length of the Co-N bond. The study correlated the bond distance with the calculated cone angle of the donating nitrogen ligand, and concluded that steric interactions play the largest role in bond lengthening. The correlation of bond distance to cone angle improved slightly when a basicity component was added to the calculation. From the data presented, this correlation holds when comparing substituted pyridines, but fails when comparing the more relevant nitrogen donors pyridine, imidazole, and 5,6-dimethylbenzimidazole. The shortest Co-N bond length thus far observed in Cobalamin is with 5,6-dimethylbenzimidazole.

An experiment can be envisioned to address the seemingly inadequate explanation of binding constant, basicity, and sterics as observed in the case of Cobalamine. Another component of this bonding interaction, such as a back bonding interaction, might help to explain these observations. By plotting proton basicity versus transition-metal binding constant, it may be possible to address relative differences of additional back bonding over strict basicity and π donation, if any. Substituted **BBIL** ligand systems effectively lend themselves to such an experiment. As previously discussed, the basicity of the substituted **BBIL** ligands can be correlated with the chemical shift of the bound proton of the analogous proton sponge compounds (**BBIL**$^+$). The activation energy for a particular M(**BBIL**)$_2$ complex in solution can be estimated from the ligand exchange experiments previously discussed by the following equation:

$$k_r = \kappa \frac{kT}{h} \exp(-\Delta G^{\ddagger}/RT)$$

where $\Delta G^{\ddagger}$ is the free energy of activation and κ is a transmission coefficient which depends on the nature of process, but is often taken as unity.[36] A slope of non-unity should be an indication of an additional bonding component.

Multidentate ligands designed to constrain the coordination geometries and denticities of metals have found several applications in chemistry. Geometrically constraining ligands impose disfavored coordination geometries and coordination numbers, which manifest themselves in unusual, or even new or rarely observed, chemical properties. These properties may lead to new or unusual spectroscopic and catalytic features. Such constraints may be further enhanced by creating hydrophobic/hydrophilic pockets near the metal center. Fundamentally, these systems may give better insight into the behavior of constrained transition metal ions. With a better understanding of these constraints, the insights gained may be applied to the design of new catalysts. The catalytic activity of these metal complexes may have more relevant impact on the commercial application of these discoveries. Instances of unusual geometric constraints on metal ions, which have provided avenues to prepare new catalysts, have been well documented. An excellent example of this is the evolution of homogeneous olefin polymerization catalysts.

A significant amount of research effort in the area of polymerization catalysis has been performed in the six decades following, the discovery of Ziegler-Natta type (heterogeneous) catalysts for the polymerization of ethylene. This work was stimulated in part by the commercial importance of polymers. The development of geometrically constrained homogeneous Group (IV) catalysts (Ti, Zr, Hf) has become an important demonstration of this evolution. The first effective homogeneous ethylene catalysts,

reported in the late 1980's, were simple Hf(Cp)$_2$Cl$_2$ organometallic complexes (Figure 10-IV).[37] These complexes produced highly linear polyethylene, but failed to incorporate any higher α-olefins. The next step in the evolution involved designated, "constrained-geometry catalysts" (CGC's), which took the form of bridged cyclopentadienyl-amido organometallic complexes (Figure 10-V).[38] These catalysts provided a more open face to the metal center than those such as IV, allowing the approach of more bulky olefins. These catalysts allowed the incorporation of up to 8 mole percent of higher α-olefins, which provided access to polymers with enhanced physical properties. Recently, such catalysts have evolved a step further (Figure 10-VI).[39] While the mechanism is not fully understood, catalyst VI is even more constrained than V and may even provide a lipophillic pocket, which has moved such catalysts into the inverted incorporation region where higher α-olefins are preferred over ethylene.
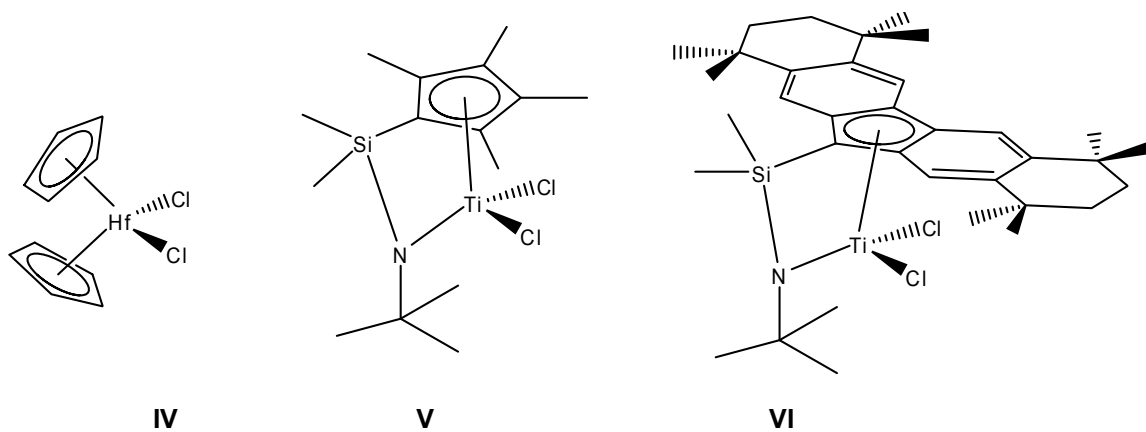
Figure 10. Moleular structures of Group (IV) constrained geometry polymerization catalysts.

Geometrically constraining bis(benzimidazole) ligands and their metal complexes have found and continue to find applications in catalysis, electron exchange, and energy conversion. Geometrically constrained bis(benzimidazoles) complexed with copper have been shown to catalyze the polymerization of α-olefins by insertion.[40,41] This is the first documented example of a copper catalyzed olefin insertion polymerization.[42] Also, as a further demonstration of binding constant as well as recoverability (environmentally friendly), a Cu(II)LCl$_2$ (where L is a bis(benzimidazole)) polymerization catalyst is shown as yellow crystals on the surface of a polymer (post-polymerization/workup) (Figure 11).[43] Recovery of any other commercial polymerization catalyst has never been demonstrated.
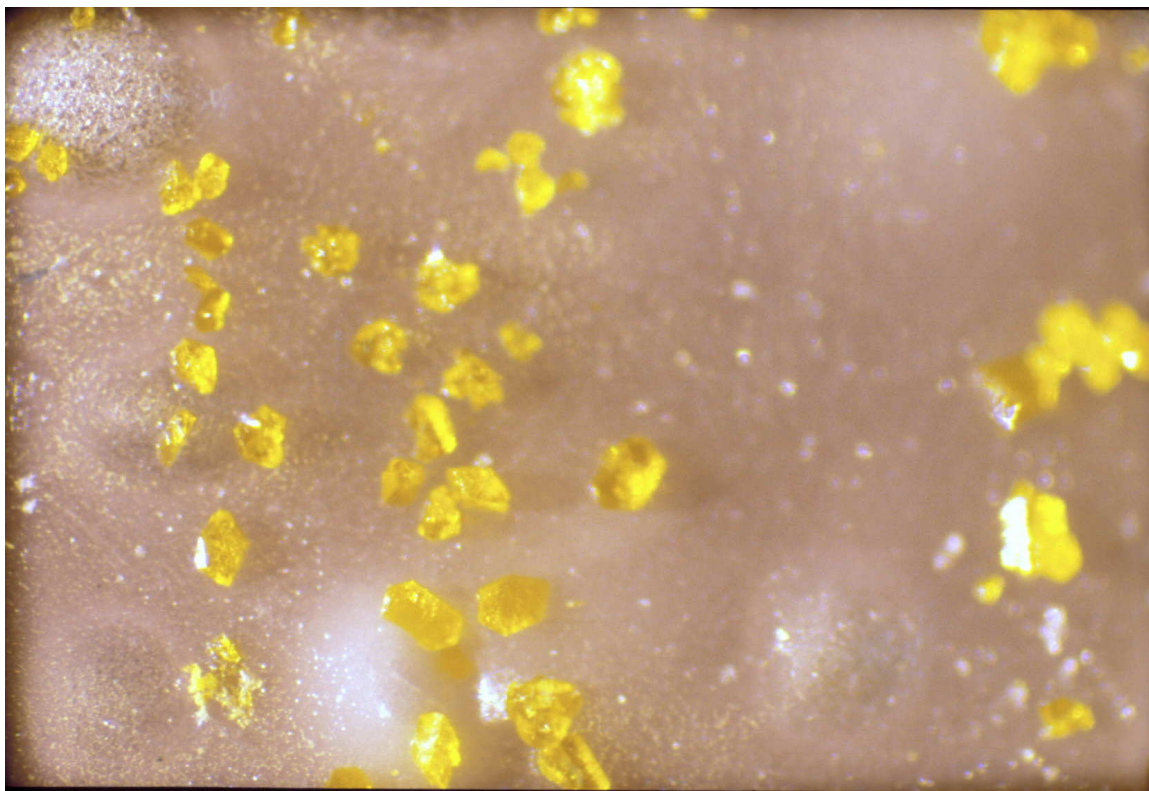
Figure 11. Crystals of a Cu(II)LCl$_2$ (where L is a bis(benzimidazole)) polymerization catalyst (post-polymerization/workup) on the surface of a polymer.

We have also begun to explore chiral, geometrically constraining bis(benzimidazole) ligands and their complexes with metal ions. The intent is to use these species to explore electron self-exchange and chiral catalysis. As noted above, the first generation ligand system **BIL** was designed to measure electron self-exchange of a Cu(I)/Cu(II) couple. Of particular interest for electron-transfer studies are Type 1 (T1) copper sites, which are mononuclear redox-active cofactors present in cupredoxins. Cupredoxins are a large family of single domain electron-transfer proteins. Nearly all T1 copper sites are four coordinate with psuedotetrahedral coordination geometries. With **BIL**, the exchange rate was estimated by using NMR relaxation times.[34] For a second

generation of ligands, chiral versions of **BBIL,** such as the *R*-2,2′-bis[2-(1-propylbenzimidazol-2-yl)]6,6′-dimethylbiphenyl (Figure 12), can be synthesized and isolated. Resolution of the Cu(I) and enantiomeric Cu(II) form will allow the direct measurement of the kinetics of electron exchange by optical rotary dispersion. Few direct measurements of electron self-exchange have ever been made on small metal complexes or biological systems. This has made Marcus theory, which allows for the indirect measurement of this phenomenon, a theory of great importance.[44]
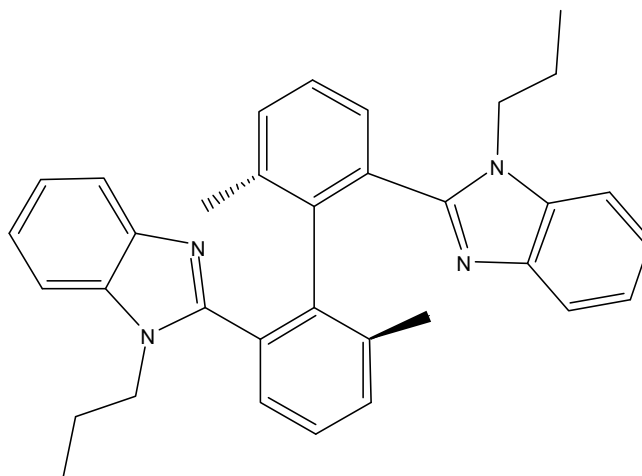
Figure 12. Molecular structure of *R*-2,2′-bis[2-(1-propylbenzimidazol-2-yl)]6,6′-dimethylbiphenyl

Asymmetric catalysis with chiral metal complexes has become increasingly important in the area of organic synthesis. Numerous catalytic enantioselective reaction types have been explored, including cyclopropanation, aziridination, aldol, Michael, allylic substitution, Diels-Alder, Henry, and ene reactions. One of the most effective catalyst compositions for these reactions consists of copper with a chiral bidentate ligand.[45] With this in mind, a number of chiral copper complexes have been prepared and characterized. One example of this is ((*S,S*)-1,2-bis(1-ethylbenzimidazol-2-yl)-1′,2′-

bis(ethoxy)ethane)copper(II) dichloride, which has been crystallographically characterized (Figure 13).[25]
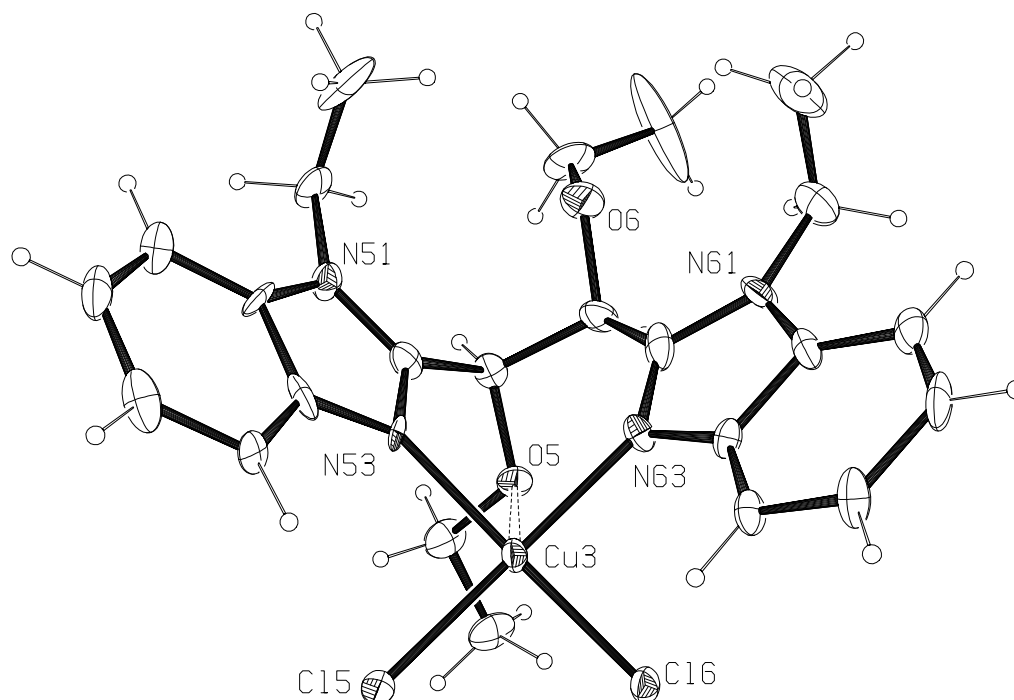
Figure 13. ORTEP[29] diagram of ((*S,S*)-1,2-bis(1-ethylbenzimidazol-2-yl)-1′,2′-bis(ethoxy)ethane)copper(II) dichloride. The thermal ellipsoids are drawn at the 25% probability level.

Another application with great potential, especially in light of the recent price surge of petroleum based energy sources, is energy conversion. Specifically, the conversion of sunlight directly into electrical energy or indirectly into chemical energy. This work is focused on dye-sensitized solar cells (DSSC) or "Grätzel"[46] cells. A dye-sensitized cell has a dye monolayer chemically absorbed on a semiconductor, such as TiO_2. The dye is intended to be the primary absorber of sunlight. The cell consists of a sandwich of TiO_2, dye, electrolyte, and catalyst (most often I^-/I_3^-) between two

conductive transparent electrodes (Figure 14). Upon illumination of the cell, charge separation occurs by electron injection from the excited-state dye molecule into the conduction band of TiO_2.
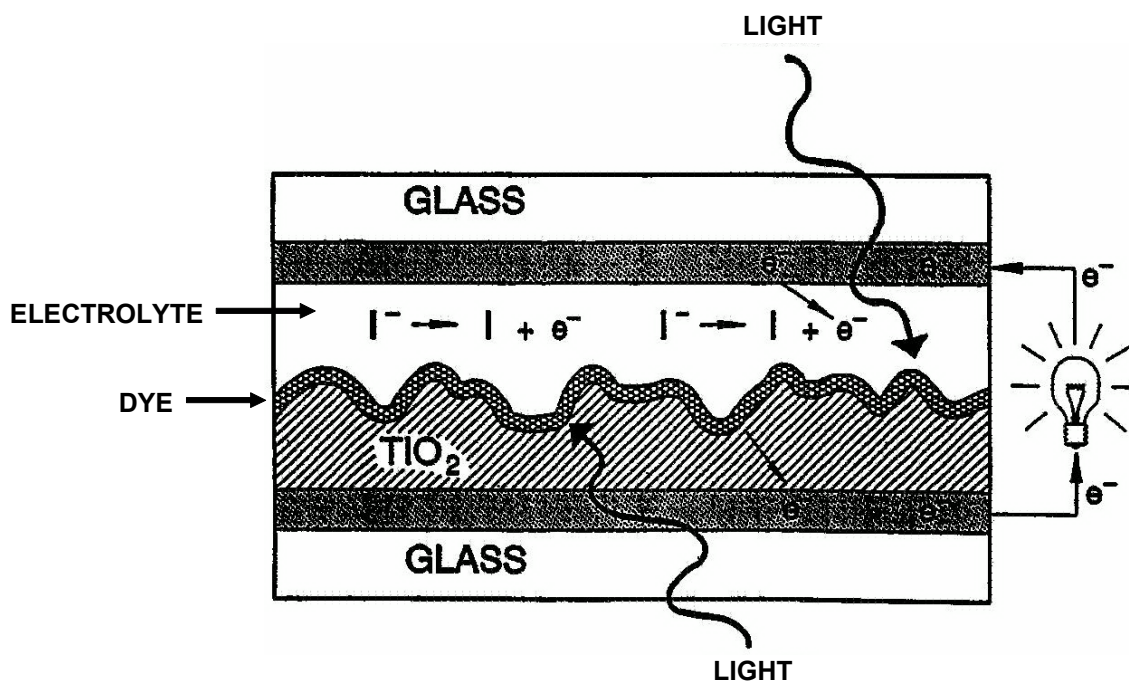
Figure 14. Schematic Diagram of a Dye-sensitized Cell.

Our goal is to synthesize dyes that absorb as much of the solar spectrum as possible with the highest quantum efficiency possible. Nearly all of the dyes that have been reported thus far have been based on the redox couple of Ru(III)/Ru(II) with pyridine-based ligands. We will examine both the ruthenium couple and the Cu(II)/Cu(I) couple with bis(benzimidazole) based ligands. Economically, copper is on the order of 100 fold less expensive than ruthenium, and much more abundant. An early version of a copper pyridine dye has already been reported.[47] That compound was shown to absorb a similar portion of the solar spectrum as the ruthenium-based dyes and remained active for

30 days. Further, geometrically constraining bis(benzimidazoles) should also maximize the quantum efficiency of the dyes by preventing loss of energy to rearrangement of the coordination environment at the metal site upon excitation.

Finally, of note is the vast literature that encompasses benzimidazole dyes and polymers of vinyl-imidazoles and vinyl-benzimidazoles. Both of these applications have a large patent estate. The dyes are known for both their relatively low cost and thermal stability, while the polymers are known for their high thermal stability. although not the focus of this work, there is surprisingly little published or patented regarding the use of bis(benzimidazoles) in these applications. Even more surprising is the lack of metal complexes reported for these applications, complexes which could be used in imaging and in electronics. This represents a compelling scientific and patent position opportunity.

Chapter 1

Synthesis of Benzimidazoles and Bis(benzimidazoles)

Discussion and Synthesis

As noted in the introduction, the synthesis of benzimidazole compounds has been investigated for over a century, yet nearly all of the compounds reported here are novel. While a number of new techniques, such as the facile oxidation of methylene bridged benzimidazoles, have been elucidated in this study, many improvements in experimental conditions have also been found in the syntheses of members of this class of compounds. To the general reader, a number of these observations and synthetic improvements may not, at first glance, seem significant, but when commercialization is considered (process chemistry), their financial importance becomes obvious. The importance of yield, selectivity, and environmentally considerate methods makes the impact of these techniques of very high value.

A wealth of reactions that result in the formation of an imidazole ring, both intended and unintended, have been reported in the literature.[1] In this study, the base benzimazole building blocks have been synthesized by using 2 of the 3 well-established condensation methods for imidazole ring formation, with minor variations. The first is the acid catalyzed carboxylate – diamine method. The second is the quinone – HMTA (hexamethylenetetramine) – ammonium acetate method. The third method, which was

not explored in this thesis, is the condensation of α-ketoaldehydes, which was first reported in 1882[48] and has continued to improve with time.[49]

There are two acid condensation techniques commonly in use for the synthesis of benzimidazoles, the first of which involves condensation in neat polyphosphoric acid at elevated temperatures.[50] Polyphosphoric acid is thought to act as a dehydrating agent. This method was used for the synthesis of bis(benzimidazoles) (**1a-1f**). The second technique utilizes refluxing 4-5M HCl and is often referred to as the "Phillips condensation method".[51] This technique was used for the synthesis of bis(benzimidazoles) (**2a-2h**).

Condensation reactions of symmetrically substituted 1,2-phenylene diamines has led to some important trends, which are not inconsistent with some previously observed trends for mono-substituted 1,2-phenylene diamines.[52] The non-substituted versions will undergo condensation with techniques involving hydrochloric acid or phosphoric acid equally well in terms of yield (H_3PO_4 > HCl in rate), with no dependence on atmospheric conditions. Electron-donating substituents, such as methyl, require the more stringent conditions of the H_3PO_4 technique to achieve good yields (> 50%). The HCl technique may produce very low yield (< 10%) even after extended reaction times. Atmospheric conditions seemed to ultimately play little role in the overall yield. Electron-withdrawing substituents, such as chloro, were more dependent on atmospheric conditions, and condensation of such compounds should be performed under inert atmosphere. When performed in air, a significant loss of product to oxidation is observed. This is generally manifested by the presence of very-dark-red material, which is difficult to remove, particularly when significant amounts are generated. Condensation of dicarboxylic acids

containing bridging groups, such as ethane-ol, ethane-thiol, and ethane-diol, which can undergo elimination, can only be achieved in good yields by using the HCl method.

Condensation of several methylene substituted malonic acids could not be achieved using either acid condensation technique. After the formation of the first benzimidazole, the intermediate undergoes decarboxylation. The reaction of diethylmalonic acid with two molar equivalents of 1,2-phenylene diamine, which results in the formation of **3a,** is depicted in Scheme 1-1. A likely mechanism for this reaction is presented in Scheme 1-2, in which a strongly bound cyclic transition state is allowed to form due to the available five-membered ring formation. This is a generally plausible mechanism for the decaboxylation of functionalized malonic acids.[53] A similar result was obtained for phenylmalonic acid which likely forms a six-membered ring transition state, resulting in 2-benzyl-1-hydrobenzimidazol-2-yl (**3c**). A milder technique, which has been reported for the synthesis of benzimidazoles, utilizes a "phosphonium anhydride" dehydrating agent.[54] This technique was not attempted for the successful synthesis of the bis(benzimidazole) product from diethylmalonic acid or phenylmalonic acid.

Scheme 1-1. Synthesis of **3a**.
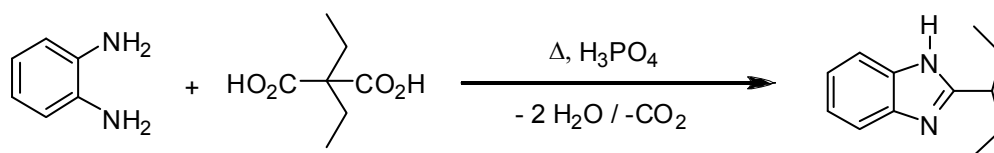
Scheme 1-2. Decarboxylation Mechanism.
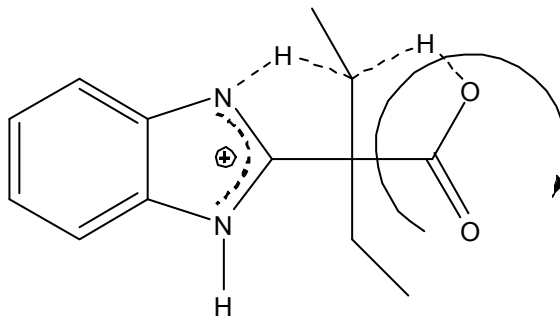
Successful syntheses of higher alkylated symmetric bis(benzimidazole)methanes were accomplished from the sequential alkylation of the four most acidic protons. The alkylations were performed in DMSO by a method adapted from a previously reported method for the alkylation of malonitriles.[55] The reactivity order for alkylation of bis(1-hydrobenzimidazole)methane (Figure 1-1) is $R_1 > R_2 \gg R_3$. This method of preparation has the advantage of being a single-pot reaction, to which different alkylating agents can be added sequentially. The only drawback of which we are aware is that the fourth alkylation can be sluggish, and may require large excess of NaH. Compounds **4a-6b** were synthesized by using this method. Because there is a large difference in reactivity for the third and fourth alkylations, the fourth alkylation can be performed on the isolated tri-alkylated product or step wise *in situ*. Once the third alkylation has been given sufficient reaction time, the fourth alkyaltion can proceed without isolation. A more expedient method for the third and fourth alkylations on a small scale utilizes *n*-butyl lithium in THF. This method was shown to give a much improved yield of **7** over the originally reported synthesis in DMSO.[42] Compounds **8a-10** were generally alkylated using sodium hydride in DMSO.
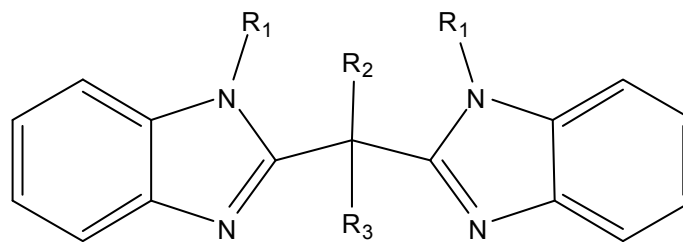
Figure 1-1. Progressive alkylation of bis(1-hydrobenzimidazole)methane.

Alkylation of hydroxylated and thiolated bis(benzimidazole)-ethane compounds could not efficiently be performed by using the NaH/DMSO technique to yield the equivalent alkyl ether and thioether compounds, owing to the propensity of the compounds to dehydrate or desulfanate under the conditions of the reaction. This NaH/DMSO technique was, however, very effective in producing the equivalent ethene compounds of the desired targets in high yields (> 90%) as a mixture of *cis* and *trans* isomers, with the *trans* isomer favored. The isomers could be separated effectively by column chromatography. The NaH/DMOS technique was used for the synthesis of **11a-12** (Scheme 1-3). An alternate synthesis of *trans*-bis(benzimidazole)ethene compounds has been reported.[56] The compounds are reportedly produced from the condensation of maleic acid, which is *cis*, with 4-bromo-1,2-phenylenediamine. The only reported method of characterization of purity is a single R_f under a single-solvent condition. Considering our results, for which both *cis* and *trans* forms are produced with the even more bulky alkylated benzimidazoles, the reported result that only *trans* would be produced from the *cis* starting material is suspect.

Scheme 1-3. Synthesis of Bis(benzimidazole)ethenes.
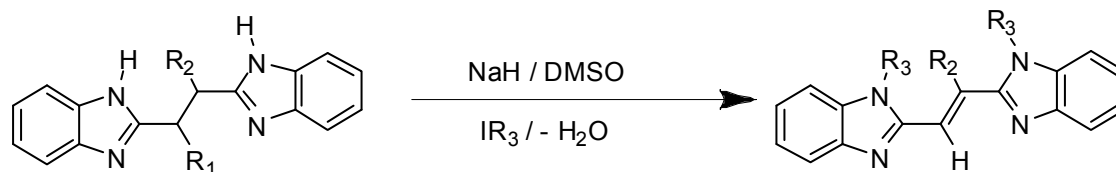
entry	R₁	R₂	R₃	compound
1	OH	H	Me	11a, 11b
2	SH	H	Et	11c, 11d
3	OH	OH	Me	12

Synthesis of alkyl ether bis(benzimidazole)ethane compounds, which contain two chiral centers, required a milder base, such as sodium hydroxide, in a mixture of DMF and 5-25% water. The addition of water helps to prevent the formation of ethylene compounds just described. The difference in acidity of the imine versus hydroxyl protons allows for stepwise alkylation, which provides a synthetic pathway to **14** (Figure 1-2). This technique, used for the synthesis of **15a-15f**, was found to retain chirality, where as more stringent conditions resulted in some racemization, leading to the isolation of (*R,S*)-1,2-bis(1-methylbenzimidazol-2-yl)-1',2'-bis(methoxy)ethane (**15b**).
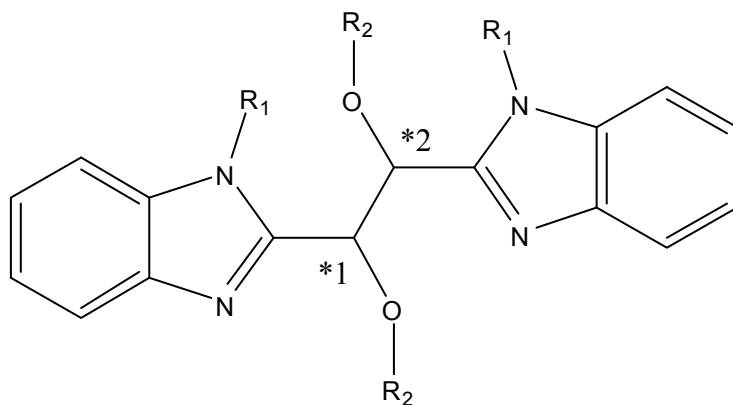
entry	R₁	R₂	*1	*2	compound
1	Me	H	*S*	*S*	13
2	Me	SiMe₃	*S*	*S*	14
3	Me	Me	*S*	*S*	15a
4	Me	Me	*R*	*S*	15b
5	Me	Me	*R*	*R*	15c
6	Et	Et	*R*	*R*	15d
7	Et	Et	*S*	*S*	15e

Figure 1-2. Synthesis of bis(benzimidazole)ethanes.

Two methods were explored for the preparation of thioether bis(benzimidazole)ethane compounds. The first is the same NaOH/DMF method as used for the alkyl-ether compounds (**15f**). The equivalent thioether was not obtained; instead, an oxidation occurred and the thioether-ethene (**16a**) was obtained. Further investigation as to the mechanism and prevention of this oxidation is required. The second method is

the acid-catalyzed conjugate addition of a thiol to a bis(benzimidazole)ethene (**11c**), as demonstrated in the synthesis of **16b**. Conjugate additions of thiols to enones have been well documented and are important in the total synthesis of many natural products.[57] Conjugate addition of a thiol to a benzimidazole-ethene has not previously been reported. Recent progress has been made in the asymmetric addition of thiols to enones,[57b] but that aspect has not been addressed in this work.

Early syntheses of bis(imidazole)ketones were first reported as two-step reactions in which the intermediates were isolated. Each step required low-temperature lithiation of a protected imidazole at the 2 position using *n*-butyl lithium, followed by subsequent addition of diethylcarbonate (DEC) and its intermediate (Scheme 1-4).[58] Isolation of the intermediate would allow for the synthesis of asymmetric bis(imidazole)ketones. This method was subsequently used to synthesize more highly substituted bis(imidazole)ketones.[59] More recently, a lithio-coupling procedure has been utilized to prepare simple *N*-protected bis(benzimidazole)ketones[60] in a single step. This reaction provides the only currently available synthetic route to substituted bis(imidazole)ketones, when the corresponding bis-(*N*-hydro-imidazole)methane compound is not readily available.

Scheme 1-4. Example of a Step-wise Synthesis of a Substituted Bis(imidazole)ketone.
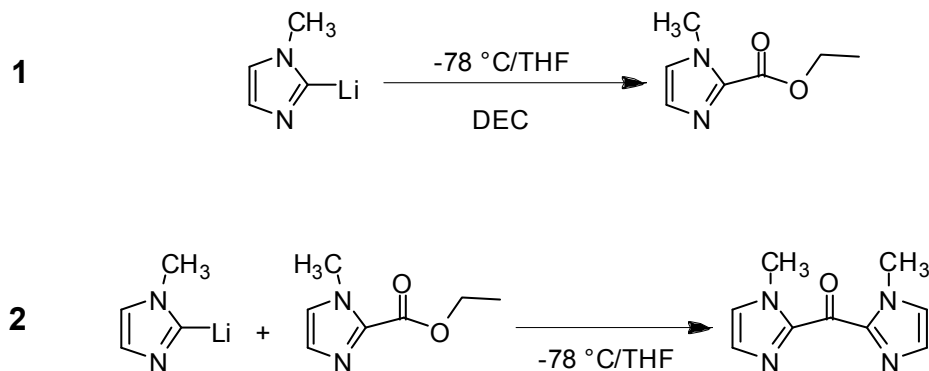
Oxidation of bis(benzimidazole)methanes directly to the corresponding bis(benzimidazole)ketones in good selectivity and yield has been a goal long sought after by numerous research groups. As previously noted, the lithio-coupling procedure has been utilized to prepare simple bis(benzimidazole)ketones.[60] In this study, the lithio-coupling procedure provided the only available route yet devised to synthesize bis(phenanthroimidazole)ketones. A metal-catalyzed air oxidation of 2-methylene-containing N-methylbenzimidazoles to the corresponding ketones has been reported (Scheme 1-5).[61] Attempts to reproduce these results in our lab resulted in low yields, which were particularly poor when R_1 was equal to H. Furthermore, we have not found subsequent citations utilizing this reported technique. Other reports, which utilized many other oxidizing reagents, failed to produce the desired ketones as well.[62]

Scheme 1-5. Oxidation of 2-Methylene-containing Benzimidazole Compounds.

entry	R$_1$	R$_2$
1	CH$_3$	—C≡N
2	CH$_3$	(acetyl methyl ester group)
3	CH$_3$	(N-methylbenzimidazol-2-yl group)
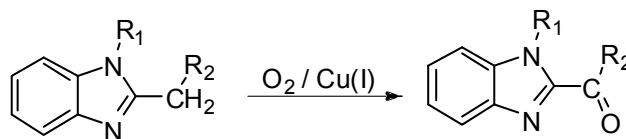
Subsequently, we found a mild, high-yield, facile procedure for preparing these desired products from bis(1-hydrobenzimidazole)methylene compounds. For example (Scheme 1-6), 1,1′bis(1-hydrobenzimidazol-2-yl)methane (**1a**) is solubilized in DMSO at rt in the presence of air and over a period of a few days, and the product ketone precipitates in various crystalline forms in quantitative yield (**17**). In contrast, a sample of **1a,** was stored under Ar, yielded no ketone product after two months. Numerous other solvents, such as DMF, acetonitrile, dichloromethane, and acetone, failed to yield any ketone product. The reaction is presumed to proceed by the formation of hydroperoxide at the methylene position, followed by rapid decomposition to eliminate water and the product ketone (Scheme 1-7). This is clearly a different mechanism than that previously reported for the selective oxidation of benzylic alcohols to aldehydes at high temperature.[64] In that case,

DMSO was shown to be the oxidant, generating dimethylsulfide. The role of DMSO in the formation of the ketone seems key, but is not yet understood. Crystal structures of the ketones show various self-assembled polymeric structures due to hydrogen-bonding interactions. The various isolable polymorphs of these compounds[25] likely explains the variability of the reported melting points of identical compounds over many decades. Upon alkylation of the amine nitrogen atoms of the benzimidazole, followed by the identical oxidation conditions, very little ketone is observed, while the bis(benzimidazoles) undergo an oxidative coupling to form selectively a terakis(benzimidazole) (**18**) (Scheme 1-6). In a comparative experiment, equal molar amounts of dipropyl (**4b**) and tripropyl (**5b**) substituted (**1a**) were combined in DMSO solution in air at rt and allowed to oxidize over several days. The reaction resulted in complete oxidative coupling of **4b** to form the terakis(benzimidazole) product **18**, while leaving **5b** unreacted. The methyl-substituted version of **18** has been reported, and was obtained by the reaction of 1,1′bis(1-methylbenzimidazol-2-yl)methane in methanol with sodium methoxide over manganese(II) acetate at rt to give a yield of 37%.[62] Oxidative addition of **1a** to form the tetrakis(benzimidazole)ethylene was performed following a literature procedure, which included refluxing in nitrobenzene.[65] The bright-yellow product was nearly insoluble in a wide variety of solvents. Attempts to alkylate the product in DMSO were unsuccessful. The only reported characterization of this compound was elemental analysis. This route was subsequently abandoned.

Scheme 1-6. Oxidation Pathways of Bis(benzimidazole)methanes.
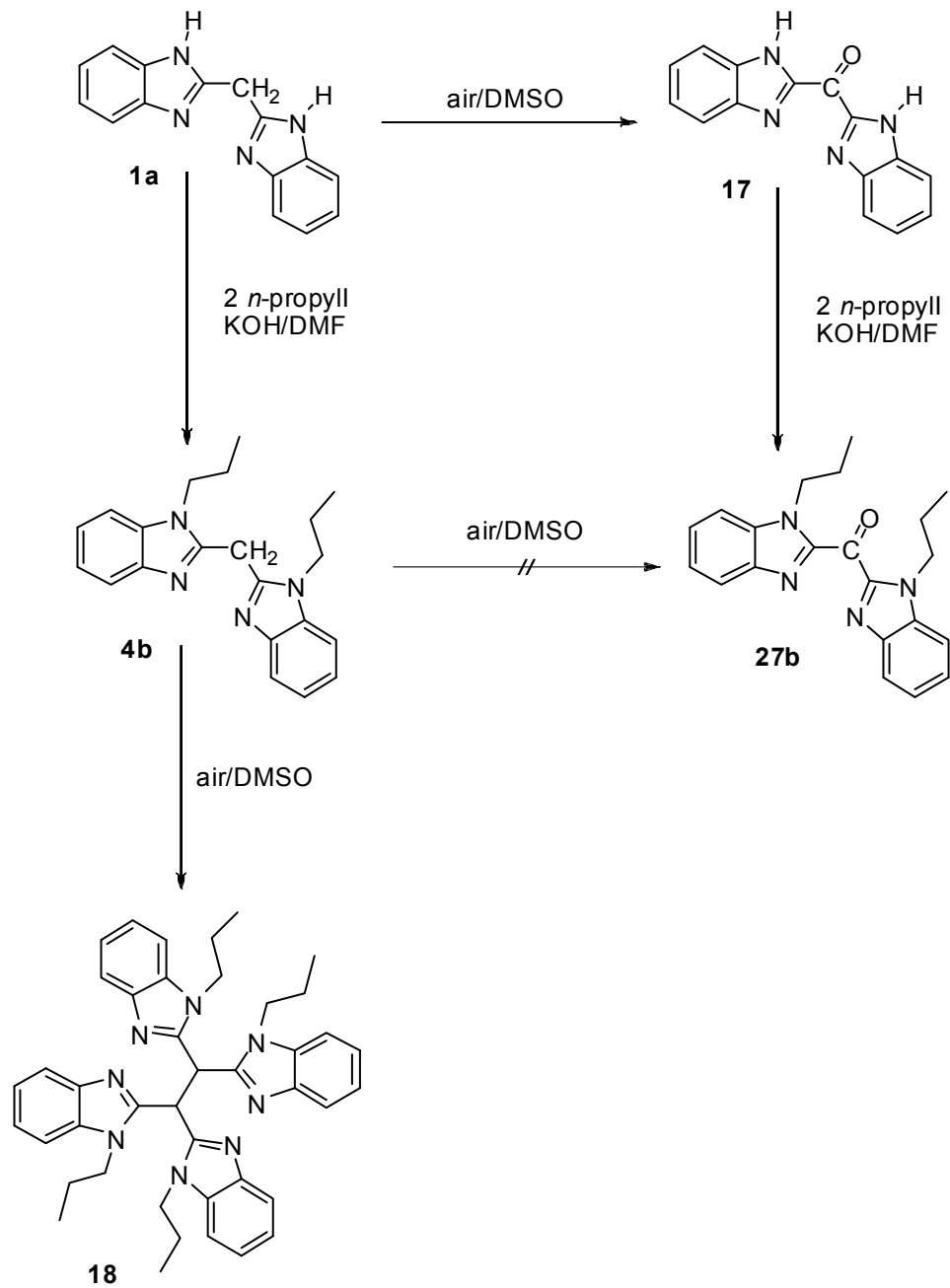
Scheme 1-7. A Possible Pathway for the Formation of Bis(benzimidazole)ketone.
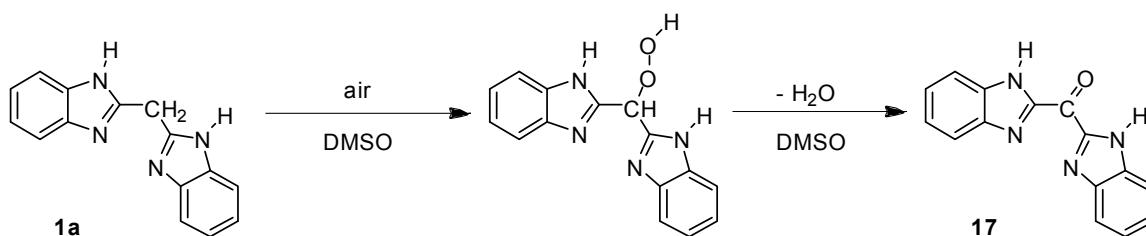
As described earlier, certain bis(benzimidazole)ketones may be synthesized by lithio-coupling with diethylcarbonate. A number of benzimidazole building blocks are reported here. Of particular inerest are extended-ring benzimidazoles for application in photo-cells; with this consideration, our synthetic work has focused on phenanthroimidazole systems. A number of reactions have been reported that result in 1-*H*-phenanthro[9,10-*d*]imidazol-2-yl. One particular reaction involving benzenecarbothioamide and 3-methylfuran under UV irradiation, resulted, quite unexpectedly, in 1-*H*-phenanthro[9,10-*d*]imidazol-2-yl in 18% yield.[66] As alluded to earlier, this is an example of the "Benzimidazole Rule", as Meth-Cohn in "*Imidazole and Benzimidazole Synthesis*" recounts, "given the right number of carbons and nitrogens, any starting material would ultimately end up as a benzimidazole".[1a] A more predictable route, the photo-oxidation of 4,5-diphenyl-1H-imidazole,[67] has been reported repeatedly and optimized to give a 65% yield.[68] In this study, phenanthroimidazoles were synthesized from the parent quinones by condensation.[69] They were single-pot reactions that generally afforded products in > 90% yield.

A number of important caveats were discovered during the syntheses of the bis(phenanthroimidazole)ketones. The lithio-coupling of non-substituted, *N*-protected

phenanthroimidazoles proceeds with high selectivity and high yields with *n*-butyl lithium at -78 °C to give **22** (Scheme 1-8). For phenanthroimidazoles that are ring-substituted with halogens, a milder base was required to maintain selectivity. Lithium diisopropylamide (LDA) was found to be the best choice to maintain selectivity and yield. Regardless of the phenanthroimidazole or base used in the coupling, homo-coupling occurs if the reaction is allowed to warm to -40 °C without the introduction of diethylcarbonate (**23**).

Scheme 1-8. Lithio-couplings of Phenanthroimidazoles.
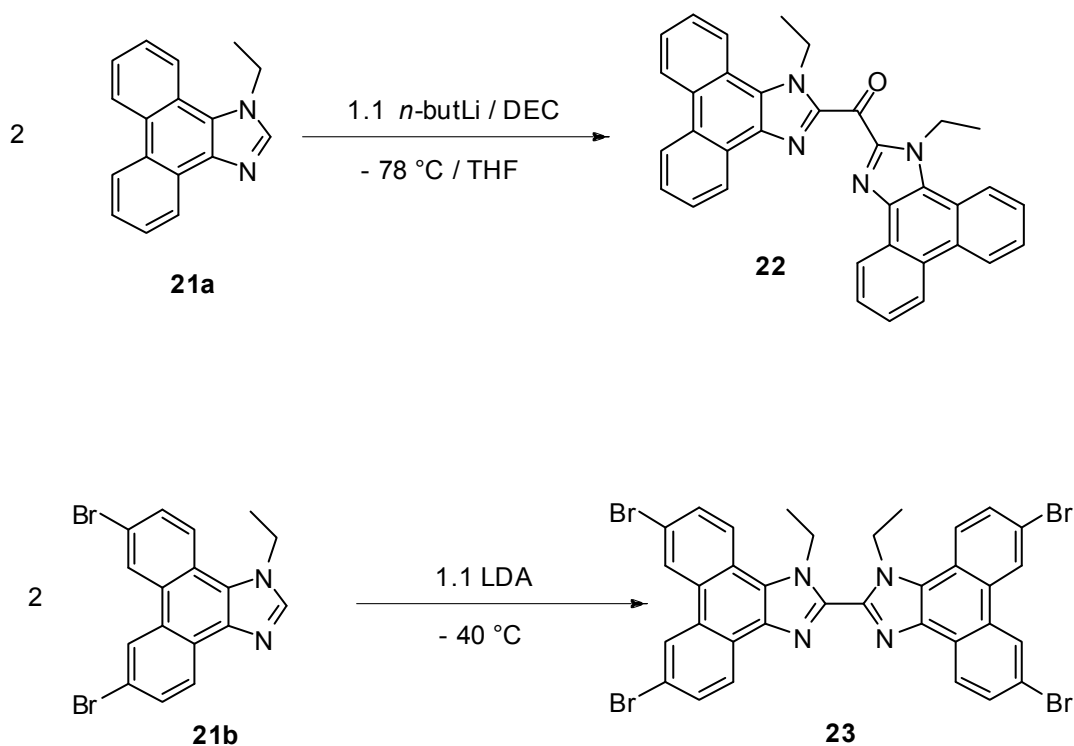
Cyanation of halogen functionalities was found to be the most expeditious route to synthesize carboxy functionalities via hydrolysis of the cyano group. A modified CuI/Pd(0) catalyzed cyanation of bromo functionalities was used.[70] A catalytic mixture of 10 mol % CuI, 5 mol % $Pd_2(dba)_3$ (tris(dibenzylideneacetone)dipalladium(0)), 5 mol % fedpp (1,1′-bis(diphenylphosphino)ferrocene), and 2 mol equiv of NaCN in acetonitrile was found to be most effective in the cyanation of the compounds that were examined (Scheme 1-9). Acetonitrile was found to be the most effective solvent. Several other reported solvents, such as THF, gave poor conversions.

Scheme 1-9. Catalyzed Cyanation of Bromo Functionalities.
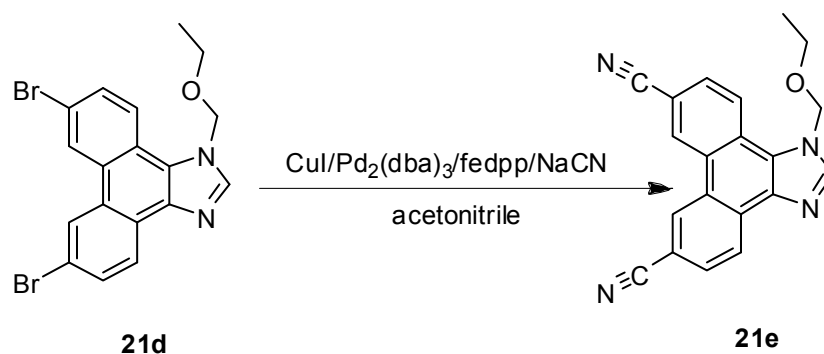
Base-catalyzed condensation of **4a** with functionalized benzaldehydes yields benzylidene derivatives, which can be either further functionalized or deprotected to yield tethered molecules that can be utilized in photovoltaic cells. The base-catalyzed

condensation of bis(benzothiazolyl)methanes has previously been reported utilizing sodium ethoxide/ethanol.[62] The synthesis of **24a** demonstrates that **4a** is a strong enough base to auto-catalyze the condensation (Scheme 1-10).

Scheme 1-10. The Auto-catalyzed Condensation of **4a** with 4-Bromobenzaldehyde to Yield **24a**.
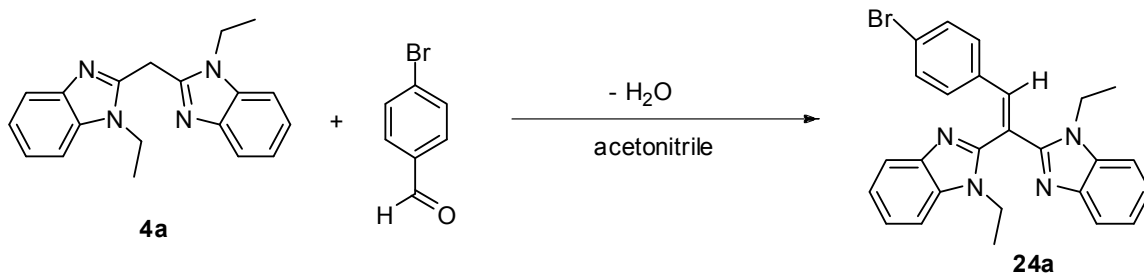
The use of catechols as tethering functionalities in compounds for possible use as photovoltaic dyes is desirable because they are known to bind strongly to TiO_2.[63] In order to prepare such dyes for use as suitable ligands, they need to be protected and deprotected efficiently. Nowhere else in the syntheses reported here was the "Goldilocks" effect found to be as crucial. When appropriate precautions were used, the cyclohexylidene ketal was found to be the most efficient route for synthesis. The methylene acetal was also utilized, owing to its availability and stability, but stringent deprotection generally gave lower yields. Silyl protection of catachol was effected, but subsequent synthetic steps led to low yield or premature deprotection. Compound **25** was prepared in high yield using a classical technique employing acid catalysis. Attempts to produce this compound using the solid acid catalyst K-10[71] were found to be ineffective. Chromatography of **25** on silica was successful, but all subsequent synthetic steps, starting with **26,** required that a base such as triethylamine be present in the solute to

avoid deprotection. An immediate indication of decomposition of the target compound on silica is the formation of a deep-indigo-blue color on the column.
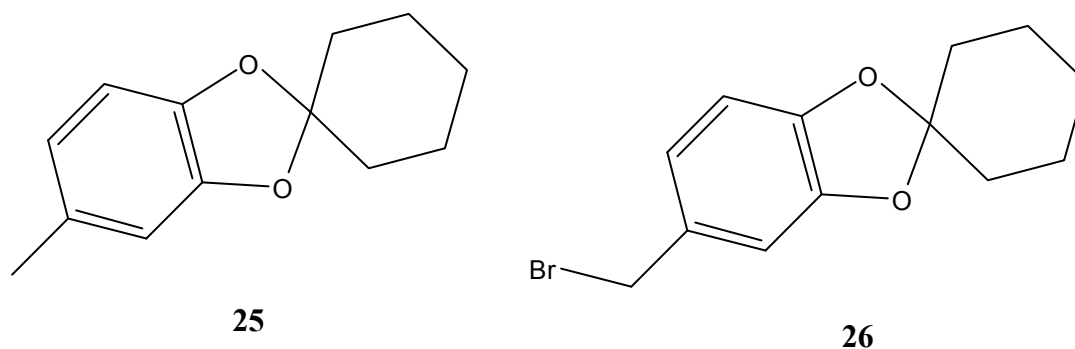
Figure 1-3. Molecular structures of **25** and **26**.

As previously mentioned in the introduction, the design and synthesis of chiral, geometrically constraining bis(benzimidazoles) for applications in electron transfer and catalysis studies has been a goal of this ongoing research. Chirality is necessarily introduced by the 2,2′-biphenyl bridge in the bis(benzimidazole)biraryls. The low rotational barrier offered by the 6,6′-proton substitution is expected to result in facile interconversion of these free ligands.[72] To avoid this interconversion, the synthesis of biaryls with larger substituents at the 6,6′ positions is required. We are unaware of the preparations of any such systems containing benzimidazoles. In our hands, the synthesis of racemization-resistant bis(benzimidazole)biaryls was found to be more difficult than was originally anticipated. For the sake of brevity, the discussion will focus on an obvious choice of binaphthyl as the bridging biaryl, the system we have examined most

thoroughly. Other bridging biaryls are being explored, but no conclusions have yet been drawn.

With the recent interest in chiral hydrogenation catalysts,[73] numerous binaphthyl-phosphine ligands have been synthesized and characterized.[74] The synthetic techniques used have not translated to equivalent synthetic routes to benzimidazole ligands. A readily available starting material is 2,2′-binaphthol, which, at first, seems to be a promising starting material. The 2,2′-binaphthol was converted into the corresponding dibromide[75] under harsh conditions (320 °C using Ph_3PBr_2) to give yields of ca. 40%. Lithiation of the dibromide, followed by introduction of carbon dioxide, has been reported to give yields of 21-90% of the dicarboxylate.[76] Attempts to reproduce this experimental procedure gave yields of 20% or less. Facile conversion of the 2,2′-binaphthol into the corresponding ditriflate has been reported and reproduced.[77] We and others have utilized several techniques to convert the ditriflate into the dinitrile, all with yields of 10% or less.[78] Attempts to produce the dicarboxylate from the ditriflate directly, using a reported palladium-catalyzed hydroxycarbonylation technique for aryl-triflates,[79] resulted in the near quantitative formation of 1,1′-binaphthalene.[80,A1] There are still promising synthetic routes to be investigated for the production of the dicarboxylate cost effectively, such as the copper-mediated homocoupling of the diazonium salt generated from 1-amino-2-naphthoic acid, or a multi-step synthesis starting from 2,2′-dimethyl-1,1′-binaphthalene. Direct oxidation of 2,2′-dimethyl-1,1′-binaphthalene to the corresponding dicarboxylate has yet to afford more than trace amounts of the product. The dicondensation reaction to give the bis(benzimidazole) from the dicarboxylates has yet to be demonstrated. As shown in Scheme 1-11, a target compound has been

synthesized using a modified Stille coupling.[81] The product is a racemic mixture; enantiomeric separation has not yet been demonstrated.

Scheme 1-11. Synthesis of *rac*-2,2′-Bis[2-(1-propylbenzimidazol-2-yl)]-1,1′-binaphthyl.
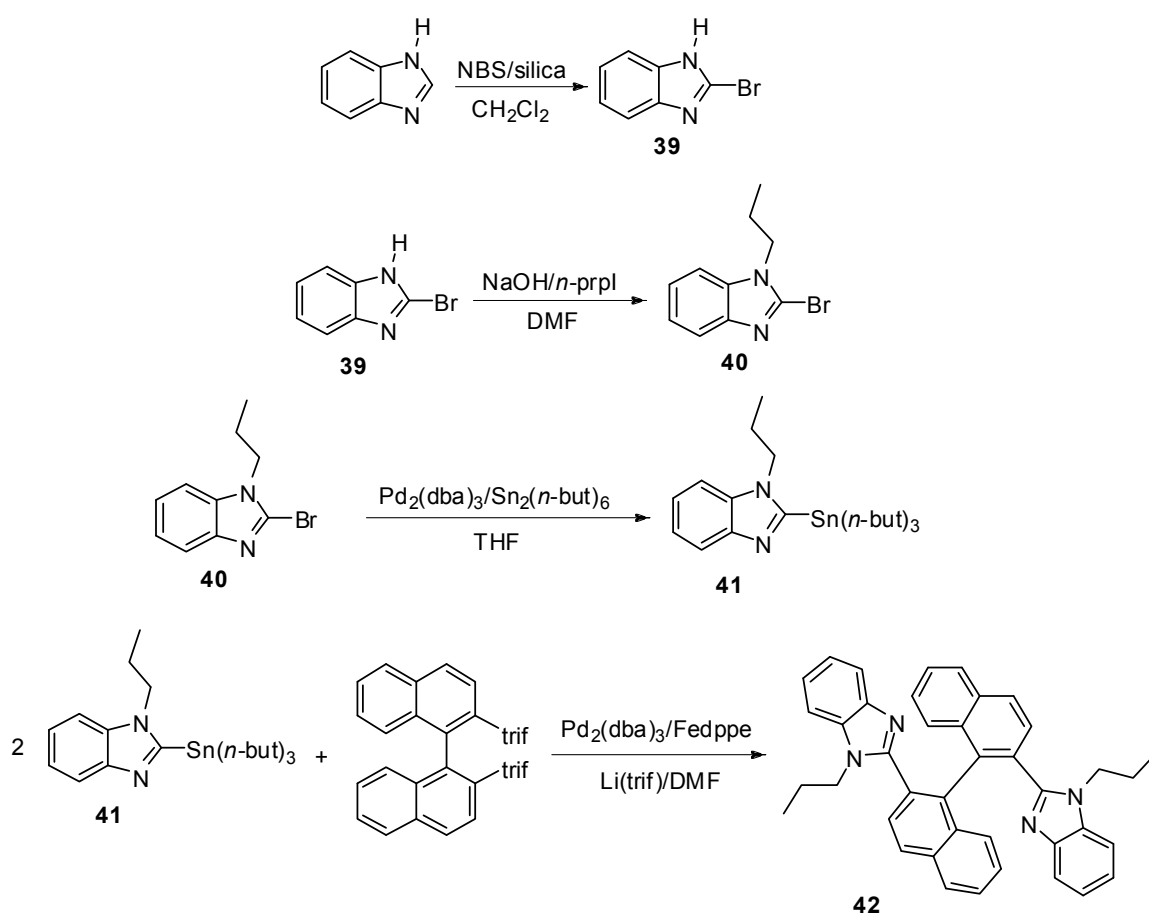
Experimental

General Conditions. Air sensitive manipulations were conducted under nitrogen or argon using standard Schlenk techniques. Dimethyl sulfoxide was dried over CaH_2. All other reagents were used as received or purified by standard methods.[82] NMR spectra were recorded using Varian 300 and 400 MHz spectrometers at rt unless otherwise noted. Melting points were determined with a hot-stage apparatus and are uncorrected. Electronic spectra were recorded with a computer-interfaced Cary Model 14 spectrometer that was upgraded by Aviv Associates. Electronic spectra were measured in spectrophotometric grade solvents. TLC was performed using 60 Å silica gel on glass with a 254 nm fluorescent indicator. Infrared spectra were measured by using a Mattson Galaxy Series FTIR 5000 spectrophotometer. ORTEP[29] diagrams of X-ray crystal structures of the compounds throughout this manuscript are noted as follows: **1a**(manuscript number), X-ray structure(I)(polymorph number), (n)(melting point Kelvin), [A(page)](appendix page number) and are provided in the appendix. Crystallographic details that are relevant to the discussion are provided in the text. Complete CIFs (crystallographic information files) are available upon request. Blanket Copyright permission has been granted by the American Chemical Society for any content included in this thesis.

Synthesis.

1,1′-Bis(1-hydrobenzimidazol-2-yl)methane. (1a)[50,83] In a 250 mL round bottom flask, 6.09 g of malonic acid (57.7 mmol), 12.47 g of 1,2-phenylene diamine (115.3 mmol), and 25 g of polyphosphoric acid were added sequentially. The mixture was heated at 190 °C for 3.5 h with stirring. The mixture was cooled to 90 °C and then neutralized to pH 8 with ammonium hydroxide. The solid was collected by filtration and repeatedly washed with water. The solid was dried to constant weight using vacuum at 80 °C for 24 h. $C_{15}H_{12}N_4$, fw = 248.28. Yield: 13.19 g, 92.1%. Mp: 331 °C (recryst. acetone/ethanol, dec.). ^{1}H NMR (CD$_3$SO$_2$CD$_3$): δ 7.53(q, J = 3.1 Hz, 4H), 7.16(q, J = 3.1 Hz, 4H), 4.54(s, 2H), 2.51(s, 2H). ^{13}C NMR (CD$_3$SO$_2$CD$_3$): δ 150.6, 139.1, 121.9, 115.1, 29.7. R_f = 0.28 (ethyl acetate/silica). FD MS: 248.2. IR (KBr pellet, cm^{-1}): 1622, 1590, 1544, 1530, 1487, 1435 s, 1309, 1271 s, 1031 s, 999, 738 s, 618, 466. Anal. Calcd for: N 22.57, H 4.87, C 72.56. Found: N 22.57, H 4.86, C 72.36.

1,1′-Bis(1-hydro-5,6-dimethylbenzimidazol-2yl)methane. (1b) In a 500 mL round bottom flask, 4.00 g of malonic acid (38.4 mmol), 10.47 g of 4,5-dimethyl-1,2-phenylene diamine (76.88 mmol), and 25 g of polyphosphoric acid were added sequentially. The mixture was heated at 200 °C for 3.5 h with stirring. The mixture was cooled to 90 °C and the mixture was then neutralized to pH 8 with ammonium hydroxide. The solid was collected by filtration and repeatedly washed with water. The solid was dried to constant weight using vacuum at 80 °C for 24 h. $C_{19}H_{20}N_4$, fw = 304.39. Yield: 11.06 g, 94.6%. Mp: 328-329 °C. ^{1}H NMR (CD$_3$SO$_2$CD$_3$): δ 7.25(s, 4H), 4.37(s, 2H), 2.51(s, 2H), 2.27(s, 12H). ^{13}C NMR (CD$_3$SO$_2$CD$_3$): δ 149.8, 137.8, 130.0, 115.5, 29.7, 20.3. R_f = 0.38 (ethyl acetate/silica).

1,1′-(1-Hydro-5-nitrobenzimidazol-2yl)methane. (1c) In a 250 mL round bottom flask, 5.00 g of malonic acid (48.0 mmol), 14.72 g of 4-nitro-1,2-phenylene diamine (96.1 mmol), and 25 g of polyphosphoric acid were added sequentially. The mixture was placed under a stream of nitrogen and heated at 190 °C for 3.5 h with stirring. The mixture was cooled to 90 °C and then neutralized to pH 8 with ammonium hydroxide. The solid was collected by filtration and repeatedly washed with water. The solid was dried to constant weight using vacuum at 80 °C for 24 h. The solid was then taken up in ethanol and refluxed with activated charcoal. The hot mixture was filtered and the solvent the removed to give an orange solid. $C_{15}H_{10}N_6O_4$, fw = 338.28. ^{1}H NMR ($CD_3SO_2CD_3$): δ 8.33(s, 1H), 8.03(d, J = 8.8 Hz, 1H), 7.59(d, J = 8.8 Hz, 1H), 7.41(d, J = 9.2 Hz, 1H), 7.40(s, 1H), 5.53(d, J = 8.4 Hz, 1H), 6.04(br s, 2H), 2.50(s, 2H). ^{13}C NMR ($CD_3SO_2CD_3$): δ 157.0, 143.7, 142.2, 137.2, 136.9, 134.2, 117.5, 116.0, 111.8, 108.4, 15.1. R_f = 0.33 (Etoac).

1-Hydro-2-methyl-5-nitrobenzimidazol-2-yl. (1c-1)[84] Compound **1c-1** was isolated as a minor decomposition product in the synthesis of **1c**. A few crystals were isolated from the slow evaporation of a DMF solution of **1c**. Crystal structure **1c-1** (I).[A6]

***trans*-1,2-Bis(1-hydrobenzimidazol-2-yl)cyclohexane. (1d)** In a 200 mL round bottom flask 5.00 g of *trans*-1,2-cyclohexane dicarboxylic acid (15.8 mmol), 3.42 g of 1,2-phenylenediamine (31.6 mmol), and 10 mL of polyphosphoric acid were added sequentially. The mixture was heated at 215 °C for 1.5 h with stirring. The mixture was cooled to 100 °C with the addition of ice. The reaction mixture was neutralized to pH 8 with ammonium hydroxide. The solid was collected by filtration and repeatedly washed with water. The solid was dried to constant weight using vacuum at 80 °C to give the

product as an amorphous pale-pink solid. $C_{20}H_{20}N_4$, fw = 316.40. Yield: 4.73 g, 94.6%. Mp: > 335 °C. ^{1}H NMR (CD$_3$SOCD$_3$): δ 7.50(m, 4H), 7.16(m, 4H), 2.12(m, 2H), 1.70(m, 6H), 1.33(m, 2H). R_f = 0.10 (ethyl acetate/silica).

***rac*-2,2′-Bis[2-(1-hydrobenzimidazol-2-yl)]biphenyl. (1e)**[12a,42] In a 1 L round bottom flask, 35.00 g of biphenyl-2,2'-dicarboxylic acid (0.145 mol), 31.25 g of 1,2-phenylene diamine (0.289 mol), and 50 g of polyphosphoric acid were added sequentially. The mixture was heated at 210 °C using a Dean-Stark trap for 3.5 h with stirring. The mixture was cooled to 150 °C and then poured into 1 L of water. A blender was used to grind the slurry. The mixture was then neutralized to pH 8 with ammonium hydroxide. The solid was collected by filtration and repeatedly washed with water. The solid was dried to constant weight using vacuum at 80 °C for 24 h. $C_{26}H_{18}N_4$, fw = 366.45. Yield: 53.98 g, 96%. Mp: 295 °C. ^{1}H NMR (CD$_3$SO$_2$CD$_3$): δ 7.73 (d, J = 7.5 Hz, 2H), 7.50(q, J = 3.5 Hz, 4H), 7.34(t, J = 7.0 Hz, 2H), 7.22(t, J = 7.0 Hz, 2H), 7.16(q, J = 3.0 Hz, 4H), 6.97(d, J = 7.5 Hz). ^{13}C NMR (CD$_3$SO$_2$CD$_3$): δ 153.2, 141.0, 138.7, 130.6, 130.4, 130.0, 128.9, 127.4, 122.1, 115.2. R_f = 0.36 (ethyl acetate/silica). FD MS: 387.3. IR (KBr pellet, cm^{-1}): 1709 m, 1621 m, 1431 s, 1369 w, 1274 m, 744 s, 531 w, 429 w. Anal. Calcd for: N 14.50, H 4.69, C 80.81. Found: N 14.41, H 4.79, C 80.65.

***rac*-2,2′-Bis[2-(1-hydro-5,6-dimethylbenzimidazol-2-yl)]biphenyl. (1f)** In a 250 mL round bottom flask, 4.00 g of biphenyl-2,2'-dicarboxylic acid (16.5 mmol), 4.50 g of 4,5-dimethyl-1,2-phenylene diamine (33.0 mmol), and 30 g of polyphosphoric acid were added sequentially. The mixture was heated at 180 °C for 4 hours. The mixture was cooled to 100 °C and then neutralized to pH 8 with ammonium hydroxide. The solid was collected by filtration and repeatedly washed with water. $C_{30}H_{26}N_4$, fw = 442.56. Yield:

6.33 g, 86.7%. M.p. 328-330 °C. ^{1}H NMR (CDCl$_3$): δ 7.48 (d, J = 7.6 Hz, 2H), 7.27 (s, 4H), 7.07 (t, J = 7.5 Hz, 2H), 6.88 (t, J = 7.5 Hz, 2H), 5.83 (s br, 2H), 2.29 (s, 12H). ^{13}C NMR (CDCl$_3$): δ 152.7, 141.0, 137.2, 131.1, 130.6, 130.1, 130.0, 128.5, 127.1, 115.2, 20.3. R_f = 0.39 (Etoac).

1,1′-Bis(1-hydrobenzimidazol-2-yl)]carbinol. (2a)[40,42] A mixture of 8.00 g of of hydroxypropanedioic acid (66.6 mmol) and 14.41 g of 1,2-phenylene diamine (133.3 mmol) in 90 mL of 4 N hydrochloric acid was refluxed for 18 h. The reaction mixture was cooled and the pH was adjusted to about 8 with ammonium hydroxide to give a pale-green solid. The solid was collected by filtration, washed with water, and dried in a vacuum oven to give of 1,1'-bis(1-hydrobenzimidazol-2-yl)carbinol as an amorphous solid. C$_{15}$H$_{12}$N$_4$O, fw = 264.28. Yield: 8.85 g, 50.3%. Mp: 198 °C (soften) 328 °C (melt). ^{1}H NMR (400 MHz, CD$_3$SO$_2$CD$_3$ 60 °C): δ 7.73 (d, J = 7.5 Hz, 2H), 7.50(q, J = 3.5 Hz, 4H), 7.34(t, J = 7.0 Hz, 2H), 7.22(t, J = 7.0 Hz, 2H), 7.16(q, J = 3.0 Hz, 4H), 6.97(d, J = 7.5 Hz). ^{13}C NMR (CD$_3$SO$_2$CD$_3$): δ 153.2, 141.0, 138.7, 130.6, 130.4, 130.0, 128.9, 127.4, 122.1, 115.2. R_f = 0.30 (ethyl acetate/silica).

(S)-1,2-Bis(1-hydrobenzimidazol-2-yl)hydroxyethane. (2b)[85] In a 500 mL round bottom flask, 14.61 g of (*l*)-malic acid (0.109 mol), 23.57 g of 1,2-phenylene diamine (0.218 mol), and 40 mL of 5N hydrochloric acid acid were added sequentially. The mixture was heated to reflux for 3 d with stirring. The mixture was cooled to RT and then the mixture was neutralized to pH 8 with ammonium hydroxide. The solid was collected by filtration and repeatedly washed with water. The solid was dried to constant weight using vacuum at 80 °C for 24 h. C$_{16}$H$_{14}$N$_4$O, fw = 278.31. Yield: 15.15 g, 50.0 %. Mp: > 320 °C. ^{1}H NMR (400 MHz, CD$_3$SO$_2$CD$_3$ 24 °C): δ 7.50 (m, 4H), 7.14(m, 4H), 6.55(br s,

1H), 5.42(m, 1H), 3.59(m, 1H), 3.39(m, 1H), 2.50(br s, 2H). ^{13}C NMR (CD$_3$SO$_2$CD$_3$): δ
156.6, 152.2, 138.5, 121.4, 117.6, 115.0, 114.4, 66.5, 35.9. R_f = 0.05 (ethyl acetate/silica).

(S)-1,2-Bis(1-hydro-5,6-dimethylbenzimidazol-2-yl)hydroxyethane. (2c) In a 125 mL
round bottom flask, 1.474 g of (*l*)-malic acid (10.99 mmol), 3.000 g of 4,5-dimethyl-1,2-
phenylene diamine (22.03 mmol), and 30 mL of 4N hydrochloric acid acid were added
sequentially. The mixture was heated to reflux for 3 d with stirring. The mixture was
cooled to RT and then the mixture was neutralized to pH 8 with ammonium hydroxide.
The solid was collected by filtration and repeatedly washed with water. The pale brown
solid was dried to constant weight using vacuum at 80 °C for 24 h. C$_{20}$H$_{22}$N$_4$O, fw =
334.41. Yield: 3.491 g, 95.1 %. Mp: > 320 °C. ^{1}H NMR (400 MHz, CD$_3$SO$_2$CD$_3$ 24 °C):
δ 7.24(s, 2H), 7.22(s, 2H), 6.42(s, 1H), 5.38(m, 1H), 3.57(m, 1H), 3.38(m, 1H), 2.47(s,
6H), 2.27(s, 6H), 2.02(s, 2H). R_f = 0.06 (ethyl acetate/silica).

***rac*-1,2-Bis(1-hydrobenzimidazol-2-yl)ethanethiol (2d)** A 7.00 g quantity of *rac*-
thiomalic acid (46.6 mmol) was added to a 500 mL round bottom flask. This was
followed by the addition of 10.10 g of 1,2-phenylenediamine (93.4 mmol). Finally, 52
mL of 4 N HCl was added to the flask. The flask was fitted with a condenser and was left
to reflux with stirring under a blanket of nitrogen. After refluxing for 70 h the reaction
mixture was cooled and the mixture was brought to pH 10 with the slow addition of conc.
ammonium hydroxide to give a yellow precipitate. The precipitate was collected by
filtration and washed with water. The solid was placed in vacuum oven at 78 °C and
dried to constant weight to give the product as a yellow solid. C$_{16}$H$_{14}$N$_4$S, fw = 294.37.
Yield: 11.61 g, 84.6%. Mp: > 370 °C. ^{1}H NMR (400 MHz, CD$_3$SO$_2$CD$_3$ 25 °C): δ
7.51(m, 4H), 7.12(m, 4H), 6.50(m, 1H), 5.43(m, 1H), 3.49(m, 2H), 2.48(m, 1H). ^{13}C

NMR (CD$_3$SO$_2$CD$_3$): δ 156.9, 152.6, 138.9, 121.7, 118.1, 115.5, 114.8, 66.8, 36.2. R_f = 0.51 (ethyl acetate/silica).

(S,S)-1,2-Bis(1-hydrobenzimidazol-2-yl)-1′,2′-bis(hydroxy)ethane. (2e)[86,87,88a] In a 300 mL round bottom flask containing 60 mL of 4N HCl, 10.00 g of *d*-tartaric acid (66.6 mmol) and 14.44 g of 1,2-phenylene diamine (134 mmol) was added. The flask was fitted with a condenser and placed under nitrogen. The mixture was left to reflux for 72 hours. The mixture was cooled and then made basic with conc. ammonium hydroxide to give a pale-green precipitate. The precipitate was collected by filtration and washed with water. The precipitate was then dried in a vacuum oven to give a pale-green powder. C$_{16}$H$_{14}$N$_4$O$_2$, fw = 294.31. Yield: 19.28 g, 98.4%.(lit. 77%)[88a] Mp: > 230 °C (onset decomp.) ^{1}H NMR (CDCl$_3$): δ 7.55(m, 4H), 7.17(m, 4H), 5.43(s, 2H), 2.50(s, 2H). ^{13}C NMR (CDCl$_3$): δ 155.9, 138.9, 121.8, 115.3, 71.3. R_f = 0.12 (ethyl acetate/silica).

(R,R)-1,2-Bis(1-hydrobenzimidazol-2-yl)-1′,2′-bis(hydroxy)ethane. (2f)[86,87,88a] In a 500 mL round bottom flask containing 80 mL of 4N HCl, 9.11 g of *l*-tartaric acid (60.7 mmol) and 13.13 g of 1,2-phenylene diamine (121.4 mmol) was added. The flask was fitted with a condenser and placed under nitrogen. The mixture was left to reflux for 72 hours. The mixture was cooled and then made basic with conc. ammonium hydroxide to give a pale-green precipitate. The precipitate was collected by filtration and washed with water. The precipitate was then dried in a vacuum oven to give a pale-green powder. C$_{16}$H$_{14}$N$_4$O$_2$, fw = 294.31. Yield: 17.84 g, 99.8%(lit. 25%)[87]. Mp: > 230 °C (onset decomp.) ^{1}H NMR (CDCl$_3$): δ 7.55(m, 4H), 7.17(m, 4H), 5.43(s, 2H), 2.50(s, 2H). ^{13}C NMR (CDCl$_3$): δ 155.9, 138.9, 121.8, 115.3, 71.3. R_f = 0.12 (ethyl acetate/silica).

(*S*,*S*)-1,2-Bis(1-hydro-5,6-dimethylbenzimidazol-2-yl)-1′,2′-bis(hydroxy)ethane. (2g)

In a 250 mL round bottom flask containing 50 mL of 5N HCl, 4.00 g of *d*-tartaric acid

(26.7 mmol) and 7.26 g of 1,2-phenylene diamine (53.3 mmol) was added. The flask was

fitted with a condenser and the mixture was left to reflux for 72 hours with stirring. The

mixture was cooled and then made basic with conc. ammonium hydroxide to give a pale-

brown precipitate. The precipitate was collected by filtration and washed with water. The

precipitate was then dried in a vacuum oven to give a pale-brown powder. $C_{20}H_{22}N_4O_2$,

fw = 350.17. Yield: 8.92 g, 95.7%. Mp: 214 (soften) 239-240 °C (melt). ^{1}H NMR (400

MHz, $CD_3SO_2CD_3$, 24 °C): δ 7.21(s, 4H), 5.87(br s, 2H), 5.20(s, 2H), 3.31(br s, 2H),

2.47(s, 6H), 2.24(s, 6H).

(*meso*)-1,2-Dibromo-1,2-bis(1-hydrobenzimidazol-2-yl)ethane. (2h) A 2.335 g

quantity of *meso*-2,3-dibromosuccinic acid (8.464 mmol) was added to a 125 mL round

bottom flask containing 40 mL of 5N hydrochloric acid. This was followed by the

addition of 1.830 g 1,2-phenylene diamine (16.92 mmol). The mixture was heated to

reflux for 3 d with stirring. The mixture was cooled to RT and then the mixture was

neutralized to pH 8 with ammonium hydroxide to give a red-brown precipitate. The solid

was collected by filtration and repeatedly washed with water. The solid was dried to

constant weight using air at 50 °C for 24 h. $C_{16}H_{12}Br_2N_4$, fw = 420.10. Yield: 1.696 g,

47.8 %. Mp: 210 °C (soften) 268-270 °C (melt decomp.). ^{1}H NMR (400 MHz,

$CD_3SO_2CD_3$, 24 °C): δ 7.20(br m, 8H), 3.40(br s, 2H), 2.47(p, J = 2.0 Hz, 2H). R_f = 0.23

(ethyl acetate/silica).

3-(1-Hydrobenzimidazol-2-yl)pentane. (3a) In a 500 mL round bottom flask, 3.00 g of

diethylmalonic acid (18.7 mmol), 4.05 g 1,2-phenylene diamine (37.5 mmol), and 40 g

of polyphosphoric acid were added sequentially. The mixture was heated at 210 °C for 3 h with stirring. The mixture was cooled to 100 °C and then slowly made basic with ammonium hydroxide. The solid was collected by filtration and repeatedly washed with water. The solid was dried to constant weight using vacuum at 80 °C for 24 h. $C_{12}H_{16}N_2$, fw = 188.27. Yield: 3.10 g, 87.9%. Mp: 261 °C (dec.). ^{1}H NMR (400 MHz, $CD_3SO_2CD_3$, 50 °C): δ 7.46(dd, J = 3.2 Hz, J = 2.7 Hz, 2H), 7.10(dd, J = 3.2 Hz, J = 2.7 Hz, 2H), 2.71(m, 1H), 1.75(m,4H), 0.81(t, J = 7.4 Hz, 6H). ^{13}C NMR ($CD_3SO_2CD_3$, 50 °C): δ 158.0, 120.9, 114.3, 43.0, 26.6, 11.7. R_f = 0.67 (ethyl acetate/silica). EI MS: 188. IR (KBr pellet, cm^{-1}): 2957 s, 2928 s, 2872 s, 1539 m, 1445 s, 1429 s, 1333 m, 1272 s, 998 m, 750 s. Crystal structure **3a**(I)$_{534}$.[88b,A7]

3-(1-Methylbenzimidazol-2-yl)pentane. (3b) To a stirred mixture of 1.00 g of **3a** (5.31 mmol) and 20 mL of dry DMSO in a 125 mL round-bottom flask fitted with a side arm and maintained under a nitrogen atmosphere, 0.75 g of sodium hydride (95%) was added over 1 h, followed by dropwise addition of 350 μL of methyl iodide (5.62 mmol) over 1 h. The reaction mixture was stirred overnight, quenched with water, then added to 100 mL of water. After stirring for 0.5 h, a pale-yellow oil separated. The oil was extracted with 50 mL of cyclohexane. The cyclohexane was then extracted repeatedly with water. The cyclohexane was dried over sodium sulfate and filtered. The cyclohexane was removed by rotary evaporation followed by high vacuum to give the product as very pale-yellow oil. $C_{13}H_{18}N_2$, fw = 202.30. Yield: 1.03 g, 95.9%. ^{1}H NMR (400 Mhz, CDCl$_3$): δ 7.76(m, 1H), 7.29(m, 1H), 7.23(m, 2H), 3.72(s, 3H), 1.88(dm, J = 43 Hz, 4H), 0.86(t, J = 7.5 Hz, 6H). ^{13}C NMR (CDCl$_3$): δ 158.4, 142.7, 135.5, 121.7, 121.6, 119.6, 109.0, 40.6, 29.7, 27.5, 12.1. R_f = 0.70 (ethyl acetate/silica). IR (KBr

plate, cm^{-1}): 2961 s, 2931 m, 2873 w, 1502 w, 1463 s, 1456 m, 1317 m, 1284 m, 744 s.

2-Benzyl-1-hydrobenzimidazol-2-yl. (3c) In a 125 mL round bottom flask, 2.50 g of phenylmalonic acid (13.9 mmol), 3.01 g 1,2-phenylene diamine (27.8 mmol), and 25 mL of 5N hydrochloric acid were added sequentially. The mixture was refluxed for 3 d with stirring. The mixture was cooled to rt and then slowly made basic with ammonium hydroxide. The solid was collected by filtration and repeatedly washed with water. The solid was recrystallized from acetonitrile to give the product as colorless prisms. $C_{14}H_{12}N_2$, fw = 208.26. Yield: 2.64 g, 91.1%. Mp: 180 °C. R_f = 0.50 (ethyl acetate/silica). Crystal structure **3c**(I)$_{453}$.[88c,A8]

1,1′Bis(1-ethylbenzimidazol-2-yl)methane. (4a) A 750 mg quantity of **1a** (3.14 mmol) was placed in a 125 mL round bottom flask containing 40 mL of THF. Then 1.00 g of powdered NaOH was added. After stirring ca. 10 min. a clear solution was obtained. Then 503 μL of iodoethane (6.29 mmol) was added. A fine white precipitate began to form after stirring ca. 10 min. The reaction mixture was left stirring overnight. The solvent was then removed by rotary evaporation. The solid was extracted with 40 mL of water and 40 mL of ethyl acetate. The ethyl acetate layer was twice extracted with 40 mL of water. The ethyl acetate was dried over sodium sulfate, filtered, and the solvent was removed by rotary evaporation to give the product as a white solid. $C_{19}H_{20}N_4$, fw = 304.39. Yield: 902 mg, 94.3%. ^{1}H NMR (400 MHz, CDCl$_3$): δ 7.67(m, 2H), 7.22(m, 6H), 4.10(q, J = 7.3 Hz, 4H), 2.56(d, J = 4.6 Hz, 2H), 1.37(t, J = 7.3 Hz, 6H). ^{13}C NMR (CDCl$_3$): δ 151.4, 143.1, 135.1, 122.2, 122.0, 119.3, 109.3, 53.9, 41.3, 15.3. R_f = 0.34 (ethyl acetate/silica).

1,1′Bis(1-propylbenzimidazol-2-yl)methane. (4b) A 2.00 g quantity of **1a** (8.05 mmol) was placed in a 125 mL round bottom flask with a side arm. This was followed by the addition of 20 mL of dry dimethyl sulfoxide. The flask was fitted with a bubbler. Then under a flow of nitrogen. Then 2.5 g of sodium hydride (95%) was added over 0.5 h with stirring. During which the the reaction mixture went from dark red to dark purple and finally to dark green. The reaction mixture was allowed to stir and cool to rt. Then 1.57 mL of 1-iodopropane (16.1 mmol) was added drop-wise over a period of 5 minutes. The reaction mixture was allowed to stir overnight under nitrogen. The reaction mixture was then quenched with water and then was further diluted with 60 mL of water to form a fluffy light-brown precipitate. The precipitate was collected by filtration and washed repeatedly with water. The precipitate was dried under vacuum at 60 °C for 24 h to give the product as a pale-brown amorphous solid. $C_{21}H_{24}N_4$, fw = 332.44. Yield: 2.67 g, 99.8%. Mp: 105-107 °C. ^{1}H NMR (400 MHz, CDCl$_3$): δ 7.75(m, 2H), 7.27(m, 6H), 4.72(d, J = 9.6 Hz, 2H), 4.29(d, J = 7.6 Hz, 4H), 1.54(p, J = 7.4 Hz, 4H), 0.87(t, J = 7.4 Hz, 6H). ^{13}C NMR (CDCl$_3$): δ 149.3, 142.8, 135.8, 123.0, 122.5, 119.9, 110.2, 46.1, 29.6, 23.3, 11.5. R_f = 0.41 (ethyl acetate/silica). IR (KBr pellet, cm^{-1}): 2969 w, 2875 w, 1653 w, 1616 w, 1456 s, 1278 w, 1022 m, 952 w, 743 s, 434 w.

1,1′Bis(1-ethylbenzimidazol-2-yl)propane. (5a)[42] A 19.10 g quantity of **1a** (0.077 mol) was placed in a 500 mL round bottom flask with a side arm. This was followed by the addition of 30 mL of purified dimethyl sulfoxide. The flask was fitted with a bubbler. Then under a flow of nitrogen 7.0 g of sodium hydride (80% dispersion in mineral oil) was added over one hour with stirring. Then 18.50 mL of iodoethane (0.231 mol) was added dropwise over one hour. The reaction mixture was left stirring under nitrogen

overnight. The reaction mixture was quenched with water and then an additional 150 mL of water was added. After stirring for one half hour, a brown solid separated from the solution. The solid was collected by filtration and repeatedly washed with water. The solid was dried in a vacuum oven for 24 hours at 60 °C. The solid was dissolved in a sufficient amount of acetone to give a yellow-brown solution. Then enough cyclohexane was added to give a cloudy solution. The mixture was refluxed on a steam bath for 10 min. followed by immersion in an ice bath for 15 min. After which a dark sticky precipitate formed. The precipitate was removed by filtration. The filtrate was concentrated to dryness under reduced pressure to give a very pale-pink solid. $C_{21}H_{24}N_4$, fw = 332.44. Yield: 18.91 g, 74%. Mp: 178 °C (dec.). ^{1}H NMR (CDCl$_3$): δ 7.80(m, 2H), 7.26(m, 6H), 4.78(t, J = 7.9 Hz, 1H), 4.32(q, J = 7.3 Hz, 4H), 2.63(qt, J = 7.5 Hz, 2H), 1.12(t, J = 7.3 Hz, 3H), 0.96(t, J = 7.2 Hz, 6H). ^{13}C NMR (CDCl$_3$): δ 151.5, 142.5, 135.2, 122.7, 122.1, 119.6, 109.6, 42.4, 38.8, 24.9, 14.6, 12.7. R_f = 0.50 (ethyl acetate/silica). FD MS: 332.2. IR (KBr pellet, cm^{-1}): 3054 w, 2969 w, 2935 w, 2871 w, 1612 w, 1460 s, 1405 s, 1372 m, 1330 m, 1259 m, 1127 m, 964 m, 750 s, 421 w. Anal. Calcd for: N 16.85, H 7.28, C 75.87. Found: N 16.21, H 7.36, C 75.77.

1,1′Bis(1-propylbenzimidazol-2-yl)butane. (5b) A 2.00 g quantity of **1a** (8.06 mmol) was placed in a 125 mL round bottom flask with a side arm. This was followed by the addition of 20 mL of purified dimethyl sulfoxide. The flask was fitted with a bubbler. Then under a flow of nitrogen 1.5 g of sodium hydride (95%) was added over one hour with stirring. Then 2.44 mL of 1-iodopropane (25.0 mmol) was added drop wise over one hour. The reaction mixture was left stirring under nitrogen overnight. The reaction mixture was quenched with water and then an additional 150 mL of water was added.

After stirring for one half hour a brown oil seperated from the solution. The oil was extracted with 40 mL of ethyl acetate. The ethyl acetate was washed three times with 40 mL water. The ethyl acetate was dried over sodium sulfate and filtered. The solvent was removed by evaporation to give a pale-brown oil. Upon standing the oil deposited the product as colorless crystals which were collected on filter paper. $C_{24}H_{30}N_4$, fw = 374.52. Yield: 2.70 g, 89.5%. Mp: 99-100 °C (dec.). ^{1}H NMR (CDCl$_3$): δ 7.80(m, 2H), 7.26(m, 6H), 4.78(t, J = 7.9 Hz, 1H), 4.32(q, J = 7.3 Hz, 4H), 2.63(qt, J = 7.5 Hz, 2H), 1.12(t, J = 7.3 Hz, 3H), 0.96(t, J = 7.2 Hz, 6H). R_f = 0.61 (ethyl acetate/silica). Crystal structure **5b** (I)$_{373}$.[A9]

1,1′Bis(1-butylbenzimidazol-2-yl)pentane. (5c)[42] A 23.00 g quantity of **1a** (0.093 mol) was placed in a 300 mL round bottom flask with a side arm. This was followed by the addition of 25 mL of purified dimethyl sulfoxide. The flask was fitted with a bubbler. Then under a flow of nitrogen 6.0 g of sodium hydride (60% dispersion in mineral oil) was added over one hour with stirring. Then 25.00 mL of 1-iodobutane (0.220 mol) was added dropwise over one hour. The reaction mixture was left stirring under nitrogen for 48 hours. The reaction mixture was quenched with water and then an additional 400 mL of water was added. After stirring for one half hour a biphasic solution was obtained. The organic layer was extracted with cyclohexane and was washed with water. The volatiles were removed under reduced pressure to leave a dark oil. The oil was chromatographed on silica gel with methylene chloride as the eluent. The solvent was removed under reduced pressure to give a very pale-pink oil which crystallized upon standing. Suitable single crystals were obtained by slow evaporation of a methylene chloride solution of the title compound. $C_{27}H_{36}N_4$, fw = 416.60. Yield: 20.44 g, 67%. Mp: 82-83 °C. ^{1}H NMR

(CDCl$_3$); δ 7.79(m, 2H), 7.24(m, 6H), 4.88(t, J = 7.9 Hz, 1H), 4.16(d sp, J = 5.0 Hz, J = 40.9 Hz, 4H), 2.59(m, 2H), 1.44(m, 4H), 1.16(m, 4H), 1.10(m, 2H), 0.99(m, 2H), 0.89(t, J = 6.8 Hz, 3H), 0.61(t, J = 7.0 Hz, 6H). ^{13}C NMR (CDCl$_3$): δ 151.8, 142.4, 135.6, 122.6, 122.0, 119.6, 109.7, 44.0, 40.9, 31.5, 31.2, 30.1, 22.5, 20.0, 14.0, 13.4. R_f = 0.73 (ethyl acetate/silica). FD MS: 416.1. IR (KBr pellet, cm^{-1}): 3050 m, 2955 m, 2931 m, 2862 m, 1613 w, 1501 m, 1458 s, 1400 s, 1331 m, 1285 m, 1008 m, 933 m, 743 s, 434 w. Crystal structure (I)$_{356}$.[42,A10]

3,3′Bis(1-ethylbenzimidazol-2yl)pentane. (6a) A 2.00 g quantity of **1a** (8.06 mmol) was placed in a 125 mL round bottom flask with a side arm. This was followed by the addition of 25 mL of purified dimethyl sulfoxide. The flask was fitted with a bubbler. Then under a flow of nitrogen 2.5 g of sodium hydride (95%) was added over 1.5 hour with stirring. Then 2.64 mL of iodoethane (33.0 mmol) was added dropwise over one hour. The reaction mixture was left stirring under nitrogen overnight. The reaction mixture was quenched with water and then an additional 150 mL of water was added. After stirring for one half hour, a brown oil separated from solution. The oil was extracted with 50 mL of ethyl acetate and repeatedly washed with water. The ethyl acetate was dried over sodium sulfate and filtered. The solvent was removed by evaporation to give the product as a pale-brown oil. C$_{23}$H$_{28}$N$_4$, fw = 360.50. Yield: 2.42 g, 83.2%. Mp: (oil). ^{1}H NMR (400 MHz, CDCl$_3$): δ 7.87(m, 2H), 7.26(m, 6H), 3.80(br s, 4H), 2.81(br s, 4H), 0.97(t, J = 7.2 Hz, 6H), 0.74(t, J = 7.5 Hz, 6H). ^{13}C NMR (CDCl$_3$): δ 153.9, 141.0, 134.5, 121.6, 121.0, 118.9, 108.8, 45.5, 38.0, 25.7, 12.9, 6.7. R_f = 0.70 (ethyl acetate/silica).

3,3′Bis(1-ethylbenzimidazol-2yl)undecane. (6b) A 2.00 g quantity of **5a** (6.02 mmol) was placed in a 125 mL round bottom flask with a side arm. This was followed by the addition of 25 mL of purified dimethyl sulfoxide. The flask was fitted with a bubbler. Then under a flow of nitrogen 1.5 g of sodium hydride (95%) was added over 1.5 hour with stirring. Then 1.14 mL of 1-iodooctane (6.32 mmol) was added dropwise over one hour. The reaction mixture was left stirring under nitrogen overnight. The reaction mixture was quenched with water and then an additional 150 mL of water was added. After stirring for one half hour, a brown oil separated from solution. The oil was extracted with 50 mL of ethyl acetate and repeatedly washed with water. The ethyl acetate was dried over sodium sulfate and filtered. The solvent was removed by evaporation to give the product as a pale-brown oil. $C_{29}H_{40}N_4$, fw = 444.66. Yield: 2.15 g, 80.2%. Mp: (oil). ^{1}H NMR (400 MHz, CDCl$_3$): δ 7.79(d, J = 6.9 Hz, 2H), 7.19(m, 6H), 3.73(br m, 4H), 2.73(br s, 2H), 2.48(br s, 2H), 1.11(br m, 12H), 0.89(t, J = 6.4 Hz, 6H), 0.75(t, J = 6.6 Hz, 3H), 0.66(t, J = 7.4 Hz, 3H). ^{13}C NMR (CDCl$_3$): δ 154.0, 140.9, 134.6, 121.7, 121.0, 118.9, 108.8, 45.2, 38.0, 32.6, 30.8, 28.8, 28.5, 28.2, 26.4, 22.3, 21.6, 13.1, 13.0, 6.8. R_f = 0.84 (ethyl acetate/silica).

1,1′-Bis(1-methylbenzimidazol-2-yl)-1″-(methoxy)ethane. (7)[40,42] A 1.00 g quantity of **2a** (3.42 mmol) was added to 35 mL of purified tetrahydrofuran. The solution was then cooled to -77 °C and 2.87 mL of 2.5 M n-butyl lithium (hexanes) (7.18 mmol) was slowly added to the solution and was stirred for 1.5 h. Then 447 μL quantity of iodomethane (7.18 mmol) was added dropwise and allowed to stir for 1.5 h and then allowed to warm to rt while stirring overnight. The reaction mixture was quenched with saturated aqueous sodium sulfate solution. Tetrahydrofuran was then removed by rotory-

evaporation. The remaining solid was washed with water and separated with methylene chloride. The product was recrystallized from a mixture of 2-propanol and cyclohexane to give a colorless solid. Suitable single crystals were obtained by slow evaporation of an acetone solution of the title compound. $C_{19}H_{20}N_4O$, fw = 320.39. Yield: 1.03 g, 94.0%. Mp: 194-195 °C. ^{1}H NMR (CDCl$_3$): δ 7.81 (m, 2H), 7.31(m, 6H), 3.67(s, 6H), 3.27(s, 3H), 2.29(s, 3H). Crystal structure (I)$_{468}$.[42,A11]

***trans*-1,2-Bis(1-methylbenzimidazol-2-yl)cyclohexane. (8a)** A 1.50 g quantity of **1d** (4.74 mmol) was placed in a 125 mL round bottom flask with a side arm. This was followed by the addition of 25 mL of purified dimethyl sulfoxide. The flask was fitted with a bubbler. Then under a flow of nitrogen 1.0 g of sodium hydride (95%) was added over 1.5 hour with stirring. Then 620 μL of iodomethane (9.95 mmol) was added dropwise over 0.5 hour. The reaction mixture was left stirring under nitrogen overnight. The reaction mixture was quenched with water and then an additional 150 mL of water was added. After stirring for one half hour, a brown solid separated from solution. The solid was collected by filtration and repeatedly washed with water. The product was air dried to give a pale-brown solid. Crystals were obtained by a slow evaporation of the product from acetone. $C_{22}H_{24}N_4$, fw = 344.45. Yield: 1.55 g, 95.2%. Mp: (precipitate) 222-223 °C; (from acetone) 206 °C(soften) 218 °C(melt). ^{1}H NMR (CDCl$_3$): δ 7.66(m, 0.5H), 7.62(m, 1H), 7.26(s, 0.5H), 7.19(m, 3H), 7.13(m, 3H), 3.73(m, 2H), 3.59(s, 4H), 3.20(s, 2H), 2.50(dm, *J* = 37.6 Hz, 1H), 2.08(m, 2H), 1.99(m, 3H), 1.63(m, 2H). ^{13}C NMR (CDCl$_3$): (chair) δ 158.0, 142.3, 135.2, 121.8, 121.6, 118.8, 109.3, 39.9, 32.7, 29.5, 25.6; (boat) δ 155.7, 142.3, 135.7, 122.1, 121.8, 119.5, 108.9, 39.2, 32.7, 28.0, 24.1. *R$_f$* =

0.45 (ethyl acetate/silica). IR (KBr pellet, cm^{-1}): 3384 m, 3051 w, 2929 s, 2853 m, 1614 w, 1468 s, 1443 s, 1329 m, 1008 w, 745 s. Crystal structure **8a** · $H_2O(I)$.[89,A12]

trans-1,2-Bis(1-propylbenzimidazol-2-yl)cyclohexane. (8b) A 1.00 g quantity of **1d** (3.16 mmol) was placed in a 125 mL round bottom flask with a side arm. This was followed by the addition of 25 mL of purified dimethyl sulfoxide. The flask was fitted with a bubbler. Then under a flow of nitrogen 900 mg of sodium hydride (95%) was added over 1.5 hour with stirring. Then 628 μL of 1-iodopropane (6.55 mmol) was added dropwise over one hour. The reaction mixture was left stirring under nitrogen overnight. The reaction mixture was quenched with water and then an additional 150 mL of water was added. After stirring for one half hour, a brown oil separated from solution. The oil was extracted with 50 mL of ethyl acetate and repeatedly washed with water. The ethyl acetate was dried over sodium sulfate and filtered. The solvent was removed by evaporation to give the product as a brown tacky solid. $C_{26}H_{32}N_4$, fw = 400.57. Yield: 1.18 g, 93.1%. ^{1}H NMR (400 MHz, CDCl$_3$): δ 7.62(m, 2H), 7.10(m, 6H), 4.23(p, J = 8.1 Hz, 1H), 3.73(mm, 3H), 2.58(s, 2H), 1.99(m, 6H), 1.71(m, 6H), 0.89(t, J = 7.4 Hz, 3H), 0.76(t, J = 7.4 Hz, 3H). ^{13}C NMR (CDCl$_3$): δ 157.8, 142.5, 134.7, 121.6, 121.5, 1118.7, 109.6, 44.7, 41.0, 33.2, 25.6, 23.3, 11.4. R_f = 0.71 (ethyl acetate/silica).

rac-2,2′-Bis[2-(1-ethylbenzimidazol-2-yl)]biphenyl · water. (9a)[42] A 12.09 g quantity of **1e** (0.031 mol) was placed in a 250 mL round bottom flask with a side arm. This was followed by the addition of 100 mL of DMSO. The flask was fitted with a bubbler. Then under a flow of nitrogen 6.0 g of sodium hydride (80% dispersion in mineral oil) was added over one hour with stirring. Then 5.20 mL of iodoethane (0.065 mol) was added drop wise over one hour. The reaction mixture was left stirring under nitrogen overnight.

The reaction mixture was quenched with water and then an additional 400 mL of water was added. After stirring for one half hour a pale-pink solid separated from the solution. The solid was collected by filtration and repeatedly washed with water. The solid was dried in a vacuum oven for 24 hours at 60 °C. The solid was dissolved in 35 mL of methylene chloride to give a dark solution. Then 150 mL of pentane was added to give a cloudy solution. The mixture was placed in an ice bath for 30 min. After which a dark sticky precipitate formed. The cloudy solute was decanted and the solvent was removed under reduced pressure to give a white crystalline solid. $C_{30}H_{28}N_4O$, fw = 460.57. Yield: 13.12 g, 92%. Mp: 166 (soften) 172 °C (melt). ^{1}H NMR (CDCl$_3$): δ 7.60(d, J = 7.0 Hz, 2H), 7.41(d, J = 6.5 Hz, 2H), 7.30(m, 6H), 7.23(m, 6H), 3.67(brd s, 4H), 1.19(t, J = 7.0 Hz, 6H). ^{13}C NMR (CDCl$_3$): δ 152.5, 143.4, 141.1, 134.5, 131.5, 130.7, 130.0, 129.4, 127.1, 122.2, 121.8, 120.0, 110.0, 38.9, 14.8. R_f = 0.62 (ethyl acetate/silica). FD MS: 442.0 (less H$_2$0). IR (KBr pellet, cm^{-1}): 3378 m (H$_2$O), 3062 m, 2968 m, 2931 m, 2871 m, 1643 s, 1447 s, 1329 s, 1276 s, 1128 m, 743 s, 476 w. Anal. Calcd for: N 12.16, H 6.13, C 78.23. Found: N 11.91, H 6.14, C 79.16. Crystal structure **9a** (I)$_{449}$.[90,A13] Crystal structure **9a·H·[ClO4]** (I).[91,A14]

***rac*-2,2′-Bis[2-(1-propylbenzimidazol-2-yl)]biphenyl. (9b)**[12a] To a stirred mixture of 4.65 g of **1e** (12.0 mmol) and 40 mL of dry DMSO in a 150 mL round-bottom flask fitted with a side arm and maintained under a nitrogen atmosphere, 0.86 g of sodium hydride (95 %) was added over 1 h, followed by drop wise addition of 2.35 mL of n-iodopropane (24.1 mmol) over one h. The reaction mixture was stirred overnight, quenched with water, then added to 400 mL of water. After stirring for ½ h, the pale-pink precipitate was collected by filtration, washed repeatedly with water, and dried in a vacuum oven for 24

h at 60 °C. The crude product was dissolved in 100 mL of ethanol containing 5 g of activated charcoal, refluxed for 15 min., filtered hot, and recovered. Rotary evaporation of the solvent, followed by drying under high vacuum gave a pale-orange amorphous solid. Crystals suitable for X-ray diffraction were obtained by slow evaporation of a solution of **9b** in a mixture of ethanol and triethylorthoformate. $C_{32}H_{30}N_4$, fw = 470.61. Yield: 5.32 g, 92%. Mp: 149 °C (melt). ^{1}H NMR (CD$_3$SO$_2$CD$_3$): δ 7.51(m, 6H), 7.36(t, J = 7.5 Hz, 2H), 7.20(m, 6H), 7.02(d, J = 7.7 Hz, 2H), 3.42(brd m, 4H), 1.65(br m,4H), 0.83(t, J = 7.3 Hz, 6H). ^{13}C NMR (CDCl$_3$): δ 152.7, 143.1, 140.8, 134.8, 131.2, 131.0, 129.5, 127.2, 122.3, 121.8, 119.8, 110.1, 45.8, 22.9, 11.3. R_f = 0.66 (ethyl acetate/silica). IR (KBr pellet, cm^{-1}): 3062 m, 2968 m, 2931 m, 2871 m, 1643 s, 1447 s, 1329 s, 1276 s, 1128 m, 743 s, 476 w. Anal. Calcd for: N 11.91, H 6.42, C 81.67. Found: N 11.97, H 6.21, C 80.83. Crystal structure (I)$_{422}$.[12a,A15]

κ^2*N^{13}*,*N$^{13'}$* Hydro- rac-2,2'-bis [2-(1-propylbenzimidazol-2yl)] biphenyl trifluoromethylsulfonate. (9b-1)[92] The salt **9b-1** was obtained by the addition of an equimolar amount of a 2.57 M solution of triflic acid in methanol to an acetonitrile solution of **9b**. Crystals were obtained by slow vapor diffusion of diethylether. $C_{33}H_{31}F_3N_4O_3S$, fw = 620.69. ^{1}H NMR (400 MHz, CDCl$_3$): δ 16.03(br s, 1H), 7.67(d, J=7.5 Hz, 2H), 7.48(m, 12H), 7.21(d, J=6.0 Hz, 2H), 4.40(m, 4H), 1.90(m, 4H), 0.97(t, J=7.2 Hz, 6H). ^{13}C NMR (400 MHz, CDCl$_3$): δ 150.6 140.3, 135.1, 133.1, 131.6, 130.4, 130.3, 129.3,125.4, 125.3, 125.0, 116.5, 112.3, 46.9, 23.2, 11.3. ^{19}F NMR (400 MHz, CDCl$_3$) δ: -78.6. Crystal structure **9b-1**(I).[92,A16] Crystal structure **9b·H[PF$_6$]**(I).[93,A17]

***N^{13}*,*N$^{43'}$*-Dihydro-[*rac*-2,2′-bis(2-(1-propylbenzimidazol-1-ium))biphenyl] di(perchlorate). (9b-2)**[94] The salt **9b-2** was obtained by the addition of two molar

equivalents of of a 2.50 M solution of perchloric acid in methanol to an acetonitrile solution of **9b**. Crystals were obtained by slow evaporation. $C_{32}H_{32}Cl_2N_4O_8$, fw = 671.52. Crystal structure **9b-2**(I).[94,A18]

***rac*-2,2′-Bis[2-(1-octylbenzimidazol-2-yl)]biphenyl. (9c)**[42] In an argon glovebox, a 16.19 g quantity of **1e** (0.042 mol) was placed in a 300 mL round bottom flask. A suspension was obtained after the addition of 60 mL of purified tetrahydrofuran. Then 3.2 g of sodium hydride powder was added over a half-hour period with stirring. After cooling 14.75 mL of 1-iodooctane (0.082 mol) was added dropwise over a half-hour period. After an hour a gray-white precipitate began to form. The mixture was allowed to stir an additional 12 hours. The reaction mixture was removed from the glove box and slowly quenched with water under nitrogen. The reaction mixture was extracted from water with methylene chloride. The methylene chloride was then dried over sodium sulfate and filtered. The methylene chloride was removed under high vacuum to give a pale-brown oil. $C_{42}H_{50}N_4$, fw = 610.87. Yield: 24.03 g, 95%. Mp: (oil) ^{1}H NMR (CDCl$_3$): δ 7.58(m, 2H), 7.41(m, 2H), 7.31(m, 4H), 7.23(m, 8H), 3.54(br s, 4H), 1.64(br s, 4H), 1.19(br m, 20 H), 0.86(t, J = 6.9 Hz, 6H). ^{13}C NMR (CDCl$_3$): δ 151.6, 142.3, 140.0, 133.7, 130.4, 129.7, 128.5, 128.4, 126.0, 121.1, 120.7, 118.9, 109.0, 43.1, 30.7, 28.4, 28.1, 27.9, 25.6, 21.6, 13.1. R_f = 0.77 (ethyl acetate/silica). CI MS (M+1): 611.3. IR (film on KBr plates, cm^{-1}): 3060 w, 2954 m. 2928 s, 2855 m, 1613 w, 1453 s, 1392 m, 1282 m, 1159 m, 744 s. Anal. Calcd for: N 9.17, H 8.25, C 82.58. Found: N 9.07, H 8.25, C 82.11.

***rac*-2,2′-Bis[2-(1-(2-ethylhexylbenzimidazol-2-yl))]biphenyl. (9d)** A 2.00 g quantity of **1e** (5.18 mmol) was placed in a 250 mL round bottom flask with a side arm. This was followed by the addition of 25 mL of anhydrous THF. The flask was fitted with a

bubbler. Then under a flow of nitrogen 1.50 g of sodium hydride (95%) was added over 1.5 hour with stirring. Then 1.89 mL of 1-bromo-2-ethylhexane (10.61 mmol) was added dropwise over one hour. The reaction mixture was left stirring under nitrogen overnight. The reaction mixture was quenched with saturated sodium sulfate water. The solvent was then removed by evaporation. Then 150 mL of water and 30 mL of ethyl acetate was added. After stirring for one half hour, the ethyl acetate was separated dried over sodium sulfate and filtered. The solvent was then removed under high vacuum to give a light brown oil separated. $C_{42}H_{50}N_4$, fw = 610.87. Yield: 2.96 g, 93.4%. Mp: (oil) ^1H NMR (CDCl$_3$): δ 7.64(br m, 4H), 7.24(br m, 12H), 4.03(br s, 4H), 1.88(br m, 2H), 1.19(br m, 14H), 0.78(br m, 14H). ^{13}C NMR (CDCl$_3$): δ 153.6, 143.4, 140.5, 135.5, 131.5, 130.0, 127.6, 122.4, 121.9, 121.6, 119.9, 111.8, 110.3, 47.7, 39.1, 30.3, 28.3, 23.5, 22.9, 14.0, 10.4. R_f = 0.80 (ethyl acetate/silica).

***rac*-2,2′-Bis[2-(1-benzylbenzimidazol-2-yl)]biphenyl. (9e)** To a stirred mixture of 2.30 g of **1e** (5.95 mmol) and 1.40 mL of benzyl chloride (12.2 mmol) in 25 mL of non-purified DMSO in a 125 mL Erlenmeyer flask, 5.0 g of powdered potassium hydroxide was added. The reaction mixture was left to stir overnight. Then 70 mL of water was added to the reaction mixture and this was extracted with 150 mL of methylene chloride. The methylene chloride layer was then extracted three times with 150 mL of water. The methylene chloride layer was dried over sodium sulfate, filtered, and the solvent was removed by rotary evaporation to give the product as a pale-brown solid. $C_{40}H_{30}N_4$, fw = 566.69.Yield: 2.73 g, 81.0%. Mp: 199 °C (soften) 219 °C (melt); 234 °C (recryst. acetone). ^1H NMR (400 MHz, CDCl$_3$): δ 7.59(br s, 2H), 7.27(m, 24H), 2.52(s, 4H). NMR (CDCl$_3$): δ 153.4, 143.6, 142.0, 137.1, 135.5, 132.6, 130.4, 129.5, 129.1, 128.9, 127.8,

127.4, 127.0, 126.3, 123.1, 123.0, 122.6, 120.5, 110.9, 47.7. R_f = 0.73 (ethyl acetate/silica). Crystal structure **9e**·HBr·HSO$_3$CF$_3$, (I).[95,A19]

rac-2,2′-Bis[2-(1-(4-bromobenzyl)benzimidazol-2-yl)]biphenyl. (9f) To a stirred mixture of 3.00 g of **1e** (7.76 mmol) and 3.88 g of 4-bromobenzyl bromide (15.5 mmol) in 25 mL of DMF in a 125 mL Erlenmeyer flask, 4.0 g of powdered potassium hydroxide was added. The reaction mixture was left to stir overnight. Then 70 mL of water was added to the reaction mixture and this was extracted with 150 mL of methylene chloride. The methylene chloride layer was then extracted three times with 150 mL of water. The methylene chloride layer was dried over sodium sulfate, filtered, and the solvent was removed by rotary evaporation to give the product as a pale-pink solid. C$_{40}$H$_{29}$BrN$_4$, fw = 645.59. Yield: 4.61g, 92.1%. Mp: 99 °C(soften) 281 °C (melt). ^{1}H NMR (400 MHz, CDCl$_3$): δ 7.61(br s, 2H), 7.29(m, 18H), 6.66(d, J = 6.5 Hz, 4H), 2.56(s, 4H). R_f = 0.40 (ethyl acetate/silica).

rac-2,2′-Bis[2-(1-(1-prpoyl(3,3-diphenyl)benzimidazol-2-yl))]biphenyl. (9g) In a 50 mL Erlenmeyer flask containing 15 mL of DMF 400 mg of **1e** (1.04 mmol) was added. This was followed by the addition of 1.0 g of powdered NaOH. After stirring for 5 min. 572 mg of 1-bromo-3,3′-diphenylpropane (2.08 mmol) was added to the flask. The mixture was left to stir for 72 hours. Then the reaction mixture was added to 70 mL of water and this was extracted with 70 mL of ethyl acetate. The ethyl acetate layer was then extracted three times with 150 mL of water. The ethyl acetate layer was separated and dried over sodium sulfate, filtered, and the solvent was removed by rotary evaporation to give a pale-pink-brown solid. The solid contained a mixture mono- and di-alkylated product. The mixture was column chromatographed over silica with ethyl acetate to give

the desired product as a pale-brown amorphous tacky solid. $C_{56}H_{46}N_4$, fw = 774.99.

Yield: 422 mg, 52.6%. ^{1}H NMR (400 MHz, CDCl$_3$): δ 7.18(m, 36H), 4.04(m, 6H),

2.13(m, 4H). R_f = 0.74 (ethyl acetate/silica).

rac-2,2′-Bis[2-(1-propyl-5,6-dimethylbenzimidazol-2-yl)]bipehenyl (10) In a 125 mL

round bottom flask with a side-arm containing 25 mL of dry DMSO, 1.00 g of **1f** (2.26

mmol) was added. This was followed by the slow addition of 1.0 g of (95%) NaH under a

flow of dinitrogen. After stiiring for 1/2 hour, 450 μL g of 1-iodopropane (4.70 mmol)

was added to the flask. The mixture was left to stir overnight. Then 70 mL of water was

added to the reaction mixture and this was extracted with 150 mL of methylene chloride.

The methylene chloride layer was then extracted three times with 150 mL of water. The

methylene chloride layer was dried over sodium sulfate, filtered, and the solvent was

removed by rotary evaporation to give a pale-brown solid. $C_{36}H_{38}N_4$, fw = 492.08. Yield:

1.10 g, 98.9%. Mp: 130 °C (soften) 171 °C (melt). ^{1}H NMR (CD$_3$Cl$_3$): δ 7.44(m, 2H),

7.29(m, 3H), 7.23(m, 3H), 7.12(m, 2H), 7.03(s, 2H), 3.66(m,4H), 2.39(s, 6H), 2.35(s,

6H), 1.26(m, 4H), 0.83(m, 6H). ^{13}C NMR (CDCl$_3$): δ 152.0, 141.9, 140.7, 133.4, 131.2,

131.0, 130.5, 129.9, 129.2, 127.7, 127.0, 119.9, 110.3, 41.0, 22.9, 20.6, 20.2, 11.3. R_f =

0.65 (ethyl acetate/silica). Crystal structure **10**·2[H(CF$_3$SO$_3$)]·H$_2$O(I).[96,A20]

(E)-1,2-Bis(1-methylbenzimidazol-2-yl)ethene. (11a)[94a] A 1.50 g quantity of **2b** (5.39

mmol) was placed in a 125 mL round bottom flask with a side arm containing 25 mL of

dry dimethyl sulfoxide. The flask was fitted with a bubbler and placed under a flow of

nitrogen. Then 1.0 g of sodium hydride (95%) was added over one hour with stirring.

After cooling to rt 705 μL of iodomethane (11.3 mmol) was added dropwise over one

hour. The reaction mixture was left stirring under nitrogen overnight. The reaction

mixture was quenched with water and then added to 250 mL of water. The mixture was extracted with 400 mL of methylene chloride. The methylene chloride was dried over sodium sulfate and filtered. The solvent was removed by rotory evaporation to give a red-brown solid that was then followed by high vacuum for 2 h at 70 °C to give 1.60 g of crude product. The solid was chromatographed over silica with 20 v/v% ethanol/cyclohexane to give 3 bands. The third yellow band was collcted and the solvent was removed by rotary evaporation to give the product as a yellow solid. Crystals of the title compound were obtained by slow evaporation of a solution of 1:1 v/v mixture of acetone and 2-propanol. Crystals of the title compound were obtained by slow evaporation of a solution of 1:1 v/v mixture of ethanol and triethylorthoformate. $C_{18}H_{16}N_4$, fw = 288.35. Yield: 1.09 g, 70%. Mp: 301 °C (melt). ^{1}H NMR (CDCl$_3$): δ 8.04 (s, 2H), 7.81(m, 2H), 7.33(m, 6H), 3.97(s, 6H). ^{13}C NMR (CDCl$_3$): δ 149.1, 143.4, 135.2, 123.2, 123.0, 120.6, 119.6, 29.8. R_f = 0.20 (ethyl acetate/silica). Crystal structure **11a(I)$_{574}$.**[94a,A21]

(Z)-1,2-Bis(1-methylbenzimidazol-2-yl)ethene. (11b) **11b** was obtained by chromatography on silica from the crude product mixture of **11a** as the second band upon removal of the solvent gave a yellow-green solid. $C_{18}H_{16}N_4$, fw = 288.35. Yield: 389 mg, 25%. Mp: 293-294 °C (melt). ^{1}H NMR (400 Mhz, CDCl$_3$): δ 7.92 (s, 2H), 7.71(m, 2H), 7.24(m, 6H), 3.85(s, 6H). ^{13}C NMR (400 MHz, CDCl$_3$): δ 150.3, 143.7, 136.7, 123.6, 123.4, 121.0, 120.0, 109.8, 30.2. R_f = 0.51 (ethyl acetate/silica).

(E)-1,2-Bis(1-ethylbenzimidazol-2-yl)ethene. (11c)[94a] A 2.00 g quantity of **2d** (6.79 mmol) was placed in a 125 mL round bottom flask with a side arm containing 25 mL of dry dimethyl sulfoxide. The flask was fitted with a bubbler and placed under a flow of

nitrogen. Then 1.0 g of sodium hydride (95%) was added over one hour with stirring. After cooling to rt 1.10 mL of iodoethane (13.6 mmol) was added dropwise over one hour. The reaction mixture was left stirring under nitrogen overnight. The reaction mixture was quenched with water and then added to 250 mL of water. The mixture was extracted with 400 mL of methylene chloride. The methylene chloride was dried over sodium sulfate and filtered. The solvent was removed by rotory evaporation to give an amorphous brown solid followed by high vacuum for 2 h at 70 °C to give 1.95 g of crude product. The solid was chromatographed over silica with 20 v/v% ethanol/cyclohexane to give 3 bands. The third yellow band was collcted and the solvent was removed by rotary evaporation to give the product as a yellow solid. Crystals of the title compound were obtained by slow evaporation of a solution of 1:1 v/v mixture of acetone and 2-propanol. $C_{20}H_{20}N_4$, fw = 316.40. Yield: 1.74 g, 81.0%. Mp: 231 °C (melt). ^{1}H NMR (400 MHz, CDCl$_3$): δ 8.01(s, 2H), 7.83(m, 2H), 7.33(m, 6H), 4.44(q, J = 7.3 Hz, 4H), 1.52(t, J = 7.3 Hz, 6H). ^{13}C NMR (CDCl$_3$): δ 149.1, 143.4, 135.2, 123.2, 123.0, 120.6, 119.7, 109.6, 38.4, 15.8 R_f = 0.54 (ethyl acetate/silica). Crystal structure **11c** (I)$_{504}$.[97a,A22], Crystal structure **11c · 2 H$_2$O** (I).[97b]

3-Ethyl-2-[(E)-2-(1-ethylbenzimidazol-2-yl)-ethenyl]benzimidazol-1-ium

perchlorate. (11c-1)[97a] Crystals of the **11c-1** were obtained by addition of perchloric acid (1 molar equivalent) to a solution of 100 mg (0.32 mmol) of **11c** in a mixture of ethanol and triethylorthoformate. Slow evaporation of the solution precipitated bright yellow blocks overnight. $C_{20}H_{21}ClN_4O_4$, fw = 416.86. Yield: 110 mg, 82.5%.^{1}H NMR (400 MHz, CD$_3$CN, 50 °C): δ [**11c**] 4.51(q, J = 7.2 Hz, 4H), [**11c-1**] 3.47(q, J = 7.0 Hz, 4H), [**11c**] 1.56(t, J = 7.2 Hz, 6H) [**11c-1**] 1.19(t, J = 7.0 Hz, 6H). K_{eq} = [**11c**]/[**11c-**

1][ClO4⁻] = 26.9. Mp: 265 °C (soften) 276 °C (melt). IR (KBr pellet, cm⁻¹): 1641 s, 1385 m, 1122 s, 1108 sh, 1059 m, 746 m. Crystal structure 7c (I).[97,A23]

(*Z*)-1,2-Bis(1-ethylbenzimidazol-2-yl)ethene. (11d) The second pink band from **11c** was collected and the solvent was removed by rotary evaporation to give the product as a orange solid. $C_{20}H_{20}N_4$, fw = 316.40. Yield: 0.31 g, 14%. ^{1}H NMR (400 MHz, CDCl$_3$): δ 7.90(s, 2H), 7.73(m, 2H), 7.30(m, 2H), 7.22(m, 4H), 4.32(q, *J* = 7.2 Hz, 4H), 1.40(t, *J* = 7.2 Hz, 6H). ^{13}C NMR (CDCl$_3$): δ 149.4, 143.7, 135.5, 123.6, 123.4, 120.9, 120.0, 110.1, 38.7, 16.1 R_f = 0.60 (ethyl acetate/silica).

(*E*)-1,2-Bis(1-methylbenzimidazol-2-yl)ethenol. (12) A 1.00 g (3.40 mmol) quantity of **2f** was placed in a 125 mL round bottom flask with a side arm containing 20 mL of dry dimethyl sulfoxide. The flask was fitted with a bubbler and placed under a flow of nitrogen. Then 1.0 g of sodium hydride (95%) was added over one hour with stirring. After cooling to rt 846 μL (13.6 mmol) of iodomethane was added drop wise over one hour. The reaction mixture was left stirring under nitrogen overnight. The reaction mixture was quenched with water and then added to 250 mL of water to give a brown precipitate. The preciptate was collected by filtration and was dried in air. The solid was chromatographed over silica with 20 v/v% ethanol/cyclohexane to give a yellow-green solution. The solvent was removed by rotary evaporation to give the product as a yellow-green solid. Crystals of the title compound were obtained by slow evaporation of a solution of 1:1 v/v mixture of ethanol and 2-propanol. $C_{18}H_{16}N_4O$, fw = 304.35. Yield: 940 mg, 90.9%. Mp: 231 °C (melt). ^{1}H NMR (400 MHz, CD$_3$SOCD$_3$): δ 10.09(s, 1H), 7.69(m, 4H), 7.27(m, 4H), 5.61(s, 1H), 4.18(3, 3H), 3.92(s, 3H). ^{13}C NMR (CDCl$_3$): δ

154.4, 151.5, 137.3, 129.6, 124.1, 124.1, 120.9, 114.5, 111.4, 69.8, 31.8. R_f = 0.38 (ethyl acetate/silica). Crystal structure **12** · 1.5 H_2O (I).[98,A24]

(*S*,*S*)-1,2-Bis(1-methylbenzimidazol-2-yl)-1,2-ethanediol. (13) In a 125 mL Erlenmeyer 3.00 g (10.2 mmol) of **2e** was added to 40 mL of DMF containing 1 mL of water. Then 2.0 g of powdered NaOH was added to the reaction mixture. Then 1.27 mL (20.4 mmol) of methyl iodide was added to the solution drop wise over 0.5 h. The flask was sealed and left to stir for 1 d at rt. The reaction mixture was then added to 200 mL of water to give the product as a pale-brown precipitate which was collected by filtration and washed with water. The solid was then dried in a vacuum oven at 60 °C overnight to give the product as a pale-brown solid. $C_{18}H_{18}N_4O_2$, fw = 322.36. Yield: 2.95 g, 89.7%. Mp: 225 °C(decomp). ^{1}H NMR (400 MHz, $CD_3SO_2CD_3$, 25 °C): δ 7.47(m, 4H), 7.15(dt, *J* = 32.2 Hz, *J* = 8.0 Hz, 4H), 5.53(s, 2H), 3.94(s, 6H), 2.50(m, 2H). ^{13}C NMR ($CD_3SO_2CD_3$, 25 °C): δ 154.6, 142.0, 136.0, 122.3, 121.7, 119.2, 110.2, 68.1, 30.3). R_f = 0.28 (ethyl acetate/silica).

(*S*,*S*)-4,5-Bis(1-methylbenzimidazol-2-yl)(2,2,7,7-tetramethyl-3,6-dioxa-2,7-disilaoctane). (14) In a 125 mL round bottom flask 850 mg of (*S*,*S*)-1,2-bis(1-methylbenzimidazol-2-yl)-1′,2′-dihydroxyethane (2.64 mmol) was added to 40 mL of THF. Then 575 mg of trimethylsilylchloride and 425 mg of pyridine was added to the solution. The flask was sealed and left to stir for 1 d at rt. The solvent was then removed from the reaction mixture by rotary evaporation. The solid was then extracted with hexanes. The hexane mixture was then extracted 3 times with 100 mL of sodium bicarbonate/water. The hexane was dried over sodium sulfate and filtered. The solvent

was then rotory evaporated to give the product as a pale yellow solid. $C_{24}H_{34}N_4O_2Si_2$, fw = 466.72. Yield: 410 mg, 33.3%. Mp: 237-239 °C(decomp). ^{1}H NMR (400 Mhz, CDCl$_3$, 50 °C): δ 7.64(m, 2H), 7.23(m, 6H), 5.63(s, 2H), 3.92(s, 6H), 0.00(s, 18H). ^{13}C NMR (CDCl$_3$, 50 °C): δ 152.7, 142.7, 136.5, 122.9, 122.3, 120.1, 109.4, 74.6, 31.1, 0.0. R_f = 0.64 (ethyl acetate/silica).

(*S*,*S*)-1,2-Bis(1-methylbenzimidazol-2-yl)-1′,2′-bis(methoxy)ethane. (15a)[99] A 1.00 g quantity of **2e** (3.40 mmol) was placed in a 125 mL round bottom flask with a side arm containing 20 mL of dry dimethyl sulfoxide. The flask was fitted with a bubbler and placed under a flow of nitrogen. Then 370 mg of sodium hydride (95%) (14.6 mmol) was added over 15 min with stirring. After cooling to rt 868 μL of iodomethane (13.9 mmol) was added drop wise over one hour. The reaction mixture was left stirring under nitrogen overnight. The reaction mixture was quenched with water and then added to 250 mL of water to give a brown precipitate. The precipitate was collected by filtration and was dried in air. The solid was purified by crystallization from acetonitrile to give X-ray quality crystals. $C_{20}H_{22}N_4O_2$, fw = 350.41. Yield: 836 mg, 70.2%. Mp: 146-147 °C. ^{1}H NMR (400 Mhz, CDCl$_3$): δ 7.64(dm, J = 6.9 Hz, 2H), 7.21(m, 6H), 5.44(s, 2H), 3.84(s, 6H), 3.44(3, 6H). ^{13}C NMR (CDCl$_3$): δ 150.1, 141.8, 135.6, 123.2, 120.3, 118.6, 109.9, 78.4, 57.1, 29.9. R_f = 0.23 (ethyl acetate/silica). IR (KBr pellet, cm^{-1}): 3037 m, 2925 m, 2894 m, 2825 m, 1612 m, 1479 s, 1394 s, 1241 m, 1087 s, 738 s. Crystal structure **15a** (I).[99,A25]

(*R*,*S*)-1,2-Bis(1-methylbenzimidazol-2-yl)-1′,2′-bis(methoxy)ethane. (15b) A few crystals were isolated by diethyl ether vapor diffusion into an acetonitrile solution of the

crude product **15c**. Crystals of **15b** were collected by filtration. $C_{20}H_{22}N_4O_2$, fw = 350.41. Yield: 80 mg, 7.3%. Mp: 248 °C. Crystal structure **15b** (I).[100,A26]

(*R*,*R*)-1,2-Bis(1-methylbenzimidazol-2-yl)-1′,2′-bis(methoxy)ethane. (15c) A 1.00 g quantity of **2f** (3.40 mmol) was placed in a 50 mL Erlenmeyer flask containing 15 mL of DMF and 4 mL of water. Then 1.0 g of powdered sodium hydroxide was added with stirring. Then 868 μL of iodomethane (13.9 mmol) was added drop wise over one hour. The reaction mixture was left stirring overnight. The reaction mixture was quenched with water and then added to 250 mL of water to give a brown precipitate. The precipitate was collected by filtration and was dried in air. The solid was purified by crystallization from acetonitrile to give X-ray quality crystals. $C_{20}H_{22}N_4O_2$, fw = 350.41. Yield: 1.02 g, 85.6%. Selectivity: 92.7%. Mp: 146-147 °C. ^{1}H NMR (400 Mhz, CDCl$_3$): δ 7.64(dm, J = 6.9 Hz, 2H), 7.21(m, 6H), 5.44(s, 2H), 3.84(s, 6H), 3.44(3, 6H). ^{13}C NMR (CDCl$_3$): δ 150.1, 141.8, 135.6, 123.2, 120.3, 118.6, 109.9, 78.4, 57.1, 29.9. R_f = 0.43 (ethyl acetate/silica). Crystal structure **15c** (I).[101a,A27]

(*R*,*R*)-1,2-Bis(1-ethylbenzimidazol-2-yl)-1′,2′-bis(ethoxy)ethane. (15d) In a 50 mL Erlenmeyer flask containing 12 mL of DMF 500 mg of **2f** (1.70 mmol) was added. To this mixture 100 mg of potassium carbonate and 500 mg of sodium hydroxide were added. Then 700 μL of iodoethane was added to the mixture. The flask was stoppered and left to stir at rt for 3 d. The reaction mixture was then quenched with 40 mL of water to give a pale-brown precipitate. The precipitate was collected by filtration and dried under air to give a pale-brown solid. The solid was recrystallized by slow evaporation of an acetonitrile solution to give the product as colorless crystals.

$C_{24}H_{30}N_4O_2$, fw = 406.52. Yield: 608 mg, 88.0%. Mp: 164 °C. ^{1}H NMR (300 MHz, CDCl$_3$): δ 7.64(m, 2H), 7.19(m, 6H), 5.58(s, 2H), 4.37(d br m, J = 52 Hz, 4H), 3.68(d m, J = 48 Hz, 4H), 1.41(t, J = 7.3 Hz, 6H), 1.21(t, J = 7.3 Hz, 6H). R_f = 0.51 (ethyl acetate/silica).

(*S*,*S*)-1,2-Bis(1-ethylbenzimidazol-2-yl)-1′,2′-bis(ethoxy)ethane. (15e) In a 50 mL Erlenmeyer flask containing 18 mL of DMF and 0.5 mL of water, a 1.043 g quantity of **2e** (3.54 mmol) was added. To this mixture 200 mg of potassium carbonate and 2.50 g of sodium hydroxide were added. Then 1.45 mL of iodoethane was added to the mixture. The flask was stoppered and left to stir at rt for 3 d. The reaction mixture was then added to 50 mL of water to give a pale-brown precipitate. The precipitate was collected by filtration and dried under air to give a pale-brown solid. $C_{24}H_{30}N_4O_2$, fw = 406.52. Yield: 1.252 g, 86.9%. Mp: 163 °C. ^{1}H NMR (300 MHz, CDCl$_3$): δ 7.64(m, 2H), 7.19(m, 6H), 5.58(s, 2H), 4.37(d br m, J = 52 Hz, 4H), 3.68(d m, J = 48 Hz, 4H), 1.41(t, J = 7.3 Hz, 6H), 1.21(t, J = 7.3 Hz, 6H). R_f = 0.54 (ethyl acetate/silica).

(*S*,*S*)-1,2-Bis(3-ethylbenzimidazol-1-ium)-1′,2′-bis(ethoxy)ethane   di(perchlorate). (15e-1)[101b] The salt **15e-2** was obtained by the addition of two molar equivalents of of a 2.50 M solution of perchloric acid in methanol to an ethanol solution of **15e**. Crystals were obtained by vapor diffusion of diethyl ether. $C_{24}H_{32}Cl_2N_4O_8$, fw = 607.44. Crystal structure **15e-1**(I).[101b,A28]

(*S*)-1,2-Bis(1-ethyl-5,6-dimethylbenzimidazol-2-yl)-1′-(ethoxy)ethane. (15f) In a 50 mL Erlenmeyer flask containing 10 mL of DMF and 5 mL of water, a 530 mg quantity of **2c** (3.54 mmol) was added. To this mixture 640 mg of of sodium hydroxide was added. Then 390 μL of iodoethane (4.88 mmol) was added to the mixture. The flask was

stoppered and left to stir at rt for 3 d. The reaction mixture was then added to 50 mL of water to give a orange-brown precipitate. The precipitate was collected by filtration and dried under air to give the product as an orange-brown solid. $C_{26}H_{34}N_4O$, fw = 418.57. Yield: 405 mg, 61.4%. Mp: > 300 °C (decomp). ^{1}H NMR (400 MHz, CDCl$_3$): δ 7.24(m, 2H), 7.01(m, 6H), 5.45(s, 1H), 4.02(m, 5H), 3.41(m, 2H), 3.22(m, 1H), 2.13(m, 6H), 1.18(m, 3H). R_f = 0.53 (ethyl acetate/silica).

(Z)-1,2-Bis(1-ethylbenzimidazol-2-yl)-1′-(ethylthio)ethene. (16a) In a 50 mL Erlenmeyer flask containing 10 mL of DMF and 5 mL of water, a 810 mg quantity of **2d** (2.75 mmol) was added. To this mixture 2.0 g of of powdered sodium hydroxide was added. Then 660 μL of iodoethane (8.25 mmol) was added to the mixture. The flask was stoppered and left to stir at rt for 3 d. The reaction mixture was then added to 100 mL of water to give a yellow-brown precipitate. The precipitate was collected by filtration and dried under air to give the product as a yellow-brown solid. $C_{22}H_{24}N_4S$, fw = 376.52. Yield: 982 mg, 94.9%. Mp: > 330 °C. ^{1}H NMR (400 MHz, CD$_3$SOCD$_3$): δ 8.55(s, 1H), 7.62(m, 4H), 7.19(m, 4H), 4.46(m, 2H), 3.34(m, 4H), 2.91(m, 3H), 1.35(m, 6H). R_f = 0.32 (ethyl acetate/silica).

rac-1,2-Bis(1-ethylbenzimidazol-2-yl)-1′-(4-fluorophenylthio)ethane. (16b) In a 50 mL round bottom flask containing 10 mL of ethyl acetate, a 128 mg quantity of **11c** (0.405 mmol) was added. To this mixture 100 mg of 4-fluorothiophenol (0.780 mmol) and 10 mg of (1S)-10-CSA was added. The mixture was then refluxed for 2 days. The reaction mixture was then twice extracted with 20 mL of 5% aqueous sodium carbonate. By TLC the ethyl acetate layer contained some unreacted **11c** and a single product. This

was reduced in volume and chromatographed with ethyl acetate on silica. The solvent was removed to give the product as a nearly colorless low melting crystalline solid. $C_{26}H_{25}FN_4S$, fw = 444.57. Yield: 98 mg, 54.4%. ^{1}H NMR (400 MHz, CDCl$_3$): δ 7.63(m, 2H), 7.15(m, 8H), 6.87(m, 2H), 5.32(m, 1H), 4.08(m, 4H), 3.55(m, 1H), 1.99(m, 1H), 1.31(m, 6H). R_f = 0.60 (ethyl acetate/silica).

1,1′-Bis(1-hydrobenzimidazol-2-yl)ketone. (17) To a beaker containing 20 mL of DMSO, 2.00 g (8.06 mmol) of **10** was added and dissolved. The beaker was left to stand in air for about a week at rt over which time crystals of two different phases precipitated. The crystals were collected by filtration and were washed with water. The crystals were then dissolved in methylene chloride and were twice extracted with water. The methylene chloride was dried over sodium sulfate and filtered. The solution was left to evaporate to give the product as colorless crystals. $C_{15}H_{10}N_4O$, fw = 262.27. Yield: 2.05 g, 97%. Mp: 320-321 °C(decomp). ^{1}H NMR (CD$_3$SO$_2$CD$_3$): δ 7.85(m, 2H), 7.47(m, 5H), 7.14(m, 1H). R_f = 0.19 (ethyl acetate/silica). IR (KBr pellet, cm^{-1}): 3057 w, 2840 w, 2724 w, 1658 s, 1438 s, 1318 s, 1221 m, 738 s. Crystal structure **17**(I)[A29], **17**·DMSO(II), **17**·DMSO(III).

1,1′,2,2′Tetra(1-propylbenzimidazol-2-yl)ethane. (18) Compound **18** was obtained by dissolving a 1.74 g quantity of **4b** (5.02 mmol) in 15 mL of DMSO placed in a 50 mL beaker. The mixture was allowed to sit in open to air at rt for 5 d. The reaction was followed by TLC. The product was precipitated by the addition to 150 mL of water. The precipitate was then dissolved in methylene chloride and was twice extracted with water. The methylene chloride was dried over sodium sulfate and filtered. The solution was left to evaporate to give the product as a colorless solid. Crystals were obtained by slow

evaporation of an acetone solution containing the product. $C_{42}H_{46}N_8$, FW = 662.87. ^1H NMR ($CDCl_3$): δ 7.98(d, J = 8.2 Hz, 2H), 7.45(m, 4H), 7.10(m, 12H), 4.25(m, 8H), 1.58(m, 8H), 0.89(t, J = 7.1 Hz, 12H). R_f = 0.74 (ethyl acetate/silica) IR (KBr pellet, cm^{-1}): 3053 m, 2958 m, 2931 m, 2874 m, 1653 m, 1457 s, 1420 m, 1283 m, 742 s. Crystal structure **18**(I).[A30]

5,6-Dichloro-1-propylbenzimidazole. (19a)[102] The precursor 5,6-dichloro-1H-benzimidazol-2-yl, first reported by Davies[103] et al., was prepared by the Phillips[51] condensation method from 4,5-dichloro-1,2-phenylenediamine and formic acid. Compound **19a** was prepared by alkylation of this product with *n*-propyliodide, using the NaH/DMSO procedure described above. Alkylation afforded an oil initially from which crystals of **19a** deposited upon standing. $C_{10}H_{10}Cl_2N_2$, fw = 229.11. ^1H NMR (400 MHz, $CDCl_3$): δ 7.89(s, 1H), 7.50(s, 1H), 7.27(s, 1H), 4.10(t, J = 7.1 Hz, 2H), 1.91 (sx, J = 7.3 Hz, 2H), 0.96(t, J = 7.4 Hz, 3H). Crystal structure **19a**(I).[102,A31]

1-Hydro-napth[2,3-d]imidazole. (19b)[104] 1-hydro-napth[2,3-d]imidazole was prepared by following a published procedure.[105] Crystals were obtained by slow evaporation of a concentrated solution of **19b** in dry dimethylsulfoxide. $C_{11}H_8N_2$, fw = 168.19. Mp: 246 °C (decomp.). Crystal structure **19b**(I).[104,106,A32]

1-Hydro-phenanthro[9,10-d]imidazol-2-yl. (20a) Compound **20a** was prepared according to a published procedure.[69] In a 250 mL round bottom flask 2.08 g of phenanthroquinone (9.99 mmol), 2.80 g of hexamethylenetetramine (20.0 mmol), and 15.5 g of ammonium acetate were added. The solids were suspended in glacial acetic acid and refluxed for 1 hour. The mixture was cooled and neutralized with conc. ammonium hydroxide, followed by the addition of water to fully precipitate the product. The product

was collected by filtration, washed with water, and dried to constant weight in a vacuum oven to give the product as an off-white solid. $C_{15}H_{10}N_2$, fw = 218.25. Yield 2.01 g, 92.2%. Mp: 291 °C. ^{1}H NMR (400 MHz, $CD_3SO_2CD_3$ 25 °C): δ 8.861(br m, 2H), 8.51(br m, 2H), 8.37(s, 1H), 7.72(br m, 2H), 7.64(br m, 2H). ^{13}C NMR ($CD_3SO_2CD_3$): δ 139.6, 136.2, 127.9, 127.8, 127.4, 125.4, 124.3, 122.0. R_f = 0.38 (ethyl acetate/silica).

1-Hydro-3,6-dibromo-phenanthro[9,10-*d*]imidazol-2-yl. (20b) Prepared by the same procedure as **20a**. In a 250 mL round bottom flask 2.08 g of 3,6-dibromophenanthro-9,10-quinone[107] (5.68 mmol), 1.59 g of hexamethylenetetramine (11.34 mmol), and 14.0 g of ammonium acetate were added. The solids were suspended in glacial acetic acid and refluxed for 1 hour. The mixture was cooled and neutralized with conc. ammonium hydroxide, followed by the addition of water to fully precipitate the product. The product was collected by filtration, washed with water, and dried to constant weight in a vacuum oven to give the product as a pale-gray solid. $C_{15}H_8Br_2N_2$, fw = 376.91. Yield 2.02 g, 94.4 %. Mp: 273 °C. ^{1}H NMR (400 MHz, 50 °C, CD_3SOCD_3): δ 8.85(s, 2H), 8.19(d, J = 6.4 Hz, 2H), 8.04(s, 1H), 7.78(dd, J = 1.8 Hz, J = 8.6 Hz, 2H). ^{13}C NMR (50 °C, CD_3SOCD_3): δ 139.7, 139.5, 130.6, 128.6, 126.7, 124.3, 119.1. R_f = 0.37 (ethyl acetate/silica).

1-Ethyl-phenanthro[9,10-*d*]imidazol-2-yl. (21a) In a 125 mL round bottom flask with a side arm containing 20 mL of dry DMSO, 2.00 g of **20a** (9.17 mmol) was added. The mixture was placed under a flow of nitrogen and this was followed by the slow addition of 1.00 g of sodium hydride (95%). After stirring for 0.5 h, 730 μL of iodoethane (9.17 mmol) was added drop wise to the reaction mixture. The reaction mixture was allowed to stir over night. The reaction mixture was quenched with water and the precipitated with

an additional 200 mL water to give a pale-brown solid which was collected by filtration and washed with an additional 200 mL of water and then dried to constant weight in a vacuum oven to give the product as a pale-brown solid. $C_{17}H_{14}N_2$, fw = 246.31. Yield: 1.14 g, 50.5%. Mp: 84 °C(soften) 100 °C(melt). ^{1}H NMR (400 MHz, 50 °C, CDCl$_3$): δ 8.70(t, J = 10.5 Hz, 2H), 8.60(d, J = 8.0 Hz, 1H), 8.08(d, J = 6.7 Hz, 1H), 7.81(s, 1H), 7.66(t, J = 6.8 Hz, 1H), 7.56(m, 3H), 4.48(q, J = 6.9 Hz, 2H), 1.56(t, J = 6.9 Hz, 3H). ^{13}C NMR (50 °C, CDCl$_3$): δ 142.2, 140.4, 139.4, 128.4, 128.1, 126.5, 126.4, 125.9, 125.4, 124.1, 123.6, 122.7, 122.1, 121.8, 120.4, 43.2, 15.9. R_f = 0.51 (ethyl acetate/silica).

1-Ethyl-3,6-dibromo-phenanthro[9,10-*d*]imidazol-2-yl. (21b) In a 125 mL round bottom flask with a side arm containing 20 mL of dry DMSO, 1.00 g of **20b** (2.66 mmol) was added. The mixture was placed under a flow of nitrogen and was followed by the slow addition of 0.50 g of sodium hydride (95%). After stirring for 0.5 h, 220 μL of iodoethane (2.75 mmol) was added dropwise to the mixture. After stirring overnight the reaction mixture was quenched with water and then precipitated with the addition of 80 mL of water to give pale-brown precipitate which was collected by filtration and washed with water and then dried to constant weight in a vacuum oven to give the product as a pale-brown solid. $C_{17}H_{12}Br_2N_2$, fw = 404.10. Yield: 985 mg, 91.7%. Mp: 160 °C (soften) 175 °C (melt). ^{1}H NMR (400 MHz, CDCl$_3$): δ 8.68(dd, J = 42.2 Hz, J = 1.7 Hz, 2H), 8.25(dd, J = 203.3 Hz, J = 8.8 Hz, 2H), 7.91(s, 1H), 7.75(qd, J = 8.8 Hz, J = 1.9 Hz, 2H), 4.58(q, J = 7.3 Hz, 2H), 1.65(t, J = 7.3 Hz, 3H). ^{13}C NMR (CDCl$_3$): δ 141.5, 138.6, 131.0, 130.3, 129.4, 128.4, 127.2, 126.4, 125.9, 124.8, 124.1, 122.2, 122.0, 119.8, 119.2, 43.0, 16.1. R_f = 0.39 (ethyl acetate/silica).

1-Propyl-3,6-dibromo-phenanthro[9,10-*d*]imidazol-2-yl. (21c) In a 50 mL Erlenmeyer flask containing 15 mL of DMF, 199 mg of **20b** (0.53 mmol) was added. Then 0.50 g of powdered sodium hydroxide was added to the mixture. After stirring for 0.5 h, 52 μL of 1-iodopropane (0.53 mmol) was added dropwise to the mixture. After stirring overnight the reaction mixture was quenched with water and then precipitated with the addition of 80 mL of water to give pale-brown precipitate which was collected by filtration and washed with water and then dried to constant weight to give the product as a pale-brown solid. $C_{18}H_{14}Br_2N_2$, fw = 418.95. Yield: 220 mg, 99.1%. Mp: 161 °C (melt) ^{1}H NMR (400 MHz, CDCl$_3$): δ 8.73(s, 1H), 8.62(s, 1H), 8.50(d, J = 8.4 Hz, 1H), 7.95(d, J = 8.8 Hz, 1H), 7.86(s, 1H), 7.73(dd, J = 8.4 Hz, J =19.8 Hz, 2H), 4.47(t, J = 7.3 Hz, 2H), 2.00(p, J = 7.3 Hz, 2H), 1.02(t, J = 7.3 Hz, 3H) R_f = 0.47 (ethyl acetate/silica).

1-Ethoxymethyl-3,6-dibromo-phenanthro[9,10-*d*]imidazol-2-yl. (21d) Under Ar 2.94 g of **20b** (7.8 mmol) was added to a 100 mL round bottom flask containing 30 mL of dry THF. Then 192 mg of NaH (95%) was added slowly to the flask and was allowed to stir for 10 min. Then 0.74 g of chloromethyl ethyl ether (7.8 mmol) was added dropwise and the mixture was allowed to stir overnight. The reaction was then quenched with sodium sulfate saturated water. The mixture was then dried over sodium sulfate and filtered. The solution was taken to dryness with rotary evaporation. The solid was extracted with cyclohexane and filtered. The cyclohexane was removed by rotary evaporation to give the product as a pale-brown solid. $C_{18}H_{14}Br_2N_2O$, fw = 434.12. Yield 2.35 g, 69.2%. Mp: 125 °C. ^{1}H NMR (400 MHz, CDCl$_3$): δ 8.64(dd, J = 27.5 Hz, J = 1.6 Hz, 2H), 8.35(dd, J = 95.5 Hz, J = 8.8 Hz, 2H), 7.93(s, 1H), 7.75(qd, J = 8.6 Hz, J =1.8 Hz, 2H), 5.75(s, 2H), 3.58(q, J = 7.0 Hz, 2H), 1.19(t, J = 7.0 Hz, 3H). ^{13}C NMR (CDCl$_3$): δ 139.4, 132.2,

131.9, 128.0, 126.6, 126.0, 125.5, 124.0, 123.8, 122.1, 64.6, 31.5, 15.8. R_f = 0.52 (ethyl acetate/silica).

1-Ethoxymethyl-3,6-dicarbonitrile-phenanthro[9,10-*d*]imidazol-2-yl. (21e) A 50 mL round bottom flask containing 20 mL of acetonitrile was placed under argon. This was followed by the sequential addition of 7 mg of Cu(I)I (0.04 mmol), 138 mg of NaCN (2.81 mmol), 7 mg of Pd$_2$(dba)$_3$ (0.015 mmol Pd), 12 mg of Fedppe (0.022 mmol), and 305 mg of **21d** (0.889 mmol). The reaction mixture was then left to reflux for 3 d under argon. The mixture was then cooled to rt and evaporated to dryness. The solids were then extracted with ethyl acetate. The ethyl acetate was removed and the cyanation was repeated due to lack of complete conversion. The product was isolated as a pale-yellow solid. C$_{20}$H$_{14}$N$_4$O, fw = 326.35. Yield 265 mg, 91.3%. Mp: 110 °C (soften) 171 °C (melt). ^{1}H NMR (400 MHz, CDCl$_3$): δ 8.42(m, 3H), 7.63(m, 4H), 5.63(s, 2H), 3.51(m, 2H), 1.12(m, 3H). R_f = 0.32 (ethyl acetate/silica).

Bis(1-ethyl-phenanthro[9,10-*d*]imidazol-2-yl)ketone. (22) In a 100 mL round bottom flask under argon, 20 mL of dry THF was added followed by the addition of 800 mg of **21a** (3.25 mmol). The mixture was cooled to -78 °C and was followed by the addition of 2.10 mL of 2.5 M *n*-butyllithium to give a red-brown solution. The mixture was stirred for 1.5 h ensuring the reaction temperature was maintained at -78 °C. Then 200 μL of diethyl carbonate (1.63 mmol) was added. After stirring for 0.5 h the mixture was slowly allowed to warm to rt. The reaction was quenched with saturated sodium chloride in water. The solvent was then removed under vacuum. The product was dissolved in 5 mL of methylene chloride and chromatographed on silica with 10 vol% ethanol in cyclohexane to give the product as a yellow solid. C$_{35}$H$_{26}$N$_4$O, fw = 518.61. Yield: 705

mg, 83.7%. Mp: 225 °C(phase change) 290 °C(decomp). ^{1}H NMR (400 MHz, CDCl$_3$): δ

8.69(dm, J = 64.8 Hz, 4H), 8.46(dm, J = 63.8 Hz, 4H), 7.67(m, 4H), 7.56(m, 4H), 4.97(q,

J = 7.1 Hz, 4H), 1.77(t, J = 7.1 Hz, 6H). ^{13}C NMR (CDCl$_3$): δ 178.2, 146.9, 139.0, 131.4,

129.0, 128.6, 128.2, 128.1, 128.0, 127.4, 127.1, 126.7, 126.0, 124.5, 124.1, 123.4, 122.9,

122.6, 43.2, 43.1, 16.7, 15.7. R_f = 0.85 (ethyl acetate/silica). crystal structure **22**(I).[A33]

2,2′-Bi(1-ethyl-3,6-dibromo-phenanthro[9,10-*d*]imidazol-2-yl). (23) In a 100 mL

round bottom flask under argon, 20 mL of dry THF was added followed by the addition

of 450 mg of **21b** (1.11 mmol). The mixture was cooled to -78 °C and was followed by

the addition of 1.17 mL of 2.0 M LDA to give a red-brown solution. The mixture was

stirred for 0.5 h ensuring the reaction temperature was maintained at -78 °C. Then the

mixture was warmed to -40 °C and stirred for 1 h. The mixture was allowed to warm to rt

and stir overnight. The reaction was quenched with saturated sodium sulfate in water.

The solvent was then removed under vacuum and the solids were extracted with ethyl

acetate. The solvent was removed by evaporation to give the product as an off white

solid. C$_{34}$H$_{22}$Br$_4$N$_4$, fw = 806.18. Yield 425 mg, 95.0%. Mp: (> 345 °C).^{1}H NMR

(CD$_3$SO$_2$CD$_3$): δ 8.79 (dd, J = 37.3 Hz, J = 1.9 Hz, 4H), 8.48(d, J = 8.6 Hz, 2H), 8.13(m,

2H), 7.78(td, J = 10.4 Hz, J = 1.6 Hz, 4H), 4.69(t, J = 7.2 Hz, 4H), 1.65(q, J = 7.2 Hz,

6H). ^{13}C NMR (CD$_3$SO$_2$CD$_3$): δ 142.3, 138.2, 130.7, 130.5, 128.2, 127.0, 126.4, 125.9,

124.7, 124.0, 122.8, 122.0, 119.3, 119.0, 42.7, 16.0. R_f = 0.38 (ethyl acetate/silica). IR

(KBr pellet, cm^{-1}): 1521 s, 1447 m, 1360 m, 1241 m, 1104 m, 840 m.

1,1′-Bis(1-ethylbenzimidazol-2-yl)-2-(2-(4-bromophenyl)ethene. (24a) In a 50 mL

Erlenmeyer flask containing 15 mL of acetonitrile, a 161 mg quantity of **4a** (0.529 mmol)

was added. This was followed by the addition of 98 mg of 4-bromobenzaldehyde (0.53

mmol). The reaction was stirred at rt and was followed by TLC. After the disappearance of **4a** the product was obtained by chromatography on silica from a crude product. $C_{26}H_{23}BrN_4$, fw = 471.39. Yield: 205 mg, 82.2%. ^{1}H NMR (400 MHz, CDCl$_3$): δ 9.95(s, 9.95), 7.70 (m, 6H), 7.28(m, 2H), 7.21(m, 4H), 4.13(q, J = 7.3 Hz, 4H), 1.39(t, J = 7.3 Hz, 6H). ^{13}C NMR (CDCl$_3$): δ 191.1, 151.1, 142.7, 135.1, 134.7, 132.4, 131.0, 129.8, 121.9, 121.7, 119.0, 109.0, 38.5, 15.1, 14.9. R_f = 0.48 (ethyl acetate/silica).

1,1′-Bis(1-ethylbenzimidazol-2-yl)-2-(1,3-benzodioxol-5-yl)ethene. (24b) A 900 mg (2.96 mmol) quantity of **4a** was added to a 125 mL Erlenmeyer flask containing 25 mL of EtOH with 500 mg of powdered NaOH. Then 444 mg (2.96 mmol) of piperonal was added to the reaction mixture. The flask was stoppered and left to stir at rt for 2 days. The solvent was reduced to ca. 5 mL and 40 mL of water was added. The mixture was neutralized (ca. pH 7) with dilute HCl. This was extracted with 40 mL of ethyl acetate. The yellow-orange ethyl acetate layer was dried over sodium sulfate and filtered. The solvent was removed by evaporation to give a yellow-orange sticky solid. $C_{27}H_{24}N_4O_2$, fw = 436.51. Yield: 1.08 g, 83.2%. ^{1}H NMR (400 MHz, CDCl$_3$): δ 8.06(m, 2H), 7.53(m, 7H), 7.12(m, 2H), 6.19(m, 1H), 4.59(m, 4H), 2.88(s, 2H), 1.21(m, 6H). R_f = 0.52 (ethyl acetate/silica).

5-Methyl-benzo[1,3]dioxole-2-spiro-1'-cyclohexane. (25) Compound **25** has been previously reported[108] and was prepared from a modified literature proceedure.[109] To a 500 mL round bottom flask 7.50 g of 4-methylcatechol (60.4 mmol) was added followed by 5.30 g of cyclohexanone (54.0 mmol) and 100 mg of p-toluenesulfonic acid. Finally 150 mL of toluene was added. The flask was fitted with a Dean-Stark trap and a condenser and was left to reflux overnight with stirring. The reaction was cooled and the

toluene mixture was extracted with 150 mL of 2% aqueous KOH 5 times. The solvent was then removed under a stream of nitrogen to give yellow oil. The oil was chromatographed on silica gel with hexane. The first band was collected and the solvent was removed by rotary evaporation to give a colorless oil. $C_{13}H_{16}O_2$, FW = 204.26. Yield: 9.87, 89.4%. ^{1}H NMR ($CDCl_3$): δ 6.61(m, 3H), 2.29(s, 3H), 1.91(m, 4H), 1.76(m, 4H), 1.52(m, 2H). R_f = 0.34 (hexane/silica).

5-Bromomethyl-benzo[1,3]dioxole-2-spiro-1'-cyclohexane. (26) Compound **26** was prepared using a modified literature proceedure.[110] To a 300 mL round bottom flask containing 25 mL of carbon tetrachloride 6.90 g of 5-methyl-benzo[1,3]dioxole-2-spiro-1'-cyclohexane (33.8 mmol) was added followed by 6.61 g of NBS (37.1 mmol) and 300 mg of potassium carbonate. Finally 500 mg of benzoyl peroxide was added. The flask was fitted with a condenser and was left to reflux overnight with stirring. The reaction was cooled and 150 mL of hexane was added to the mixture and then was extracted with 150 mL of 2% aqueous $NaHCO_3$ 3 times. The solvent was then removed by rotary evaporation to give a pale yellow-orange oil. The oil was chromatographed on silica gel with hexane. The second band was collected and the solvent was removed by rotary evaporation to give a colorless oil. The oil was stored over 100 mg potassium carbonate at -20 °C. Over a few days the oil crystallized as a white solid. $C_{13}H_{15}BrO_2$, fw = 283.16. Yield: 4.57 g, 89.4%. ^{1}H NMR ($CDCl_3$): δ 6.61(m, 3H), 2.29(s, 3H), 1.91(m, 4H), 1.76(m, 4H), 1.52(m, 2H). R_f = 0.34 (hexane/silica).

1,1'-Bis(1-methylbenzimidazol-2-yl)ketone. (27a) Compound **27a** was prepared as previously reported.[60] Crystal structure **27a**(I)$_{421}$[A34], **27a**(II)$_{447}$, **27a·2 H₂O**(III)$_{383}$.

1,1′-bis(1-propylbenzimidazol-2-yl)ketone. (27b) In a 50 mL Erlenmeyer flask containing 20 mL of DMF, 1.00 g of **17** (3.81 mmol) was added. Then 1.00 g of powdered sodium hydroxide was added to the mixture. After stirring for 0.5 h, 449 μL of 1-iodopropane (7.62 mmol) was added dropwise to the mixture. After stirring overnight the reaction mixture was quenched with water and then precipitated with the addition of 80 mL of water to give pale-brown precipitate which was collected by filtration and washed with water and then dried to constant weight to give the product as a pale-brown solid. $C_{21}H_{22}N_4O$, fw = 346.43. Yield: 1.18 g, 89.4%. ^{1}H NMR (CDCl$_3$): δ 7.79(m, 2H), 7.61(m, 2H), 7.42(m, 2H), 7.32(m, 2H), 4.52(t, J = 7.4 Hz, 4H), 1.96(sp, J = 7.4 Hz, 4H), 1.10(t, J = 7.4 Hz, 6H). R_f = 0.47 (hexane/silica).

1,1′-bis(1-(5-methyl-benzo[1,3]dioxole-2spiro-1′-cyclohexane)benzimidazol-2-yl)ketone. (27c) In a 125 mL Erlenmeyer flask containing 25 mL of DMF, 1.00 g of **17** (3.81 mmol) was added. Then 1.00 g of powdered sodium hydroxide was added to the mixture. After stirring for 0.5 h, 2.16 g of **26** (7.62 mmol) was added dropwise to the mixture. After stirring overnight the reaction mixture was quenched with water and then precipitated with the addition of 80 mL of water to give pale-brown oily precipitate which was extracted with 50 mL of ethyl acetate. The mixture was then extracted with 50 mL of water 3 times. The ethyl acetate was then removed by rotary evaporation to give a pale-brown oil. The oil was chromatographed on silica gel with hexanes. The second band was collected and the solvent was removed by rotary evaporation to give a pale-brown sticky solid. $C_{41}H_{38}N_4O_5$, fw = 666.76. Yield: 1.65 g, 64.8%. ^{1}H NMR (CDCl$_3$): δ 7.88(m, 2H), 7.27(m, 6H), 6.59(m, 6H), 2.50(br s, 4H), 1.75(m, 4H), 1.58(m 8H), 1.37(m, 4H), 1,13(m, 4H). R_f = 0.47 (hexane/silica).

1,1′-bis(1-(4-bromobenzyl)benzimidazol-2-yl)ketone. (27d) In a 25 mL Erlenmeyer flask containing 15 mL of DMF, 500 mg of **17** (1.91 mmol) and a 955 mg quantity of 4-bromobenzylbromide (3.82 mmol) were added. This was followed by the addition of 750 mg of powdered NaOH. The flask was stoppered and left to stir at rt for two days. The reaction mixture was then added to 100 mL of water and the product precipitated out of solution. The solid was collected by filtration and washed with water. The solid was then dried in a vacuum oven overnight at 60 °C. The product was isolated as a brown sticky amorphous solid. $C_{29}H_{20}Br_2N_4O$, fw = 600.30. Yield: 942 mg, 82.2%. ^1H NMR (400 MHz, $CDCl_3$): δ 7.62(m, 2H), 7.11(m, 8H), 6.45(m, 6H), 2.50(s, 4H). ^{13}C NMR ($CDCl_3$): δ 152.5, 141.9, 137.2, 134.9, 134.5, 123.5, 122.9, 120.8, 119.9, 110.1, 40.9. R_f = 52 (ethyl acetate/silica). IR (KBr pellet, cm^{-1}): 3051 m, 2968 m, 2938 m, 1900 m, 1611 m, 1501 s, 1487 s, 1459 m, 1297 m, 1071 s, 1011 s, 810 m, 751 s.

1-*H*-2-bromobenzimidazole. (39) Compound **39** was prepared by a literature procedure.[111] A 1.133 g (9.59 mmol) quantity of 1-*H*-benzimidazole was added to a 125 mL round bottom flask containing 5 g of silica gel and 30 mL of methylene chloride. Thiis was followed by the addition of 1.707 g (9.59 mmol) of NBS. The flask was sealed and left to stir at rt for two days. The solvent was then removed by rotary evaporation. The solid was then extracted with 40 mL of methanol and filtered. The solvent was then removed from the filtrate by rotary evaporation. The residue was then extracted with water and methylene chloride. The methylene chloride was separated and dried over sodium sulfate and filtered. The solvent was removed by rotary evaporation to give a pale yellow sticky amorphous solid. $C_7H_5BrN_2$, fw = 197.03. Yield: 1.17 g, 61.9%. R_f = 0.34 (ethyl acetate/silica).

1-propyl-2-bromobenzimidazole. (40) In a 125 mL Erlenmeyer flask containing 20 mL of DMF, a 380 mg quantity of **39** (1.93 mmol) was added followed by the addition of 500 mg of powdered NaOH. Then 188 μL of *n*-propyl iodide (1.93 mmol) was added. The mixture was stirred for 1 h giving a yellow solution. The reaction mixture was then added to 50 mL of water. This initially resulted in a white precipitate which quickly turned to an oil. The oil was extracted with ethyl acetate and washed with water. The ethyl acetate was dried over sodium sulfate and filtered to give a clear solution. The solvent was removed by evaporation to give the product as a colorless oil. $C_{10}H_{11}BrN_2$, fw = 239.11. Yield: 440 mg, 95.4%. ^{1}H NMR (400 MHz, CDCl$_3$): δ 8.01(m, 1H), 7.40 (m, 3H), 4.13(t, J = 7.0 Hz, 2H), 1.90(m, 2H), 0.96(t, J = 7.0 Hz, 3H). R_f = 0.47 (ethyl acetate/silica).

tri-*n*-butyl(2-(1-propylbenzimidazol-2-yl)stannane (41) A 50 mL round bottom flask containing 20 mL of THF was placed under argon. This was followed by the sequential addition of 95 mg of **40** (0.40 mmol), 260 mg of hexa-*n*-butylditin (0.45 mmol), 10 mg of Pd$_2$(dba)$_3$ (0.022 mmol Pd), and 10 mg of fedppe (0.018 mmol). The reaction mixture was then left to reflux for 2 d under argon. The mixture was then cooled to rt and evaporated to dryness. The solids were added to 20 mL water containing 20 mg NaF. The aqueous mixture was then extracted with ethyl acetate. The product was isolated from the ethyl acetate as a pale-brown oil. $C_{22}H_{38}N_2Sn$, fw = 449.26. Yield 146 mg, 81.5 %. Mp: (oil). ^{1}H NMR (400 MHz, CDCl$_3$): δ 7.81(m, 2H), 7.33(m, 2H), 4.05(br s, 2H), 1.85(br s, 2H), 1.54(br s, 6H), 1.28(br s, 6H), 1.11(br s, 6H), 1.03(br s, 3H), 0.86(br s, 9H). R_f = 0.39 (ethyl acetate/silica).

***rac*-2,2′-bis[2-(1-propylbenzimidazol-2-yl)]-1,1′-binaphthyl (42)** A 50 mL round bottom flask containing 15 mL of DMF was placed under argon. This was followed by the sequential addition of 80 mg of **41** (0.18 mmol), 50 mg of 1,1′-bi-2-naphthol bis(trifluoromethanesulfonate) (0.090 mmol), 10 mg of Pd$_2$(dba)$_3$ (0.022 mmol Pd), 20 mg of fedppe (0.037 mmol), and 10 mg of lithium trifluoromethanesulfonate (0.064 mmol). The reaction mixture was then left to reflux for 3 d under argon. The mixture was then cooled to rt and evaporated to dryness. The solids were added to 20 mL water. The aqueous mixture was then extracted with ethyl acetate. The extract was then chromatographed on silica wth ethyl acetate. The product was isolated from the ethyl acetate as a soft pale-yellow solid. C$_{40}$H$_{34}$N$_2$, fw = 570.72. Yield 36 mg, 70%. Mp: 91-91 °C. ^{1}H NMR (400 MHz, CDCl$_3$): δ 7.96(dd, *J* = 8.8 Hz, *J* = 53.8 Hz, 6H), 7.50(m, 6H), 7.32(m, 4H), 7.18(m, 4H), 4.05(m, 4H), 1.83(m, 4H), 0.87(m, 6H). *R$_f$* = 0.68 (ethyl acetate/silica).

Chapter 2

Geometrically Constrained Metal Complexes

Introduction

Multidentate ligands designed to constrain the coordination geometries of metals have found several applications in chemistry. For example, geometrically constraining ligands have been used with Ti, Zr and Hf as polymerization catalysts,[112] which has spawned a large academic and industrial research effort,[113] one which continues today.[114] These Group IV catalysts have also been reported to be efficient hydrosilation catalysts.[115] Further, geometrically constraining ligands have been used to effect a particular coordination geometry, such as trigonal-pyramidal,[116] an unusual oxidation state, such as Ni(I),[117] or to ensure the formation of a given isomer.[118] In bioinorganic chemistry, they have been used extensively to help model the active sites of metalloproteins.[119] Some time ago, we designed the bis(imidazole) biphenyl-based bidentate ligand **BIL** (introduction) as a tetrahedrally constraining moiety to study electronic features and Cu(I)/Cu(II) electron self-exchange for the structurally similar, distorted-tetrahedral tetrakis(imidazole) Cu(I)(**BIL**)$_2$ and Cu(II)(**BIL**)$_2$ coordination geometries.[34] Recently, we found that **9b**, an alkylated benzimidazole analogue of **BIL**, forms more nearly-tetrahedral complexes with divalent first-row transition metals ranging from Cr(II) to Zn(II), and with Cu(I) and Cd(II); **9b** also acts as a highly basic proton sponge.[27a,c] In some instances, one bis(benzimidazole) species, such as the ligand **2-1**[120a] (Figure 2-1) or ligand **9a**[120b,c,d] is sufficient to produce a distorted-tetrahedral

coordination geometry (e. g., with X = N or Cl, the following angular ranges were found:

for Mn(II)(**2-1**)Cl$_2$, X-Mn(II)-X′, 96.8-115.7°,[120a]; Ni(II)(**9a**)Cl$_2$, X-Ni(II)-X′, 102.1-123.4°,[120c]; Cu(II)(**9a**)Cl$_2$, X-Cu(II)-X′, 96.6-133.7°,[121].

There are numerous examples of lanthanide complexes that are both isomorphous and isostructural.[122] This is due to the spherical nature of the outer shell orbitals of the lanthanide ions. Except for a few specific examples, such as porphyrin complexes[123] (square-planar/square-bipyramidal) and **BIL** complexes[34] (distorted tetrahedral), there are few examples of both isomorphous and isostructural substitution for the transition metals. There are two other examples of note. The first is a "porphyrin like" ring system that utilizes benzimidazole in the ring.[124] The second is a distorted square-bipyramidal example.[125] Both systems were structurally characterized with several transition metals. We report here the preparation and characterization of two systems with constrained coordination geometries. The first consists of tetrahedrally constrained complexes using bis(benzimidazole analogues) of **BIL** characterized with several transition metal ions. The second consists of square-bipyramidally constrained complexes using bis(**15a,c,d,e**) with first- and second-row transition-metal ions.
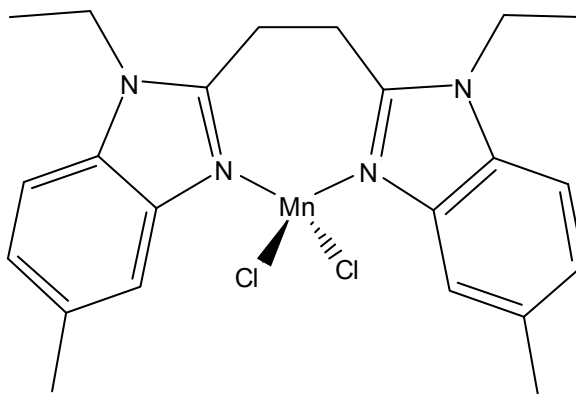

Figure 2-1. Structure of 1,2-bis(1-ethyl-5-methylbenzimidazol-2-yl)manganese(II) dichloride (**2-1**).

Experimental Section

All reagents were used as received or purified by standard methods.[82] Melting points were determined with a hot-stage apparatus and are uncorrected. Densities of the crystalline products were measured by flotation.

Safety Note. While we experienced no difficulty handling these materials, it should be noted that perchlorate salts of metal complexes with organic ligands are potentially explosive. Only small amounts of such materials should be prepared, and these should be handled with great care.

Tetrahedrally Constrained Metal Complexes

Preparation of the Complexes.

rac- bis- {2,2'-bis [2-(1-propylbenzimidazol-2-yl)] biphenyl)} manganese(II) bis (perchlorate), *rac*-Mn(II)(9b)$_2$·(ClO$_4$)$_2$. (2-2)[12a] A mixture containing two equivalents of **9b** (400 mg, 0.85 mmol), 154 mg of Mn(ClO$_4$)$_2$ · 6H$_2$O (0.425 mmol), 20 mL of acetonitrile, and 2 mL of triethyl orthoformate was heated briefly to gentle reflux. Following vapor diffusion of diethyl ether into the room-temperature mixture, pale-yellow-brown crystals suitable for X-ray diffraction were deposited, collected by filtration, and dried in air. C$_{64}$H$_{60}$Cl$_2$MnN$_8$O$_8$, fw = 1195.05. Yield: 480 mg, 94.5 %. IR (KBr pellet, cm^{-1}) 3061 m, 2967 m, 2930 m, 1615 m, 1464 s, 1420 s, 1287 m, 1088 s, 903 s, 760 s, 623 m. Anal. Calcd for N, 9.38 ; H, 5.06; C, 64.32; Cl, 5.93. Found: N, 9.45; H, 5.29; C, 63.19; Cl, 6.09. Crystal structure (**2-2**).[12a,A35]

rac-bis-{2,2'-bis[2-(1-propylbenzimidazol-2-yl)]biphenyl)}iron(II)   bis(perchlorate), *rac*-Fe(II)(9b)$_2$·(ClO$_4$)$_2$. (2-3)[12a] Two equivalents of **9b**, (520 mg, 1.10 mmol) were added to a stirred mixture of 110 mg of FeCl$_2$ · 4H$_2$O (0.55 mmol), 20 mL of acetonitrile

and 5 mL of triethyl orthoformate. After 10 min, 229 mg of $AgClO_4$ (1.10 mmol) was added; the mixture was stirred overnight, then filtered through a 0.2 μ poly(tetrafluoroethylene) membrane to give a clear, pale-orange-brown solution. Vapor diffusion of diethyl ether into the filtrate afforded pale-orange-brown crystals suitable for X-ray diffraction, which were collected by filtration and dried in air. $C_{64}H_{60}Cl_2FeN_8O_8$, fw = 1195.96. Yield: 606 mg, 92.1 %. IR (KBr pellet, cm^{-1}) 3063 m, 2967 m, 2930 m, 1615 m, 1466 s, 1420 s, 1287 m, 1092 s, 907 s, 758 s, 621 m. Anal. Calcd for N, 9.37; H, 5.06; C, 64.27; Cl, 5.93. Found: N, 9.64; H, 5.36; C, 64.09; Cl, 5.78. Crystal structure (**2-3**).[12a,A36]

rac- bis-[2,2'-bis [2-(1-propylbenzimidazol-2-yl)] biphenyl)] manganese(II)$_{0.03}$ zinc(II)$_{0.97}$ bis(perchlorate), rac-Mn(II)$_{0.03}$Zn$_{0.97}$(II)(9b)$_2$·(ClO$_4$)$_2$. (2-4) A mixture containing two equivalents of **9b** (316 mg, 0.672 mmol), 4 mg of $Mn(ClO_4)_2 \cdot 6H_2O$ (0.011 mmol), 121 mg $Zn(ClO_4)_2 \cdot 6H_2O$ (0.325 mmol), 8 mL of acetonitrile, and 1 mL of triethyl orthoformate was heated briefly to gentle reflux and allowed to cool to rt. Following vapor diffusion of diethyl ether into the room-temperature reaction mixture, very pale-pink crystals suitable for X-ray diffraction were deposited, collected by filtration, and dried in air. $C_{64}H_{60}Cl_2Mn_{0.03}N_8O_8Zn_{0.97}$, fw = 1205.20. Yield: 112 mg, 55.3 %. Epr (Figure 2-14).

rac-bis-[2,2'-bis[2-(1-propylbenzimidazol-2-yl)]biphenyl)]cobalt(II) bis(perchlorate), rac-Co(II)(9b)$_2$·(ClO$_4$)$_2$. (2-5) A mixture containing two equivalents of **9b** (203 mg, 0.43 mmol), 79 mg of $Co(ClO_4)_2 \cdot 6H_2O$ (0.22 mmol), 10 mL of acetonitrile, and 4 mL of triethyl orthoformate was heated to reflux. Following vapor diffusion of diethyl ether into the room-temperature mixture, blue-purple crystals suitable for X-ray diffraction were

deposited, collected by filtration, and dried in air. $C_{64}H_{60}Cl_2CoN_8O_8$, fw = 1199.05. Yield: 185 mg, 71.5%. IR (KBr pellet, cm^{-1}) 2966 w, 1614 w, 1464 m, 1419 m, 1286 w, 1085 s, 935w, 783 w, 749 m. Crystal structure (**2-5**).[A37]

***rac*-bis-[2,2'-bis[2-(1-propylbenzimidazol-2-yl)]biphenyl)]nickel(II) bis(perchlorate), *rac*-Ni(II)(9b)$_2$·(ClO$_4$)$_2$. (2-6)** A mixture containing two equivalents of **9b** (203 mg, 0.43 mmol), 79 mg of Ni(ClO$_4$)$_2$ · 6H$_2$O (0.22 mmol), 10 mL of acetonitrile, and 4 mL of triethyl orthoformate was heated to reflux. Following vapor diffusion of diethyl ether into the room-temperature mixture, dark-green crystals, exhibiting brown – green dichroism, suitable for X-ray diffraction were deposited, collected by filtration, and dried in air. $C_{64}H_{60}Cl_2N_8NiO_8$, fw = 1198.81. Yield: 231 mg, 87.6%. IR (KBr pellet, cm^{-1}) 3062 w, 2966 w, 2877 w, 1613 w, 1471 m, 1425 m, 1288 w, 1095 s, 787 m, 752 m. Crystal structure (**2-6**).[A38]

***rac*-bis-[2,2'-bis[2-(1-hydrobenzimidazol-2-yl)]biphenyl)]copper(II) bis(perchlorate), *rac*-Cu(II)(1e)$_2$·(ClO$_4$)$_2$. (2-7)** A mixture containing two equivalents of **1e** (200 mg, 0.518 mmol), 96 mg of Cu(ClO$_4$)$_2$ · 6H$_2$O (0.26 mmol), 15 mL of acetonitrile, and 1 mL of triethyl orthoformate was heated to reflux. Following vapor diffusion of diethyl ether into the room-temperature mixture, small dark-maroon crystals suitable for X-ray diffraction were deposited, collected by filtration, and dried in air. $C_{52}H_{36}Cl_2CuN_8O_8$, fw = 1035.34. Yield: 241 mg, 89.5%. Crystal structure (**2-7**).[A39]

***rac*- bis- [2,2'-bis [2-(1-propylbenzimidazol-2-yl)] biphenyl)] copper(II) bis(perchlorate), *rac*-Cu(II)(9b)$_2$·(ClO$_4$)$_2$. (2-8)** A mixture containing two equivalents of **9b** (210 mg, 0.446 mmol), 83 mg of Cu(ClO$_4$)$_2$ · 6H$_2$O (0.22 mmol), 8 mL of acetonitrile, and 1 mL of triethyl orthoformate was heated to reflux. Following vapor

diffusion of THF into the room-temperature mixture, dark-maroon crystals suitable for X-ray diffraction were deposited, collected by filtration, and dried in air. $C_{64}H_{60}Cl_2CuN_8O_8$, fw = 1203.66. Yield: 214 mg, 79.4%. Crystal structure (**2-8**).[A40]

***rac-* bis-[2,2'-bis [2-(1-propylbenzimidazol-2-yl)] biphenyl)] copper(II) bis(trifluoromethanesulfonate), *rac*-Cu(II)(9b)₂·(CF₃SO₃)₂. (2-9)** A mixture containing two equivalents of **9b** (180 mg, 0.382 mmol), 69 mg of $Cu(CF_3SO_3)_2$ (0.19 mmol), 8 mL of acetonitrile, and 1 mL of triethyl orthoformate was heated to reflux. Following vapor diffusion of diethyl ether into the room-temperature mixture, dark-maroon crystals suitable for X-ray diffraction were deposited, collected by filtration, and dried in air. $C_{66}H_{60}CuF_6N_8O_6S_2$, fw = 1302.90. Yield: 191 mg, 76.8%. Crystal structure (**2-9**).[A41]

***rac-* bis-[2,2'-bis [2-(1-octylbenzimidazol-2-yl)] biphenyl)] copper(II) bis(trifluoromethanesulfonate) · ethanol, *rac*-Cu(II)(9c)₂·(CF₃SO₃)₂·CH₃CH₂OH. (2-10)** A mixture containing two equivalents of **9c** (250 mg, 0.409 mmol), 74 mg of $Cu(CF_3SO_3)_2$ (0.20 mmol), 15 mL of ethanol, and 1 mL of triethyl orthoformate was heated to reflux. The mixture was allowed to crystallize by slow evaporation; dark-puple block-shaped crystals suitable for X-ray diffraction were deposited, collected by filtration, and dried in air. $C_{88}H_{106}CuF_6N_8O_7S_2$, fw = 1629.50. Yield: 312 mg, 95.7%. Crystal structure (**2-10**).[A42]

***rac-* bis-[2,2′-bis (1-ethylbenzimidazol-2-yl) biphenyl)] copper(I) trfluoromethanesulfonate toluene solvate dihydrate, *rac*-Cu(I)(9a)₂ · (CF₃SO₃)·(C₇H₈)·(H₂O). (2-11)**[12b] To a 10 mL mixture of 1:1 *v/v* acetonitrile/toluene containing 50 mg of $[Cu(CH_3CN)_4](CF_3SO_3)\cdot CH_3CN$ (0.12 mmol), 106 mg of **9a** (0.24 mmol) was added. A clear, pale-yellow solution resulted, which was sealed in a jar

containg diethyl ether to allow vapor diffusion. No steps were taken to exclude water from the system. Pale-yellow crystals of **2-11** precipitated over a three day period. $C_{68}H_{64}CuF_3N_8O_5S$, fw = 1225.08. Yield: 119 mg, 80.7%. ^1H NMR (400 MHz, CDCl$_3$): δ = 7.38 (d, J = 8.1 Hz, 4H), 7.28(m, 6H), 7.11(m, 11H), 6.91(d, J = 7.6 Hz, 4H), 6.76(d, J = 7.6 Hz, 4H), 6.52(t, J = 7.6 Hz, 4H), 5.87(d, J = 8.1, 4H), 4.27(d sextet, J = 54.5 Hz, J = 7.2 Hz, 8H), 2.37(s, 3H), 1.85(s, 2H, water), 1.53(t, J = 7.1 Hz, 12H). IR (KBr pellet, cm^{-1}) 3660 s, 3474 br, 3059 m, 2976 m, 2935 m, 1613 m, 1466 s, 1407 s, 1276 s, 1150 s, 1031 s, 638 s. Crystal structure (**2-11**).[12b,A43]

rac- bis-[2,2′-bis [2-(1-propylbenzimidazol-2-yl)] biphenyl)] copper(I) (perchlorate)·(CH$_3$CH$_2$OCH$_2$CH$_3$), _rac_-Cu(I)(9b)$_2$·(ClO$_4$)·(CH$_3$CH$_2$OCH$_2$CH$_3$). (2-12) A mixture containing two equivalents of **9b** (200 mg, 0.425 mmol), 70 mg of [Cu(CH$_3$CN)$_4$]·(ClO$_4$) (0.21 mmol), 10 mL of acetonitrile, and 2 mL of triethyl orthoformate was heated to reflux. Following vapor diffusion of diethyl ether into the room-temperature mixture, pale-yellow crystals, exhibiting colorless – pale-yellow dichroism, suitable for X-ray diffraction were deposited, collected by filtration, and dried in air. $C_{68}H_{70}ClCuN_8O_5$, fw = 1178.31. Yield: 211 mg, 83.7%. ^1H NMR (sample powdered and dried in vacuum) (400 MHz, CD$_3$CN): δ = 7.38 (d, J = 8.2 Hz, 4H), 7.10(t, J = 6.9 Hz, 4H), 7.03(t, J = 7.6 Hz, 4H), 6.86(t, J = 6.3 Hz, 8H), 6.74(d, J = 7.4 Hz, 4H), 6.43(t, J = 7.7 Hz, 4H), 5.92(d, J = 8.1, 4H), 4.06(d septet, J = 74.9 Hz, J = 4.8 Hz, 8H), 1.85(br m, 8H), 0.86(t, J = 7.3 Hz, 12H). ^{13}C NMR (CD$_3$CN): δ = 153.1, 142.9, 134.7, 131.0, 130.5, 129.5, 128.6, 123.8, 122.8, 121.3, 111.4, 47.4, 24.0, 11.5. Crystal structure (**2-12**).[A44]

***rac*-bis-[2,2'-bis[2-(1-propylbenzimidazol-2-yl)]biphenyl)]zinc(II)   bis(perchlorate),**

***rac*-Zn(II)(9b)$_2$·(ClO$_4$)$_2$. (2-13)**   A mixture containing two equivalents of **9b** (146 mg,

0.310 mmol), 158.0 mg Zn(ClO$_4$)$_2$ · 6H$_2$O (0.156 mmol), 8 mL of acetonitrile, and 1 mL

of triethyl orthoformate was heated briefly to gentle reflux. Following vapor diffusion of

diethyl ether into the room-temperature mixture, very-pale-pink crystals suitable for X-

ray diffraction, were deposited, collected by filtration, and dried in air. C$_{64}$H$_{60}$Cl$_2$N$_8$O$_8$Zn,

fw = 1205.51. Yield: 71 mg, 38.7 %. ^{1}H NMR (400 MHz, CD$_3$CN, 50 °C): δ = 7.69 (d, *J*

= 8.3 Hz, 4H), 7.35(dt, *J* = 25.8 Hz, *J* = 7.8 Hz, 8H), 7.12(q, *J* = 7.8 Hz, 8H), 7.03(d, *J* =

7.8 Hz, 4H), 6.70(t, *J* = 8.3 Hz, 4H), 5.67(d, *J* = 8.3, 4H), 4.26(d m, *J* = 64.4 Hz, 8H),

1.92(p, *J* = 2.5 Hz, 8H), 1.00(t, J = 7.4 Hz, 12H). Crystal structure (**2-13**).[A45]

***rac*-   bis-[2,2'-bis   [2-(1-propylbenzimidazol-2-yl)]   biphenyl)]   cadmium(II)**

bis(perchlorate), *rac*-Cd(II)(9b)$_2$·(ClO$_4$)$_2$. (2-14) A mixture containing two equivalents

of **9b** (179 mg, 0.38 mmol), 80 mg of Cd(ClO$_4$)$_2$ · 6 H$_2$O (0.19 mmol), 10 mL of

acetonitrile, and 1 mL of triethyl orthoformate was heated to reflux. Following vapor

diffusion of diethyl ether into the room-temperature mixture, colorless crystals suitable

for X-ray diffraction were deposited, collected by filtration, and dried in air.

C$_{64}$H$_{60}$CdCl$_2$N$_8$O$_8$, fw = 1252.53. Yield: 217 mg, 91%. Crystal structure (**2-14**).[A46]

***rac*-   bis-[2,2'-bis   [2-(1-propylbenzimidazol-2-yl)]   biphenyl)]   copper(II)$_{0.03}$**

cadmium$_{0.97}$(II)   bis(perchlorate),   *rac*-Cu(II)$_{0.03}$Cd$_{0.97}$(II)(9b)$_2$·(ClO$_4$)$_2$. (2-15)   A

mixture containing two equivalents of **9b** (150 mg, 0.319 mmol), 65.0 mg (0.155 mmol)

of Cd(ClO$_4$)$_2$ · 6 H$_2$O, 2.0 mg (0.005 mmol) of Cu(ClO$_4$)$_2$ · 6 H$_2$O, 10 mL of acetonitrile,

and 1 mL of triethyl orthoformate was heated to reflux. Following vapor diffusion of

diethyl ether into the room-temperature mixture, very pale-pink prisms suitable for X-ray

diffraction were deposited, collected by filtration, and dried in air. $C_{64}H_{60}Cd_{0.97}Cl_2Cu_{0.03}N_8O_8$, fw = 1251.06. Yield: 136 mg, 68.2%. Crystal structure (**2-15**).[A47]

Spectroscopic and Electrochemical Studies. NMR spectra were recorded using a Bruker AVANCE 400 Ultrashield spectrometer. Infrared spectra were measured using a Mattson Galaxy Series 5000 spectrophotometer. Electronic-spectral measurements were made using Cary instruments upgraded and computer-interfaced by Aviv Associates. Reflectance measurements were made using a Perkin-Elmer 330 spectrophotometer fitted with a 60 mm diameter integrating sphere. EPR spectra were measured with a Varian E-12 spectrometer calibrated with a Hewlett-Packard Model 5245-L frequency counter and a diphenyl picryl-hydrazyl crystal (g = 2.0036). Magnetic susceptibilities were measured from 2 K to 295 K using a Quantum Design SQUID magnetometer (MPMS-XL) operated at 1000 Oersted. Diamagnetic corrections for the sample holder and for the ligands and counterions (calculated from Pascal's constants) were applied to the susceptibilities.

All electrochemical measurements were carried out with a conventional three-electrode system. A glassy carbon disk of approximately 0.28 cm^2 surface area served as the working electrode. The reference electrode was a commercial saturated-calomel electrode (SCE), and a platinum wire was used as the counter electrode.

Both differential pulse polarography (DPP) and cyclic voltammetry (CV) experiments were performed using a BAS 100B electrochemical analyzer interfaced to a PC. Potentials for the manganese, **2-2**, oxidations were determined by DPP, while iron, **2-3**, oxidation and reduction potentials, as well as the cobalt, **2-5**, and copper, **2-8**,

oxidation potentials, were determined from CVs. All measurements were performed under nitrogen. CV measurements were made at scan rates of 25-300 mV/s. DPP measurements were made at 4 mV/s. Calibration was checked against ferrocene. Solutions were made from HPLC-grade dichloromethane that was distilled from CaH_2. A stock solution 0.05 M in tetra n-butyl ammonium hexafluorophosphate was prepared. Solutions of the complexes were prepared having concentrations of 1 x 10^{-4} to 2 x 10^{-4} M.

X-ray Crystallography. Diffraction measurements were made with a Bruker SMART CCD area detector system using ϕ and ω scans. In all cases, a hemisphere of data was collected. Initial cell parameters and data collection were performed using SMART software.[126a] The SAINT package[126a] was used for integration of data, cell refinement, Lorentz, polarization, and decay corrections, and for merging data. Absorption corrections were applied using SADABS.[126b]

Structures were solved and refined on F^2 using the SHELX system and all data.[126c,d] Partial structures were obtained by direct methods; the remaining non-hydrogen atoms in each structure were located using difference Fourier techniques. H atoms were located on difference Fourier maps or placed at calculated positions. For H atoms whose thermal parameters were not refined, isotropic temperature factors were set equal to 1.2-1.5 U_N, where N is the atom bonded to H. Views of the structures were prepared using ORTEP32 for Windows.[29] Additional metric details of the structures are presented in table 2-1 and ORTEP[29] diagrams are presented in the appendix.

Results and Discussion

Syntheses.

The facile syntheses of crystalline, tetrahedrally constrained metal complexes

were all effected by vapor diffusion of an ether into an acetonitrile solution of the metal complex with the single exception of **2-10**, which was obtained by slow evaporation. We have also discovered polymorphs of the geometrically constrained metal complex *rac*-bis-[2,2'-bis [2-(1-propylbenzimidazol-2-yl)] biphenyl)]] metal(II)] bis(perchlorate) (Figure 4-III (introduction)), where the metals are cobalt, nickel, copper, and zinc. These polymorphs were induced by altering the solvent from which the crystals were grown; this is by far the best known method for preparing polymorphs. When diethyl ether is utilized, the complexes crystallize in the orthorhombic space group *Pnn2*, and when tetrahydrofuran is utilized, the complexes crystallize in the monoclinic space group *Cc*.

Description of the Structures.

Ligand **9b** crystallizes in space group *P2₁/n* with two molecules in the asymmetric unit (Figure A14). Its bis complexes with Mn(II) **2-2**, Fe(II) **2-3**, Co(II) **2-5**, Ni(II) **2-6**, Zn(II) **2-13**, Cd(II) **2-14**, and Cu(II)$_{0.03}$Cd(II)$_{0.97}$ **2-15**, crystallize in space group *Pnn2* and are isomorphous. The polymorphic structure Cu(II) **2-8** crystallizes in the space group *Cc*. A view of one of the isostructural cations in **2-13,** is shown in Figure 2-2, in which hydrogen atoms important to the NMR discussion are labeled. In each structure, the benzimidazole and phenyl groups are planar to within 0.01-0.02 Å and, ligand flexibility is provided by torsional twist about the C-C bonds linking the planar groups. In effect, **9b** behaves as a three-hinged species. As suggested by the phenyl-phenyl dihedral angles (Table 2-1), the free and bound ligands **9b** exhibit significantly different conformations; **9b** adopts an extended, "trans" conformation with the benzimidazole fragments on opposite sides of the biphenyl group, while the bound ligands are of necessity "cis." In **9b**, the C12-N13 distances (Table 2-1) are significantly

shorter than the C12-N11 distances, implying substantial imine and amine character, respectively, for these linkages. Ligation results in substantial equilibration of the C12-N13 and C12-N11 distances in the isostructural compounds, consistent with electron delocalization over the N11-C12-N13 units, a common feature of imidazolium and benzimidazolium salts.[27a] In the crystal, molecules of **9b** pack with little or no π-overlap among the several aromatic groups. In contrast, the ethyl analog of **9b, 9a,** adopts an unusual, compact, twisted-clamshell conformation with intramolecular distances between *nearly-eclipsed*, slightly diverging imidazole fragments indicative of strong π-π interactions.[90a]

In the isomorphous compounds, both cations and anions exhibit crystallographically imposed 2-fold symmetry with the metal ions and one perchlorate Cl atom located on 2a sites (0, 0, z) and the other Cl atom located on 2b sites (0, ½, z). Perchlorate groups utilizing the 2b sites are ordered, while those on the 2a sites have one of the four oxygen atoms located on the 2-fold axis, and, as a consequence, three of the four oxygen atoms are disordered. The chelating benzimidazole ligands and metal ions form nine-membered rings whose conformation (Figure 2-3) is best described as twist-boat-boat (Figure 2-4), one of the 16 symmetrical conformations characteristic of 9-membered rings.[127] In the solid state, the chelate rings are effectively rigid and chiral. In a given cation, the ligands are related by crystallographic 2-fold axes and, therefore, must have the same handedness (*R, R* or *S, S*). Glide plane operations convert one enantiomer to the other; hence, each unit cell contains an equal number of *R, R* and *S, S* cations, and crystals of the isomorphic compounds are racemic salts. Individual cations also contain

approximate 2-fold axes normal to each other and to the crystallographically imposed 2-fold axis, giving them effective 222 (D$_2$) site symmetry.
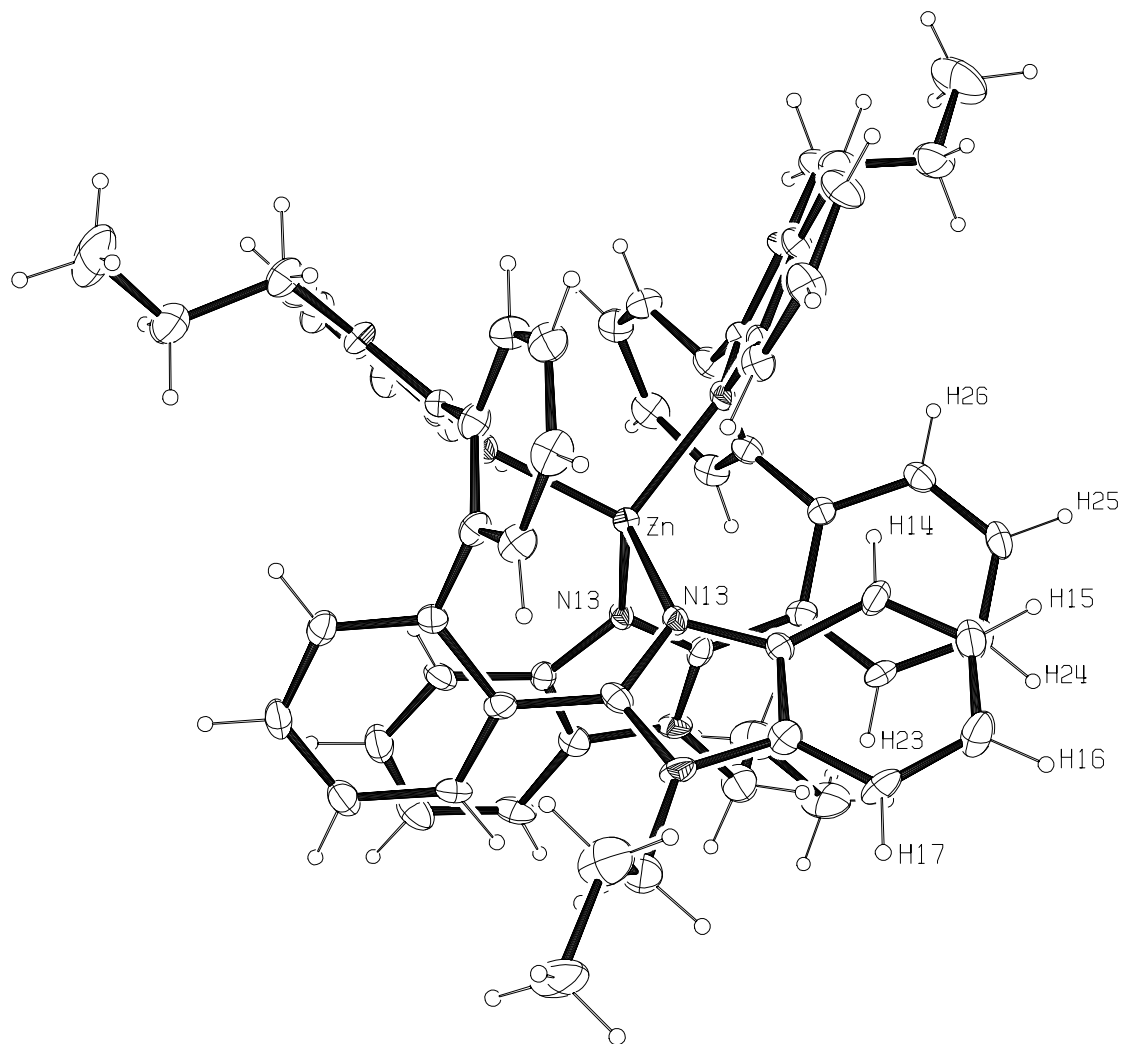

Figure 2-2. An ORTEP[29] view of one of the isostructural cations in **2-13**, *rac*-bis-[2,2'-bis[2-(1-propylbenzimidazol-2-yl)]biphenyl)]zinc(II). The thermal ellipsoids are drawn at the 25% probability level.

Table 2-1. Metric Parameters for the Species Studied (Å, deg).

complex	9b[a]	9b[a]	2-2	2-3	2-5
	9b-A	9b-B	Mn(II)(9b)$_2$(ClO$_4$)$_2$	Fe(II)(9b)$_2$(ClO$_4$)$_2$	Co(II)(9b)$_2$(ClO$_4$)$_2$
R group	propyl	propyl	propyl	propyl	propyl
space group	P2$_1$/n	P2$_1$/n	Pnn2	Pnn2	Pnn2
a	8.2663(17)	8.2663(17)	15.2527(15)	15.290(4)	15.1861(6)
b	16.200(3)	16.200(3)	17.1915(17)	17.226(4)	17.1390(7)
c	39.351(8)	39.351(8)	11.0902(11)	11.119(3)	11.0841(4)
α	90.0000	90.0000	90	90	90
β	90.700(3)	90.700(3)	90	90	90
γ	90.0000	90.0000	90	90	90
Volume	5269.2(18)	5269.2(18)	2908.0(5)	2928.7(12)	2884.91(19)
Z	8.0000	8.0000	2	2	2
T(K)	298(1)	298(1)	298(1)	298(1)	297(1)
M-N13			2.138(4)	2.078(4)	2.040(3)
M-N43			2.130(4)	2.078(4)	2.045(3)
M-N53					
M-N83					
Average M-N			2.134(4)	2.078(4)	2.043(3)
N13-M-N43			119.95(15)	120.89(14)	119.81(12)
N13-M-N13′			100.8(2)	99.8(2)	99.80(18)
N13-M-N43′			107.60(15)	108.35(15)	108.95(13)
N43-M-N43′			102.1(2)	100.0(2)	100.72(19)
N43-M-N53					
N53-M-N83					
φ-φ	126.7(1)	129.9(1)	50.2(2)	52.2(2)	66.4(1)
φ-φ′					
φ-Bz$_1$	52.2(1)	64.51(8)	56.7(2)	56.9(1)	58.7(1)
φ-Bz$_2$	62.1(1)	67.33(9)	58.0(1)	59.3(1)	57.1(1)
φ-Bz$_3$					
φ-Bz$_4$					
N1-C2(amine)	1.372(4)	1.368(4)	1.350(7)	1.334(6)	1.341(5)
N1-C2(amine)	1.374(4)	1.380(4)	1.338(6)	1.335(6)	1.352(5)
N3-C2(imine)	1.306(4)	1.311(3)	1.339(7)	1.351(6)	1.333(5)
N3-C2(imine)	1.314(4)	1.311(4)	1.336(6)	1.330(6)	1.332(5)

Table 2-1. Continued

2-6	2-7[a]	2-7[a]	2-8
Ni(II)(**9b**)$_2$(ClO$_4$)$_2$	Cu(II)(**1e**)$_2$(ClO$_4$)$_2$-A	Cu(II)(**1e**)$_2$(ClO$_4$)$_2$-B	Cu(II)(**9b**)$_2$(ClO$_4$)$_2$
propyl	hydro	hydro	propyl
Pnn2	Pbcn	Pbcn	Cc
15.191(3)	21.258(2)	21.258(2)	15.9272(19)
17.173(3)	20.264(2)	20.264(2)	22.997(3)
11.091(2)	21.453(2)	21.453(2)	16.1721(18)
90	90	90	90
90	90	90	93.279(2)
90	90	90	90
2893.4(10)	9241.5(16)	9241.5(16)	5913.9(12)
2	8	8	4
297(1)	100(2)	100(2)	297(1)
2.006(6)	1.979(5)	1.989(5)	1.977(7)
2.019(6)	1.988(5)	1.992(5)	1.989(6)
			2.007(6)
			2.012(6)
2.012(6)	1.984(5)	1.991(2)	1.997(14)
124.2(2)	138.8(2)	133.2(3)	135.7(2)
100.2(4)	95.8(3)	98.0(2)	96.06(11)
105.1(3)	97.3(2)	98.0(2)	96.93(11)
100.2(4)	98.0(3)	100.4(2)	100.3(3)
	97.3(2)	100.4(2)	102.0(2)
	138.8(2)	132.7(3)	132.2(2)
68.6(3)	69.4(2)	73.1(2)	68.53(27)
			67.99(28)
59.4(2)	51.3(2)	56.2(2)	66.30(19)
57.2(2)	60.0(2)	52.2(2)	68.53(27)
			67.87(22)
			65.94(23)
1.326(10)	1.349(8)	1.343(8)	1.371(9)
1.359(10)	1.352(8)	1.338(8)	1.339(10)
1.325(10)	1.330(7)	1.337(8)	1.327(9)
1.341(10)	1.332(8)	1.355(7)	1.335(10)

Table 2-1. Continued

2-9	2-10	2-11	2-12
Cu(II)(**9b**)$_2$(trif)$_2$	Cu(II)(**9b**)$_2$(trif)$_2$(EtOH)	Cu(I)(**9a**)$_2$(trif)(tol)(H$_2$O)$_2$	Cu(I)(**9b**)$_2$(ClO$_4$)(Et$_2$O)
propyl	propyl	ethyl	propyl
Cc	P-1	P2$_1$/c	Cc
16.386(5)	14.491(3)	11.1715(7)	16.506(3)
22.732(7)	16.454(4)	24.1173(10)	22.856(4)
16.858(5)	18.345(4)	23.0286(9)	16.341(3)
90	92.722(4)	90	90
96.968(4)	109.658(4)	95.190(4)	92.450(4)
90	98.020(4)	90	90
6233(3)	4058.0(15)	6179.1(5)	6158.9(19)
4	2	4	4
297(1)	100(1)	297(1)	
1.933(9)	1.994(3)	2.088(3)	2.074(7)
1.964(9)	1.996(3)	2.072(2)	2.089(7)
2.003(8)	1.996(3)	2.121(3)	2.106(7)
2.003(9)	2.004(3)	2.119(2)	2.112(7)
1.976(29)	1.998(4)	2.100(2)	2.095(7)
136.2(3)	136.21(13)	118.16(9)	119.2(3)
95.80(17)	95.66(13)	99.15(10)	98.51(11)
97.63(15)	98.70(13)	111.57(10)	110.9(3)
99.3(4)	98.80(13)	100.48(10)	98.71(12)
99.8(4)	99.87(13)	109.51(10)	110.6(3)
135.4(4)	134.63(13)	119.01(9)	120.3(3)
71.30(38)	68.97(14)	69.7(1)	64.5(3)
69.44(39)	67.44(14)	61.0(1)	63.0(3)
72.72(28)	71.77(12)	66.7(1)	70.4(2)
63.56(33)	67.12(11)	74.7(1)	71.1(2)
66.75(29)	55.23(11)	64.8(1)	71.8(2)
72.46(26)	65.32(12)	70.5(1)	70.2(2)
1.369(13)	1.358(5)	1.363(4)	1.368(12)
1.359(13)	1.353(5)	1.366(4)	1.362(13)
1.332(14)	1.331(5)	1.321(4)	1.321(13)
1.324(13)	1.336(5)	1.320(4)	1.320(12)

Table 2-1. Continued

2-13	2-14	2-15
Zn(II)(**9b**)$_2$(ClO$_4$)$_2$	Cd(II)(**9b**)$_2$(ClO$_4$)$_2$	Cu(II)$_{0.03}$Cd(II)$_{0.97}$(**9b**)$_2$(ClO$_4$)$_2$
propyl	propyl	propyl
Pnn2	Pnn2	Pnn2
15.176(3)	15.3374(15)	15.3773(17)
17.219(3)	17.2247(17)	17.2806(19)
11.069(3)	11.0491(11)	11.0846(12)
90	90	90
90	90	90
90	90	90
2892.5(10)	2919.0(5)	2945.5(6)
2	2	2
297(1)	297(1)	
2.035(8)	2.217(6)	2.206(3)
2.036(9)	2.233(7)	2.216(3)
2.036(8)	2.225(6)	2.211(5)
119.5(3)	119.2(2)	119.42(10)
100.6(5)	102.1(3)	102.20(16)
108.6(5)	107.8(2)	107.58(10)
101.2(4)	101.7(4)	101.68(16)
68.2(4)	60.1(3)	59.68(13)
59.7(3)	58.2(2)	58.07(9)
57.9(3)	56.9(2)	56.84(9)
1.346(14)	1.340(11)	1.355(4)
1.361(14)	1.350(11)	1.340(5)
1.323(14)	1.315(9)	1.322(4)
1.360(14)	1.338(11)	1.320(5)

[a]Two molecules in the asymmetric unt.
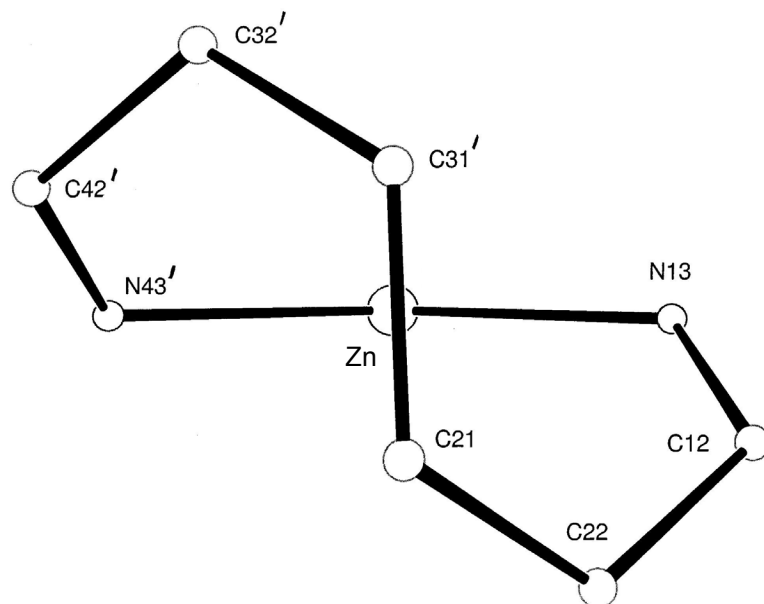
Figure 2-3. Nine-membered ring in one of the enantiomeric cations in **2-13**.
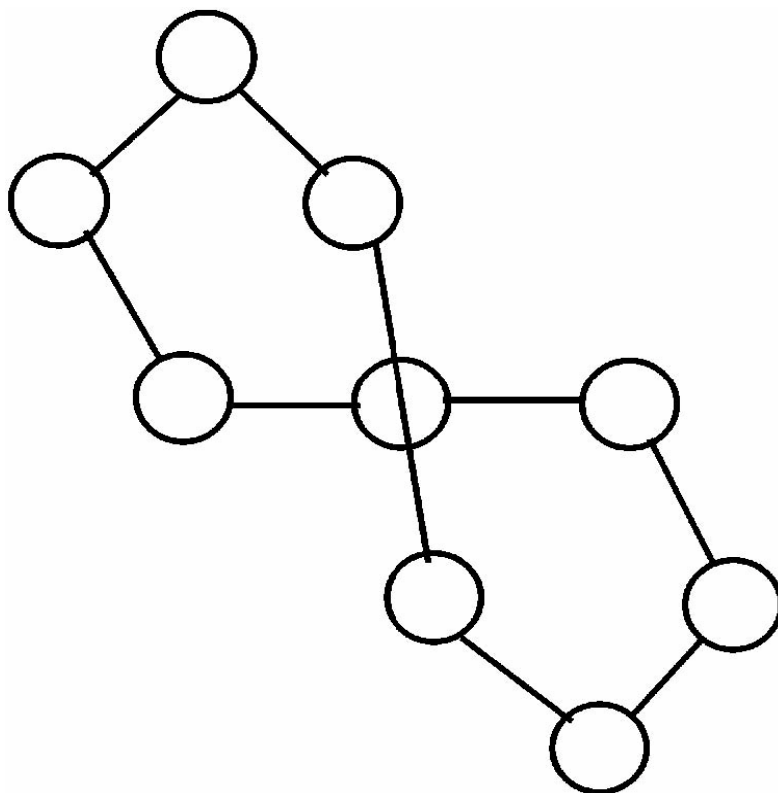
Figure 2-4. Twist-boat-boat conformation of a puckered nine-membered ring.

To our knowledge, **2-2** provides the first example of a structurally-characterized, four-coordinate Fe(II) complex containing an Fe-N(benzimidazole) bond, while cations **2-2** and **2-3** provide the first examples of four-coordinate Mn(II) and Fe(II) ions ligated exclusively by benzimidazoles. Relatively uniform ligation is expected to make these isostructural species especially attractive for spectroscopic studies.

In sum, the isostructural cations exhibit D_2-distorted-tetrahedral coordination geometries (Figure 2-5), with the largest variation of N-M-N bond angles found in the Cu(II) complex, **2-7**, which vary from 95.8(3) to 138.8(2)°. A major difference among the cations are the M-N distances: the average first row M(II)-N bond lengths are plotted in Figure 2-6 and show a periodic trend in which the shortest distance occurs for Cu(II). These are plotted alongside with the ionic radii of the M(II) ions in a T_d environment.[128] The differences in the M(II) distances appear to be attributable[129] primarily to the difference in ionic radii of the metals, rather than to crystal-field effects, which are expected to be small for tetrahedral complexes.
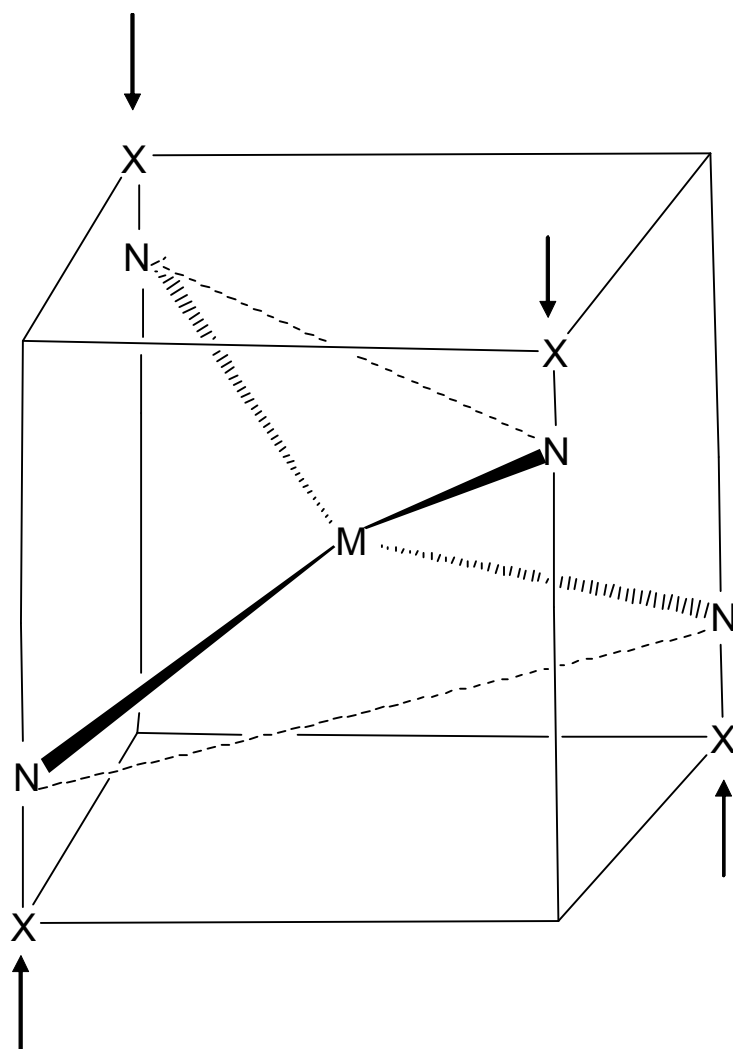
Figure 2-5. Sketch showing an idealized D_{2d} MN$_4$ coordination geometry for the isostructural ML$_2$ species. The four corners (X) of the cube indicate ligand N-atom locations for tetrahedral geometry (T_d); the arrows indicate the direction of motion required to produce D_{2d} geometry. The complexes **2-2** - **2-15** exhibit lower D_2 symmetry because the dihedral angle between the N-M-N planes in not 90°.
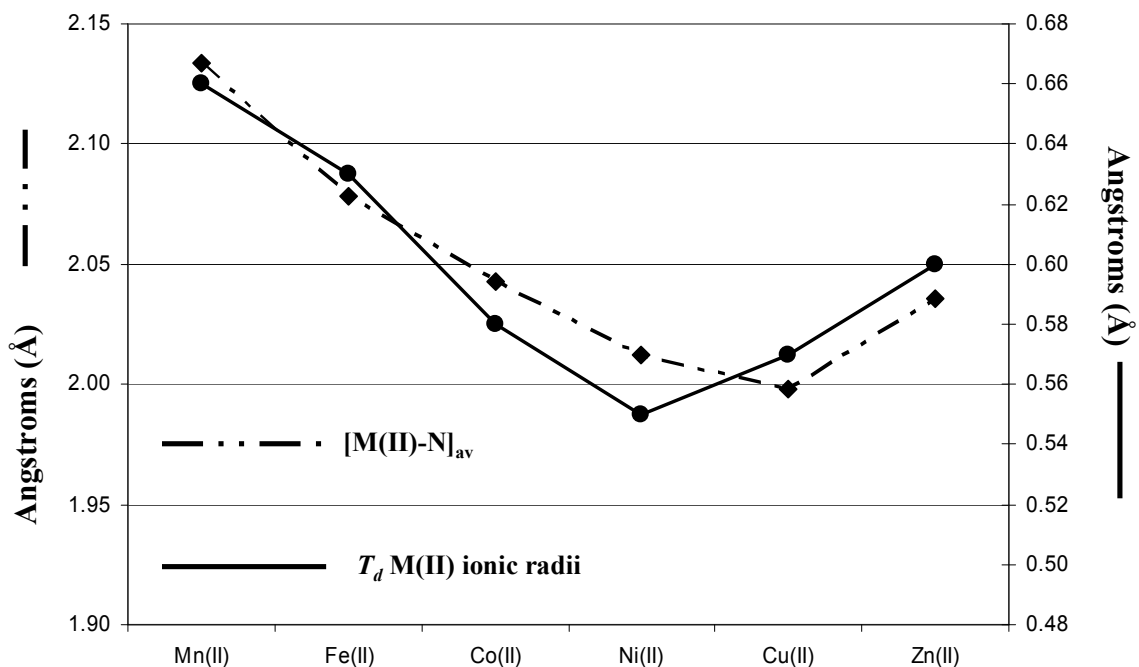
Figure 2-6. Periodic M(II)-N$_{av}$ bond lengths and T_d ionic radii.

While Figure 2-6 exhibits the expected periodic trend for M(II) species, a second plot (Figure 2-7) and third plot (Figure 2-8) correlate to other, possibly less expected, parameters. Figure 2-7 shows a plot of the average difference in M-N distance minus the ionic radius (T_d)[128] in angstroms and a plot of the deviation from tetrahedralality in degrees defined as $- |109.47 - (N\text{-}M\text{-}N)|_{av}$. Figure 2-8 shows plots of the average difference in M-N distance minus the ionic radius (T_d)[128] in angstroms and a plot of -Z, the negative of the scaled Lewis acid strength.[130] In Figure 2-7, there is a reasonable correlation between Δ(distance) and Δ(angle) for the metal ions with unfilled d-subshells (Mn(II)-Cu(II)) species. There is, however, no reasonable agreement or correlation for

those species whose metal ions have filled *d*-subshells [Cu(I), Zn(II), and Cd(II)]. Results

for the latter three species indicate that the differences in ionic radii of these metal ions

do not greatly influence the deviation from tetrahedrality. For these species, the Lewis

acid strength of the ion appears to be a better determinant. In Figure 2-8, the correlation

for the filled d^{10} species Cu(I), Zn(II), and Cd(II) and d^9 Cu(II) with the negative of

Lewis acid strength is reasonable, indicating that the strong Lewis acid Zn(II) forms a

stronger bond to the benzimidazole N(imine) base than does the weak Lewis acid Cu(I).

This observation will be examined further by the NMR ligand-exchange studies

presented below.
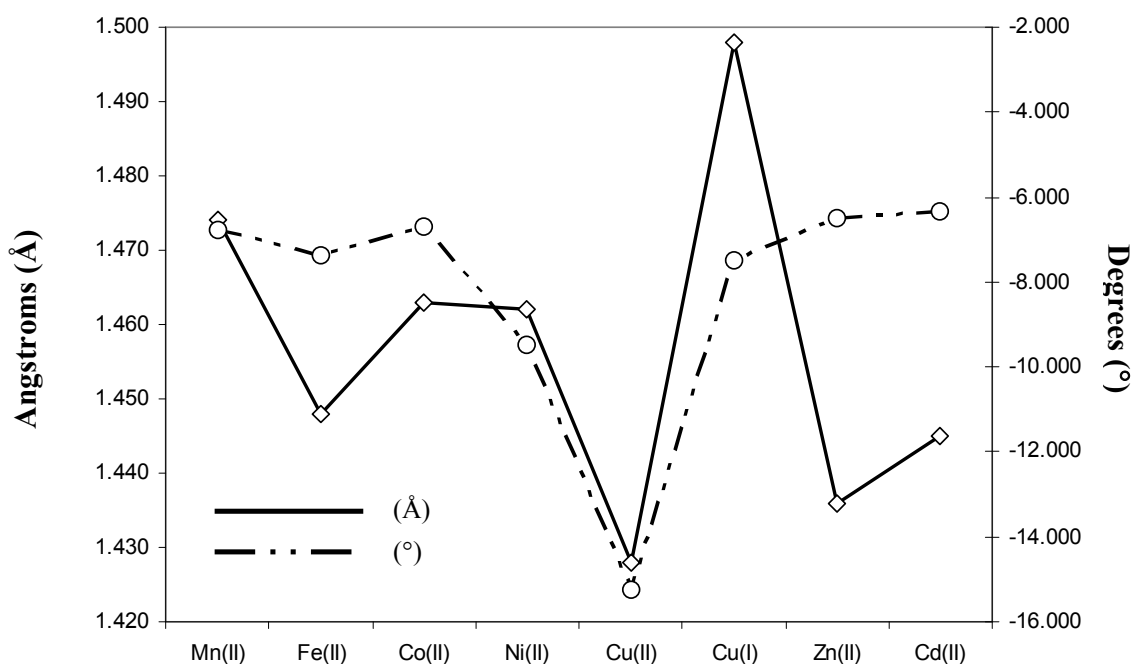
Figure 2-7. Plots of [(M-N)$_{av}$ - ionic radius (T_d)], Δ(Å) and deviation from tetrahedrality,

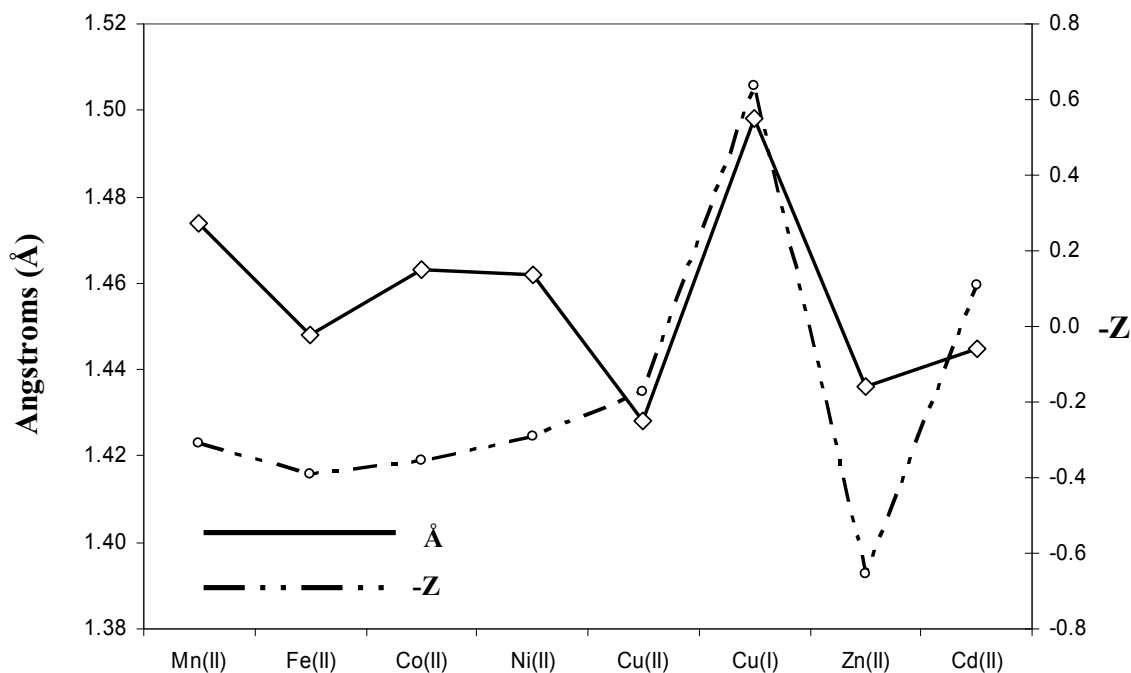Δ(°) defined by $-|$ 109.47 - (N-M-N)$|$ $_{av}$.

Figure 2-8. Plots of [(M-N)$_{av}$ - ionic radius (T_d)] (Å) and -Z, the negative of the scaled Lewis acid strength.

3. Electrochemical Studies

The reference compound **2-13** displayed no oxidations or reductions over the potential range studied for **2-2**, **2-3**, **2-5**, and **2-8**. The cation in **2-3** shows a one-electron reduction at $E_{1/2}$ = -1.60 V (Figure 2-9) corresponding to Fe(II) → Fe(I), as well as a one-electron oxidation at $E_{1/2}$ = 1.76 V (Figure 2-10) corresponding to Fe(II) → Fe(III). These potentials varied little for scan rates ranging from 25 to 300 mV/s for the oxidation (1.74 to 1.76 V) and from 50 to 300 mV/s for the reduction (-1.596 to −1.599 V). Over the same scan ranges, the difference between cathodic and anodic peak potentials

decreased with decreasing scan rate (from 238 mV to 108 mV for the Fe(II) oxidation

and from 135 mV to 115 mV for the Fe(II) reduction) towards the value expected[131] (59

mV) for reversible one-electron processes. The electrochemical stability of the Fe(III)

oxidation state in this system suggests that it might be possible to isolate an Fe(III)(**9b**)$_2$

complex and, we are currently attempting to do so. We are unaware of any structurally

characterized tetrahedral Fe(III)N$_4$ complexes. The cation in **2-2** shows a broad, quasi-

reversible, one-electron oxidation at $E_{1/2} = 0.64$ V (Figure 2-11) corresponding to Mn(II)

$\rightarrow$ Mn(III), as well as an irreversible oxidation at $E_{1/2} = 1.36$ V corresponding to Mn(III)

$\rightarrow$ Mn(IV). The cation in **2-5** shows a one-electron reduction at $E_{1/2} = -1.289$ V (Figure 2-

12) corresponding to Co(II) $\rightarrow$ Co(I). A one-electron oxidation corresponding to Co(II)

$\rightarrow$ Co(III) was not observed under our conditions. The cation in **2-8** shows a one-electron

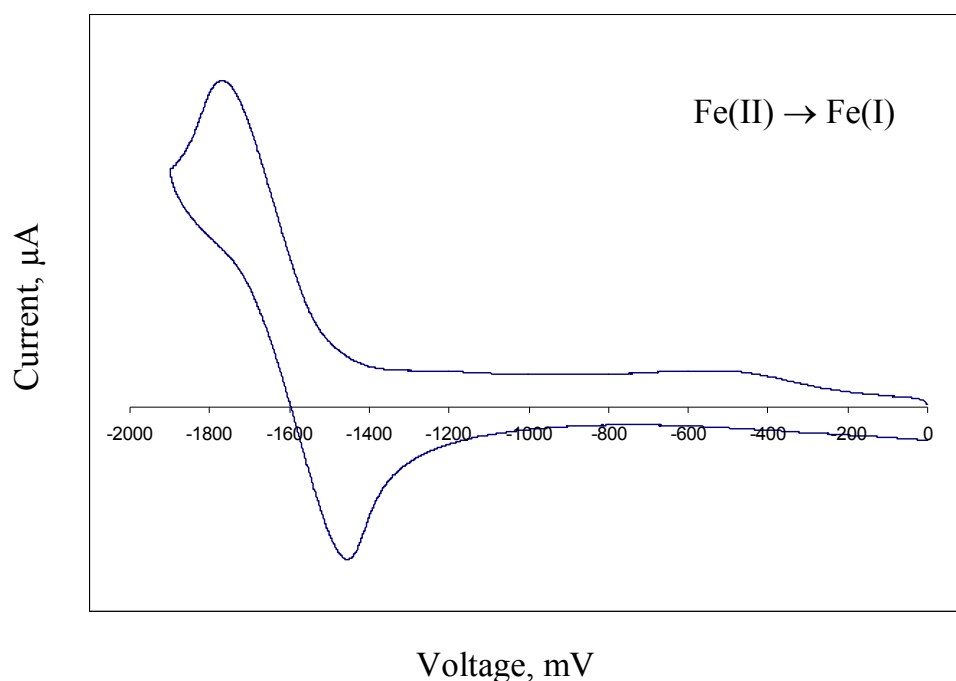oxidation at $E_{1/2} = 0.632$ V (Figure 2-13) corresponding to Cu(II) $\rightarrow$ Cu(III).

Figure 2-9. Cyclic voltammogram of the cation in **2-3** showing a Fe(II) → Fe(I) reduction; measured with a scan rate of 300 mV/s.
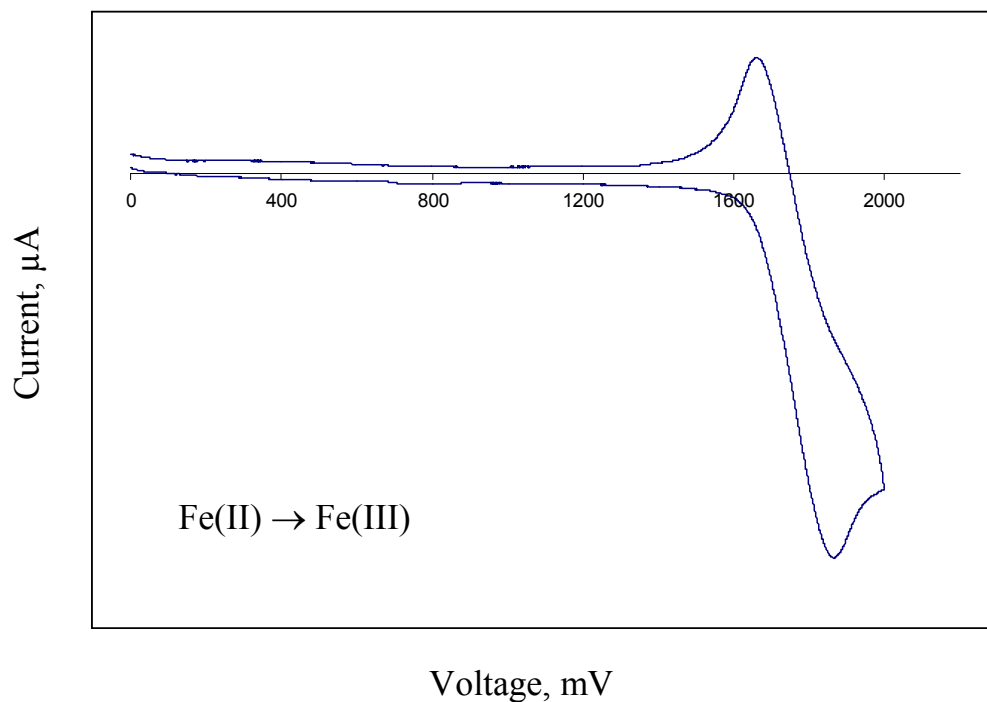

Figure 2-10. Cyclic voltammogram of the cation in **2-3** showing a Fe(II) → Fe(III) oxidation; measured with a scan rate of 300 mV/s.
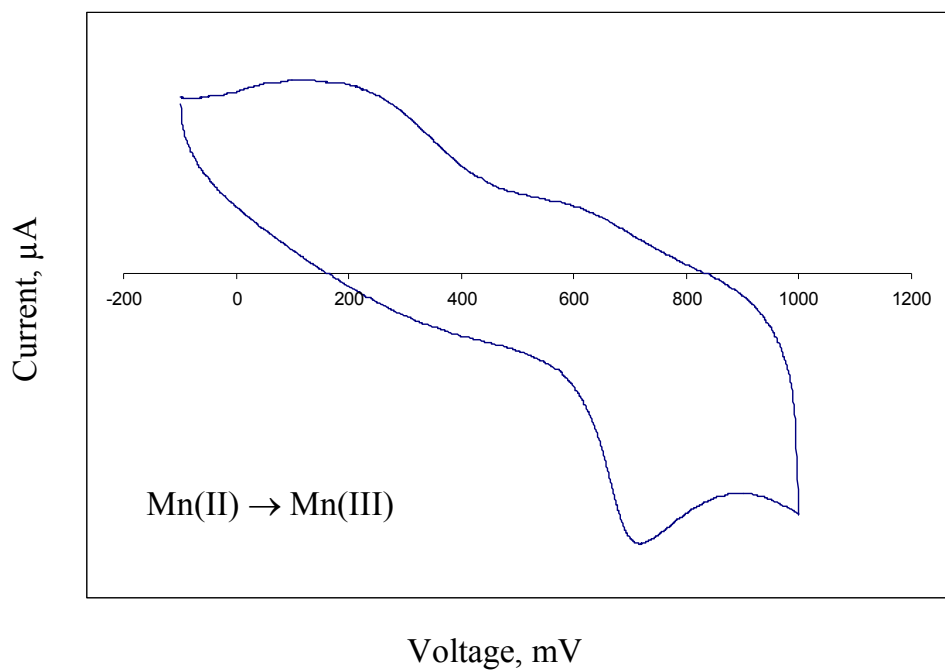
Voltage, mV

Figure 2-11. Cyclic voltammogram of the cation in **2-2** showing a Mn(II) $\rightarrow$ Mn(III) oxidation; measured with a scan rate of 50 mV/s.
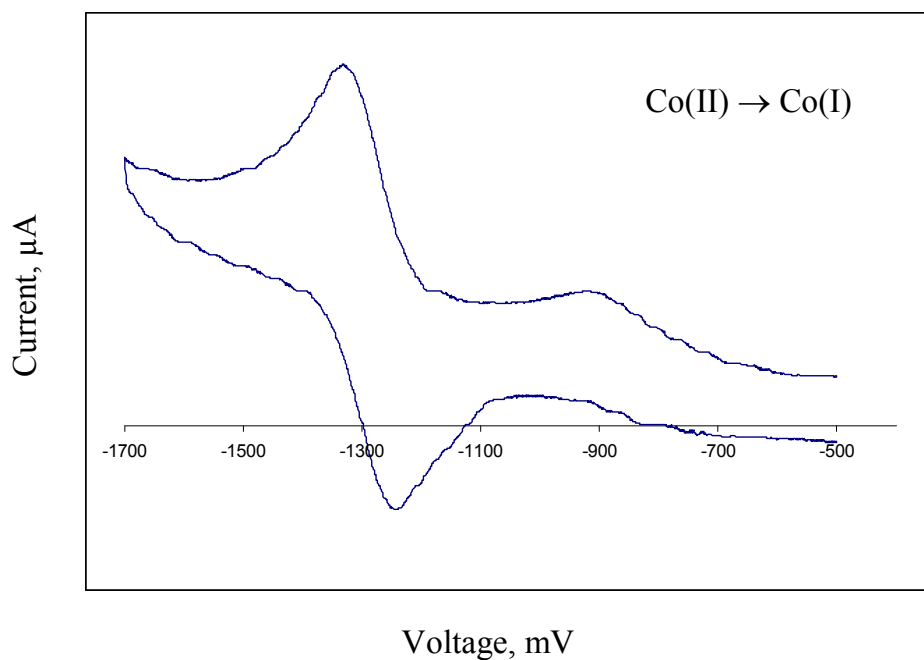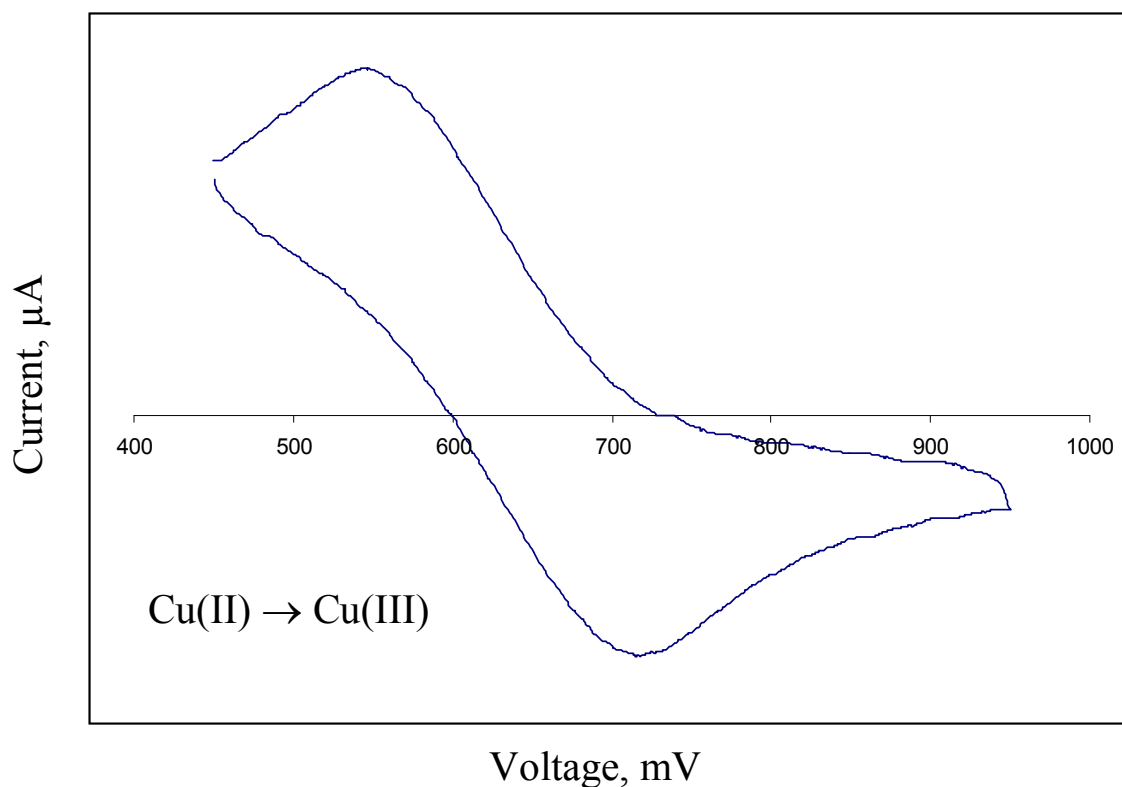

Voltage, mV

Figure 2-12. Cyclic voltammogram of **2-5** showing a Co(II) $\rightarrow$ Co(I) reduction; measured with a scan rate of 50 mV/s.

Figure 2-13. Cyclic voltammogram of the cation in **2-8** showing a Cu(II) → Cu(III) oxidation; measured with a scan rate of 50 mV/s.

Magnetic Studies

At room temperature, dichloromethane solutions of **2-2** exhibited broad X-band EPR spectra centered at g ~ 2.0 with few distinguishing features; these spectra did not sharpen noticeably at 77 K. The poorly-resolved Mn(II) hyperfine coupling constant was estimated to be ~ 100 Gauss (90 x 10^{-4} cm^{-1}). Improved resolution (Figure 2-14) was obtained when the powdered polycrystalline isostructural nominally 3% Mn(II)-doped Zn(II) analogue **2-4** was measured. The spectrum exhibits the characteristic 6-line Mn(II) hyperfine structure, along with additional structure whose origin is uncertain. Recent

studies have shown that axial and rhombic zero-field splitting (ZFS) effects, which can contribute to hyperfine structure exhibited by Mn(II) chromophores, are difficult to simulate convincingly at X-band;[132] however, studies at considerably higher frequencies have allowed axial and rhombic ZFS effects to be quantified for a distorted-tetrahedral Mn(II) complex.[133] The observed g value [2.003(1)] is typical for a sextet ground state Mn(II) ion (see magnetic susceptibility results) which can not spin-orbit couple to excited ligand-field states, all of which carry lower spin multiplicities. Moreover, in **2-2**, Mn(II) is bound to N-donor atoms that can not introduce substantial ligand-supplied spin-orbit effects. Smaller Mn coupling (65-79 Gauss) has been reported for several tetrahedral Mn(II) complexes, whereas larger coupling (86-93 Gauss) appears to be characteristic of octahedral Mn(II) chromophores.[134] The trend of increased Mn hyperfine coupling reported for octahedral Mn(II) complexes relative to their regular tetrahedral analogs might not extend to the case of low-symmetry, nearly-tetrahedral Mn(II) chromophores such as, **2-2,** which exhibits C_2 crystallographic and approximate D_2 site symmetry.
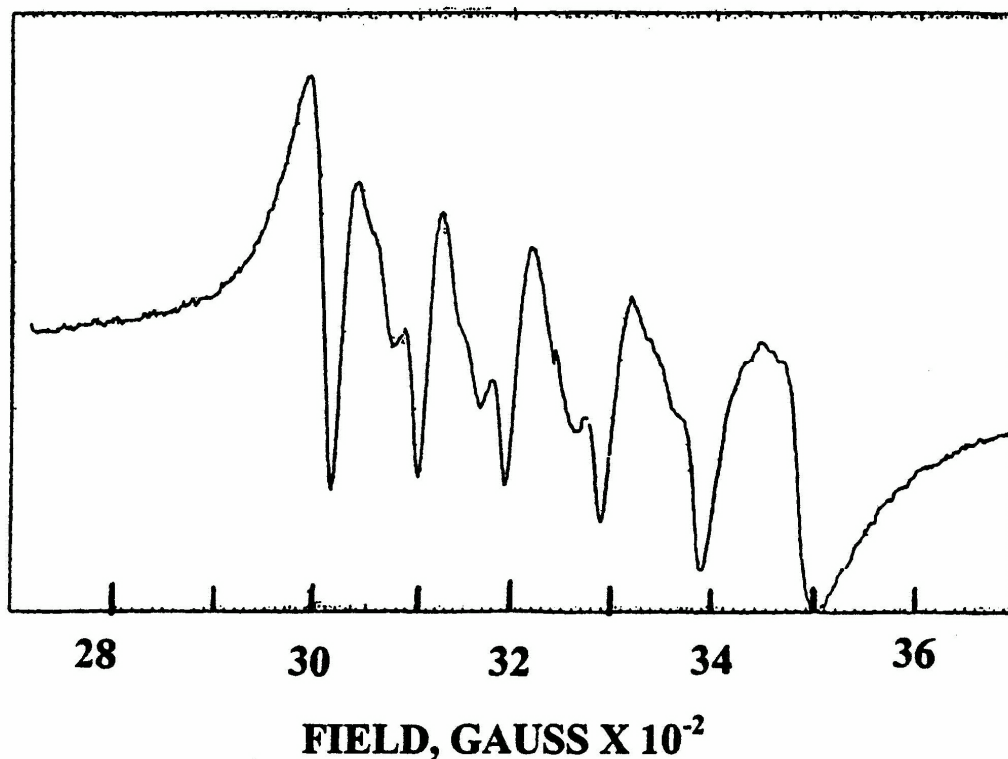
Figure 2-14. X-Band EPR spectrum at 90 K of polycrystalline, nominally 3% Mn(II)-doped Zn(II), **2-4**.

Dichloromethane solutions of **2-3** were EPR-silent at X-band both at room temperature and at 77 K. As is typical for high-spin Fe(II) complexes, zero-field splitting (see below) for **2-3** exceeds the available microwave energy of about 0.3 cm^{-1} at X-band (ca. 9 GHz) frequencies. Higher frequency EPR spectrometers (> 94 GHz) are required to obtain energies large enough to pump the $\Delta m_s = 1$ transitions of non-Kramers S = 2 Fe (II) complexes showing zero-field splitting.[135]

Corrected magnetic susceptibilities and magnetic moments of **2-2** and **2-3** from 5-295 K are shown in Figure 2-15. The magnetic moment of **2-2** is close to the spin-only

value (5.92 μ_B) for an S = 5/2 Mn(II) system. As noted above, spin-orbit contributions are not expected for the $^6A_1$ ground state, consonant with the modest decrease in magnetic moment from 6.05 μ_B at 295 K to 5.92 μ_B at 15 K. The magnetic moment of **2-3** at 295 K is increased slightly from the spin-only moment (4.90 μ_B) to 5.02 μ_B, possibly owing to an orbital contribution which is allowed for this approximately-tetrahedral high-spin d^6 Fe(II) complex.[136a] Upon cooling to 50 K, A slow decrease to 4.81 μ_B is observed, followed by a more pronounced falloff to 3.97 μ_B as the temperature is decreased to 5 K. The latter behavior is characteristic of Fe(II) complexes exhibiting positive zero-field splitting.[137-139]

As noted above, the *R, R* and *S, S* Fe(II) chromophores in **2-3** adopt flattened, nearly-tetrahedral geometries with apparent D_2 symmetry (three perpendicular 2-fold axes), even though only one 2-fold axis is crystallographically required. This latter axis is positioned perpendicular to the direction of flattening, a structural feature previously noted for the Ni(II) and Co(II) complexes of a related bidentate bis(imidazole)biphenyl ligand.[34] Although the chirality of individual cations precludes point symmetry containing mirror planes or centers of symmetry, the spectroscopically effective site symmetry of the bare Fe(II)N_4 subunits in **2-3** could be as high as D_{2d}. The energy level diagram for a D_{2d}-flattened pseudotetrahedral Fe(II) complex (Figure 2-16) shows the split ligand-field (LF) transitions Δ_1 and Δ_2 (see the electronic-spectral studies section below) and a positive zero-field splitting parameter D arising from spin-orbit coupling of the $^5A_1$ (d_{z^2}) ground state. D values for four pseudotetrahedral Fe(II) complexes have been measured by combined Mossbauer/magnetic susceptibility studies and that of a fifth complex by independent Mossbauer, far-infrared absorption, and high frequency EPR

spectroscopies. The reported D values span the range -5 to 11.6 cm^{-1}. An estimate of D

for **2-3** may be obtained from LF theory using the relationship $D = \dfrac{3\lambda^2}{\Delta_1}$, where λ is the

spin-orbit coupling constant and Δ_1 is the energy separation between the ^{5}E excited state

and the ^{5}A$_1$ (d_{z^2}) ground state (Figure 2-16).[139] The free-ion value of λ for Fe(II) is 107

cm^{-1}, and is thought to be reduced by covalency in Fe(II) complexes to ~ 80 cm^{-1}.[135,137,139]

If Δ_1 is taken to be 5 000 cm^{-1}, the average of the two lowest LF absorptions (see

electronic-spectral studies section below), the estimated value of D is ~ 4 cm^{-1}.

Although none of the D values reported in the literature is based solely upon

magnetic susceptibility data, we attempted to estimate D, the zero-field splitting, and g

values from a detailed analysis of low-temperature susceptibility data for **2-3**. A fresh

sample was prepared, recrystallized twice, ground to a fine powder, and pressed into a

pellet to minimize any preferential orientation of the crystallites in the magnetic field.

Susceptibility data were recorded at ~ 0.25 K intervals over the 2-50 K temperature range

and attempts were made, using non-linear least-squares methods, to fit the data to the

following expression for the molar susceptibility, χ_M, which was derived for the D$_{2d}$

symmetry case:[137,140]

$$\chi_M = \frac{1}{3}\chi_\parallel + \frac{2}{3}\chi_\perp = \left(\frac{2N\beta^2 g_\parallel^2}{3kT}\right)\left(\frac{e^{-d} + 4e^{-4d}}{1 + 2e^{-d} + 2e^{-4d}}\right) + \left(\frac{4N\beta^2 g_\perp^2}{9D}\right)\left(\frac{9 - 7e^{-d} - 2e^{-4d}}{1 + 2e^{-d} + 2e^{-4d}}\right)$$

where $d = \dfrac{D}{kT}$ and $\dfrac{N\beta^2}{3k} = 0.1251$.

The results are summarized as follows. The non-linear least-squares fit is initial-

conditions dependent, and, for example, similar, stable and reproducible fits could be

obtained yielding positive or negative D values, starting from different positive or negative D values, respectively. The values obtained for the two minima are: $D = 2.1(5)$ cm^{-1}, $g_{//} = 2.41(9)$ and $g_{\perp} = 1.54(8)$; $D = -6.82(4)$ cm^{-1}, $g_{//} = 1.769(1)$, and $g_{\perp} = 2.063(2)$. The second set of values corresponds to the "best" fit, i. e., the one with the lowest χ^2 value. With $g_{//}$ and $g_{\perp}$ each fixed at 2.0, the resulting D value is -28 ± 3 cm^{-1}, and the fit is substantially inferior. When g and D are allowed to vary independently, g values significantly less than 2.0 are obtained, a physically impossible result for a d^6 Fe(II) ion with a greater than half-filled d subshell. These difficulties suggest that the equation above is unsuitable for rhombically split sites because, among other things, χ_M no longer is equal to $\frac{1}{3}\chi_{//} + \frac{2}{3}\chi_{\perp}$. As a result, neither an unambiguous value of D nor reasonable g values could be extracted from an analysis of the low-temperature magnetic susceptibility data. For a distorted-tetrahedral Fe(SPh)$_4$$^{2-}$ chromophore, the rhombic contribution to ZFS was calculated to be $+1.4$ cm^{-1}, a substantial fraction of the axial contribution, $+5.8$ cm^{-1}.[135]

Finally, the susceptibility data closely follow Curie-Weiss behavior with $C = 3.00$ and $\theta = -3.3$ K. The relationship $g_{eff} = 2.828\left(\dfrac{C}{S(S+1)}\right)^{1/2}$ with $S = 2$ gives a plausible g value of 2.00. However, the substantial size of ligand **9b** suggests that that **2-3** is magnetically dilute, and therefore, that a finite value of θ need not signify a magnetic interaction between the complexes. It merely means that a Curie-Weiss analysis of a magnetically non-interacting complex can effectively mask whatever phenomena actually are contributing to the observed magnetic behavior. For Fe(II), the well-documented ZFS may be obscured.[136b]
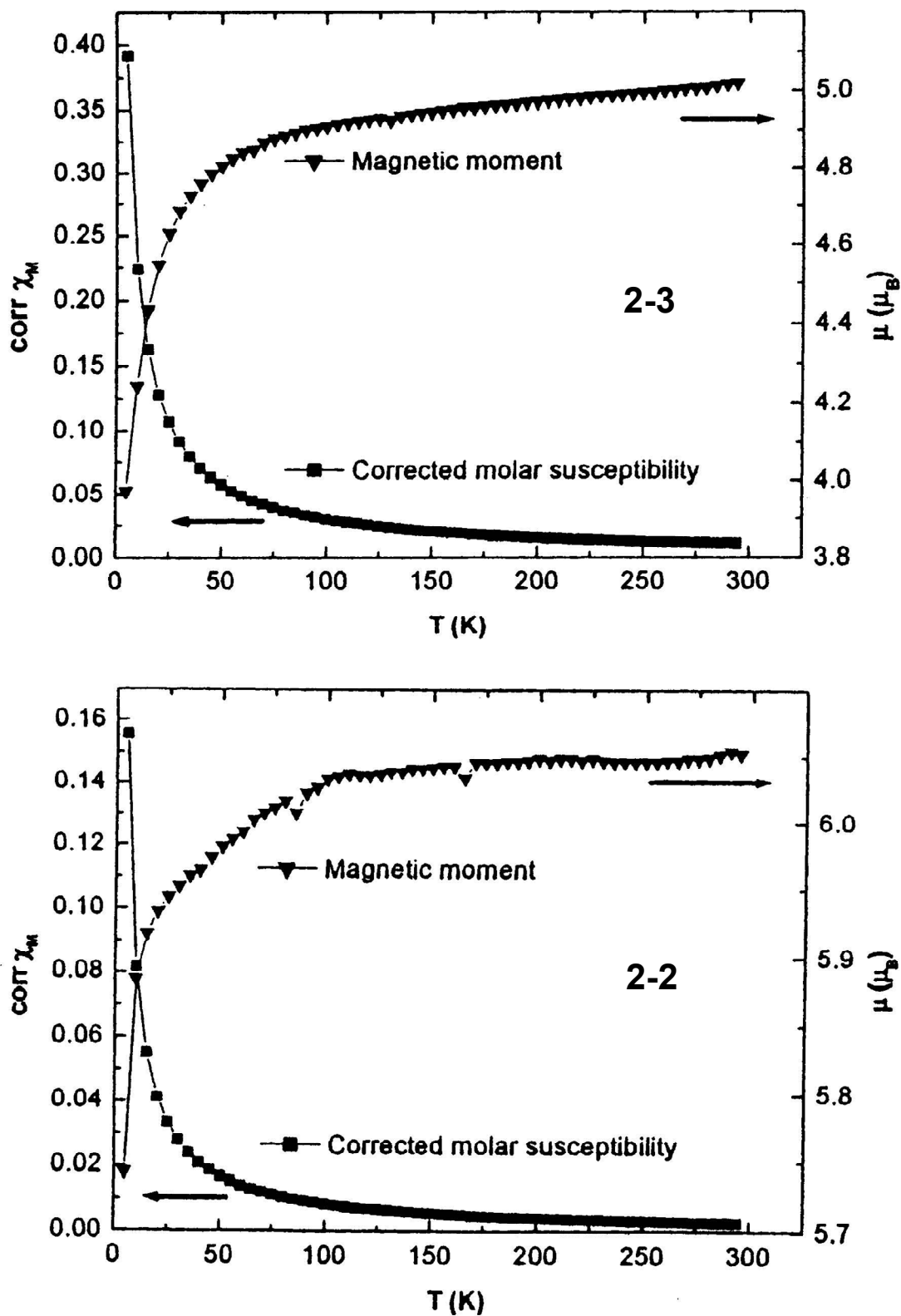
Figure 2-15. Magnetic susceptibilities in emu/mole and magnetic moments of a) **2-3**; and b) **2-2** over the 5-295K temperature range.
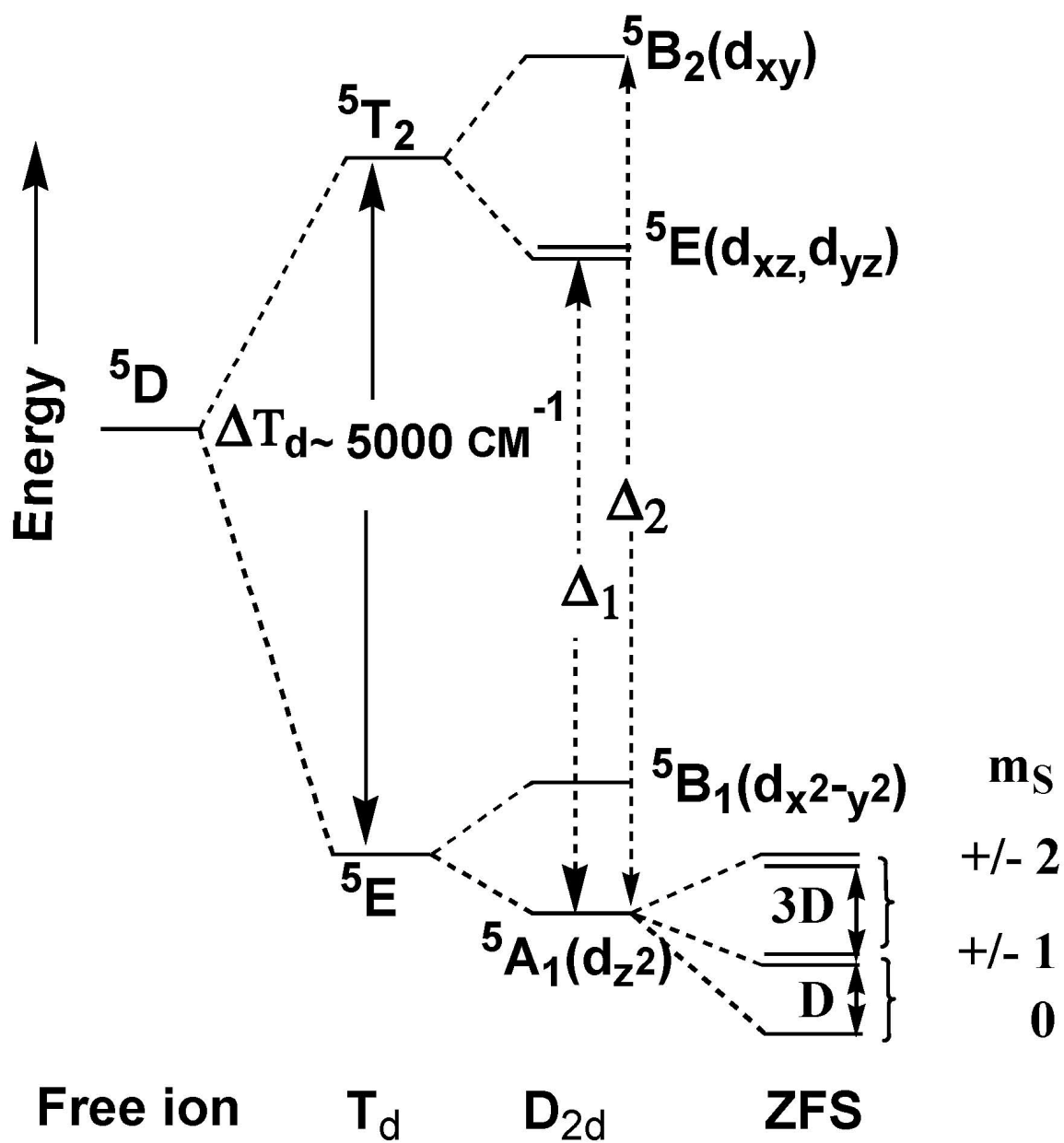
Figure 2-16. Energy level diagram for a D_{2d}-flattened pseudotetrahedral Fe(II) complex.

Electronic-Spectral Studies.

Electronic spectra of **9b, 2-2**, **2-3**, **2-5**, **2-6** and **2-8** are summarized in Table 2-2. The deconvoluted spectrum of **9b** shows three broad overlapping absorptions centered at 33 000 (ε = 20 000), 40 700 (ε = 54 000), and 48 100 (ε = 150 000) cm^{-1}. The positions and intensities of these bands correspond roughly to the composite absorptions of its biphenyl and benzimidazole subunits. Biphenyl[141a] shows a broad absorption at 40 500 cm^{-1} (ε = 19 300), whereas benzimidazole and 2-alkyl-substituted benzimidazoles show progressions of absorptions[141b] centered at ~ 35 600 cm^{-1} (ε ~ 6 000) and ~ 40 000 cm^{-1} (ε ~ 6 000), along with a more intense absorption at 47 600 cm^{-1} (ε ~ 27 900). These benzimidazole extinction coefficients should be doubled to place them and the spectrum of **9b**, which contains two benzimidazole units, on the same scale. A recent study of benzimidazole[142] suggests that the band system at ~ 35 600 cm^{-1} has mixed, but predominantly HOMO $\rightarrow$ LUMO orbital character. The flanking higher-energy pattern at ~ 40 000 cm^{-1} is thought to contain HOMO $\rightarrow$ LUMO + 1 character, whereas the highest-energy absorption was assigned as predominantly HOMO - 1 $\rightarrow$ LUMO + 1. Ultraviolet spectra of **2-3** and **2-2** are dominated by the absorptions of ligand **9b,** blue-shifted by ~ 2 000 to 3 000 cm^{-1}. Possible charge-transfer and/or LF absorptions in the uv region are obscured by the more intense ligand absorptions.

In both the solution and reflectance spectra of high-spin **2-2**, the expected spin-forbidden sextet $\rightarrow$ quartet LF absorptions were too weak to characterize clearly. Measurements of such absorptions typically require low-temperature, single-crystal studies.[143] In contrast, the more intense low-energy LF absorptions expected for high-spin

2-3 were readily seen in the room temperature reflectance spectra. The reflectance

spectrum of **2-2** was used as a control to identify absorptions in this region due to ligand

infrared vibrational overtones. LF absorptions of tetrahedral Mn(II) are not observed at

energies below 18 000 cm^{-1}.[143-145] Broad absorptions of **2-3** at 4 700 and 5 300 cm^{-1},

are attributed to $^5A_1 \rightarrow {}^5E$ absorptions (Δ_1 in Figure 2-16) of this approximately D_{2d}

Fe(II) chromophore split by the reduction of symmetry to D_2 as noted in the

crystallographic discussion. The broad shoulder at $\sim$ 6 000 cm^{-1} is assigned to the

expected $^5A_1 \rightarrow {}^5B_2$ transition shown as Δ_2 in Figure 2-16.[145] The solution spectrum of **2-

5** exhibits a LF triplet with transitions at 16 500, 17 300, and 18 500 cm^{-1}. This transition

is attributed to $^4A_2 \rightarrow {}^4T_1({}^4P)$ absorptions and are commonly observed for Co(II) ions in a

tetrahedral environment.[146] The LMCT is likely obscured by the intense ligand

absorptions, and near-infrared spectra were not measured. The solution spectrum of **2-6**

exhibits three LF bands at 12 700, 15 600, and 20 900 cm^{-1}. These bands are attributed to

$^3T_2(P) \rightarrow {}^3T_1(F)$ absorptions and are commonly observed for Ni(II) ions in a tetrahedral

environment.[147] These three LF bands are similar in intensity and energy to those

reported for the Ni(II)-imidazole analogue.[34] The LMCT band is likely obscured by the

intense ligand absorptions. Near-infrared spectra were not measured. The solution

spectrum of **2-8** exhibits two LF bands at 13 900 and 19 600 cm^{-1}. These compare to the

two LF bands of 12 500 and 15 400 cm^{-1} reported for the Cu(II)-imidazole analogue.[34]

The shoulder observed at 23 300 is assigned as the LMCT and compares to 22 700 cm^{-1}

reported for Cu(II)-imidazole analogue.[34] The blue shift in all of the observed transitions

in **2-8** compared to the analogous imidazole complex, may be attributed to the more

nearly tetrahedral environment of **2-8**. In both cases only two bands are observed when

three possible transitions exist for Cu(II) with D_{2d} coordination symmetry.[148] The near-infrared spectra were not measured.

Table 2-2. Summary of Deconvoluted Electronic and Reflectance Spectra

substance	energy, cm^{-1})	ε^a
9b	33 100	20 000
	40 700	54 000
	48 100	150 000
2-3	4 700^b	broad
	5 300^b	broad
	~ 6 000^b	shoulder
	35 900	22 000
	43 200	2 750
	~50 000	92 500

2-2	35 200	19 000
	42 600	31 000
	~50 000	110 000

2-5	16 500	570
	17 300	400
	18 500	290
	35 300	19 500

2-6	12 700	15
	15 600	90
	20 900 sh	130
	35 200	21 900

2-8	13 900	180
	19 600	720
	23 300 sh	430
	35 200	23 200

[a] Extinction coefficients are normalized to one ligand **9b**. [b] Reflectance data.

NMR Studies

To examine the solution chemistry and to determine the extent of ligand exchange, solutions of the diamagnetic species **2-12** and **2-13** with **9b** in deuterioacetonitrile were examined. The proton-numbering scheme is shown in Figure 2-17. For the ligand exchange experiments, the terminal methyl fragments of the n-propyl groups (1A, Figure 2-18) were followed as a function of temperature. The ligand exchange experiments were followed over a temperature range of 30 to 75 °C monitoring the spectra at 10 °C intervals, except for the high-temperature measurement. The extremes of the temperature range for **2-12** and **2-13** are depicted in Figures 2-19 and 2-20, respectively.
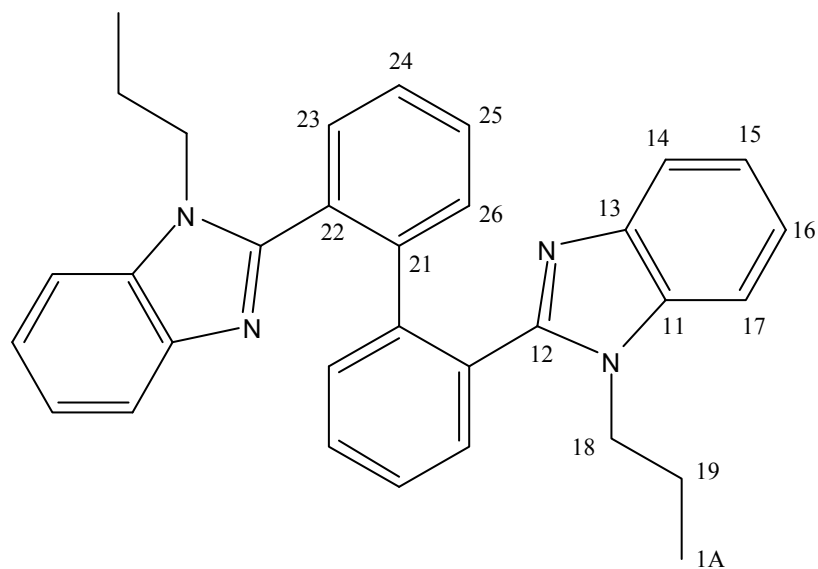
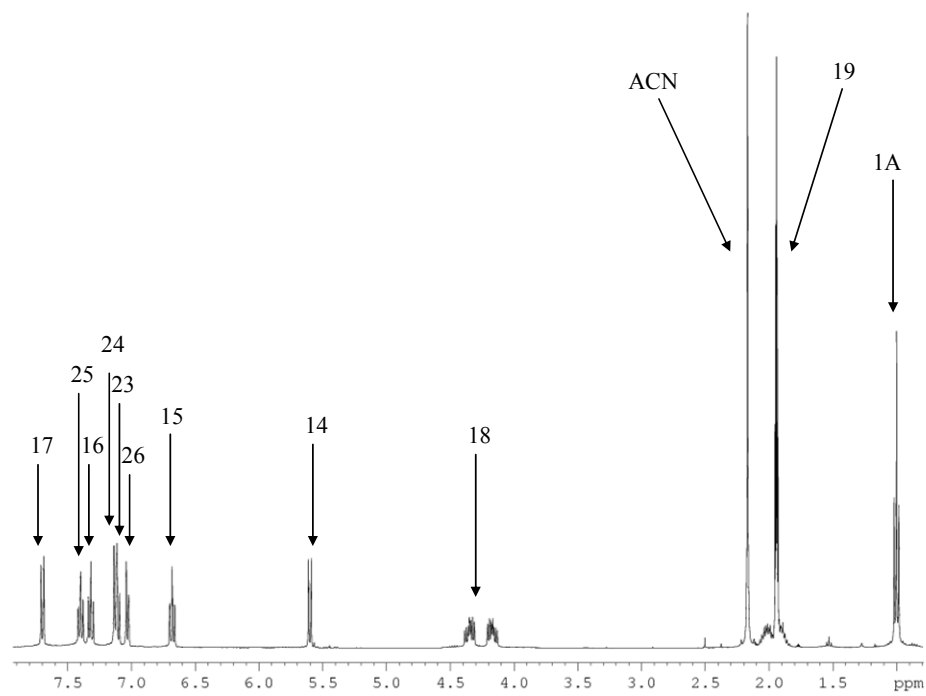**Figure 2-17.** Proton numbering scheme for **9b, 2-12, and 2-13**.

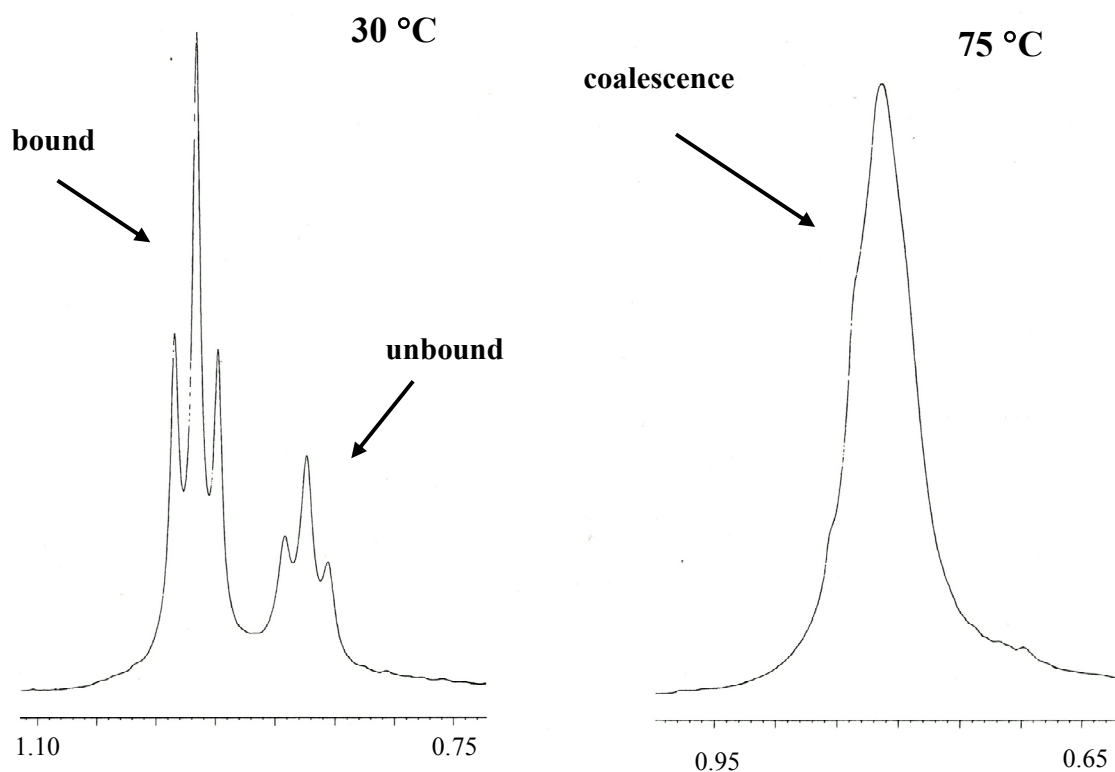**Figure 2-18.** ^{1}H NMR spectra (400 MHz, CD$_3$CN) at 30 °C of a solution 8.0 mM in **2-13**.

Figure 2-19. ^{1}H NMR spectra (400 MHz, CD$_3$CN) at 30 and 75 °C of a solution 8.0 mM in **2-12** and 4.0 mM in **9b**.
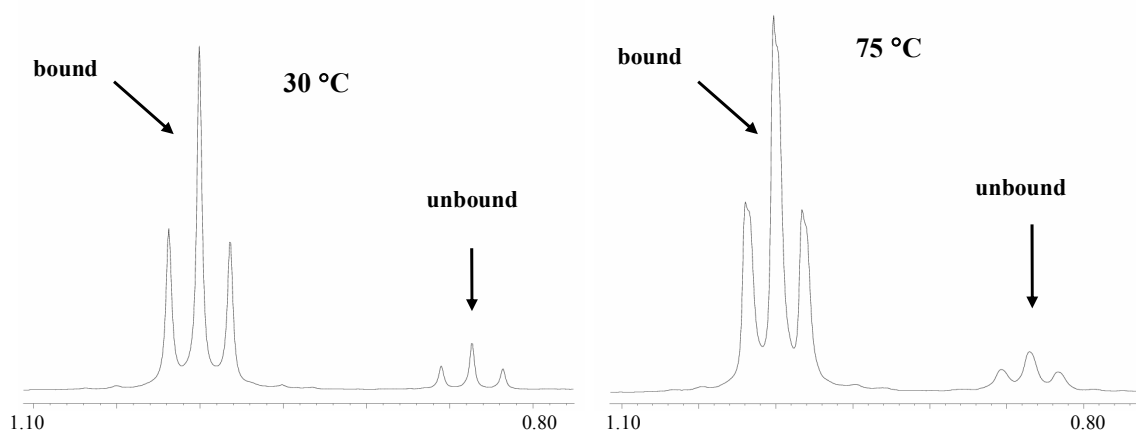

Figure 2-20. ^{1}H NMR spectra (400 MHz, CD$_3$CN) at 30 and 75 °C of a solution 8.0 mM in **2-13** and 4.0 mM in **9b**.

As the temperature of the solution of **2-12** (Figure 2-20) was raised to 75 °C the signals of the 1A protons fully coalesced, indicating facile ligand exchange at the higher temperature on the NMR time scale. The coalescence temperature is 60 °C higher than that of the analogous Cu(I)-imidazole complex,[34] indicating that benzimidazole forms much stronger metal-ligand bonds than imidazole. This higher stability is an important aspect when considering applications of these complexes in areas such as catalysis. The solution of **2-13** shows little evidence of ligand exchange even at 75 °C. These results, suggest that the binding constant of **9b** with Zn(II) is considerably greater than that with Cu(I), reinforcing the observations derived from the crystallographic analysis of these isostructural complexes.

Figure 2-2 illustrates the through-space proximity of protons H23-H26 and H14-H17. The protons H14 and H15 undergo significant shielding from the phenyl group of the adjacent ligand. Proton H15 is shifted upfield by approximately 0.3 ppm and proton H14 is shifted upfield by approximately 1.3 ppm. The assignment of the aryl protons in complex **2-13** can be completed by use of splitting, coupling constant, and the ROESY experiment performed on the d_3ACN solution of **2-13** (Figure 2-21). Within the complex, the closest intraligand proton distances in the solid state are H15 – H24 at 3.07 Å. The final assignments of the protons are tabulated in Table 2-3.
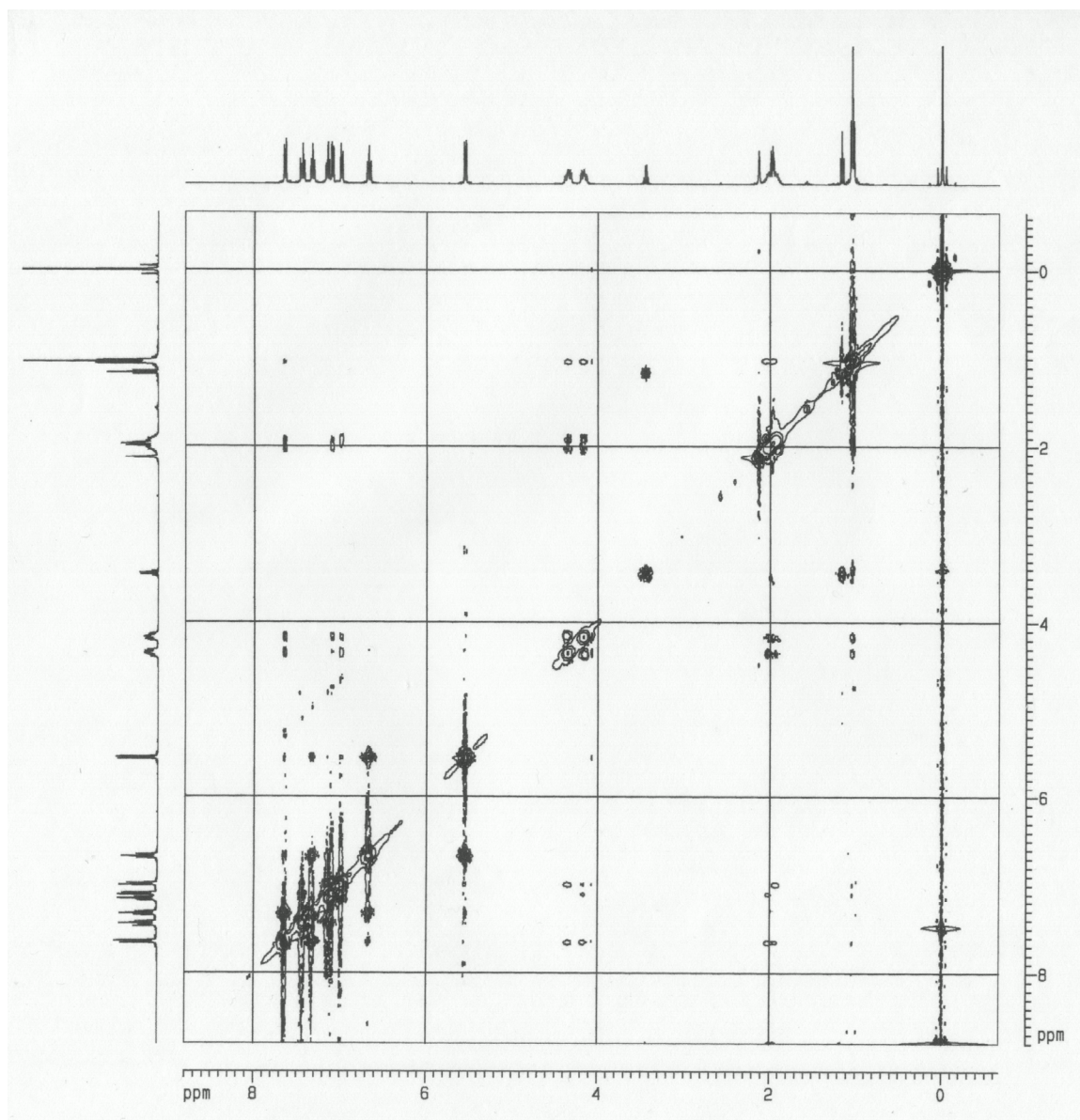
Figure 2-21. ROESY spectra (^{1}H NMR, 400 MHz, CD$_3$CN) at 30 °C of a solution 6.0 mM in **2-13**.

Table 2-3. Proton assignments for **2-13**.

proton	Chemical shift	splitting	J(Hz)
14	5.71	d	8.3
15	6.70	t	8.3
26	7.01	d	7.7
23	7.09	d	7.7
24	7.13	t	7.7
16	7.32	t	8.3
25	7.37	t	7.7
17	7.67	d	8.3

Conclusions

2,2'-Bis[2-(1-propylbenzimidazol-2-yl)]biphenyl, **9b**, with four planar groups and three connecting "hinges" acts as a geometrically constraining bidentate ligand. With Fe(II) and Mn(II), high-spin nearly-tetrahedral complexes containing $M(II)(9b)_2$ cations are formed. Ligation yields rigid, chiral 9-membered M(**9b**) rings, resulting in cations with *R, R* or *S, S* stereochemistry. Crystals of $Fe(II)(9b)_2 \cdot (ClO_4)_2$ and

Mn(II)(**9b**)$_2$·(ClO$_4$)$_2$ are isomorphous racemates with equal numbers of *R, R* and *S, S* cations in each unit cell. Mn(II)(**9b**)$_2$·(ClO$_4$)$_2$ exhibits a Mn(II) → Mn(III) oxidation at E$_{1/2}$ = 0.64 V. The corresponding Fe(II) → Fe(III) oxidation at E$_{1/2}$ = 1.76 V is suggests the possibility of isolating an unusual pseudotetrahedral Fe(III)N(BzIm)$_4$ species. Ultraviolet spectra of the Fe(II) and Mn(II) complexes are dominated by absorptions of ligand **9b** blue-shifted by approximately 2 000 to 3 000 cm^{-1}. LF absorptions were observed for the Fe(II) chromophore; those expected for the Mn(II) analogue were too weak to be observed above the background of the tailing uv absorptions. Magnetic susceptibility studies show that Mn(II)(**9b**)$_2$·(ClO$_4$)$_2$ behaves as a simple, high-spin paramagnet, whereas the falloff in magnetic moment shown by Fe(II)(**9b**)$_2$·(ClO$_4$)$_2$ from 5.02 μ_B at 295 K to 3.97 μ_B at 5 K is indicative of zero-field splitting. From LF considerations, the ZFS parameter D was estimated to be ~ 4 cm^{-1}.

Square-Bipyramidally Constrained Metal Complexes

Preparation of the Complexes.

(***OC*-6-12)-bis[(*S,S*)-1,2-bis(1-methylbenzimidazol-2-yl)-1′,2′-bis(methoxy)ethane]copper(II) bis(tetrafluoroborate) acetonitrile disolvate, Cu(II)(15a)$_2$·(BF$_4$)$_2$ · (acetonitrile)$_2$. (2-16)** A pale-blue solution of 41.6 mg of Cu(BF$_4$)$_2$ · 3 H$_2$O (0.14 mmol) was prepared in 10 mL of acetonitrile and 2 mL of triethylorthoformate. Addition of 100 mg of **15a** (0.28 mmol) yielded a green solution from which purple crystalline prisms formed upon slow evaporation of the solvent. The crystalline product was collected by filtration and vacuum dried to give a pale-purple powder. C$_{44}$H$_{50}$B$_2$F$_8$CuN$_{10}$O$_4$, fw = 1020.10. Yield: 112 mg, 85.3% (less solvent). IR

(KBr pellet, cm^{-1}) 3430 br, 2954 w, 1616 w, 1501 m, 1460 m, 1337 m, 1084 s, 813 w, 754 m. Crystal structure (**2-16**).[149,A48] EPR LN$_2$ green ACN soln g$_\perp$ = 2.04, A$_\perp$ = 16 x 10^{-4} cm^{-1}, g$_\parallel$= 2.275, A$_\parallel$= 92 x 10^{-4} cm^{-1}.

(*OC*-6-12) - **bis[(*S*,*S*)-1,2-bis(1-methylbenzimidazol-2-yl)-1′,2′-bis(methoxy)ethane] palladium(II) dichloride, Pd(II)(15a)$_2$·Cl$_2$. (2-17)** Triethyl orthoformate (1 mL) was added to a 50 mL Erlenmeyer flask containing a yellow-orange solution of bis(acetonitrile)palladium(II) dichloride (30 mg, 0.12 mmol) and **15a** (81 mg, 0.23 mmol) in acetonitrile (10 mL). After gentle warming of the solution for 5 min, slow evaporation afforded pale-yellow plates of the product. C$_{40}$H$_{44}$Cl$_2$N$_8$O$_4$Pd, fw = 878.15. Yield: 71 mg, 67%. IR (KBr pellet, cm^{-1}) 3435 br, 2942 w, 1645 w, 1533 m, 1477 m, 1334 m, 1155 w, 746 m. Crystal structure (**2-17**).[150,A49]

(*OC*-6-12) - **bis[(*R*,*R*)-1,2-bis(1-ethylbenzimidazol-2-yl)-1′,2′-bis(ethoxy)ethane] copper(II) bis(perchlorate), Cu(II)(15d)$_2$·(ClO$_4$)$_2$. (2-18)** A pale-blue solution of 45.6 mg of Cu(ClO$_4$)$_2$ · 6 H$_2$O (0.123 mmol) was prepared in 10 mL of acetonitrile and 2 mL of triethylorthoformate. Addition of 100 mg of **15d** (0.246 mmol) yielded a green solution from which purple crystalline rods formed upon slow diffusion of diethyl ether. The crystalline product was collected by filtration and vacuum dried to give a pale-purple powder. C$_{48}$H$_{60}$Cl$_2$CuN$_8$O$_{10}$, fw = 1075.48. Yield: 107 mg, 81.0%. Crystal structure (**2-18**).[A50]

Results and Discussion

Octahedral coordination is commonly found for the first-row transition metals; however, it is much less common to find these metals in constrained chiral octahedral environments. Species with constrained chiral octahedral environments would be useful

in applications for which chirality is important. Species with chiral constrained octahedral environments have been prepared with second-row transition metals, specifically, palladium(II) (**2-17**). Stable, isolable six-coordinate octahedral complexes of Pd(II) are quite rare. We believe **2-17** to be the first structurally characterized example with $N_4 + O_2$ (*OC*-6-12) donation; Cambridge Structural Database (Version 5.25).[151] In our analysis of distorted-octahedral Pd(II) complexes, we have omitted carbon, halide, and metal bonding interactions with palladium, leaving us with two types of donor ligand sets that provide distorted-octahedral coordination. The first is provided by two 10-crown-S3 thioethers to give $S_4 + S_2$ ligation. The axial S atoms were found to influence the electronic absorption spectrum of the complex, despite the relatively long Pd(II)-S(thioether) distance of 3.11 Å.[152] The second donor set was provided by *cis*-$P_2O_2 + O_2$ (*OC*-6-22) ligation. In the two complexes reported, the complex containing axial Pd(II)-O(ether) bond lengths of 2.632(7) and 2.671(7) Å inkages, were considered to be bonding while, in the second complex containing axial Pd(II)-O(ether) distances of 2.887 and 3.025 Å were considered non-bonding.[153] In **2-17,** the Pd-O distances of 2.867(4) and 2.871(4) Å are long, and the extent to which these interactions are bonding is not known.

Ligands **2b**, **2e**, and **2f** have been previously reported, and have been used to prepare metal complexes with Ni(II)[154] and Cu(II)[85,155]. While discrete ML_2 cations could be isolated and crystallographically characterized, all were also found to dimerize[85,154] in solution and in the solid state; further, they form tetramers,[155] which have been crystallographically characterzed. The instability of these complexes makes the study of discreet ML_2 cations difficult. In all cases, the lack of alkylation was found to be the cause of the formation of oligomeric species. Alkylation of these ligands to give newly

reported ligands, such as **15a** and **15d**, has eliminated the pathway for the formation of oligomeric species, allowing the syntheses of discrete chiral species such as **2-16**, **2-17**, and **2-18**, which are suitable for spectroscopic studies.

The cations in **2-16**, **2-17**, and **2-18** are coordinated facially by the imine N atoms of the planar benzimidazole fragments and by one of the alkoxy O atoms from each of two ligands, to yield a distorted tetragonal $N_4 + O_2$ coordination geometry, in which the N atoms form a nearly square-planar base (Table 2-4). The axial O atoms are displaced from the axis normal to the MN_4 plane towards the ligand to which they are attached. These geometric features of the coordination geometry are qualitatively similar for each of the cations, the major differences being the M-O distances, which are substantially longer in the Pd cation in **2-17**, and several of the N-M-O angles, which indicate a greater deviation from regular tetragonal symmetry for the Pd species (Table 2-4).

Ligands **15a** and **15d** have three torsional degrees of freedom, which may be characterized by the torsion angles χ_1, χ_2, and χ_3, shown in Figure 2-22, and defined in the legend for Table 2-2. In the cationic species, the three torsion angles compare favorably except for χ_3 in **2-18** which differs on the order of 30°. This significant deviation results from changing the R group in **2-18** from methyl to ethyl.
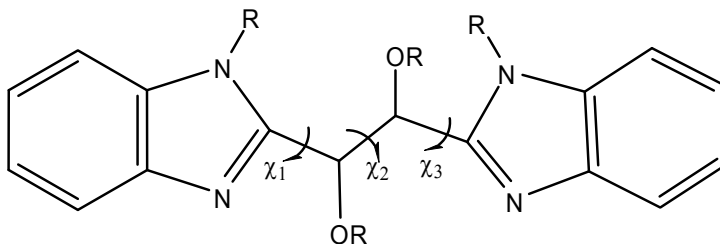

Figure 2-22. The three torsion angles χ_1, χ_2, and χ_3, found in ligands **15a** and **15d**.

Table 2-4. Comparison of selected bond lengths (Å), bond angles (°), and torsion angles (°) for **2-16**, **2-17**, and **2-18**. The torsion angles χ_1, χ_2, and χ_3 correspond to (R)N-C-C-O(M), O(M)-C-C-O, and O-C-C-N′(R), respectively, where O(M) is the O atom coordinated to the metal.

	2-16	2-18	2-17		2-16	2-18	2-17
	Cu(II)	Cu(II)	Pd(II)		Cu(II)	Cu(II)	Pd(II)
M-N43	2.028(6)	2.034(6)	2.006(5)	M-N33	2.006(6)	2.010(7)	2.058(5)
M-N13	2.032(5)	2.042(7)	2.011(5)	M-O4	2.520(5)	2.551(6)	2.867(4)
M-23	1.973(6)	1.969(7)	2.027(5)	M-O1	2.483(4)	2.435(6)	2.871(4)
N43-M-N13	92.2(2)	88.8(3)	90.4(2)	N23-M-O4	99.9(2)	105.6(3)	110.57(16)
N43-M-N23	177.4(3)	174.8(3)	177.27(18)	N33-M-O4	73.9(2)	82.1(3)	79.37(16)
N13-M-N23	89.7(2)	90.6(3)	89.2(2)	N43-M-O1	106.24(19)	101.8(3)	104.51(16)
N43-M-N33	90.3(2)	89.6(3)	87.8(2)	N13-M-O1	81.39(19)	73.1(3)	70.04(16)
N13-M-N33	177.4(3)	176.6(4)	176.39(18)	N23-M-O1	72.4(2)	82.9(3)	77.85(16)
N23-M-N33	89.8(2)	91.2(3)	92.8(2)	N33-M-O1	98.4(2)	104.2(3)	107.40(15)
N43-M-O4	81.15(19)	69.5(3)	66.92(15)	O4-M-O1	169.55(15)	169.5(2)	169.30(15)
N13-M-O4	106.05(19)	100.2(3)	102.79(16)				
χ_1(ligand 1)	-145.2(7)	-141.5(9)	-140.9(6)	χ_1(ligand 2)	-134.9(7)	-127.9(10)	-132.1(6)
χ_2(ligand 1)	-177.3(7)	-174.5(7)	-178.8(5)	χ_2(ligand 2)	-178.6(5)	-179.4(7)	-176.3(4)
χ_3(ligand 1)	-62.1(8)	-32.3(11)	-59.8(8)	χ_3(ligand 2)	-56.0(8)	-29.5(11)	-58.0(7)

Chapter 3

# Applications of Bis(benzimidazole) Complexes

Introduction

As demonstrated in the previous chapter, bis(benzimidazoles) can be used to ligate and constrain the coordination geometry of many of transition metal ions. This chapter will focus specifically on the application of bis(benzimidazoles) ligated with copper to provide catalysts with a variety of applications. These copper complexes have been found to catalyze the oxidative carbonylation of methanol to form dimethyl carbonate. Such complexes have also been found to be remarkable polymerization catalysts, with the ability to homopolymerize and copolymerize olefins and acrylates. Finally, some of these complexes have been used as catalysts for novel cyclopropanation reactions.

Dimethyl Carbonate – Copper Bis(benzimidazole) Catalysts

Industrially, dimethyl carbonate (DMC) is used for the production of aromatic polycarbonates. Since DMC is a nontoxic compound,[156] it also has the potential to be used as an environmentally friendly fluid for numerous solvent related applications, and conceivably even as a fuel oxygenate (e. g., a methyl tertiary butyl ether (MTBE) replacement). It may also be used as a *green chemistry* replacement for methyl iodide, dimethyl sulfate, or phosgene, reagents which are used for methylation and carbonylation reactions,[156] both on small and large scales. Historically, aromatic polycarbonates have been prepared from the polycondensation of BPA (bisphenol A) and the highly toxic intermediate phosgene, $COCl_2$. Currently, aromatic polycarbonates are prepared by trans-

esterification of DMC with phenol to afford DPC (diphenylcarbonate), which is subsequently transesterified with BPA to afford the aromatic polycarbonate (Scheme 3-1).[157]

Scheme 3-1. Production of a polycarbonate.
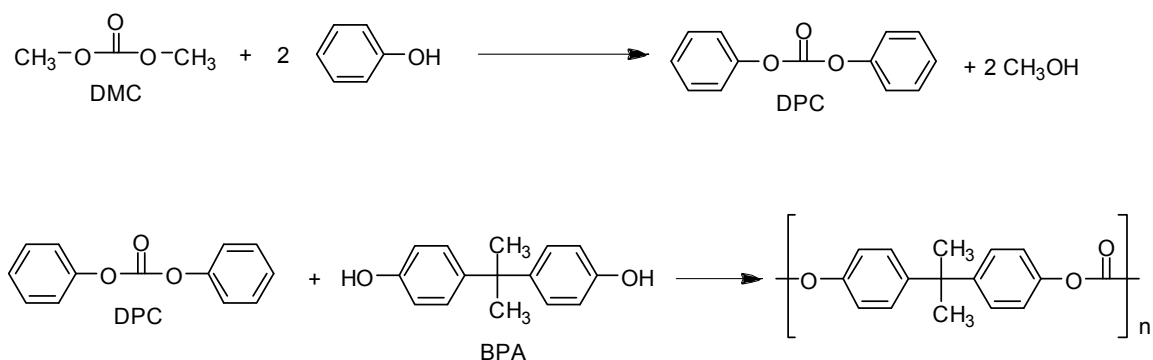
Well over 200 patents have been documented and evaluated for the production of DMC.[158] Two notable processes have been patented for the production of DMC, but have not been commercialized. The first is based on the reaction of urea with methanol to form initially the carbamate, which is further reacted to form DMC, ammonia and carbon dioxide (Scheme 3-2).[159] Current inefficiencies in the recycles, including the conversion of NH_3 and CO_2 to urea make this process unattractive.

Scheme 3-2. The urea process.

$$NH_2CONH_2 + CH_3OH \rightarrow NH_2COOCH_3 + NH_3 \rightarrow CH_3OH + NH_2COOCH_3 \rightarrow DMC + NH_3$$
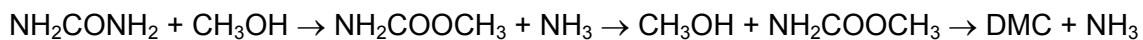
In another process, methylnitrite is reacted with carbon monoxide over a heterogeneous catalyst to form DMC and NO (Scheme 3-3).[160] This process suffers from significant disproportionation of methylnitrite to generate $(NO)_x$ which is toxic, and is a regulated emission substance.

Scheme 3-3. The methylnitrite process.

$$2\ NO + 2\ CH_3OH + 1/2\ O_2 \longrightarrow 2\ CH_3ONO + H_2O$$

$$CO + 2\ CH_3ONO \xrightarrow{PdFe/C} DMC + 2\ NO$$
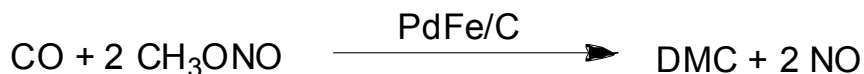
Currently, DMC is prepared industrially via oxidative carbonylation of methanol using a copper catalyst. This method utilizes copper(I) chloride as the catalyst and is practiced by Enichem.[161] The overall copper catalyzed reaction is shown in Scheme 3-4.

Scheme 3-4. Oxidative carbonylation of methanol using cuprous chloride catalyst in the liquid phase.

$$2\ CuCl + 2\ CH_3OH + \tfrac{1}{2}\ O_2 \rightarrow 2\ Cu(OCH_3)Cl + H_2O$$

$$2\ Cu(OCH_3)Cl + CO \rightarrow 2\ CuCl + DMC$$
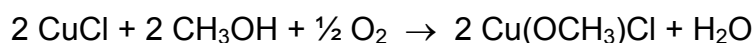
In the commercial liquid-phase process, copper(I) chloride is very sparingly soluble in the reaction mixture, and is, therefore, a limiting component in the catalytic cycle. Since copper(I) is thought to be the active species in this system, hydrochloric acid is also added as a component in the commercial catalytic system to inhibit the oxidation of Cu(I) to Cu(II) in the presence of oxygen and water. The commercial process, which is run

between 120 - 160 °C, is extremely corrosive and requires costly components such as glass lined reactors. Further, failure in the glass lining could lead to rupture or explosion. Consequently, a less corrosive catalyst system would be greatly desired.

The use of a well defined, oxidatively stable, soluble copper catalyst with strongly bound bidentate ligands and weakly coordinating anions would seem to be a logical system to try as a replacement to the Enichem process. This has been exemplified using the catalyst [1,1'(1-butylbenzimidazol-2yl)pentane] copper(II) di(trifluoromethanesulfonate) (**3-1**) (Figure 3-1), which contains a copper(II) cation ligated by a bidentate bis(benzimidazole) and two weakly coordinating triflate anions.[162]
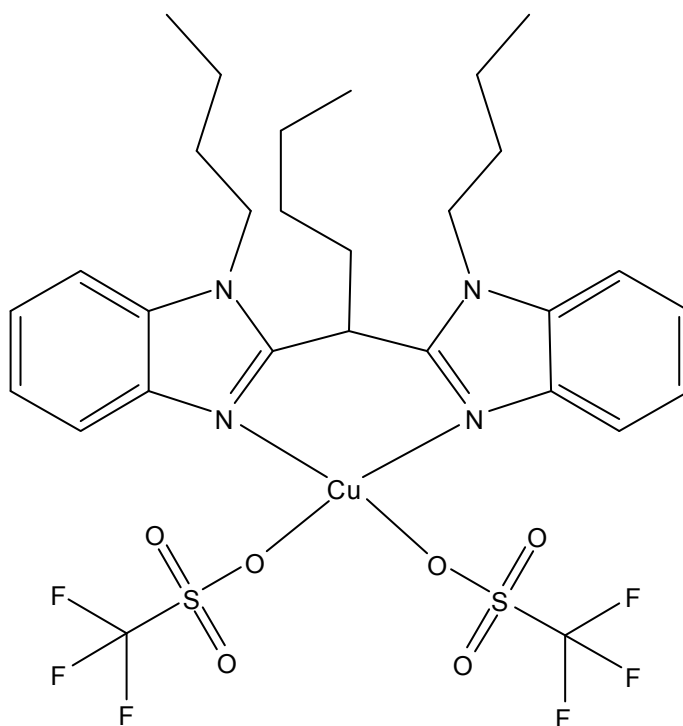

Figure **3-1.** Drawing of [1,1'(1-butylbenzimidazol-2yl)pentane]copper(II) di(trifluoromethanesulfonate) (**3-1**).

Results[162] thus far have demonstrated that a catalytic system based on soluble copper catalysts can be run without the generation of toxic side products. More importantly, the process can be run under non-corrosive conditions (e.g. non-acidic and free of halogen ions (F⁻, Cl⁻, Br⁻, I⁻)).

Polymerization – Copper Bis(benzimidazole) Catalysts

There has been considerable recent activity in the area of late transition-metal polymerization catalysis.[163,164] In the last two decades, metallocenes have revolutionized the commercial polymerization of olefins. In many cases, such catalysts are now used in place of Ziegler-Natta catalysts to produce better performing HDPE (high-density polyethylene) and LLDPE (linear low-density polyethylene). Metallocenes are based on early transition metals, predominantly Ti, Zr, and Hf, which are very oxophillic and which are very easily poisoned by polar monomers and contaminants.[165] Catalysts with the ability to incorporate polar monomers may give rise to new high-performance materials with high adhesive, toughness, and dyability.[166] These catalysts may also be more tolerant of minor contaminants in ethylene polymerization. The search for such polymerization catalysts has led to the late transition metals.

Olefin Polymerization

Reports of nickel and palladium bis(imine) catalysts[167,168] have spurred the research in late transition-metal-catalyzed polymerization. Further, iron and cobalt catalysts containing tridentate nitrogen ligands have also been found to be active polymerization catalysts.[169,170] The polymerization of ethylene with nickel and palladium bis(imine) catalysts has generally yielded substantial branching in the polyethylenes

produced, while cobalt and iron catalysts produced far fewer branches. However, early work also showed considerable chain transfer to aluminum, which results from the cocatalyst, methylaluminoxane (MAO), in these systems.

We report here the polymerization of ethylene with the use of copper bis(benzimidazole) catalysts that produce very highly linear polyethylenes of substantial molecular weight and low polydispersity. These catalysts also incorporate certain α-olefins.[40,171,172] A particular challenge to chemists who study single-site polymerization catalysts is the characterization of the active metal site. Many direct and indirect probes have been used to study such metal sites before, during, and after polymerization. Catalyst species which contain ferromagnetic or paramagnetic metals offer a special challenge in part because they render conventional ^{1}H and ^{13}C NMR techniques ineffective. High Pressure ^{19}F NMR has been found to be a useful indirect method for studying copper-based polymerizations of this sort. The synthesis and structure of a bis(benzimidazole)copper ^{19}F probe catalyst will be described. Catalyst structural-reactivity relationships with ethylene and α-olefins will also be discussed.

Experimental

The probe copper complex was prepared in three synthetic steps as illustrated in Scheme 3-5. The condensation reaction of malonic acid in polyphosphoric acid with two equivalents of 4-fluoro-1,2-phenylenediamine, subsequent alkylation of the resulting bis(benzimidazole) (**3-2**) to give **3-3** were performed by the synthetic methods described in chapter 1. Finally, the alkyalated bisbenzimidazole was metalated using $CuCl_2 \cdot 2H_2O$ in a mixture of ethanol and triethylorthoformate to yield **3-4**. Triethylorthoformate (TEOF) is added to promote dehydration in the reaction mixture and to aid in the crystallization of

the metal complex. The solid yellow-green crystalline complex was then isolated by filtration. Suitable X-ray quality crystals were obtained by the slow evaporation of a filtered methanol solution of **3-4** (Figure 3-2).

Scheme 3-5. Synthetic steps for the preparation of the bis(benzimdazole)copper ^{19}F probe catalyst (**3-4**).
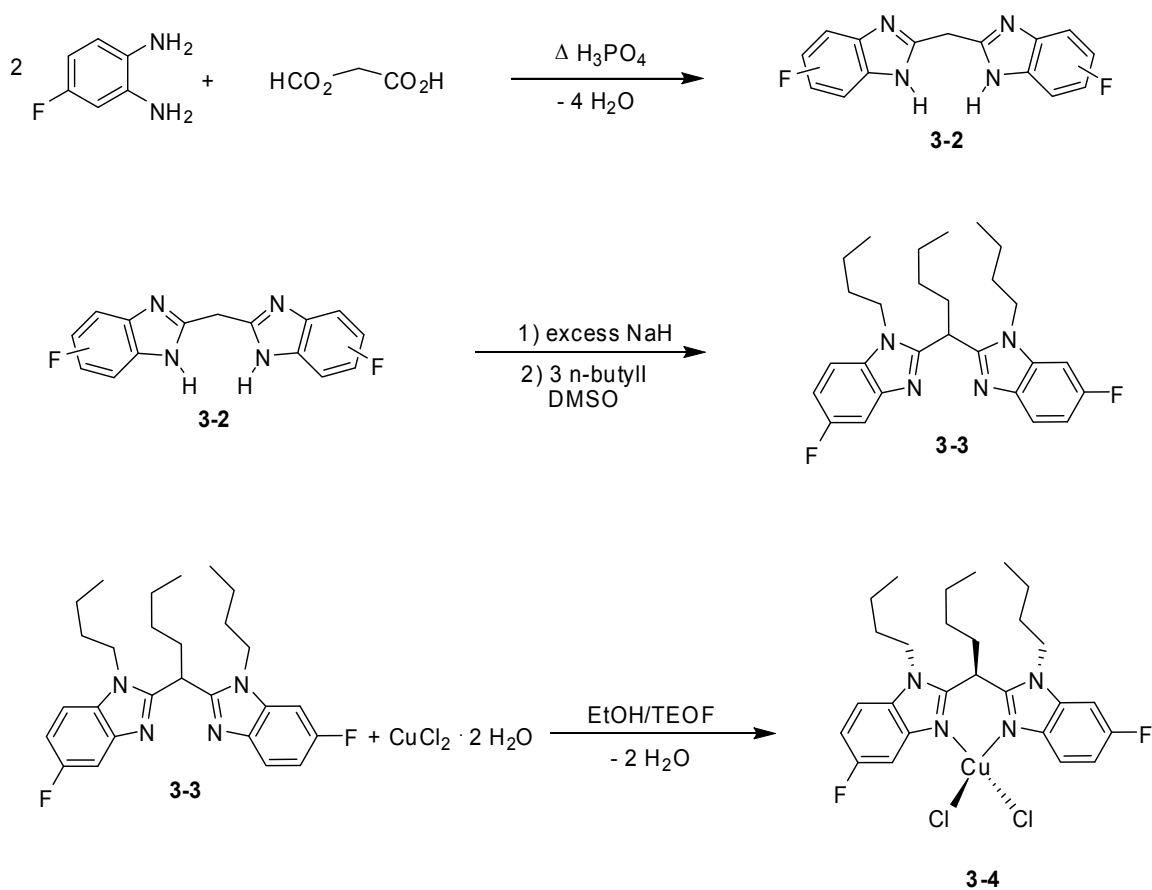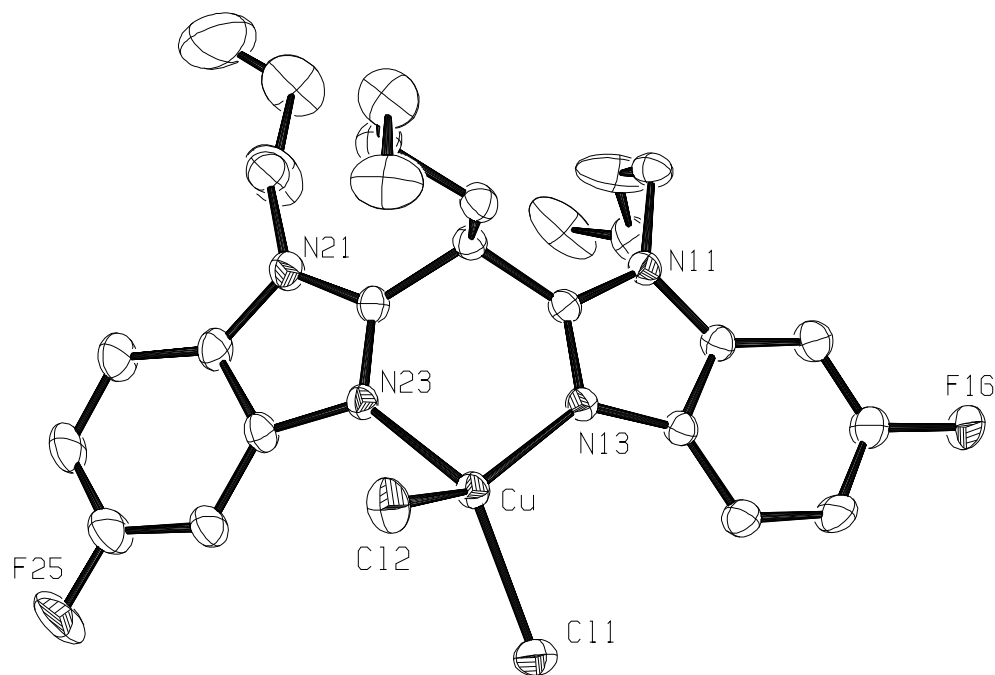
Figure 3-2. Structure of **3-4**, [1-(1-butyl-5-fluorobenzimidazol-2yl)-1'-(1-butyl-6-fluorobenzimidazol-2yl)pentane] Copper(II) dichloride. The hydrogen atoms have been omitted for clarity.

High-Pressure ^{19}F NMR Polymerization Conditions

For high-pressure (500 psig) ^{19}F NMR studies, a custom made high pressure sapphire tube[173] was used to conduct ethylene polymerizations, wth purified toluene-d_8 as the solvent. The spectra were obtained unlocked and without spinning, and the ^{19}F-NMR chemical shifts were referenced to an external C_6F_6 standard. Postulated species for the polymerization using pre-catalyst **3-4** are presented in Table 3-1. For the actual polymerization experiment, the NMR tube was charged with toluene-d_8, **3-4**, MAO, and 500 (psig) of ethylene. After mixing, the reaction was monitored at ambient temperature

for 0.5 h (exp. 4). The reaction was then heated to 80 °C and monitored for 5 h, during which time, polyethylene was produced (exp. 5). The reaction was then returned to ambient temperature and monitored once again (exp. 6). A detailed explanation of the postulated species will be presented later.

Table 3-1. ^{19}F NMR Data for High-Pressure Ethylene Polymerization Experiments 1-6.

Exp.	Chemical Shift (ppm)	Δ (Hz)	Conditions	Postulated Species
1	-118.2, -120.4	880	Ambient Solution	Free Ligand **3-3**
2	-117.6, -119.9	920	Ambient Solution	MAO/TMA Interaction **3-3a**[a]
3	-115.1, -119.0	1560	Ambient Solution	Cu Complex **3-4**
4	-109.7, -110.9[b]	480	Ambient Temp.	Tight Ion Pair **3-5**
	-112.7, 114.7[c]	800	MAO, 500 (psig)	Transient Species **3-5a**
5	-109.7, -110.9[d]	480	80 °C, 5 h	Tight Ion Pair **3-5**
	-110.2, -111.2[c]	400	Polymerization	Active Catalyst **3-6**
6	-109.7, -110.9	480	Return to Ambient	Tight Ion Pair **3-5**

[a]Interaction of the free ligand **3-3** wth excess MAO/TMA (trimethylaluminum) in solution. [b]Sharp signal. [c]Minor broad short lived species. [d]Sharp signal 60 % by integration. [e]Broad signal 40 % by integration.

Comparative Ethylene/α-Olefin Polymerization Conditions

A typical olefin polymer was obtained from an equimolar mixture of comonomer and ethylene pressurized to 700 psig. A non-fluorinated copper catalyst solution (Figure 3-3) in toluene with MAO (methylaluminoxane); Al:Cu $\Rightarrow$ 220:1, 80 °C. The resulting polymer compositional data is given in (Table 3-2). The data will be discussed in detail later.
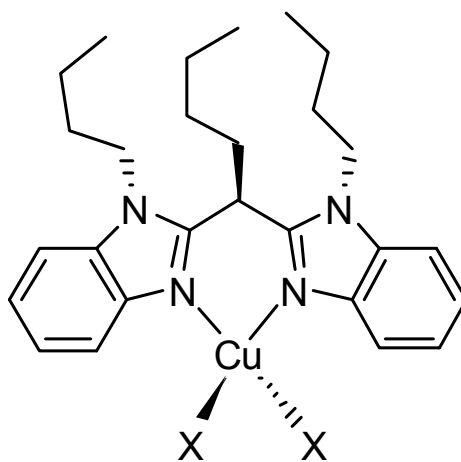

Figure 3-3. Non-fluorinated copper catalyst used for comparative α-Olefin polymerization studies.

Table 3-2. Compositional Data for Ethylene/α-Olefin Copper-Catalyzed Polymerization.

Comonomer	Yield (g)	Mol %[a]	Mw x 10^{-3}	MWD	Tm °C
None	6.74	-	150	2.50	136
Propylene	0	-	-	-	-
Isobutylene	0.15	-	-	-	-
3-methylbutene	0.30	-	-	-	134
1-butene	15.20	2.2	88	3.00	122
1-hexene	14.98	0.5	511	2.19	122
1-octene	14.75	1.8	152	2.64	115
1-octadecene	13.04	1.0	309	2.63	17^{b}/115
norbornene	1.51	2.7	467	2.43	120

[a] Mole percent incorporation of α-olefin. [b] Initial mp attributed to side chain crystallinity.

Results and Discussion

The facile synthesis of the copper probe molecule **3-4**, which is presented in Scheme 3-5, had an unexpected synthetic result. In the alkylation step, the possibility exists for generating three isomers with respect to the fluorine substitution, i.e., 5,5', 6,6', and 5,6'. Based on results from the alkylation of mono-benzimidazoles, all three isomers were expected.[174] Under our experimental conditions, however, only the 5',6 isomer was observed. In Table 3-3 and Figure 3-4, the downfield portion of the ^{13}C NMR spectrum of **3-3** can clearly be assigned. The identity and purity of the ligand are further supported by TLC and by the crystal structure of **3-4**. Also of note is the observation that the asymmetrically electron-withdrawing, nitro-substituted bis(benzimidazole) **1c** appears to

exists as the 5′,6 isomer in DMSO solution at rt. Further study is needed to explain the selectivity of the reaction.

Table 3-3. Downfield ^{13}C NMR Chemical Shifts and Assignment for **3-3**, 1-(1-butyl-5-fluorobenzimidazol-2-yl)-1′-(1-butyl-6-fluorobenzimidazol-2-yl)pentane.

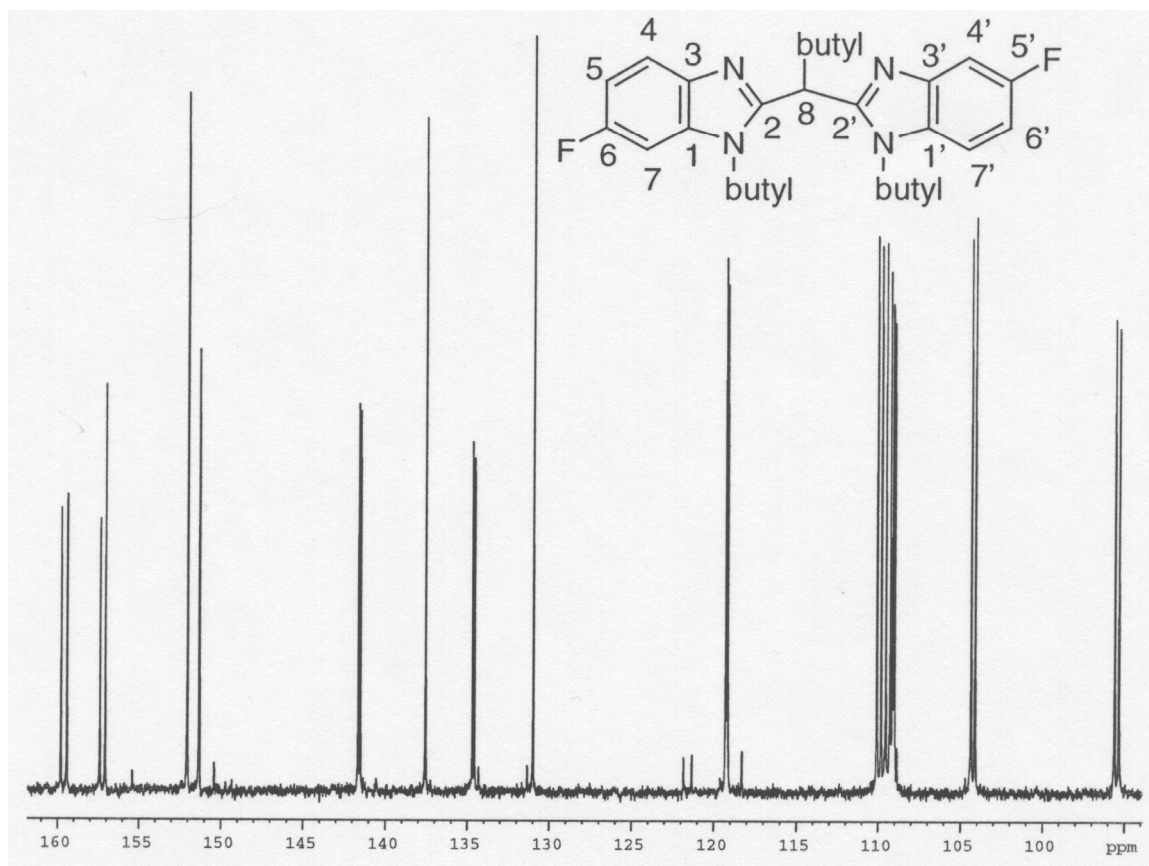| C atom number	Chemical shift (ppm)	J (Hz)
2	152.0	-
3	137.6	-
4	119.2	10.0
5	109.4	25.1
6	159.6	34.8
7	95.5	27.4
1	134.6	12.9
2'	151.3	-
3'	141.6	12.6
4'	104.2	24.0
5'	157.2	32.4
6'	110.0	26.1
7'	109.1	10.5
1'	131.0	-
8	44.7	-

Figure 3-4. Downfield ^{13}C NMR and atom numbering for **3-3**, 1-(1-butyl-5-fluorobenzimidazol-2-yl)-1′-(1-butyl-6-fluorobenzimidazol-2-yl)pentane.

The use of ^{19}F NMR to study ferromagnetic and paramagnetic species has been slowly evolving,[175] and very few examples of this technique have been reported for studying Cu(II) paramagnetic species.[176] In our case, because the fluorine substituents are far removed from the metal center, line broadening and chemical shift effects are minimized. The 5′,6′ substitution in **3-3** allows pairs of signals to be easily recognized. This has the added benefit that chemical shift differences arising from the different environment of the two fluorine atoms, can be used as a diagnostic tool. This tool is especially effective in this instance because the differences in chemical shifts are greatly

influenced by the metal center. Furthermore, the electron-withdrawing effect of the fluorine atoms leads to a dramatic reduction of the turnover rate of the catalyst, with the result that reaction intermediates can be observed in some instances. The use of pressure (500 psig of ethylene) allows for the study of such intermediates under realistic polymerization conditions.

In Table 3-1, six distinct species can be identified, which account for most of the species that could reasonably be envisioned for the polymerization reaction using probe molecule **3-4**. The first three species; **3-3**, **3-3a**, and **3-4**, were identified in solution without ethylene present. A distinct pair of signals was assigned to the free ligand **3-3**. A second distinct pair of signals, **3-3a**, was identified for the interaction of **3-3** with methylaluminumoxane (MAO) and trimethylaluminum (TMA), assuming that the copper metal ion was displaced by aluminum to form the complex. The paramagnetic Cu(II) species, **3-4**, gives rise to a pair of signals with the largest chemical shift difference in Table 3-1. A difference of 1560 Hz is significantly larger than those assigned to the other 5 species identified. We attribute this large difference to the strong chemical- shift effect of the paramagnetic metal center. During all the polymerizations, only diamagnetic copper species were found to be present. NEXAFS and epr data suggest that diamagnetic copper species are Cu(I) and Cu(III).[177]

In the initial polymerization activation of **3-4**, a short-lived transient species, **3-5a**, was observed. This is likely one of the chloride-containing intermediates that is lost during activation with MAO. After the loss of this species, only one persistent pair of signals, corresponding to species **3-5**, is observed. This is designated as a "tight ion pair". As previously mentioned, electron-withdrawing groups dramatically lower the

productivity of the copper catalyst. In fact, under such circumstances at ambient temperature, no polyethylene is formed. Presumably, the electron-withdrawing effect of the fluorines increases the coulombic attraction between the metal center and the anion, leading to the formation of a tight ion pair, which prevents an open site for ethylene binding.[178] Upon heating the polymerization mixture to 80 °C, during which polyethylene begins to form, a second set of broadened signals, **3-6**, is observed. The formation of polyethylene and the expected line broadening suggest that these signals arise from the active catalyst species. As the reaction mixture is returned to ambient temperature, only the pair of signals, **3-5**, attributed to the tight ion pair, is observed. Polymerization also ceases upon cooling.

In Table 3-2, copolymerization data are presented for ethylene and selected hydrocarbon olefins with the non-fluorinated precatalyst in Figure 3-3 under identical conditions of temperature and pressure for each polymerization example. The homopolymerization of ethylene yields a remarkable polyethylene. Not only are substantial molecular weights achieved with low polydispersity, but branching is less than 1 for every 1000 carbon atoms (Figure 3-5) and crystallinities of greater than 65 percent are achieved.[179] This is in contrast to the first generation nickel and palladium bis(imine) catalysts that often produce polymers with 80-150 branches per 1000 carbon atoms.[167,168] The addition of C_4-C_{18} α-olefin comonomers has the effect of increasing catalyst productivity by more than two fold. This type of "comonomer effect" has been well documented for a number of metallocenes.[180]

Another striking result of the study of this catalyst is that the addition of propylene completely inhibits polymerization. Possibilities for the inhibition include the formation

by propylene of an allylic interaction or a strong γ-agostic interaction. The low yields observed with isobutylene and 3-methylpentene are attributed to similar, but diminished' inhibition, as with propylene. Further mechanistic study is required to reveal the nature of this interaction.
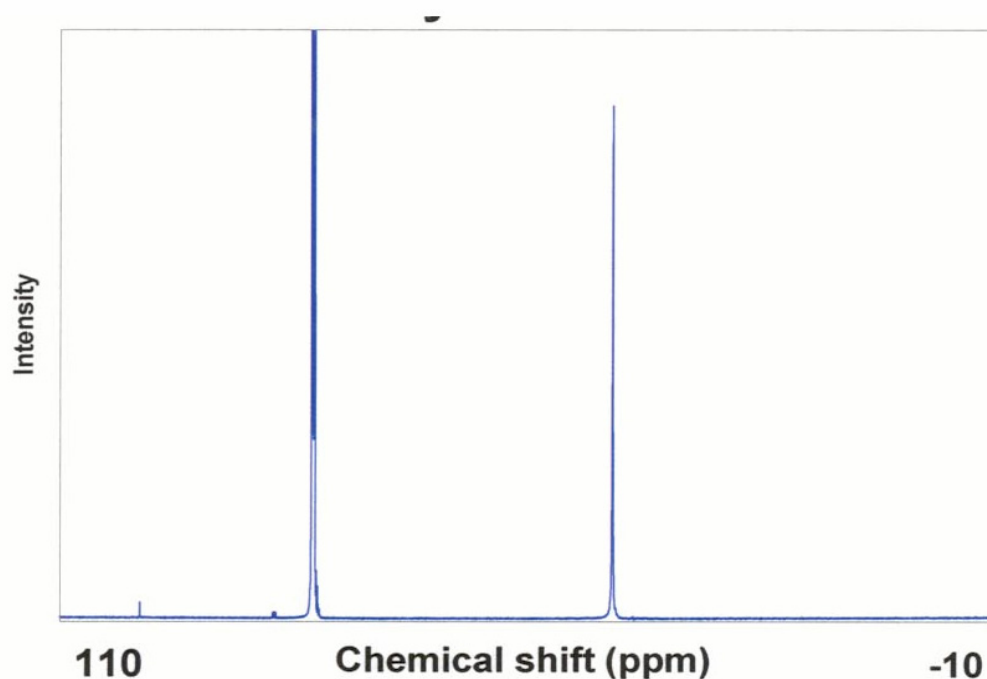

Figure 3-5. ^{13}C NMR spectrum of a polyethylene sample. No branches were detected above the signal to noise ratio; which was greater than 4000:1.

Conclusions

Fluorine-19 NMR

Fluorine-19 NMR has been shown to be a useful tool for the characterization of fluorine-labeled copper complexes. The identification of various fluorine-containing species provides a method to study copper-catalyzed polymerizations. Trends in chemical

shift, splitting, and coupling all provide information about the coordination sphere of the metal center. Use of this technique to characterize homogeneous copper catalysts indicates that, these catalysts are likely single site due to the emergence of specific resonances during polymerization. The simplicity of the spectra argues against a multi-site catalyst, and is consistent with the physical properties of the polymers produced.

Polymerization of Acrylates and Copolymerization of Ethylene/Acrylates by Cu Catalysts

The formation of copolymers of olefins with acrylate monomers by organometallic catalysts has been elusive. Acrylate monomers tend to poison Ziegler-Natta and metallocene catalysts.[165] Late-transition-metal catalysts[166,181], in general, are relatively insensitive to polar species. However, the known late-metal catalysts still have difficulty forming acrylate homopolymers and/or in-chain olefin/acrylate copolymers. For example, the Grubbs neutral nickel catalyst[182] only copolymerizes ethylene with functional monomers in which a spacer group separates the functionality and the reactive double bond. Brookhart's early cationic Pd and Ni diimine catalysts[183] have produced only low-acrylate-content ethylene copolymers (<20 mol %), which have the acrylate group at the ends of branches rather than in the polymer backbone chain. More recent versions[184] of the Ni diimine catalysts are able to make in-chain copolymers, but they tend to be low molecular weight materials with little incorporation of polar monomers (<1.4 mol %). Similarly, Drent's[185] recently reported [P,O]-ligated palladium catalysts also tend to produce low molecular weight, low acrylate copolymers.

With the exclusion of ATRP (atom transfer radical polymerization) catalysts, which have been reported for many catalysts containing a variety of transition metals, polymerization catalysts based on copper are rare. One rather ambiguous example has been reported.[186] A second example is Shibayama's[187] aminidate-ligated Cu catalyst system; however, only homopolymers have been reported by using these initiators. Cu ATRP catalysts are exemplified by the pioneering work of Matyjaszewki[188] and more recently Sen.[189] However, these systems are free radical initiators, albeit living radical ones. (A living free radical is defined as producing a polymer with a polydispersity of unity.) Free radical initiators do not readily homopolymerize ethylene under low pressure, low temperature conditions.

Certain Cu(bis(benzimidazole)) pre-catalysts (activated by MAO) were the first copper catalysts found not only to homopolymerize both ethylene and various acrylates, but also to copolymerize these two monomer classes.[40,42,190] Unlike conventional Brookhart Pd diimine-catalyzed ethylene/acrylate copolymers, the Cu-catalyzed copolymers are in-chain copolymers, with high levels of acrylate incorporation; using these Cu catalysts, a range of low to high molecular weight products has been prepared. We report here the details of the Cu bis(benzimidazole) (Cu BBIM)/MAO catalyzed homo-acrylate-polymerization with initial chiral catalyst implications, and copolymerizations of ethylene and alkyl (meth)acrylates, as well as the characterization of the products formed from these systems.

Experimental

Three copper complexes were used to study the homopolymerization of *tert*-butyl acrylate (*t*-BA) and copolymerization of ethylene and *t*-BA. These complexes were

prepared as in Scheme 3-5; (1,1′-bis(1-methylbenzimidazol-2-yl)-1″-(methoxy)ethane)copper(II) dichloride, Cu(II)(**7**)Cl$_2$, (**3-7**)[42,A51]; *rac*-(2,2′-bis[2-(1-octylbenzimidazol-2-yl)]biphenyl)copper(II) dichloride, Cu(II)(**9c**)Cl$_2$, (**3-8**)[42]; (*R,R*)-(1,2-bis(1-ethylbenzimidazol-2-yl)-1′,2′-bis(ethoxy)ethane)copper(II) dichloride, *R,R*-Cu(II)(**15d**)Cl$_2$, (**3-9**) (the enantiomeric form (*S,S*) is depicted in Figure 13 of the Introduction); (1,1′bis(1-ethylbenzimidazol-2-yl)propane)copper(II) dichloride, Cu(II)(**5a**)Cl$_2$, (**3-10**)[42]; and (1,1′bis(1-butylbenzimidazol-2-yl)pentane)copper(II), Cu(II)(**5c**)Cl$_2$, (**3-11**)[42]. All were all isolated as solid crystalline products.

**Table 3-4.** Copper-Catalyzed Homopolmerization of *t*-BA[a]**.**

catalyst	Cu/Al/*t*-BA mole ratio	polymer yield (%)	*M*n, *M*w, MWD (x10^{-3})	*Tacticity* *mm, mr, rr (%)*
3-7	0/1/14	trace		
3-7	1/5/940	5		
3-7	1/12/1010	33	280, 620, 2.2	16, 45, 39
3-7	1/13/1320	57	470, 850, 1.8	
3-7	1/12/980	77	320, 640, 2.0	
3-8	1/10/980	52		19, 43, 38
3-9	1/75/1245	92		mm = 99
radical[b]				mm = 44-46
radical[c]		99	54, 89, 1.66	mm = 44
epimerization[d]	1/12/1000	97	58, 92, 1.59	mm = 44

[a]Reaction conditions: 0.045 mmol of catalyst; toluene as solvent; exclusion of light; mol Al/MAO; 25 °C; 18 h. [b]Reference 191. Polymers produced over a range of 0-60 °C.

[c]Poly(*t*-BA) prepared with benzoyl peroxide as in ref. 191. [d]Epimerization verification of polymer in footnote c. Mole ratio of *t*-BA based on monomer segment.

Activation of **3-7** with MAO generates an active polymerization catalyst which homopolymerizes ethylene and acrylates; the catalyst also copolymerizes ethylene with acrylates (Scheme 3-6). Under the copolymerization conditions described below, the order of monomer reactivity is *tert*-butyl acrylate (*t*-BA) 3910 (mol of monomer/(g of Cu h)) > *n*-butyl acrylate (*n*-BA) 1790 (mol of monomer/(g of Cu h)) > methyl methacryalte (MMA) 860 (mol of monomer/(g of Cu h)). CuBBIM/MAO does not homopolymerize traditional free radical polymerizable monomers like styrene, vinyl acetate, or butadiene. Also, unlike Brookhart's Pd diimine catalysts, it does not homopolymerize cyclopentene.[192]

Scheme 3-6. Copper Catalyzed Polymers.
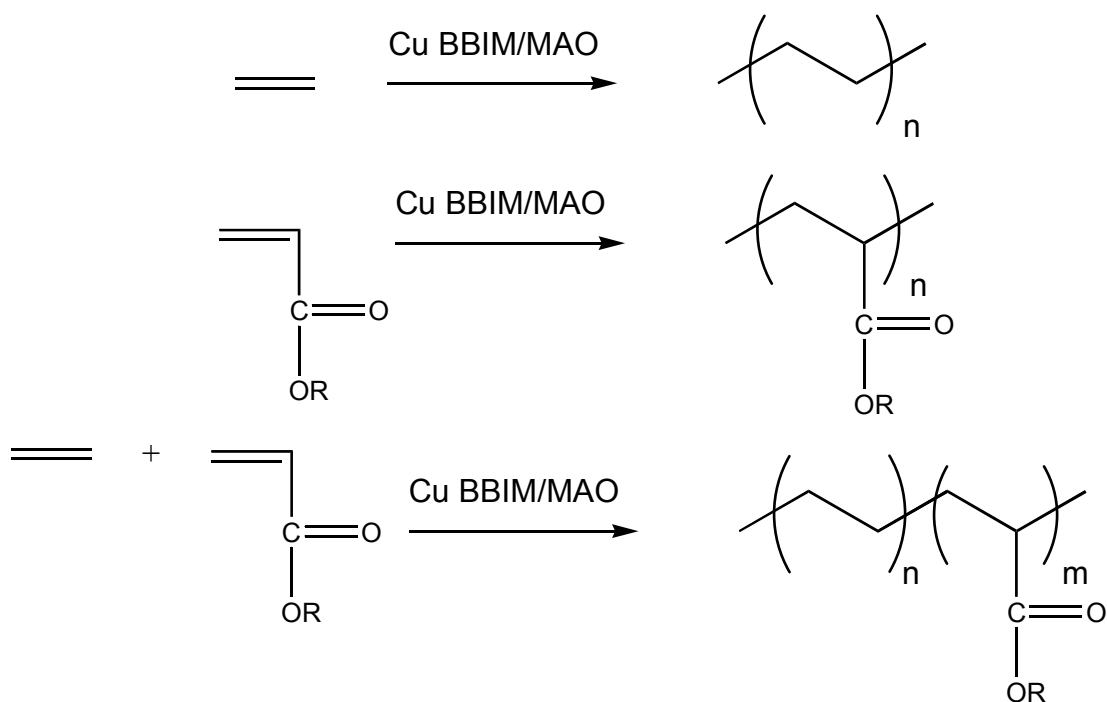
Epimerization Study

Radically initiated poly *t*-BA was produced according to the procedures in reference 191. The polymer was produced on a 15 g scale by using 3% benzoyl peroxide at 25 ºC. Characterization of the polymer compares well to that reported previously.[191] The epimerization experiment was carried out identically to that of the Cu-catalyzed homopolymerization of *t*-BA, with the exception that radically produced poly *t*-BA (3.0 g) was introduced in place of *t*-BA monomer. After the attempted epimerization, the polymer remained unchanged within experimental error. This result suggests that the tacticity of the Cu-catalyzed polymer is significantly different from those produced via radically initiated processes.[193] This also argues that the Cu catalyst is not simply acting as an epimerization catalyst to change the tacticity of a radically initiated polymer.

EPR Studies

EPR spectra were measured with a Varian E-12 spectrometer calibrated with a Hewlett-Packard Model 5245-L frequency counter and a DPPH crystal (g = 2.0036). Samples were taken of a typical *t*-BA homopolymerization product described previously, and which was prepared using catalyst **3-10**. In an Ar glovebox, samples were taken at 0.25, 2, 6, and 24 hours, and were sealed in 3 mm quartz tubes under Ar. The spectra were measured at 296 and 77 K. No detectable signal was observed in any of the samples. Cu ATRP polymerizations were also monitored by this technique, and signals attributable to both Cu(II) and free radicals were observed.[194] The absence of any signal indicates that, if present, any Cu(II) and carbon-centered radical species are below $\sim 10^{-8}$ M. One of

the samples was also examined at 353 K, in order to look for any zero-field splitting. Again, no signal was found, eliminating, to a great extent, the possibility of Cu(II) dimers in any significant concentration.

Homopolymerizations of acrylates by Cu BBIM/MAO are typically run at lower temperatures (~25 $^{\circ}$C) and lower ratios of Al/Cu (<75) than ethylene/α-olefin polymerizations. Table 3-4 shows the results of homopolymerization of t-BA with these Cu BBIM/MAO catalyst systems. Although not shown in the Table, conversion typically increases with increasing MAO concentration and reaction time. Little or no polymer is formed in the absence of Cu BBIM catalysts. GC and ^{1}H NMR analyses of the reaction mixtures showed only monomer, polymer and solvent. The resulting products are high molecular weight, narrow MWD polymers. The tacticities of both chiral and non-chiral CuBBIM/MAO-catalyzed polymers are considerably different from those of poly(t-BA) prepared by free-radical polymerization.

The chiral catalyst, **3-9**, produces a highly isotactic poly(t-BA), which has significant mechanistic implications. Syntheses of isotactic poly(t-BA) has been known for some time;[195] they are formed at low temperature (-78 °C) using "living (MWD $\approx$ 1.0)" anionic initiators and very pure reagents at low temperature.[196] Highly isotactic poly(t-BA) has been prepared more recently using chiral cationic *ansa*-Zirconocene. Ziconocene polymerizations are thought to proceed via an enantiomorphic, site-control mechanism.[197] A second mechanism has been suggested that has the active propagating species serving as a non-metallic, 1,4-conjugate-addition pathway.[198] Given the polymerization results in Table 3-4, the Cu BBIM/MAO catalyzed homopolymerization of t-BA does not appear likely to proceed via a non-Cu-centered 1,4-conjugate-addition

pathway. A more likely mechanism might involve cationic, enantiomorphic site control, along with a 1,4-conjugate addition involving a two-electron-transfer process [Cu(I)-Cu(III)] at the metal center.

Ethylene and *tert*-butyl acrylate have been copolymerized at 600 - 800 psig and 80 $^{\circ}$C using Cu BBIM/MAO catalysts. In contrast to the Brookhart Pd and Ni diimine catalysts, high levels of acrylate incorporation are possible (45-100 %). Also, high molecular weight, narrow MWD copolymers with low levels of branching can be prepared (Table 3-5). The products have been shown to be true copolymers by ^{13}C NMR and GPC/UV. Figure 3-6 shows the ^{13}C NMR spectra for the Cu BBIM/MAO catalyzed E/*t*-BA copolymers compared with homopoly(*t*-BA). The presence of EAE, and EAA/AAE triads in the former is a clear indication of copolymer formation. Additional support for the presence of copolymers is a uniform distribution of UV activities across the MWD in the GPC/UV trace (Figure 3-7).

Table 3-5. Copper-Catalyzed Copolymerization of Ethylene and *t*-BA[a].

Cu/Al/*t*-BA mole ratio	Polymer Yield (g)	*M*n, *M*w (MWD) (x10^{-3})	triads EAE:EAA/ AAE:AAA	Branches/ 1000 C	mol % *t*-BA[b]
1/230/1740	6.0	39, 85 (2.2)	6:35:58	<<1	65
1/130/1780	5.9	44, 89 (2.0)	6:34:60	6	72
1/230/950	2.4		11:35:54	10	55

[a]Reaction conditions: 0.045 mmol of **3-8**; toluene as solvent; exclusion of light; mol Al/MAO; 80 °C; 720 psig of ethylene; concentration *t*-BA 1.9 M. [b]Mole fraction of the copolymer consisting of *t*-BA units.
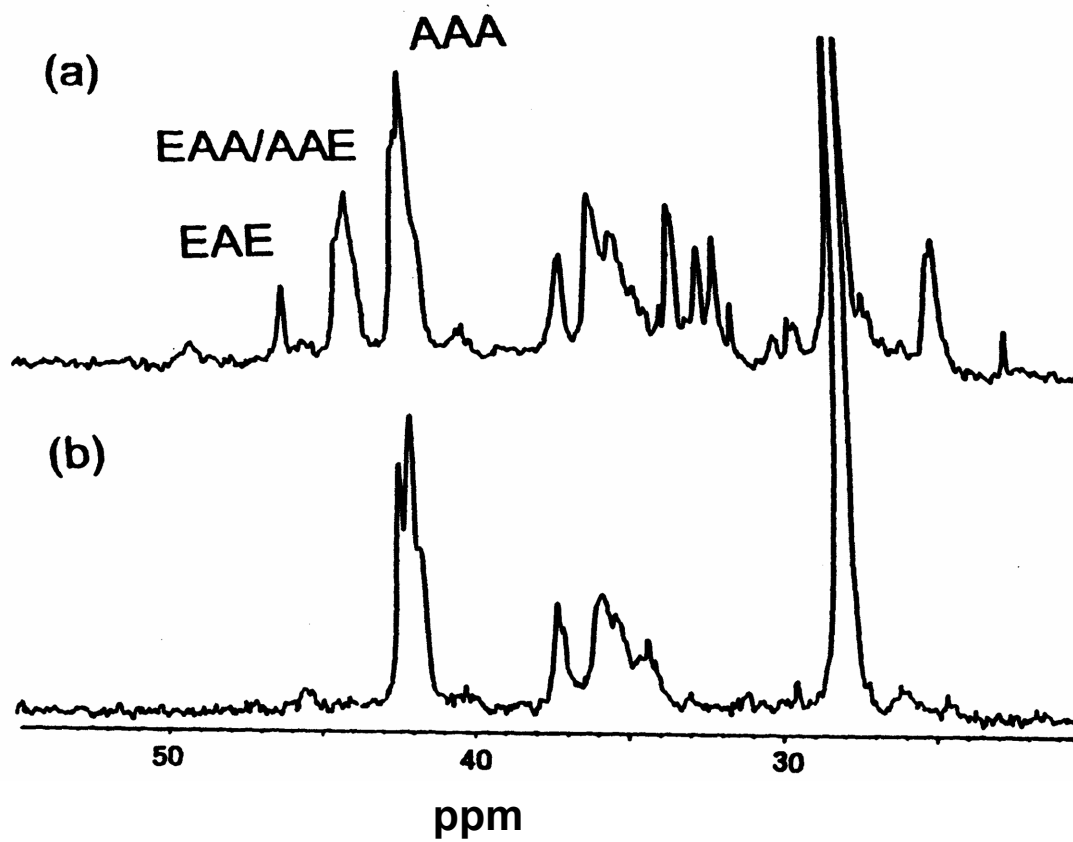
Figure 3-6. ^{13}C NMR spectra of (a) ethylene/*t*-butyl acrylate copolymer and (b) *t*-butyl acrylate homopolymer
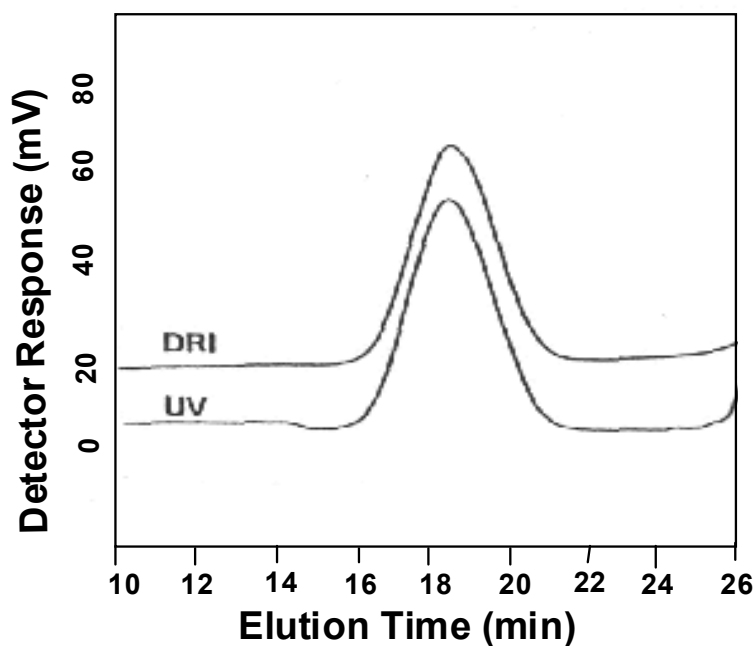
Figure 3-7. GPC of ethylene/*t*-butyl acrylate copolymer with DRI and UV detectors

While the mechanism of CuBBIM/MAO polymerizations is not completely determined, based upon the high degree of linearity and narrow MWD in the product, the ethylene homopolymerization data are consistent with a single-site coordination/insertion mechanism. Along with the ability to incorporate certain α-olefins, this mechanism is supported further by indirect mechanistic studies performed using fluorine-labeled copper catalysts.[41,177] The acrylate homopolymerization and copolymerization cases may proceed via one or more different mechanisms. However, conventional free-radical or ATRP mechanisms are less likely. Conventional free-radical chemistry is unlikely

because CuBBIM/MAO 1) does not polymerize other traditional free-radical monomers (e.g., styrene, butadiene, vinyl acetate,) and 2) can induce polymerization in the presence of known free-radical inhibitors, such as phenothiazine or MEHQ (commercial samples of acrylate monomers containing 10-100 ppm of inhibitor can be polymerized "as received" without removal of inhibitor). In our hands, **3-11** failed to induce ATRP with 1-chloroethylbenzene (PhEtCl) or reverse ATRP with 2,2′-azobis(2-methylpropionitrile) (AIBN). Tacticities for acrylate homopolymers catalyzed by CuBBIM/MAO do not match those expected for free-radical products.[191] Attempts to epimerize a radically produced homopolymer of *t*-BA was monitored under CuBBIM/MAO polymerization conditions failed to alter the tacticity of the polymer. Additionally, room-temperature experiments, in which the CuBBIM/MAO catalysis of the homopolymerization of *t*-BA by epr failed to detect the presence of any radical or Cu(II) signal.

In summary, CuBBIM/MAO is a highly versatile catalyst system that homopolymerizes ethylene and acrylates and, more significantly, induces ethylene/acrylate copolymerization. This new system is remarkable in that it spans homopolymerization space broadly, while still enabling copolymerization of traditionally transition-metal-catalyzed incompatible monomer classes.

References

1.   a) Grimmett, M. R. In *Imidazole and Benzimidazole Synthesis*; Meth-Cohn, O., Ed.; Academic Press: San Diego, 1997. b) Preston, P. N. "Benzimidazoles and Cogeneric Tricyclic Compounds" In *The Chemistry of Heterocyclic Compounds v.40*; Preston, P. N., Ed.; Wiley: New York, 1981. c) Preston, P. N. *Chem. Rev.* **1974**, *74*, 279-314.

2.   Heintz, W. *Ann. Chem.* **1862**, *123*, 325-341.

3.   a) Huang, W.; Scarborough, R. M. *Tet. Lett.* **1999**, *40*, 2665-2668. Refs. therein. b) Yeh, C.-M.; Tung, C.-L.; Sun, C.-M. *J. Comb. Chem.* **2000**, *2*, 341-348.

4.   Private communications.

5.   Saranteas, K.; Bakale, R.; Hong, Y.; Luong, H.; Foroughi, R.; Wald, S. *Org. Proc. Res. Dev.* **2005**, *9*, 911-922.

6.   Chong, C. R.; Chen, X.; Shi, L.; Liu, J. O.; Sullivan, Jr., D. J. *Nature Chem. Bio.* **2006**, *2*, 415-416.

7.   In *Comprehensive Medicinal Chemistry: The Rational Design, Mechanistic Study and Therapeutic Applications of Chemical Compounds*; Hansch, C., Sammes, P. G., Taylor, J. B., Eds.; Pergamon Press: New York, 1990.

8.   Katz, B. A.; Clark, J. M.; Finer-More, J. S.; Jenkins, T. E.; Johnson, C. R.; Ross, M. J.; Luong, C.; Moore, W. R.; Stroud, R. M. *Nature* **1998**, *391*, 608-612.

9.   Hanson, M. A.; Oost, T. K.; Sukonpan, C.; Rich, D. H.; Stevens, R. C. *J. Am. Chem. Soc.* **2000**, *122*, 11268-11269.

10.   Janc, J. W.; Clark, J. M.; Warne, R. L.; Elrod, K. C.; Katz, B. A.; Moore, W. R. *Biochem.* **2000**, *39*, 4792-4800.

11.   Paul, J. J.; Kircus, S. R.; Sorrell, T. N.; Ropp, P. A.; Thorp, H. H. *Inorg. Chem.* **2006**, *45*, 5126-5135.

12.   a) Stibrany, R. T.; Lobanov, M. V.; Schugar, H. J.; Potenza, J. A. *Inorg. Chem.* **2004**, *43*, 1472-1480. b) Stibrany, R. T.; Schugar, H. J.; Potenza, J. A. *Acta Cryst.* **2004**, *E60*, m1836-m1840.

13.   a) Kroeger Smith, M. B.; Hose, B. M.; Hawkins, A.; Lipchock, J.; Farnsworth, D. W.; Rizzo, R. C.; Tirado-Rives, J.; Arnold, E.; Zhang, W.; Hughes, S. H.;

Jorgensen, W. L.; Michejda, C. J.; Smith, R. H., Jr. *J. Med. Chem.* **2003**, *46*, 1940-1947. b) Roth, T.; Morningstar, M. L.; Boyer, P. L.; Hughes, S. H.; Buckheit, R. W., Jr.; Michejda, C. J. *J. Med. Chem.* **1997**, *40*, 4199-4207.

14.   Stibrany, R. T.; Schugar, H. J. unpublished results.

15.   a) Tajima, K.; Hasegawa, Y. U. S. Patent 5,173,479, 1992. b) Perry, N. B.; Anderson, R. E.; Brennan, N. J.; Douglas, M. H.; Heaney, A. J.; McGimpsey, J. A.; Smallfield, B. M. *J. Agric. Food Chem.* **1999**, *47*, 2048-2054. c) Dudai, N.; Lewinsohn, E.; Larkov, O.; Katzir, I.; Ravid, U.; Chaimovitsh, D.; Sa′adi, D.; Putievsky, E. *J. Agric. Food Chem.* **1999**, *47*, 4341-4345.

16.   Sell, C. S. In *A Fragrant Introduction to Terpenoid Chemistry*; Royal Society of Chemistry: Cambridge, UK, 2003.

17.   a) Hoffman, A. M. U. S. Patent 7,105,187, 2006. b) Chang, C.; Tong, X. U. S. Patent 6,939,978, 2005.

18.   Dines, M. B. *Separation Sci.* **1973**, *8*, 661-672.

19.   Cavallo, L.; Cucciolito, M. E.; De Martino, A.; Giordano, F.; Orabona, I.; Vitagliano, A. *Chem. Eur. J.* **2000**, *6*, 1127-1139.

20.   a) Cucciolito, M. E.; Flores, G.; Vitagliano, A. *Organomet.* **2004**, *23*, 15-17. b) Kieken, E.; Wiest, O.; Helquist, P.; Cucciolito, M. E.; Flores, G.; Vitagliano, A.; Norrby, P.-O. *Organomet.* **2005**, *24*, 3737-3745.

21.   McCrone, W. C. In *Physics and Chemistry of the Organic Solid State*; Fox, D.; Labes, M. M.; Weissberger, W. Eds.; Wiley Interscience: New York, 1965.

22.   Almarsson, O.; Hickey, M. B.; Peterson, M. L.; Morissette, S. L.; Soukasene, S.; McNutly, C.; Tawa, M.; MacPhee, J. M.; Renenar, J. F. *Cryst. Growth Des.* **2003**, *3*, 927-933.

23.   Stibrany, R. T.; Schugar, H. J.; Potenza, J. A. *Acta Cryst.* **2004**, *E60*, o1182-o1184.

24.   Harris, N. V.; Smith, C.; Ashton, M. J.; Bridge, A. W.; Bush, R. C.; Coffee, E. C. J; Dron, D. I.; Harper, M. F.; Lythgoe, D. J.; Newton, C. G.; Riddell, D. *J. Med. Chem.* **1992**, *35*, 4384-4392.

25.   Stibrany, R. T.; Potenza, J. A. **2006**, unpublished results
.

26.   Stibrany, R. T.; Schugar, H. J.; Potenza, J. A. **2006**, unpublished results.

27. a) Stibrany, R. T.; Schugar, H. J.; Potenza, J. A. *Acta Cryst.* **2002**, *E58*, o1142-o1144. b) Stibrany, R. T.; Potenza, J. A. Private Communication CCDC 604501, 2006. c) Stibrany, R. T.; Potenza, J. A. Private Communication CCDC 612691, 2006.

28. Stibrany, R. T.; Potenza, J. A. Private Communication CCDC 609179, 2006.

29. a) Burnett, M. N.; Johnson, C. K. *ORTEP*III; Report ORNL-6895. Oak Ridge National Laboratory; Oak Ridge, TN, 1996. b) Farrugia, L. *J. Appl. Cryst.* **1997**, *30*, 565.

30. Llamas-Saiz, A. L.; Foces-Foces, C.; Elguero, J. *J. Mol. Struct.* **1994**, *328*, 297-323.

31. Sjöberg, S. *Pure Appl. Chem.* **1997**, *69*, 1549-1570.

32. a) Hoorn, H. J.; de Joode, P.; Dijkstra, D. J.; Driessen, W. L.; Kooijman, H.; Veldman, N.; Spek, A. L.; Reedijk, J. *Mater. Chem.* **1997**, *7*, 1747-1754. b) Kapinos, L. E.; Song, B.; Sigel, H. *Chem. Eur. J.* **1999**, *5*, 1794-1802.

33. Cheng, K., L.; Sheu, S., C.; Lee, G., H.; Lin, Y., C.; Wang, Y.; Ho, T., I. *Acta Cryst.* **1997**, *C53*, 1238-1240.

34. Knapp, S.; Keenan, T. P.; Zhang, X.; Fikar, R.; Potenza, J. A.; Schugar, H. J. *J. Am. Chem. Soc.* **1990**, *112*, 3452-3464.

35. Siega, P.; Randaccio, L.; Marzilli, P. A.; Marzilli, L. G.; *Inorg. Chem.* **2006**, *45*, 3359-3368.

36. Harris, R. K. In *Nuclear Magnetic Resonance Spectroscopy: A Physicochemical View*; Pittman Books Limited: London, 1983.

.
37. a) Turner, H. W. U. S. Patent 4,752,597, 1988. b) Turner, H. W. U. S. Patent 6,121,395, 2000.

38. Canich, J. A. M. U. S. Patent 5,026,798, 1991.

39. Irwin, L. J.; Reibenspies, J. H.; Miller, S. A. *J. Am. Chem. Soc.* **2004**, *126*, 16716-16717.

40. Stibrany, R. T. U. S. Patent 6,180,788, 2001.

41. Stibrany, R. T.; "Copper-Based Olefin Polymerization Catalysts: High-Pressure ^{19}F NMR Catalyst Probe" In *Beyond Metallocenes: Next-Generation Polymerization Catalysts*. Patil A. O.; Hlatky G. G. Eds.; ACS Symp. Ser. 857; Am. Chem. Soc.: Washington, DC, 2003, 210–221.

42. Stibrany, R. T.; Schulz, D. N.; Kacker, S.; Patil, A. O.; Baugh, L. S.; Rucker, S. P.; Zushma, S.; Berluche, E.; Sissano, J. A. *Macromolecules* **2003**, *36*, 8584–8586.

43. Stibrany, R. T. MetCon2002, Houston, TX, 2002.
.
44. a) Ritter, S. K. *Chem. Eng. News* **2006**, *84*, 42:45-48. b) Rorabacher, D. B. *Chem. Rev.* **2004**, *104*, 651-697.

45. Desimoni, G.; Faita, G., Jørgensen, K. A. *Chem. Rev.* **2006**, *106*, 3561-3651.

46. Grätzel, M. *Inorg. Chem.* **2005**, *44*, 6382-6390.

47. Sakaki, S.; Kuroki, T.; Hamada, T. *J. Chem. Soc., Dalton Trans.* **2002**, 840-842.

48. Radziszewski, B. *Chem. Ber.* **1882**, *15*, 2706-2708.

49. Bredereck, H.; Theillig, G. *Chem. Ber.* **1953**, *86*, 88-96.

50. Vyas, P. C.; Oza, C. K.; Goyal, A. K. *Chem. Ind.* **1980**, 287-288.

51. Phillips, M. A. *J. Chem. Soc.* **1931**, 1143-1153.

52. Wang, L. L.; Joullié, M. M. *J. Am. Chem. Soc.* **1957**, *79*, 5706-5708.

53. Zielinski, M. In *The Chemistry of Carboxylic Acids and Esters*; Patai, S., Ed.; Wiley- Interscience: New York, 1969; pp.453-503.

54. Hendrickson, J. B.; Hussoin, M. S. *J. Org. Chem.* **1987**, *52*, 4139-4140.

55. Bloomfield, J. J. *J. Org. Chem.* **1961**, *26*, 4112-4115.

56. Dann, O.; Volz, G.; Deamnt, E.; Pfeifer, W.; Bergen, G.; Fick, H.; Walkenhorst, E. *Lieb. Ann. Chem.* **1973**, 1112-1140.

57. a) Argade, A. B.; Haugwitz, R. D.; Devraj, R.; Kozlowski, J.; Fanwick, P. E.; Cushman, M. *J. Org. Chem.* **1998**, *63*, 273-278. b) Nishimura, K.; Tomioka, K. *J. Org. Chem.* **2002**, *67*, 431-434.

58. Canty, A. J.; George, E. E.; Lee, C. V. *Aust. J. Chem.* **1983**, *36*, 415-418.

59. Isele, K.; Broughton, V.; Matthews, C. J.; Williams, A. F.; Bernardinelli, G.; Frans, P.; Decurtins, S. *J. Chem. Soc. Dalt. Trans.* **2002**, 3899-3905.

60. Gorun, S. M.; Stibrany, R. T.; Katritzky, A. R.; Slawinski, J. J.; Raid-Allah, H.; Brunner, F. *Inorg. Chem.* **1996**, *35*, 3-4.

61. a) Sprecher, C. A.; Zuberbühler, A. D. *Angew. Chem. Int. Ed. Engl.* **1977**, *16*, 189. b) Sprecher, C. A.; Zuberbühler, A. D. *Chimia* **1977**, *31*, 68.

62. Bradamante, S.; Facchetti, A.; Pagini, G. A. *Gazz. Chim. Ital.* **1996**, *126*, 329-337.

63. Rego, L. G. C.; Batista, V. S. *J. Am. Chem. Soc.* **2003**, *125*, 7989-7997.

64. Traynelis, V. J.; Hergenrother, W. L. *J. Am. Chem. Soc.*, **1964**, *86*, 298-299.

65. Arnold, R. G.; Barrows, R. S.; Brooks, R. A. *J. Org. Chem.* **1958**, *23*, 565-568.

66. Oda, K.; Sakai, M.; Tsujita, H.; Machida, M. *Synth. Comm.* **1997**, *27*, 1183-1189.

67. Stibrany, R. T.; Potenza, J. A.; Schugar, H. J. Private Communication CCDC 172750, 2001.

68. Krebs, F. C.; Spanggaard, H. *J. Org. Chem.* **2002**, *67*, 7185-7192, and references therein.

69. Steck, E. A.; Day, A. R. *J. Am. Chem. Soc.* **1943**, *65*, 452-456.

70. Anderson, B. A.; Bell, E. C.; Ginah, F. O.; Harn, N. K.; Pagh, L. M.; Wepsiec, J. P. *J. Org. Chem.* **1998**, *63*, 8224-8228.

71. Li, T.-S.; Li, L.-J.; Lu, B.; Yang, F. *J. Chem. Soc. Perkin Trans. I* **1998**, 3561-3564.

72. Stibrany, R. T.; Matturro, M. G.; Zushma, S.; Patil, A. O. *Acta Cryst.* **2004**, *E60*, m188-m189.

73. Genet, J.-P. *Acc. Chem. Res.* **2003**, *36*, 908-918.

74. a) Cai, D.; Payack, J. F.; Bender, D. R.; Hughes, D. L.; Verhoeven, T. R.; Reider, P. J. *J. Org. Chem.* **1994**, *59*, 7180-7181. b) Horiuchi, T.; Ohta, T.; Shirakawa, E.; Nozaki, K.; Takaya, H. *J. Org. Chem.* **1997**, *62*, 4285-4292. c) Shimada, T.; Cho, Y.-H.; Hayashi, T. *J. Am. Chem. Soc.* **2002**, *124*, 13396-13397.

75. a) Takaya, H.; Mashima, K.; Koyano, K.; Yagi, M.; Kumobayashi, H.; Takatomi, T.; Akutagawa, S.; Noyori, R. *J. Org. Chem.* **1986**, *51*, 629-635. b) Takaya, H.; Akutagawa, S.; Noyori, R. *Org. Synth.* **1989**, *67*, 20-32.

76. Hoshi, T.; Nozawa, E.; Katano, M.; Suzuki, T.; Hagiwara, H. *Tet. Lett.* **2004**, *45*, 3485-3487.

77. a) Uozumi, Y.; Tanahashi, A.; Lee, S.-Y.; Hayashi, T. *J. Org. Chem.* **1993**, *58*, 1945-1948. b) Frantz, D. E.; Weaver, D. G.; Carey, J. P.; Kress, M. H.; Dolling, U. H. *Org. Lett.* **2002**, *4*, 4717-4718.

78. Kasák, P.; Putala, M. *Collect. Czech. Chem. Commun.* **2000**, *65*, 729-740.

79. Cacchi, S.; Fabrizi, G.; Goggiamani, A. *Org. Lett.* **2003**, *5*, 4269-4272.

80. Stibrany, R. T.; Potenza, J. A. Private Communication CCDC 604806, 2006.

81. Li, D.; Zhao, B.; LaVoie, E. J. *J. Org. Chem.* **2000**, *65*, 2802-2805.

82. Perrin, D. D.; Armarego, W. L. F. *Purification of Laboratory Chemicals* Pergamon Press: New York, 1988.

83. Duan, G. -Y.; Sun, Y. -W.; Liu, J. –Z.; Wang, J. –W. *Acta Cryst.* **2005**, *E61*, o3476-o3477.

84. Stibrany, R. T.; Potenza, J. A. Private Communication CCDC 635590, 2007.

85. van Albada, G. A.; Reedijk, J.; Hamalainen, R.; Turpeinen, U.; Spek, A. L. *Inorg. Chim. Acta* **1989**, *163*, 213-222.

86. Johnstone, R. A. W.; Rose, M. E. *Tetrahedron.* **1979**, *35*, 2169-2173.

87. Isele, K.; Broughton, V.; Matthews, C. J.; Williams, A. F.; Bernardinelli, G.; Franz, P.; Decurtins, S. *J. Chem. Soc. Dalt. Trans.* **2002**, 3899-3905.

88. a) Roderick, W. R.; Nordeen, C. W. Jr.; Von Esch, A. M.; Appell, R. N. *J. Med. Chem.* **1972**, *15*, 655-658. b) Stibrany, R. T.; Potenza, J. A. Private Communication CCDC 652811, 2007. c) Stibrany, R. T.; Potenza, J. A. Private Communication CCDC 653352, 2007.

89. Stibrany, R. T.; Schugar, H. J.; Potenza, J. A. *Acta Cryst.* **2006**, *C62*, o140-o142.

90. a) Stibrany, R. T.; Schugar, H. J.; Potenza, J. A. *Acta Cryst.* **2003**, *E59*, o693-o695. b) Stibrany, R. T.; Schugar, H. J.; Potenza, J. A. *Int. Union Cryst. Newslet.* **2003**, *11*, 7.

91. Stibrany, R. T.; Potenza, J. A. Private Communication CCDC 604501, 2006.

92. Stibrany, R. T.; Schugar, H. J.; Potenza, J. A. *Acta Cryst.* **2002**, *E58*, o1142-o1144.

93. Stibrany, R. T.; Potenza, J. A. Private Communication CCDC 612691, 2006.

94. Stibrany, R. T.; Potenza, J. A. Private Communication CCDC 604897, 2006.

95. Stibrany, R. T.; Potenza, J. A. Private Communication CCDC 621180, 2006.

96 Stibrany, R. T.; Potenza, J. A. Private Communication CCDC 621178, 2006.

97. a) Stibrany, R. T.; Schugar, H. J.; Potenza, J. A. *Acta Cryst.* **2005**, *C61*, o354-o357. b) Stibrany, R. T.; Potenza, J. A. *Acta Cryst.* **2006**, *E62*, o828-o830.

98. Stibrany, R. T.; Potenza, J. A. Private Communication CCDC 619256, 2006.

99. Stibrany, R. T.; Schugar, H. J.; Potenza, J. A. *Acta Cryst.* **2003**, *E59*, o1448-o1450.

100. Stibrany, R. T.; Potenza, J. A. Private Communication CCDC 617708, 2006.

101. a) Stibrany, R. T.; Potenza, J. A. Private Communication CCDC 613440, 2006. b) Stibrany, R. T.; Potenza, J. A. Private Communication CCDC 660562, 2007.

102. Stibrany, R. T.; Schugar, H. J.; Potenza, J. A. *Acta Cryst.* **2004**, *E60*, o1603-o1605.

103. Davies, M. T.; Mamalis, P.; Petrow, V.; Sturgeon, B. *J. Pharm. Pharmacol.* **1951**, *3*, 420-430.

104. Stibrany, R. T.; Schugar, H. J.; Potenza, J. P. *Acta Cryst.* **2004**, *E60*, o1648-o1651.

105. Fries, K.; Walter, R.; Schilling, K. *Annal. Chem.* **1935**, *516*, 248-285.

106. Stibrany, R. T.; Potenza, J. P. Private Communication CCDC 619078, 2006.

107. a) Schmidt, J.; Eitel, M. *J. Prakt. Chem.* **1932**, *134*, 167-176. b) Bhatt, M. V. *Tett.* **1964**, *21*, 803-821.

108. Anselmi, C.; Centini, M.; Sega, A.; Napolitano, E.; Pelosi, P.; Scesa, C. *Int. J. Cosmetic Sci.* **1996**, *18*, 67-74.

109. Cole, E. R.; Crank, G.; Hai Minh, H. T. *Aust. J. Chem.* **1980**, *33*, 675-680.

110. Berkowitz, D. B.; Smith, M. K. *J. Org. Chem.* **1995**, *60*, 1233-1238.

111. Mistry, A. G.; Smith, K.; Bye, M. R. *Tet. Lett.* **1986**, *27*, 1051-1054.

112.   (a) Shapiro, P. J.; Bunel, E.; Schaefer, W. P.; Bercaw, J. E. *Organometallics* **1990**, *9*, 867-869. (b) Canich, J. A. M. U. S. Patent 5,026,798, 1991.

113.   McKnight, A. L.; Waymouth, R. M. *Chem. Rev.* **1998**, *98*, 2587-2598.

114.   (a) Zi, G; Li, H.-W.; Xie, Z. *Organometallics* **2002**, *21*, 3850-3855. (b) Wang, H.; Wang, Y.; Li, H.-W.; Xie, Z. *Organometallics* **2001**, *20*, 5110-5118.   (c) Juvaste, H.; Pakkanen, T. T.; Iiskola, E. I. *J. Organomet. Chem.* **2000**, *606*, 169-175. (d) Lanza, G.; Fragalà, I. L.; Marks, T. J. *J. Am. Chem. Soc.* **2000**, *122*, 12764-12777. (e) Juvaste, H.; Pakkanen, T. T.; Iiskola, E. I. *Organometallics* **2000**, *19*, 1729-1733. (f) Lu, H. L.; Hong, S.; Chung, T. C. *Macromolecules* **1998**, *31*, 2028-2034.

115.   Trifonov, A. A.; Spaniol, T. P.; Okuda, J. *Organometallics* **2001**, *20*, 4869-4874.

116.   Raab, V.; Kipke, J.; Burghaus, O.; Sundermeyer, J. *Inorg. Chem.* **2001**, *40*, 6964-6971.

117.   Dietrich-Buchecker, C. O.; Guilhem, J.; Kern, J.-M.; Pascard, C.; Sauvage, J.-P. *Inorg. Chem.* **1994**, *33*, 3498-3502.

118.   Bond, A. M.; Colton, R.; Kevekordes, J. E.; Panagiotidou, P. *Inorg. Chem.* **1987**, *26*, 1430-1435.

119.   (a) Lee, W.-Z.; Tolman, W. B. *Inorg. Chem.* **2002**, *41*, 5656-5658. (b) Holland, P. L.; Tolman, W. B. *J. Am. Chem. Soc.* **2000**, *122*, 6331-6332. (c) Randall, D. W.; George, S. D.; Hedman, B.; Hodgson, K. O.; Fujisawa, K.; Solomon, E. I. *J. Am. Chem. Soc.* **2000**, *122*, 11620-11631, and references cited therein.

120.   (a) Broughton, V.; Bernardinelli, G.; Williams, A. F. *Inorg. Chim. Acta* **1998**, *275*, 279-288. (b) Stibrany, R. T.; Matturro, M. G.; Zushma, S.; Patil, A. O. U. S. Patent 6,501,000, 2002. (c) Stibrany, R. T.; Matturro, M. G.; Zushma, S.; Patil, A. O. *Acta Cryst.* **2004**, *E60*, m188-m189. (d) Patil, A. O.; Zushma, S.; Stibrany, R. T.; Rucker, S. P.; Wheeler, L. M. *J. Polym. Sci.: Part A: Polymer Chem.* **2003**, *41*, 2095-2106.

121.   Stibrany, R. T.; Patil, A. O.; Zushma, S. **2002**, 223rd ACS Meeting, Orlando, FL.

122.   a) Clegg, W.; Sage, I.; Oswald, I.; Brough, P.; Bourhill, G. *Acta Cryst.* **2000**, *C56*, 1323-1325. b) Farrugia, L. J.; Peacock, R. D.; Stewart, B. *Acta Cryst.* **2000**, *C56*, e435-e436. c) Estrader, M.; Ribas, J.; Tangoulis, V.; Solans, X.; Font-Bardia, M.; Maestro, M.; Diaz, C. *Inorg. Chem.* **2006**, *45*, 8239-8250.

123.   a) Byrn, M. P.; Curtis, C. J.; Goldberg, I.; Hsiou, Y.; Khan, S. I.; Sawin, P. A.; Tendick, S. K.; Strouse, C. E. *J. Am. Chem. Soc.* **1991**, *113*, 6549-6557. b) Byrn,

M. P.; Curtis, C. J.; Hsiou, Y.; Khan, S. I.; Sawin, P. A.; Tendick, S. K.; Terzos, A.; Strouse, C. E. *J. Am. Chem. Soc.* **1993**, *115*, 9480-9497.

124.　Payra, P.; Zhang, H.; Kwok, W. H.; Duan, M.; Gallucci, J.; Chan, M. K. *Inorg. Chem.* **2000**, *39*, 1076-1080.

125.　a) Bernhardt, P. V.; Mattsson, J.; Richardson, D. R. *Inorg. Chem.* **2006**, *45*, 752-760. b) Ambundo, E. A.; Ochrymowycz, L. A.; Rorabacher, D. B. *Inorg. Chem.* **2001**, *40*, 5133-5138. c) Xie, B.; Wilson, L. J.; Stanbury, D. M. *Inorg. Chem.* **2001**, *40*, 3606-3614. d) Xie, B.; Elder, T.; Wilson, L. J.; Stanbury, D. M. *Inorg. Chem.* **1999**, *38*, 12-19.

126.　(a) Bruker, **2000.** *SHELXTL* (Version 6.10), *Saint-Plus* (Version 6.02) and *SMART-WNT2000* (Version 5.622). Bruker AXS Inc., Madison, Wisconsin, USA. (b) Blessing, R. H. *Acta Cryst.* **1995**, *A51*, 33-38. (c) Sheldrick, G. M. *SHELXS-97. Acta Cryst.* **1990**, *A46*, 467-473. (d) Sheldrick, G. M. *SHELXL-97. A Computer Program for the Refinement of Crystal Structures*; University of Göttingen: Germany.

127.　Evans, D. G.; Boeyens, J. C. A. *Acta Cryst.* **1990**, *B46*, 524-532.

128.　Holm, R. H.; Kennepohl, P.; Solomon, E. I. *Chem. Rev.* **1996**, *96*, 2239-2314.

129.　Chen, H.-J.; Zhang, L.-Z; Cai, Z.-G.; Yang, G.; Chen, X.-M. *J. Chem. Soc., Dalton Trans.* **2000**, 2463-2466
.

130.　Zhang, Y. *Inorg. Chem.* **1982**, *21*, 3889-3893.

131.　Skoog, D. A.; Holler, F. J.; Nieman, T.A. *Principles of Instrumental Analysis*; Harcourt Brace, Philadelphia 1998, 5th Edition, Chapter 25, pp 639-672.

132.　Coffino, A. R.; Peisach, J. *J. Magn. Reson. Series B* **1996**, *111*, 127-134.

133.　Wood, R. M.; Stucker, D. M.; Jones, L. M.; Lynch, W. B.; Misra, S. K.; Freed, J. H. *Inorg. Chem.* **1999**, *38*, 5384-5388.

134.　a) Manson, J. L.; Buschmann, W. E.; Miller, J. S. *Inorg. Chem.* **2001**, *40*, 1926-1935. b) Chan, S. I.; Fung, B. M.; Lütje, H. *J. Chem. Phys.* **1967**, *47*, 2121-2130. c) Tsay, F.-D.; Helmholz, L. *J. Chem. Phys.* **1969**, *50*, 2642-2650. d) Olender, Z.; Goldfarb, D.; Batista, J. *J. Am. Chem. Soc.* **1993**, *115*, 1106-1114.

135.　Knapp, M. J.; Krzystek, J.; Brunel, L.-C.; Hendrickson, D. N. *Inorg. Chem.*, **2000**, *39*, 281-288.

136.　a) Mabbs, F. E.; Machin, D. J. *Magnetism and Transition Metal Complexes*; Chapman and Hall: London, England, 1973: pp 20 and 21. b) Mabbs, F. E.;

Machin, D. J. *Magnetism and Transition Metal Complexes*; Chapman and Hall: London, England, 1973: pp 15 and 16.

137. Edwards, P. R.; Johnson, C. E.; Williams, R. J. P. *J. Chem. Phys.* **1967**, *47*, 2074-2082.

138. Dockum, B. W.; Reiff, W. M. *Inorg. Chim. Acta* **1986**, *120*, 61-76.

139. Solomon, E. I.; Pavel, E. G.; Loeb, K. E.; Campochiaro, C. *Coord. Chem. Revs*. **1995**, *144,* 369-460.

140. O'Connor, C. J. in *Progress in Inorganic Chemistry*, Lippard, S. J., Ed.; Wiley: New York, N. Y., 1982; pp 232 and 233.

141. a) *Stadler Handbook of Ultraviolet Spectra*: Simons, W. W., Ed.: Stadler Research Laboratories: Philadelphia, PA, 1979; p 21, spectrum 171. b) *Stadler Handbook of Ultraviolet Spectra*: Simons, W. W., Ed.: Stadler Research Laboratories: Philadelphia, PA, 1979; pp 182 and 183, spectra 738 and 739.

142. Borin, A. C.; Serrano-Andrés, L. *Chem. Phys.* **2000**, *262*, 253-265.

143. Siiman, O.; Gray, H. B. *Inorg. Chem.* **1974**, *13*, 1185-1191, and references therein.

144. Lever, A. P. B. *Inorganic Electronic Spectroscopy*, 2nd ed.; Elsevier: New York, 1984; p 450.

145. Forster, D.; Goodgame, D. M. L. *Inorg. Chem.* **1965**, *4*, 1712-1716.

146. Lever, A. P. B. *Inorganic Electronic Spectroscopy*, 2nd ed.; Elsevier: New York, 1984; p 496.

147. Lever, A. P. B. *Inorganic Electronic Spectroscopy*, 2nd ed.; Elsevier: New York, 1984; p 503.

148. Lever, A. P. B. *Inorganic Electronic Spectroscopy*, 2nd ed.; Elsevier: New York, 1984; p 569.

149. Stibrany, R. T.; Schugar, H. J.; Potenza, J. A. *Acta Cryst.* **2004**, *E60*, m1147-m1150.

150. Stibrany, R. T.; Schugar, H. J.; Potenza, J. A. *Acta Cryst.* **2005**, *E61*, m1991-m1994.

151. Allen, F. H. *Acta Cryst.* **2002**, *B58*, 380-388.

152. Grant, G. J.; Sanders, K. A.; Setzer, W. N.; VanDerveer, D. G. *Inorg. Chem.* **1991**, *30*, 4053-4056.

153. Sun, J. -S.; Uzelmeier, C. E.; Ward, D. L.; Dunbar, K. R. *Polyhedron*, **1998**, *17*, 2049-2063.

154. Van Albada, G. A.; Reedijk, J. *Inorg. Chim. Acta* **1989**, *163*, 213-222.

155. Isele, K.; Franz, P.; Ambrus, C.; Bernardelli, G.; Decurtins, S.; Williams, A. F. *Inorg. Chem.* **2005**, *44*, 3896-3906.

156. Tundo, P.; Selva, M. *Acc. Chem. Res.* **2002**, *35*, 706-716.

157. Kim, W. B.; Joshi, U. A.; Lee, J. S. *Ind. Eng. Chem. Res.* **2004**, *43*, 1897-1914.

158. Pacheco, M. A.; Marshall, C. L. *Energy and Fuels* **1997**, *11*, 2-29.

159. Ryu, J. Y. U. S. Patent 6,010,976, 2000.

160. Jentsch, J.-D.; Klausener, A.; Landscheidt, H.; Lenders, B.; Pennemann, B.; Wolters, E.; Zirngiebl, E. U. S. Patent 5,498,744, 1996.

161. Rivetti, F.; Romano, U. U. S. Patent 5,686,644, 1997.

162. Stibrany, R. T.; Mehnert, C. P.; Matturro, M. G. U. S. Patent 7,049,457, 2006.

163. Britovsek, G. J. P.; Gibson, V. C.; Wass, D. F. *Angew. Chem. Int. Ed.* **1999**, *38*, 428-447.

164. Ittel, S. D.; Johnson, L. K.; Brookhart, M. *Chem. Rev.* **2000**, *100*, 1169-1203.

165. Schulz, D. N.; Patil A. O. In *Functional Polymers - Modern Synthetic Methods and Novel Structures*; Patil, A. O., Schulz, D. N., Novak, B. M., Eds.; ACS Symp. Ser. 704; American Chemical Society: Washington, DC, 1998; pp 1-14.

166. Abu-Surrah, A.; Rieger, B. *Angew. Chem. Int. Ed. Engl.* **1996**, *35*, 2475-2477.

167. Brookhart, M. S.; Johnson, L. K.; Killian, C. M.; Arthur, S. D.; Feldman, J.; McCord, E. F.; McLain, S. J.; Kreutzer, K. A.; Bennett, M. A.; Coughlin, E. B.; Ittel, S. D.; Parthasarathy, A.; Wang, L.; Yang, Z. U. S. Patent 5,866,663, 1999.

168. Johnson, L. K.; Killian, C. M.; Arthur, S. D.; Feldman, J.; McCord, E. F.; McLain, S. J.; Kreutzer, K. A.; Bennett, M. A.; Coughlin, E. B.; Ittel, S. D.; Parthasarathy, A.; Temple, D. J.; Brookhart, M. S. WO Patent 9623010, 1996.

169. Small, B. L.; Brookhart, M.; Bennet, A. M. A. *J. Am. Chem. Soc.* **1998**, *120*, 4049-4050.

170. Britovsek, G. J. P.; Bruce, M.; Gibson, V. C.; Kimberley, B. S.; Maddox, P. J.; Mastroianni, S.; McTavish, S. J.; Redshaw, C.; Solan, G. A.; Strömberg, S.; White, A. J. P.; Williams, D. J. *J. Am. Chem. Soc.* **1999**, *121*, 8728-8740.

171. Stibrany, R. T.; Schulz, D. N.; Kacker, S.; Patil, A. O., WO Patent 9930822, 1999.

172. Stibrany, R. T.; Schulz, D. N.; Kacker, S.; Patil, A. O., U. S. Patent 6,037,297, 2000.

173. Stibrany, R. T.; Gorun, S. M. *J. Organomet. Chem.* **1999**, *579*, 217-221.

174. Mathias, L. J.; Burkett, D. *Tet. Lett.* **1979**, *49*, 4709-4712.

175. Birnbaum, E. R.; Hodge, J. A.; Grinstaff, M. W.; Schaefer, W. P.; Henling, L.; Labinger, J. A.; Bercaw, J. E.; Gray, H. B. *Inorg. Chem.* **1995**, *34*, 3625-3632.

176. Belle, C.; Beguin, C.; Gautier-Luneau, I.; Hamman, S.; Philouze, C.; Pierre, J. L.; Thomas, F.; Torelli, S.; Saint-Aman, E.; Bonin, M. *Inorg. Chem.* **2002**, *41*, 479-491.

177. Stibrany, R. T.; Patil, A. O.; Zushma, S. **2002**, 223rd ACS Meeting, Orlando, FL.

178. Richardson, D. E. In *Electron Transfer Reactions*; Isied, S. S., Eds.; American Chemical Society: Washington, D.C.; 1997: pp79-90.

179. Stibrany, R. T.; Patil, A. O.; Zushma, S. *Poly. Mat. Sci. Eng.* **2002**, *86*, 323-324.

180. Seppala, J. V.; Koivumaki, J.; Liu, X. J. *Poly. Sci., Part A: Poly. Chem.* **1993**, *31*, 3447-3452.

181. Brookhart, M.; Wagner, M. I.; *J. Am. Chem. Soc.* **1994**, *116*, 3641- 3642.

182. a) Wang, C.; Friedrich, S.; Younkin, T. R.; Li, R. T.; Grubbs, R. H.; Bansleben, D. A.; Day, M. W. *Organometallics* **1998**, *17*, 3149-3151. b) Bansleben, D. A.; Friedrich, S.; Younkin, T. R.; Grubbs, R. H.; Wang, C.; Li, R. T.; WO Patent 9842665, 1998. c) Younkin, T. R.; Connor, E. F.; Henderson, J. I.; Friedrich, S. K.; Grubbs, R. H.; Bansleben, D. A. *Science* **2000**, *287*, 460-462.

183. a) Johnson, L. K.; Mecking, S.; Brookhart, M. *J. Am. Chem. Soc.* **1996**, *118*, 267-268. b) Johnson, L. K.; Killian, C. M.; Authur, S. D.; Feldman, J.; McCord, E. F.; Kreutzer, K. A.; Coughlin, E. B.; Parthasarathy, A.; Brookhart, M. S. WO Patent

Application 96/23010 (1996). c) Mecking, S.; Johnson, L. K.; Wang, L.; Brookhart, M. *J. Am. Chem. Soc*. **1998**, *120*, 888-899.

184.   Johnson, L.; Bennett, A.; Dobbs, K.; Hauptman, E.; Lonkin, A.; Ittel, S.; McCord, E.; McLain, S.; Radzewich, C.; Yin, Z.; Wang, L.; Wang, Y.; Brookhart, M. *Polym. Mater. Ssci. Eng.* **2002**, *86*, 319.

185.   Drent, E.; van Dijk, R.; Van Ginkel, R.; Van Oort, B.; Pugh, R. I.; *J. Chem. Soc., Chem. Commun*. **2002**, 744-745.

186.   Gibson, V. C.; Tomov, A.; Wass, D. F.; White, A. J. P. *J. Chem. Soc., Dalton Trans*. **2002**, 2261-2262.

187.   Shibayama, K.; Ogasa, M. WO Patent 9835996, 1998.

188.   a) Matyjaszewski, K. in *Controlled Radical Polymerization*; Matyjaszewski, K., Ed.; ACS Symp. Ser. 685; American Chemical Society: Washington, DC, 1998, pp 258-283. b) Xia, J.; Matyjaszewski, K. *Macromolecules* **1997**, *30*, 7697-7700.

189.   a) Liu, S.; Elyashiv, S.; Sen, A. *J. Am. Chem. Soc*. **2001**, 123, 12738-12739. b) Sen, A.; Elyashiv, S.; Greinert, N.; Liu, S. *Polym. Mater. Sci. Eng.* **2002**, *86*, 330.

190.   a) Stibrany, R. T.; Schulz, D. N.; Kacker, S.; Patil, A. O., WO Patent 9930822, 1999. b) Stibrany, R. T.; Schulz, D. N.; Kacker, S.; Patil, A. O. U. S. Patent 6,037,297, 2000. c) Stibrany, R. T.; Schulz, D. N.; Kacker, S.; Patil, A. O. U. S. Patent 6,417,303, 2002.

191.   Matsuzaki, K.; Uryu, T.; Kanai, T.; Hosonuma, K.; Matsubara, T.; Tachikawa, M.; Yamada, M.; Okuzono, S. *Makromol. Chem*. **1977**, *178*, 11-17.

192.   McLain, S. J.; Feldman, J.; McCord, E. F.; Gardner, K. H.; Teasley, M. F.; Coughlin, E. B.; Sweetman, K. J. *Macromolecules* **1998**, *31*, 6705-6707.

193.   Matyjaszewski, K. *Macromolecules* **1998**, *31*, 4710-4717.

194.   Wang, A. R.; Zhu, S. *Macromolecules* **2002**, *35*, 9926-9933.

195.   Aylward, N. N. *J. Polym. Sci.: Polym. Phys.* **1981**, *19*, 1805-1816 and references therein.

196.   a) Fayt, R.; Forte, R.; Jacobs, C.; Jerome, R.; Ouhadi, T.; Teyssie, Ph.; Varshney, S. K. *Macromolecules* **1987**, *20*, 1442-1444. b) Hatada, K. *J. Polym. Sci., Part A: Chem.* **1999**, *37*, 245-260.

197.   Collins, S.; Ward, D. G.; Suddaby, K. H. *Macromolecules* **1994**, *27*, 7222-7224.

198.   Bolig, A. D.; Chen, E. Y. –X. *J. Am. Chem. Soc.* **2004**, *126,* 4897-4906.

Appendix

All ORTEP[29] views are shown with 25% probability thermal ellipsoids.

193. $N^{13},N^{43'}$-dihydro-*rac*-2,2'-bis[2-(1-propylbenzimidazol-1-ium)]biphenyl bis(perchlorate). (**9b-2**)

194. $N^{13},N^{43'}$-dihydro-[*rac*-2,2'-bis(2-(1-benzylbenzimidazol-1-ium))biphenyl] (trifluoromethanesulfonate)(bromide). (**9e·HBr·H(SO$_3$CF$_3$)**)

195. $N^{13},N^{43'}$-dihydro-[*rac*-2,2'-bis(2-(1-propyl-5,6-dimethylbenzimidazol-1-ium))biphenyl] di(trifluoromathanesulfonate) · hydrate. (**10·2[H(CF$_3$SO$_3$)]·H$_2$O**)

196. (*E*)-1,2-Bis(1-methylbenzimidazol-2-yl)ethene. (**11a**)

197. (*E*)-1,2-Bis(1-ethylbenzimidazol-2-yl)ethene. (**11c**)

198. 3-Ethyl-2-[(*E*)-2-(1-ethylbenzimidazol-2-yl)-ethenyl]benzimidazol-1-ium perchlorate. (**11c-1**)

199. (*E*)-1,2-(1-methylbenzimidazol-2-yl)ethenol · 1.5 water. (**12**)

200. (*S,S*)-1,2-Bis(1-methylbenzimidazol-2-yl)-1',2'-bis(methoxy)ethane. (**15a**)

201. (*R,S*)-1,2-Bis(1-methylbenzimidazol-2-yl)-1',2'-bis(methoxy)ethane. (**15b**)

202. (*R,R*)-1,2-Bis(1-methylbenzimidazol-2-yl)-1',2'-bis(methoxy)ethane. (**15c**)

203. (*S,S*)-1,2-Bis(3-ethylbenzimidazol-1-ium)-1',2'-bis(ethoxy)ethane di(perchlorate). (**15e-1**)

204. 1,1'-Bis(1-hydrobenzimidazol-2-yl)ketone. (**17**)

205. 1,1',2,2'Tetra(1-propylbenzimidazol-2-yl)ethane. (**18**)

206. 5,6-dichloro-1-propylbenzimidazole. (**19a**)

207. 1-hydro-napth[2,3-d]imidazole. (**19b**)

208. Bis(1-ethyl-phenanthro[9,10-d]imidazol-2-yl)ketone. (**22**)

209. 1,1'-Bis(1-methylbenzimidazol-2-yl)ketone. (**27a**)

210. *rac*- bis- {2,2'-bis [2-(1-propylbenzimidazol-2-yl)] biphenyl)} manganese(II) bis (perchlorate), *rac*-Mn(II)(**9b**)$_2$·(ClO$_4$)$_2$. (**2-2**)

211. *rac*-bis-{2,2'-bis[2-(1-propylbenzimidazol-2-yl)]biphenyl}iron(II) bis(perchlorate), *rac*-Fe(II)(**9b**)$_2$·(ClO$_4$)$_2$. (**2-3**)

212. *rac*-bis-[2,2'-bis[2-(1-propylbenzimidazol-2-yl)]biphenyl)]cobalt(II) bis(perchlorate), *rac*-Co(II)(**9b**)$_2$·(ClO$_4$)$_2$. (**2-5**)

213. *rac*-bis-[2,2'-bis[2-(1-propylbenzimidazol-2-yl)]biphenyl)]nickel(II) bis(perchlorate), *rac*-Ni(II)(**9b**)$_2$·(ClO$_4$)$_2$. (**2-6**)

214. *rac*-bis-[2,2'-bis[2-(1-hydrobenzimidazol-2-yl)]biphenyl)]copper(II) bis(perchlorate), *rac*-Cu(II)(**1e**)$_2$·(ClO$_4$)$_2$. (**2-7**)

215. *rac*- bis- [2,2'-bis [2-(1-propylbenzimidazol-2-yl)] biphenyl)] copper(II) bis(perchlorate), *rac*-Cu(II)(**9b**)$_2$·(ClO$_4$)$_2$. (**2-8**)

216. *rac*- bis-[2,2'-bis [2-(1-propylbenzimidazol-2-yl)] biphenyl)] copper(II) bis(trifluoromethanesulfonate), *rac*-Cu(II)(**9b**)$_2$·(CF$_3$SO$_3$)$_2$. (**2-9**)

217. *rac*- bis-[2,2'-bis [2-(1-octylbenzimidazol-2-yl)] biphenyl)] copper(II) bis(trifluoromethanesulfonate) · ethanol, *rac*-Cu(II)(**9c**)$_2$·(CF$_3$SO$_3$)$_2$·CH$_3$CH$_2$OH. (**2-10**)

218. *rac*- bis-[2,2′-bis (1-ethylbenzimidazol-2-yl) biphenyl)] copper(I) trfluoromethanesulfonate toluene solvate dihydrate, *rac*-Cu(I)(**9a**)$_2$·(CF$_3$SO$_3$)·(C$_7$H$_8$)·(H$_2$O). (**2-11**)

219. *rac*- bis-[2,2′-bis [2-(1-propylbenzimidazol-2-yl)] biphenyl)] copper(I) (perchlorate)·(CH$_3$CH$_2$OCH$_2$CH$_3$), *rac*-Cu(I)(**9b**)$_2$·(ClO$_4$)·(CH$_3$CH$_2$OCH$_2$CH$_3$). (**2-12**)

220. *rac-* bis-[2,2'-bis [2-(1-propylbenzimidazol-2-yl)]biphenyl)] zinc(II) bis (perchlorate), *rac*-Zn(II)(**9b**)$_2$·(ClO$_4$)$_2$. (**2-13**)

221. *rac-* bis-[2,2'-bis [2-(1-propylbenzimidazol-2-yl)] biphenyl)] cadmium(II) bis(perchlorate), *rac*-Cd(II)(**9b**)$_2$·(ClO$_4$)$_2$. (**2-14**)

222. *rac-* bis-[2,2'-bis [2-(1-propylbenzimidazol-2-yl)] biphenyl)] copper(II)$_{0.03}$ cadmium$_{0.97}$(II) bis(perchlorate), *rac*-Cu(II)$_{0.03}$Cd$_{0.97}$(II)(**9b**)$_2$·(ClO$_4$)$_2$. (**2-15**)

223. (*OC*-6-12)- bis[(*S*,*S*)-1,2-bis (1-methylbenzimidazol-2-yl)-1′,2′- bis(methoxy)ethane]copper(II) bis(tetrafluoroborate) acetonitrile disolvate, Cu(II)(**15a**)$_2$·(BF$_4$)$_2$ · (acetonitrile)$_2$. (**2-16**)

224. (*OC*-6-12)- bis[(*S*,*S*)-1,2-bis (1-methylbenzimidazol-2-yl)-1′,2′- bis(methoxy)ethane]palladium(II) dichloride, Pd(II)(**15a**)$_2$·Cl$_2$. (**2-17**)

225. (*OC*-6-12) - bis[(*R*,*R*)-1,2-bis(1-ethylbenzimidazol-2-yl)-1′,2′-bis(ethoxy)ethane] copper(II) bis(perchlorate), Cu(II)(**15d**)$_2$·(ClO$_4$)$_2$. (**2-18**)

226. (1,1′-bis(1-methylbenzimidazol-2-yl)-1″-(methoxy)ethane)copper(II) dichloride, Cu(II)(**7**)Cl$_2$. (**3-7**)
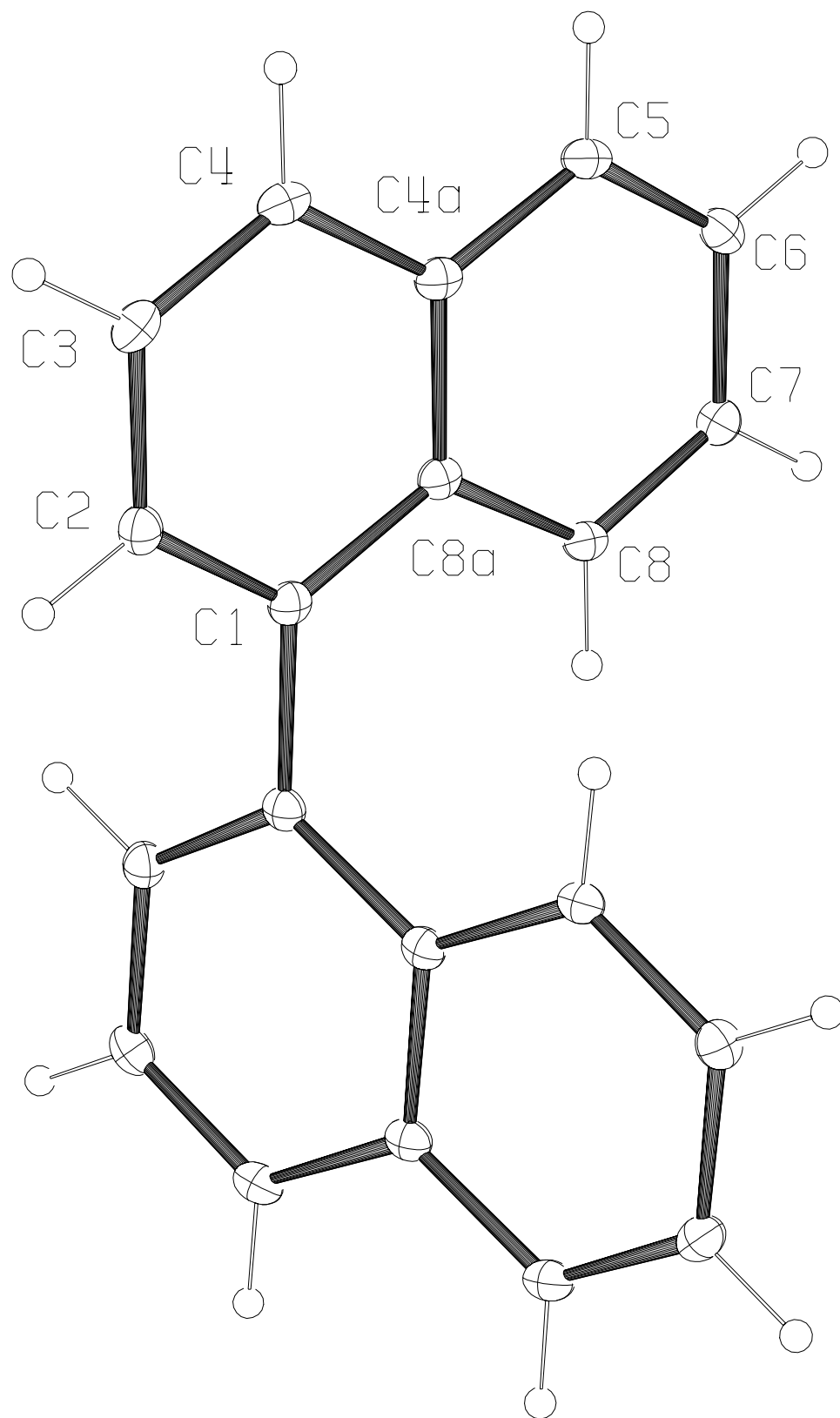
1,1′-binaphthyl.
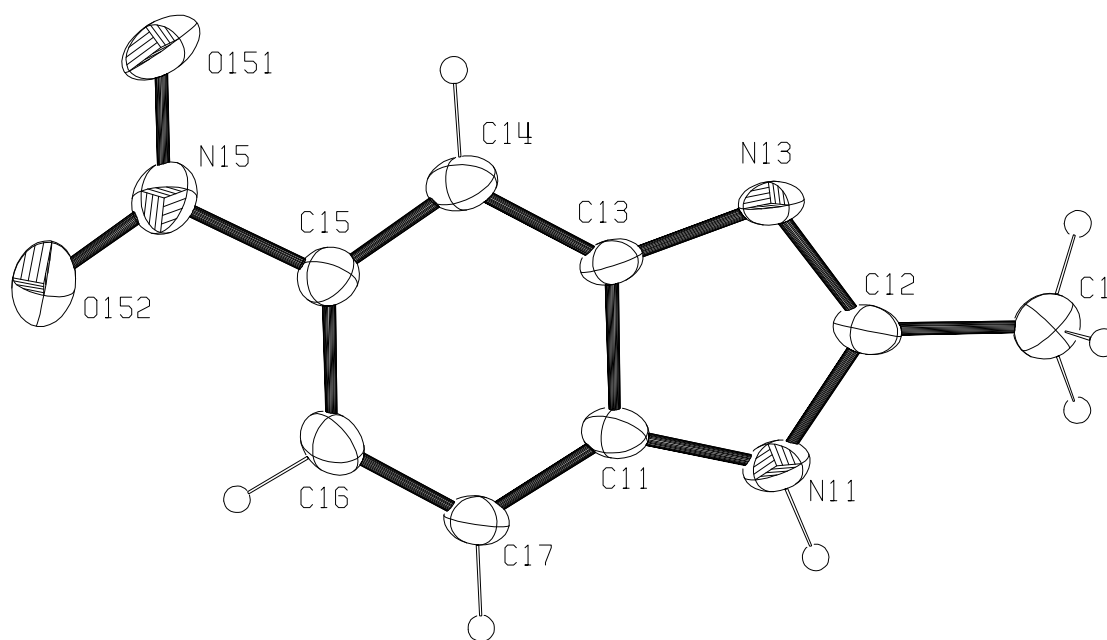
1-hydro-2-methyl-5-nitrobenzimidazol-2-yl. (**1c-1**)

3-(1-hydrobenzimidazol-2-yl)pentane. (**3a**)
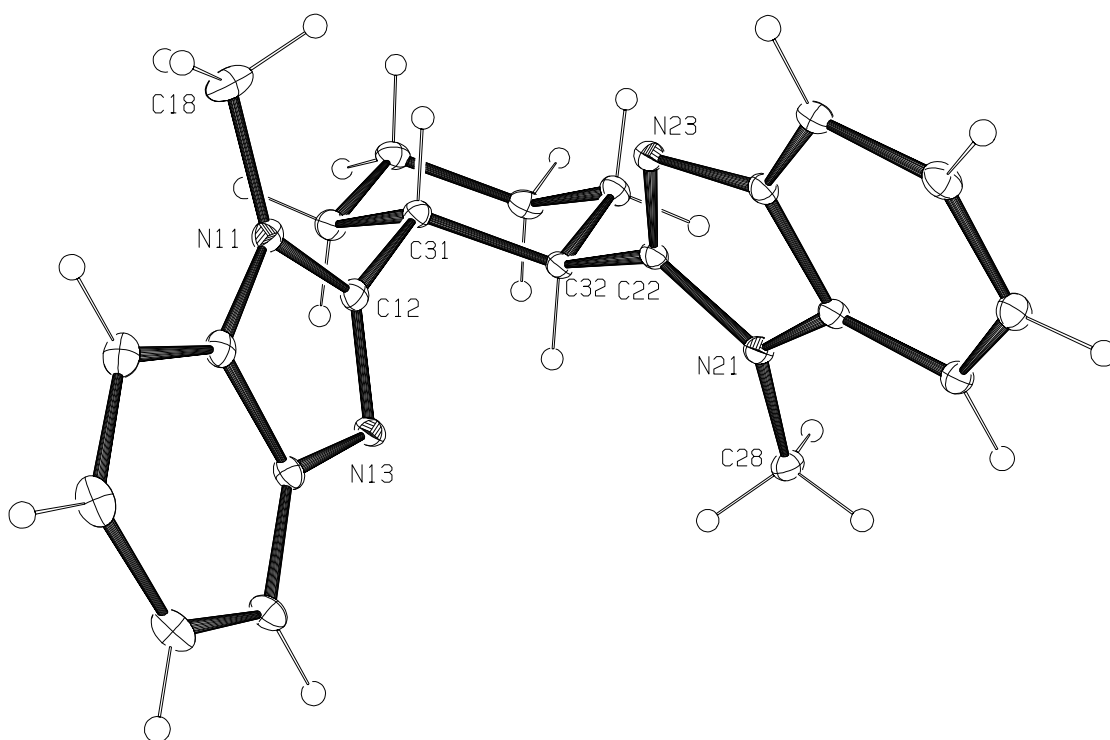
N13

N11
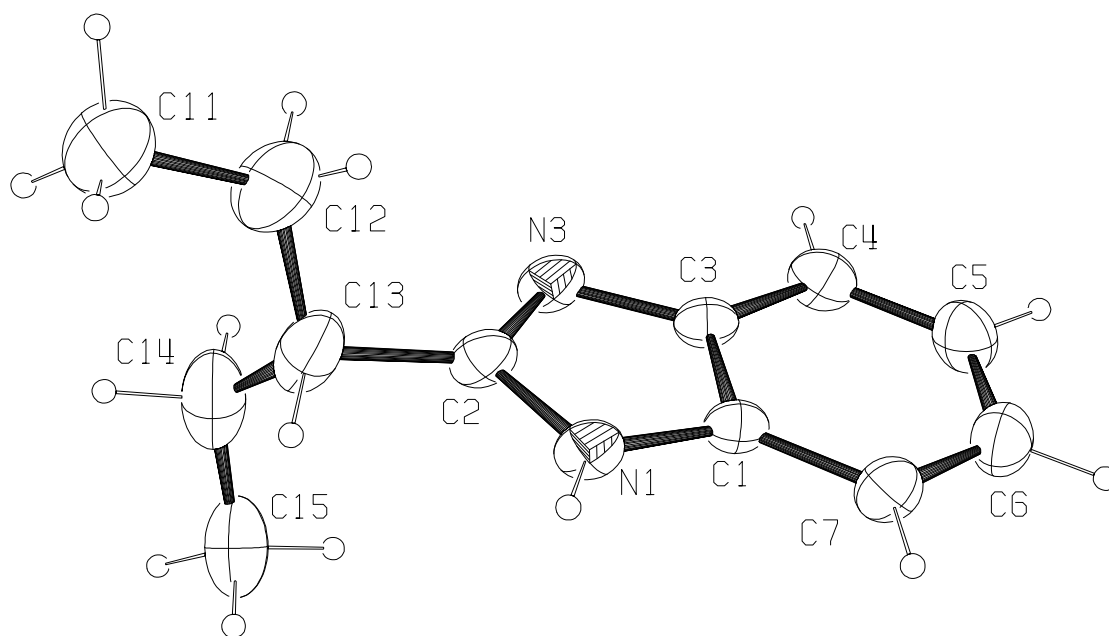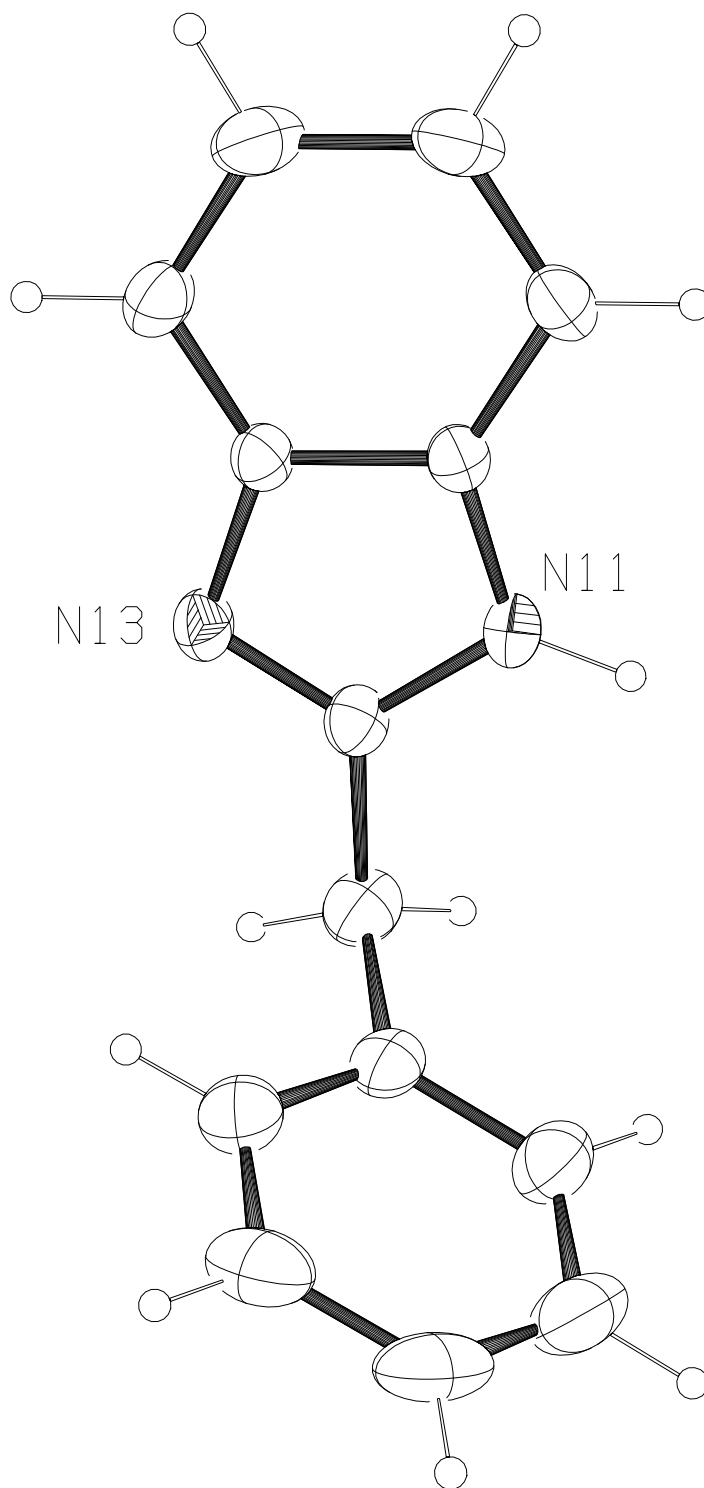
2-Benzyl-1-hydrobenzimidazol-2-yl. (**3c**)
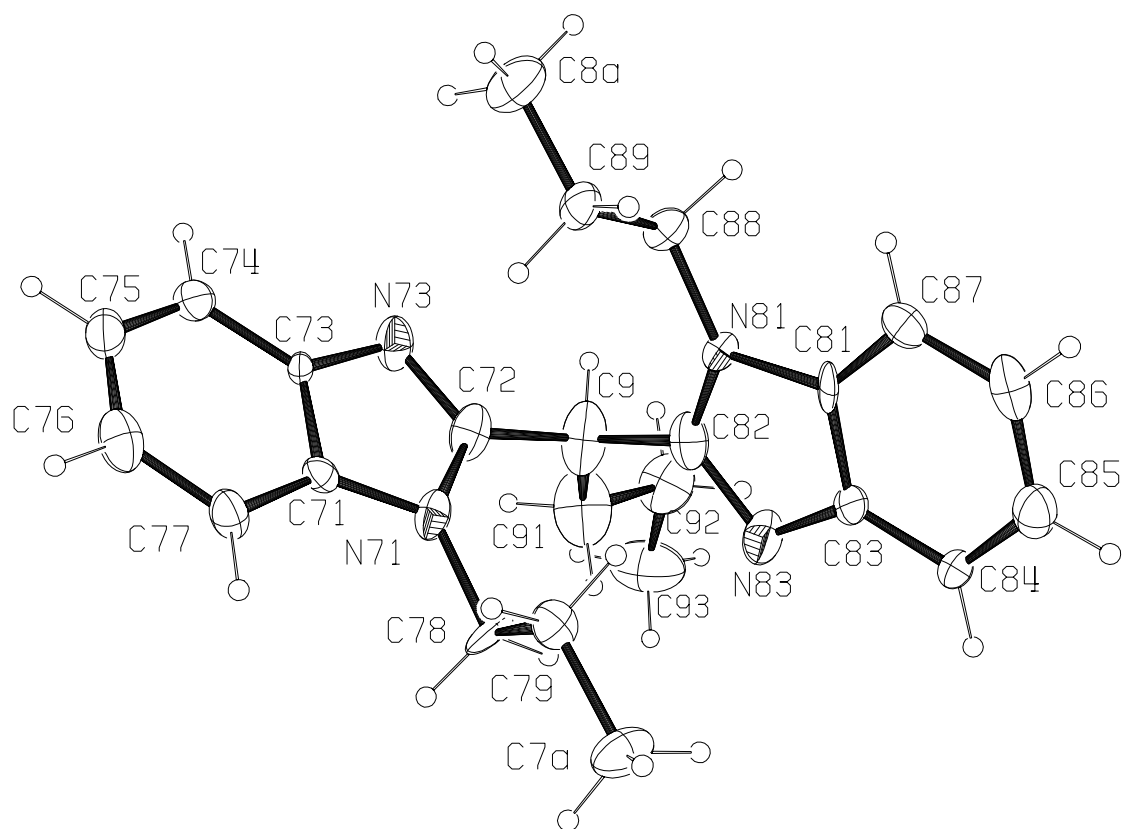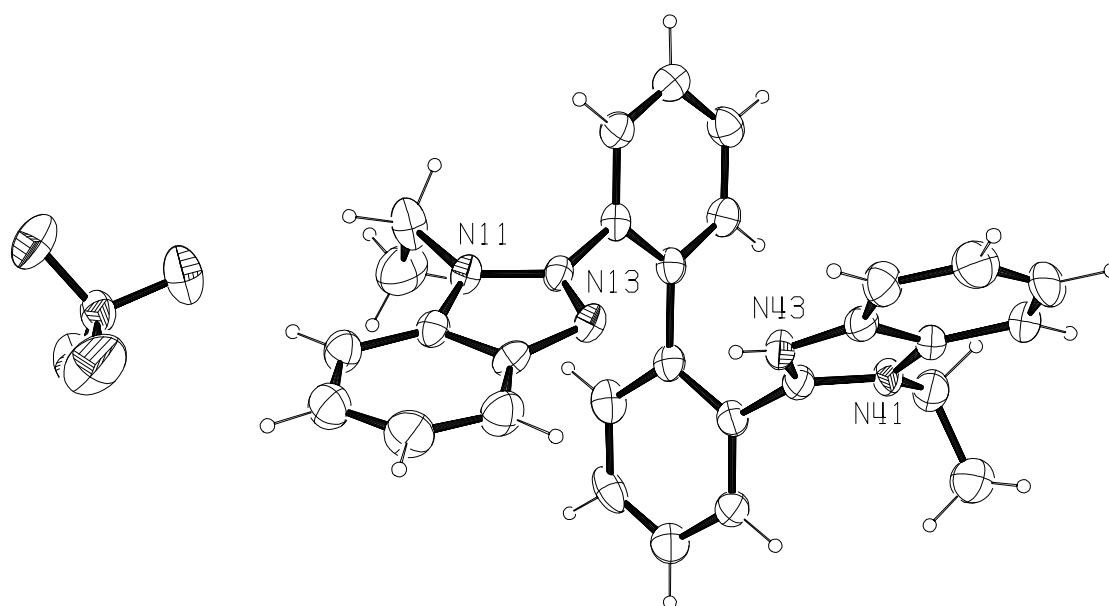
1,1′bis(1-propylbenzimidazol-2-yl)butane. (**5b**)
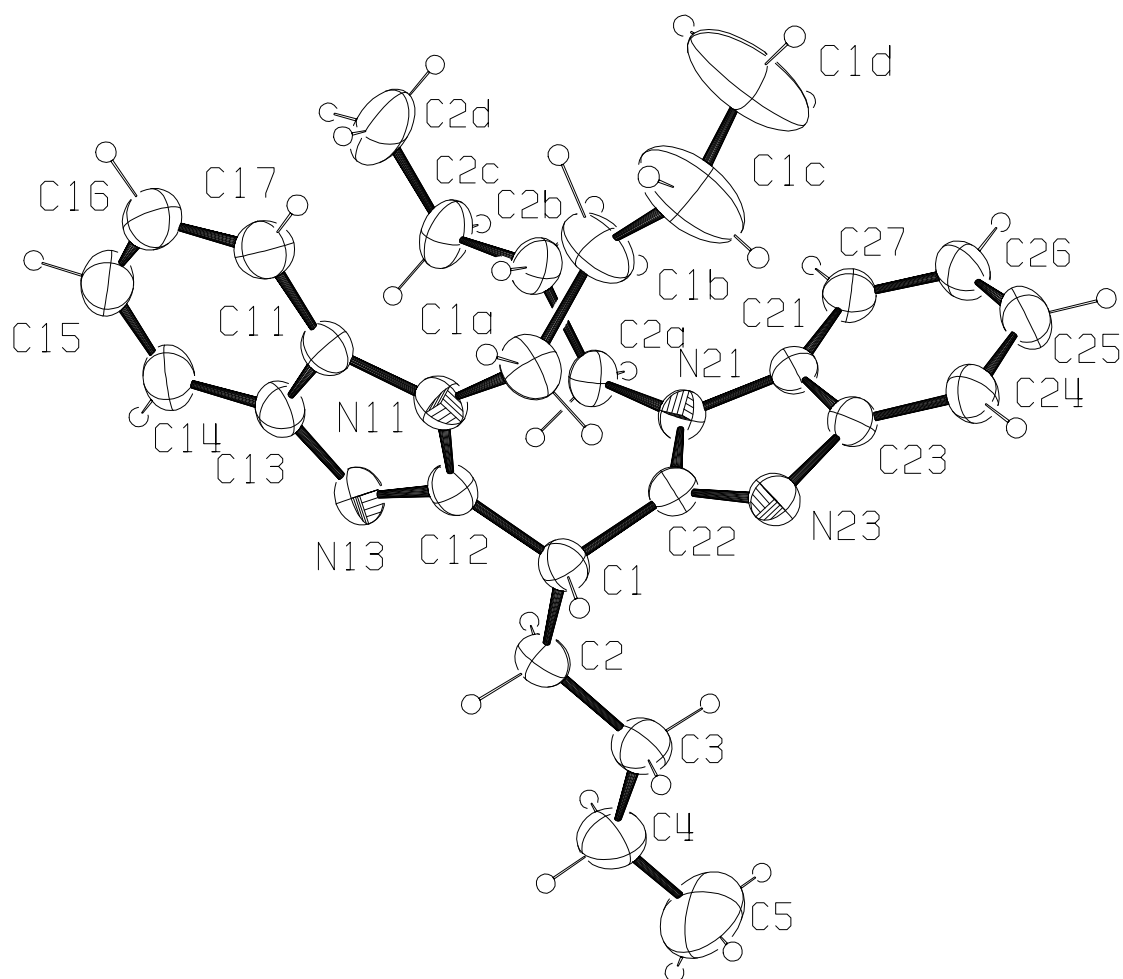
1,1′bis(1-butylbenzimidazol-2-yl)pentane. (**5c**)
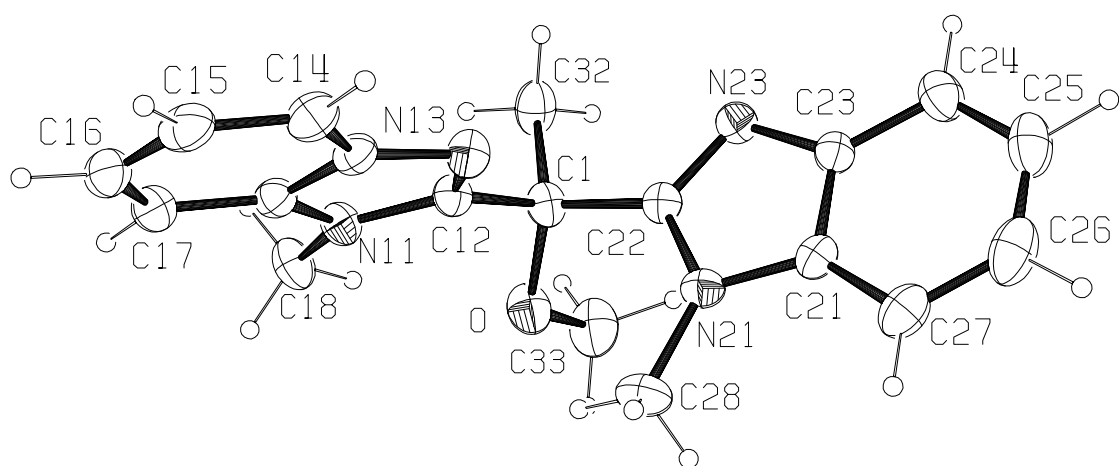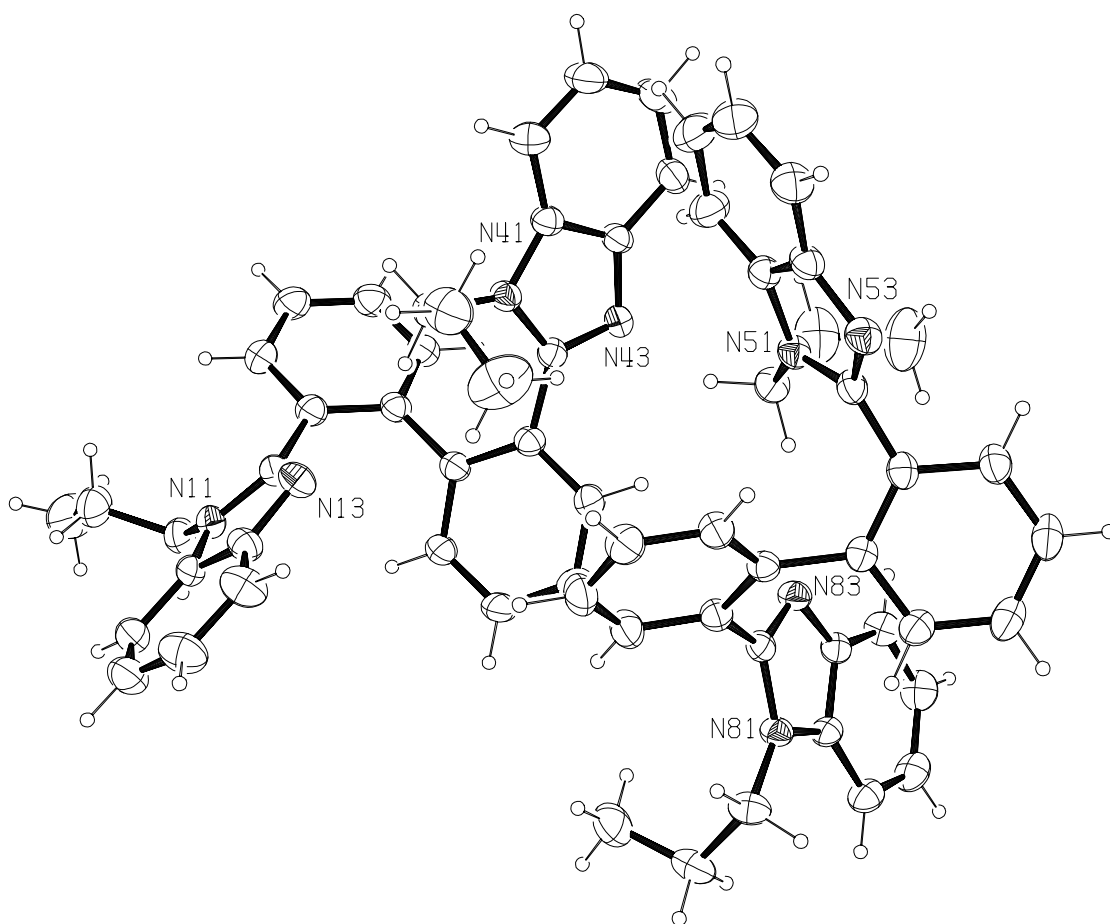
1,1'-bis(1-methylbenzimidazol-2-yl)-1"-(methoxy)ethane. (**7**)

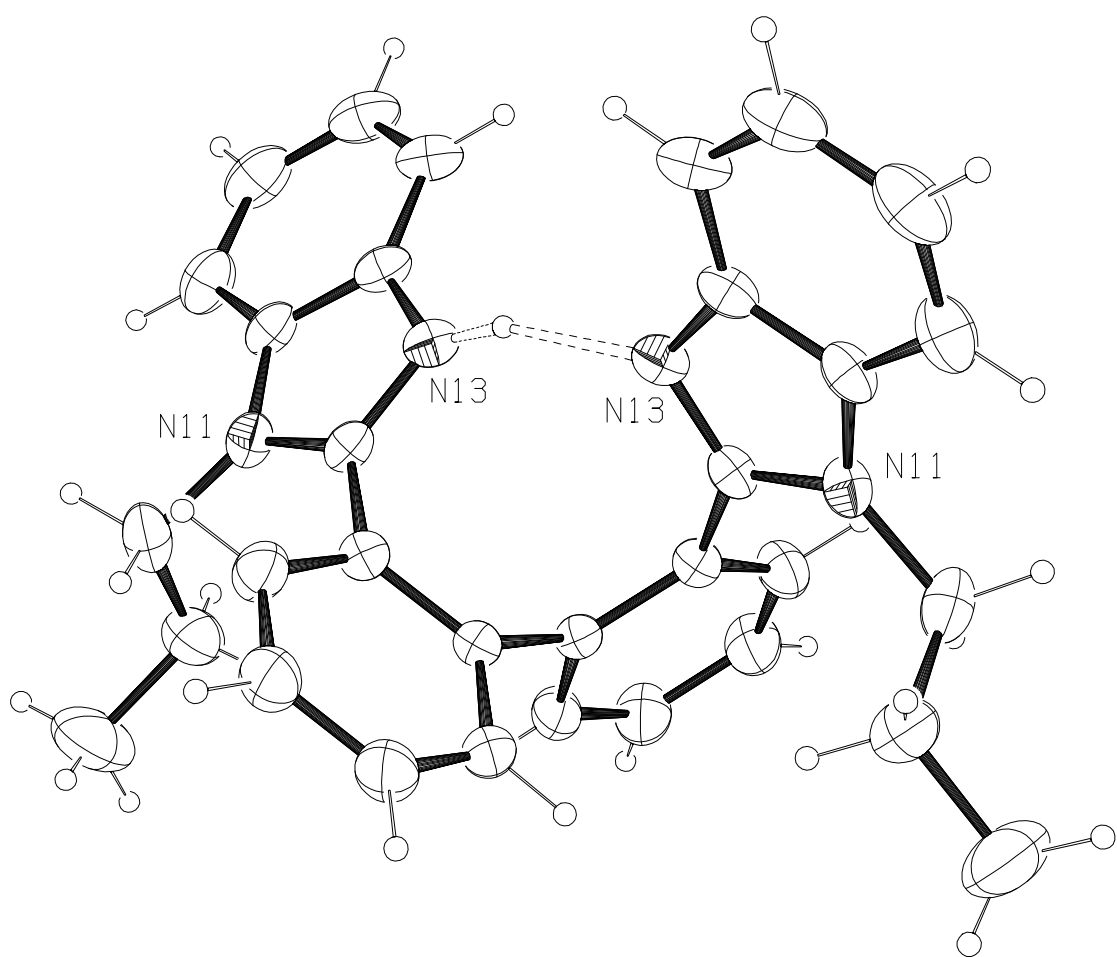*trans*-1,2-bis(1-methylbenzimidazol-2yl)cyclohexane. (**8a** · H₂O)

rac-2,2′-bis[2-(1-ethylbenzimidazol-2-yl)]biphenyl. (**9a**)

κ²*N*¹³,*N*⁴³′-Hydro-*rac*-2,2'-bis[2-(1-ethylbenzimidazol-2-yl)]biphenyl perchlorate.

(**9a**·H(ClO₄))

rac-2,2′-bis[2-(1-propylbenzimidazol-2-yl)]biphenyl. (**9b**)

The cation of κ²*N*¹³,*N*¹³′-Hydro-*rac*-2,2′-bis[2-(1-propylbenzimidazol-2yl)]biphenyl trifluoromethanesulfonate. (**9b-1**)
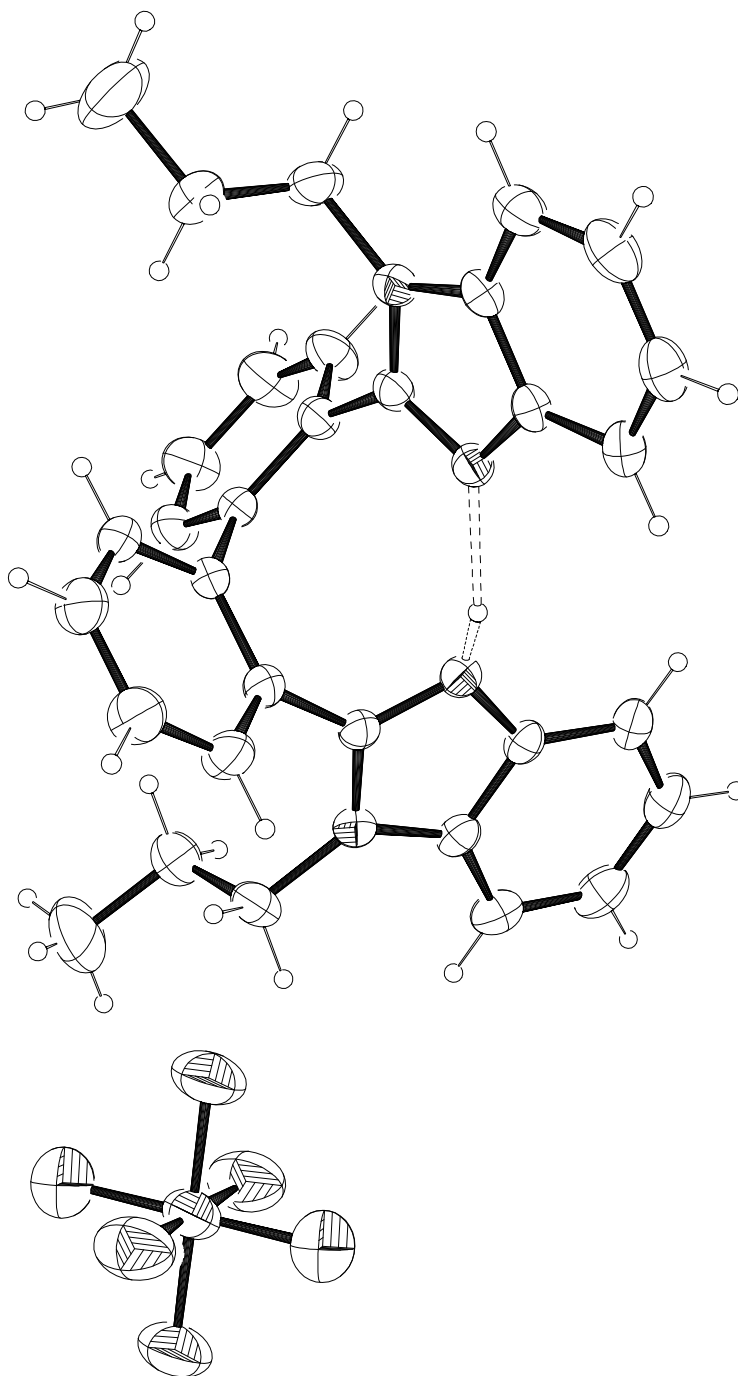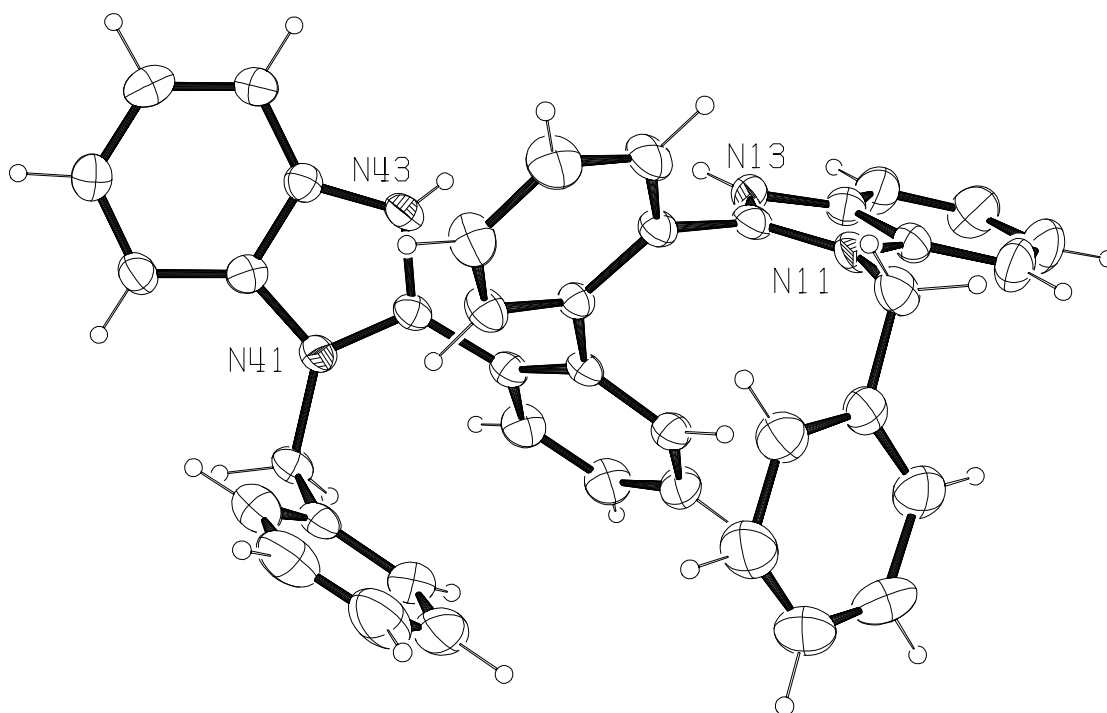
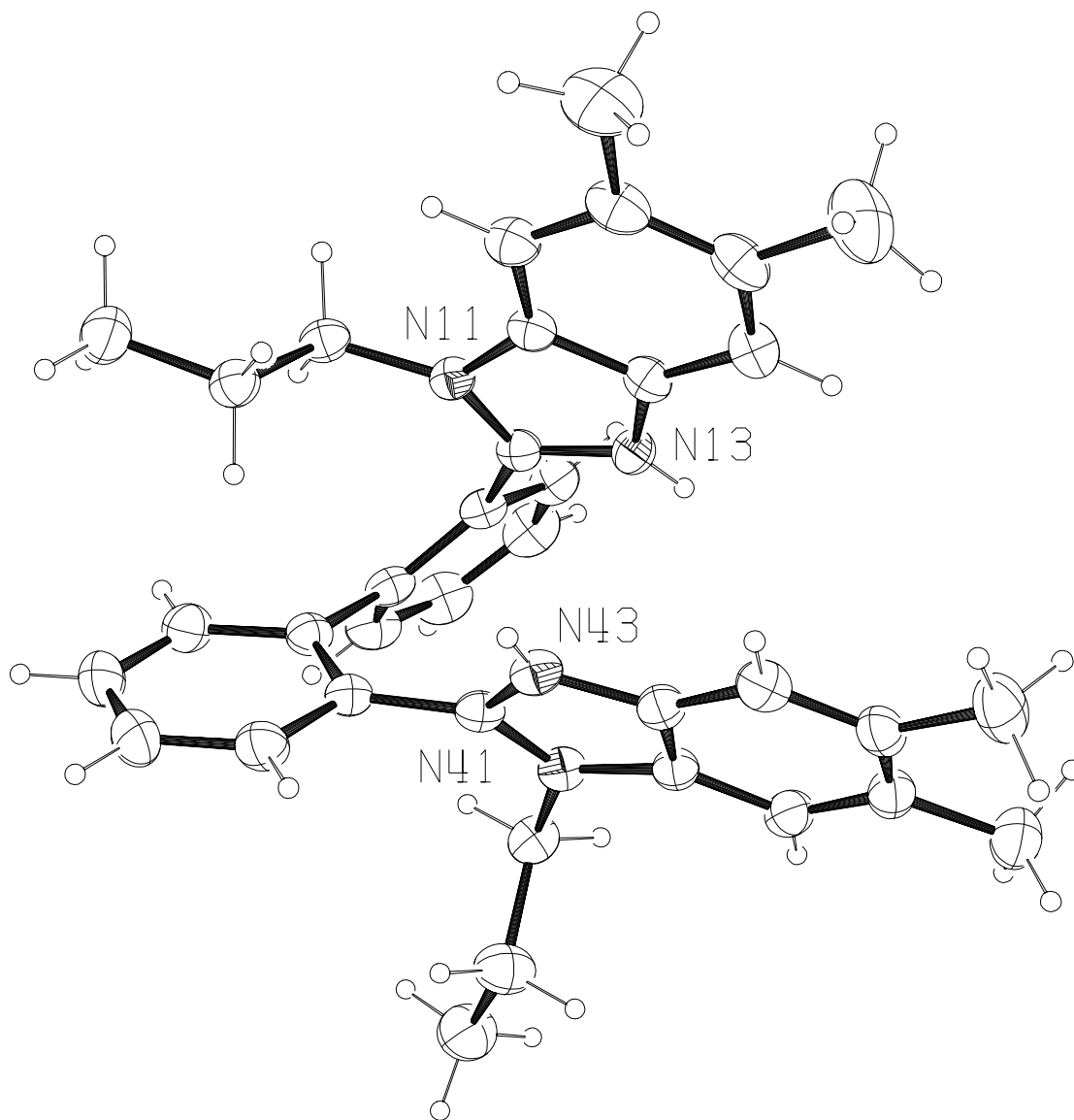$\kappa^2 N^{13}, N^{13'}$-Hydro-*rac*-2,2′-bis[2-(1-propylbenzimidazol-2-yl)]biphenyl

(hexafluorophosphate). (**9b**·H(PF$_6$))
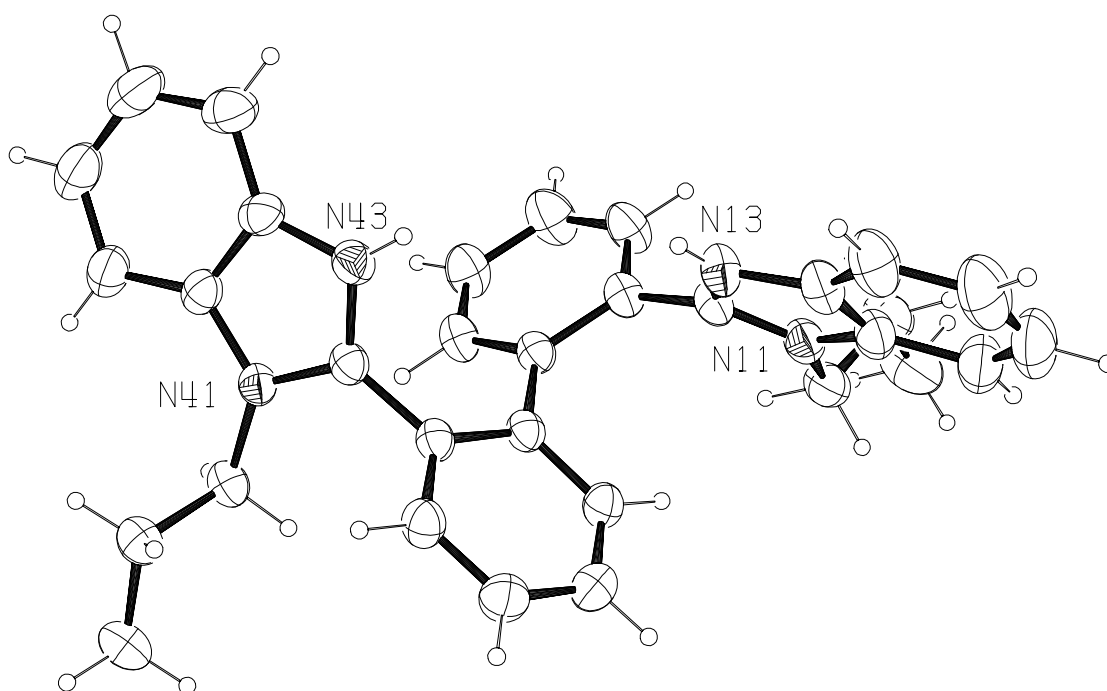
The cation of N^{13},$N^{43'}$-dihydro-*rac*-2,2′-bis[2-(1-propylbenzimidazol-1-ium)]biphenyl bis(perchlorate). (**9b-2**)
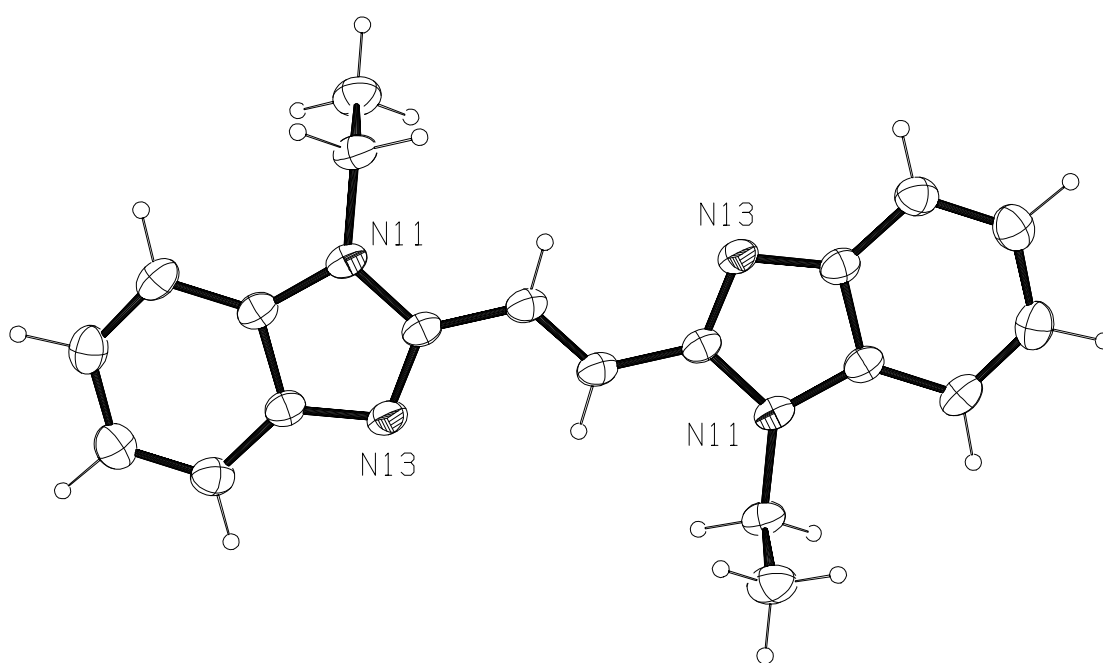
The cation of N^{13},$N^{43'}$-dihydro-[*rac*-2,2′-bis(2-(1-benzylbenzimidazol-1-

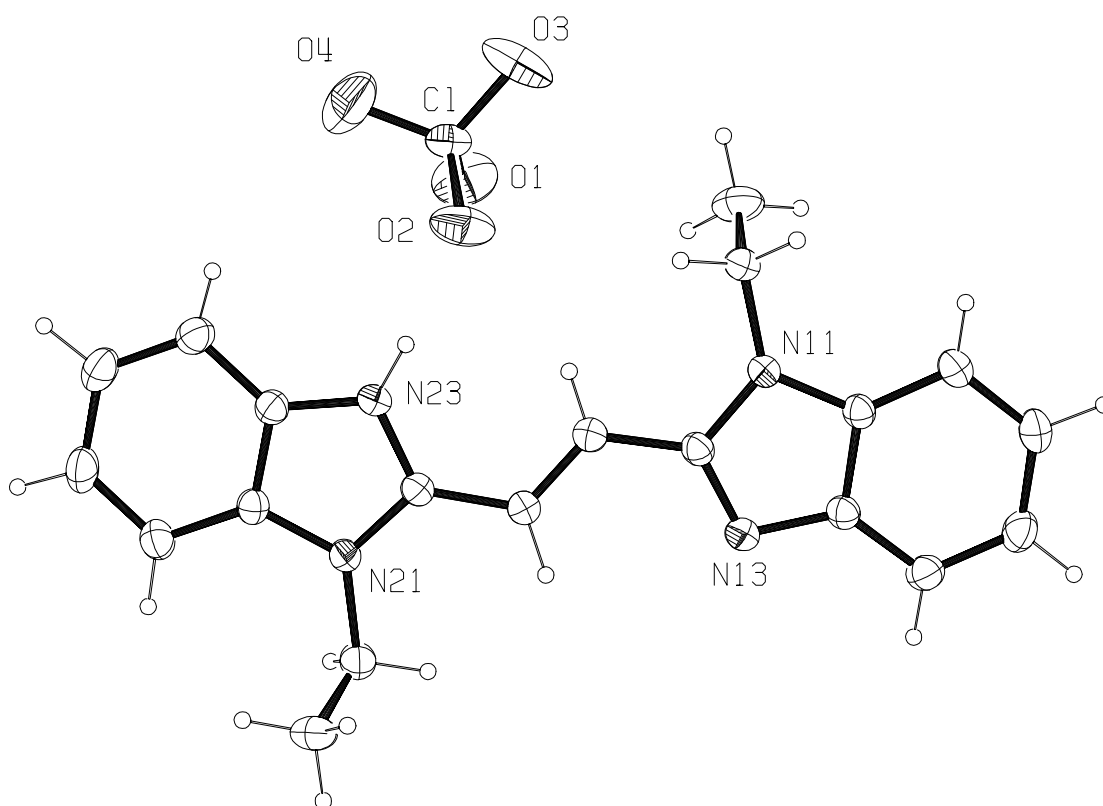ium))biphenyl](trifluoromethanesulfonate)(bromide). (**9e**·HBr·H(SO$_3$CF$_3$))

The cation of $N^{13},N^{43'}$-dihydro-[*rac*-2,2′-bis(2-(1-propyl-5,6-dimethylbenzimidazol-1-ium))biphenyl] di(trifluoromathanesulfonate) · hydrate. (**10**·2[H(CF$_3$SO$_3$)]·H$_2$O)
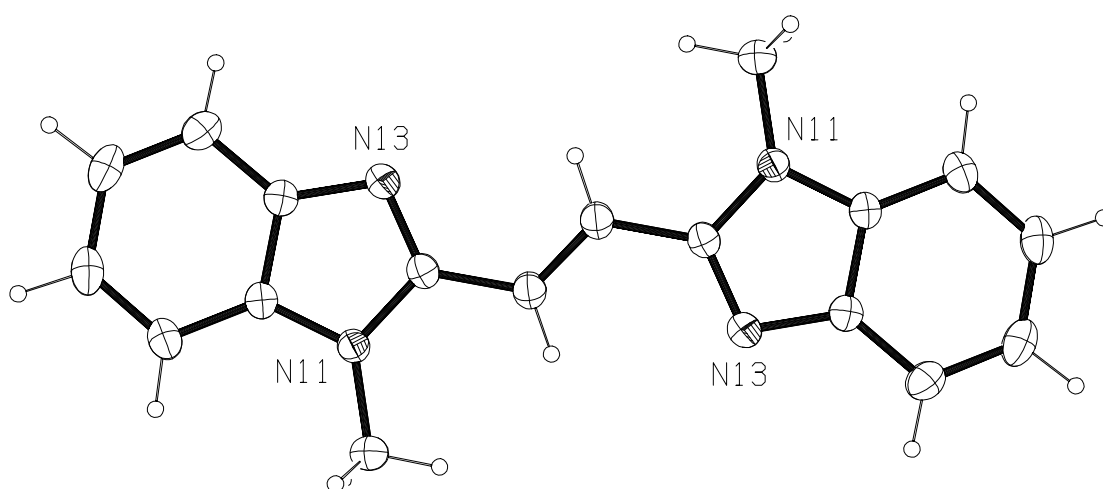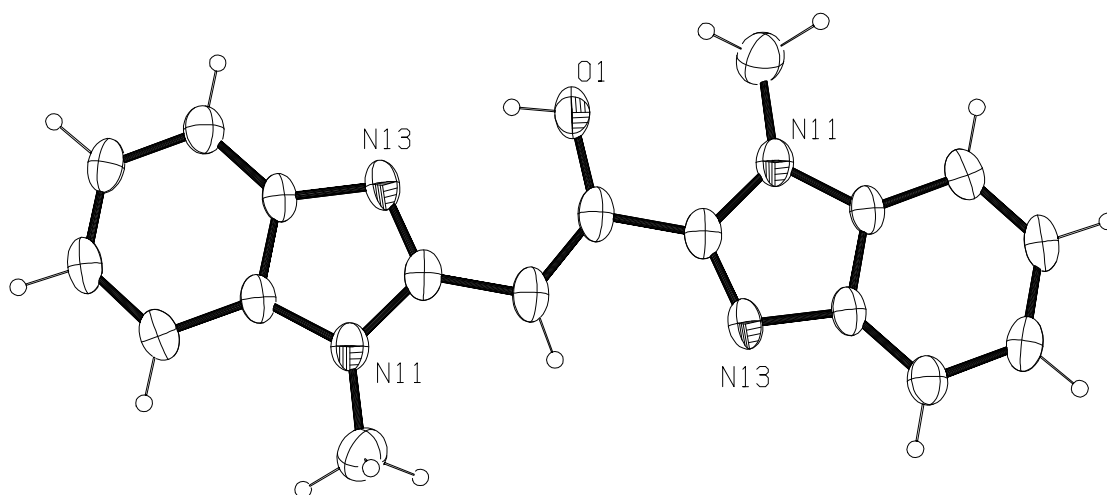
(*E*)-1,2-Bis(1-methylbenzimidazol-2-yl)ethene. (**11a**)
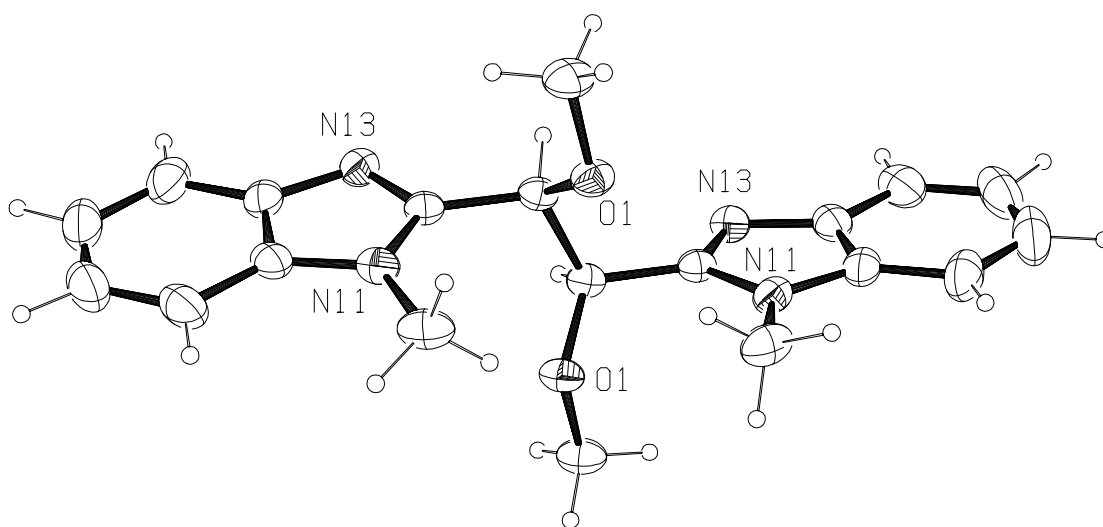
(*E*)-1,2-Bis(1-ethylbenzimidazol-2-yl)ethene. (**11c**)

3-Ethyl-2-[(*E*)-2-(1-ethylbenzimidazol-2-yl)-ethenyl]benzimidazol-1-ium   perchlorate.

(**11c-1**)

(*Z*)-1,2-(1-methylbenzimidazol-2-yl)ethenol · 1.5 water. (**12**)

(*S*,*S*)-1,2-Bis(1-methylbenzimidazol-2-yl)-1',2'-bis(methoxy)ethane. (**15a**)
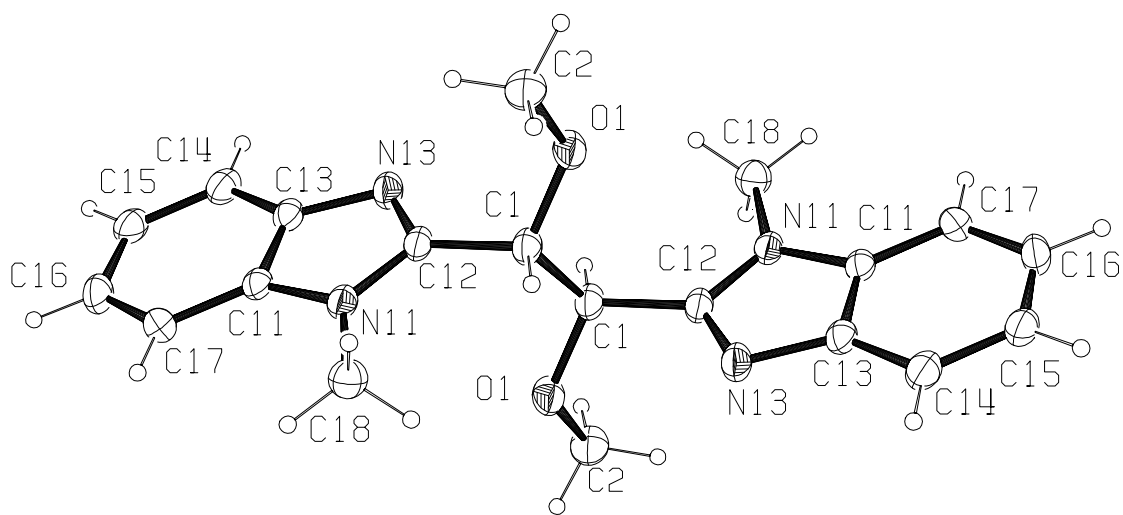
(*R*,*S*)-1,2-Bis(1-methylbenzimidazol-2-yl)-1',2'-bis(methoxy)ethane. (**15b**)
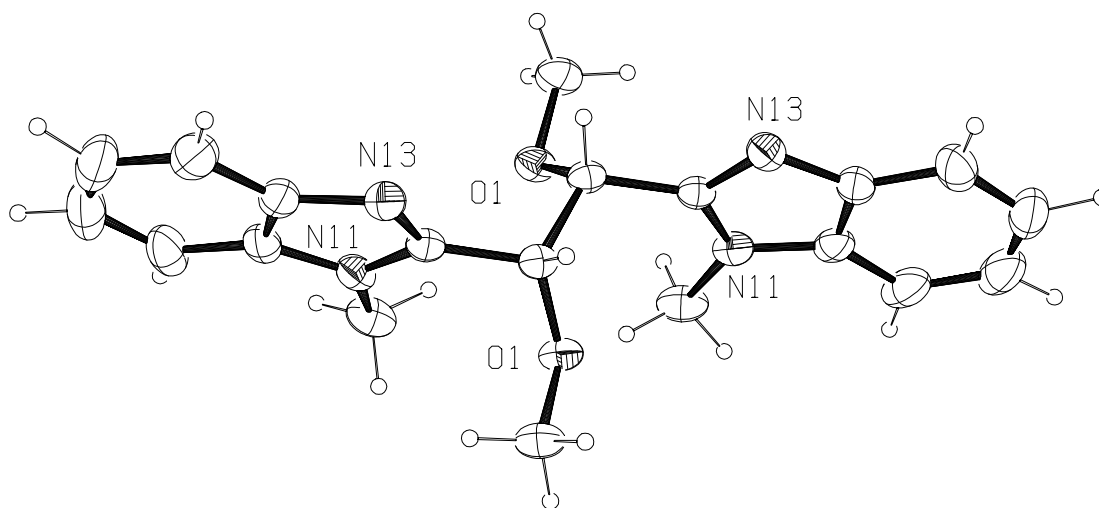
(*R*,*R*)-1,2-Bis(1-methylbenzimidazol-2-yl)-1',2'-bis(methoxy)ethane. (**15c**)
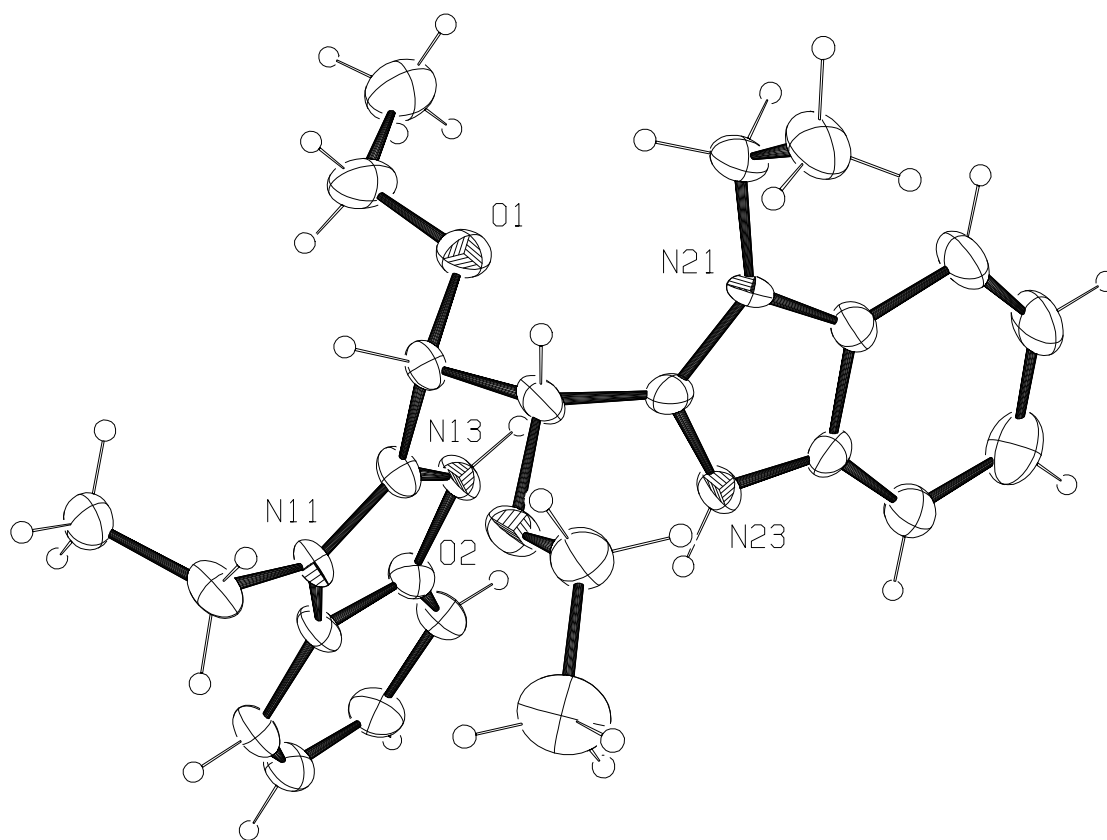
The cation of (*S*,*S*)-1,2-Bis(3-ethylbenzimidazol-1-ium)-1′,2′-bis(ethoxy)ethane di(perchlorate). (**15e-1**)
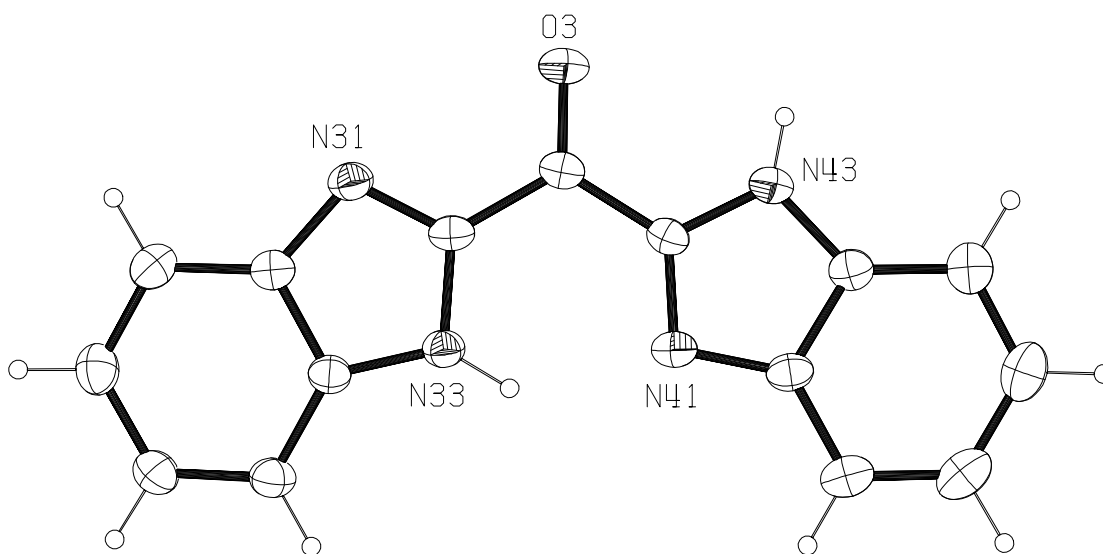
1,1′-Bis(1-hydrobenzimidazol-2-yl)ketone. (**17**)
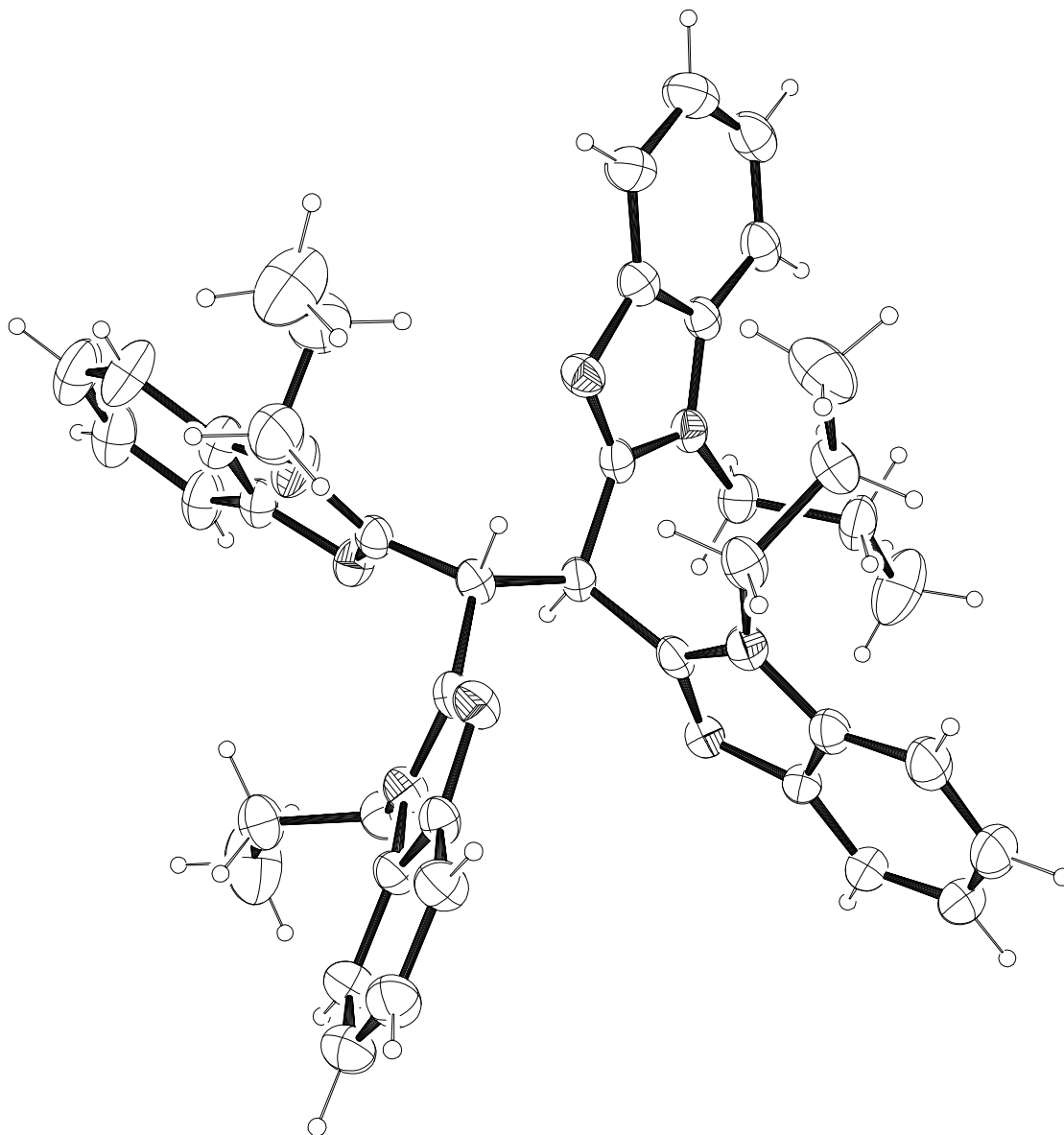
1,1′,2,2′Tetra(1-propylbenzimidazol-2-yl)ethane. **(18)**
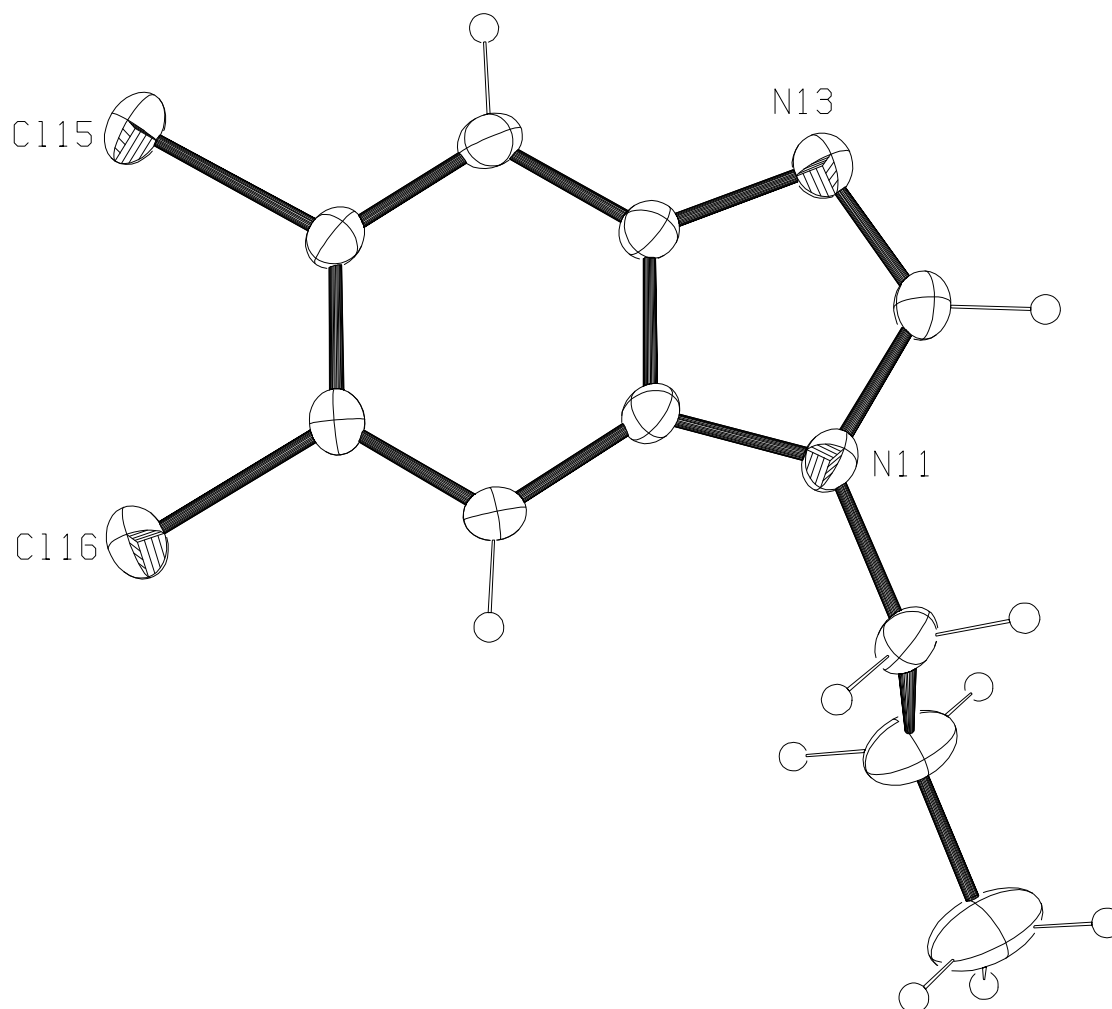
5,6-dichloro-1-propylbenzimidazole. (**19a**)
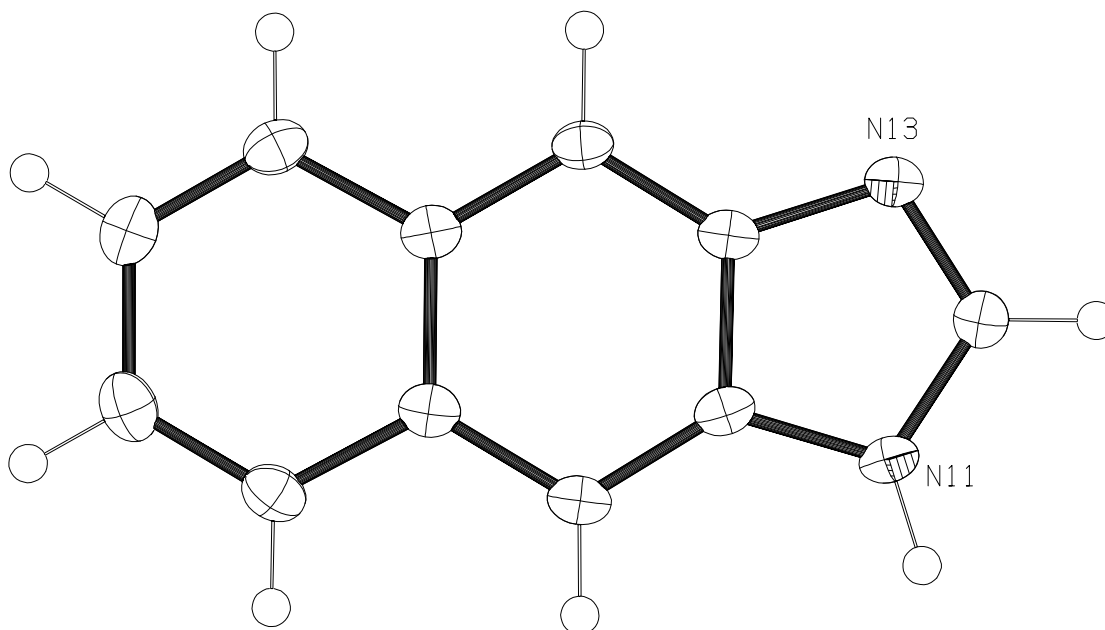
1-hydro-napth[2,3-d]imidazole. (**19b**)
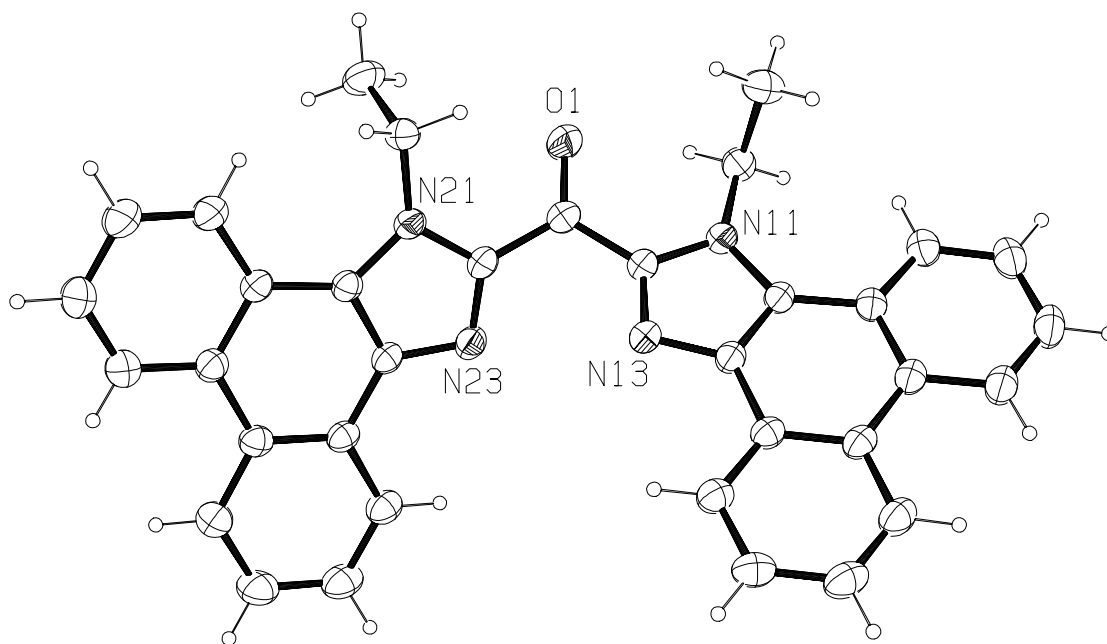
Bis(1-ethyl-phenanthro[9,10-d]imidazol-2-yl)ketone. (**22**)
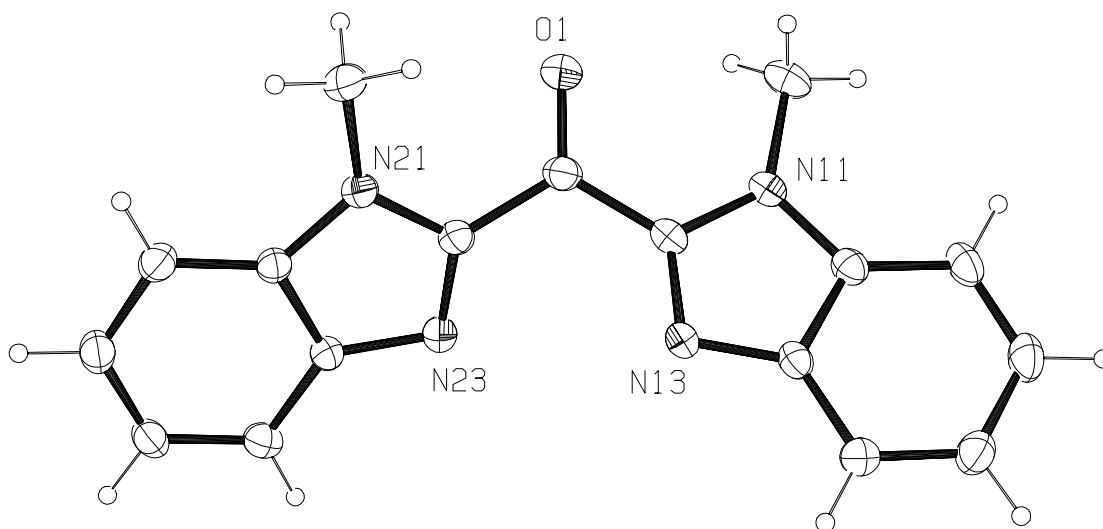
1,1′-Bis(1-methylbenzimidazol-2-yl)ketone. (**27a**)
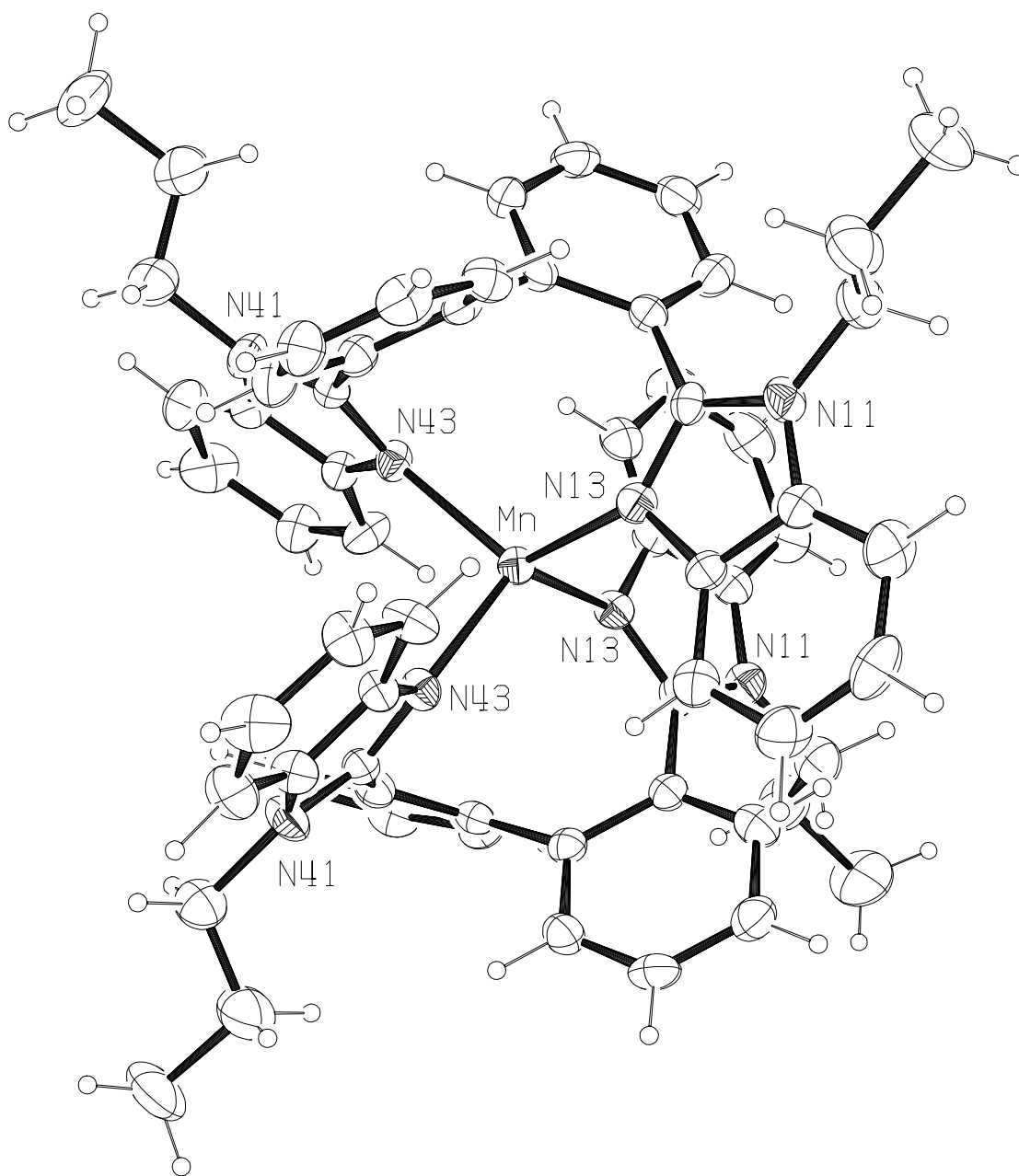
The cation of *rac*- bis-{2,2'- bis [2-(1-propylbenzimidazol-yl)]biphenyl)}manganese(II)bis(perchlorate), *rac*-Mn(II)(**9b**)$_2$·(ClO$_4$)$_2$. (**2-2**)
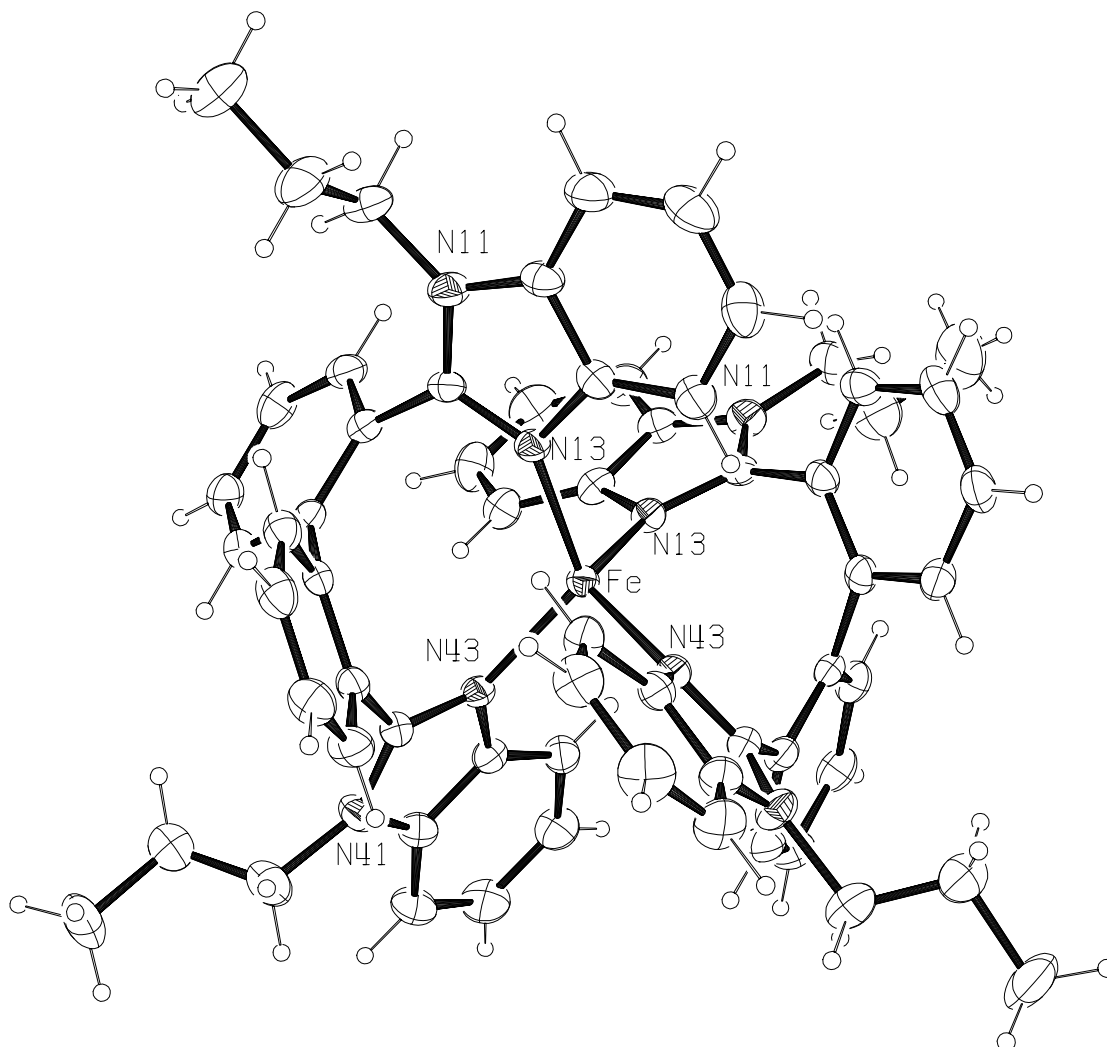
The cation of *rac*-bis-{2,2'-bis[2-(1-propylbenzimidazol-2-yl)]biphenyl)}iron(II) bis(perchlorate), *rac*-Fe(II)(**9b**)$_2$·(ClO$_4$)$_2$. (**2-3**)
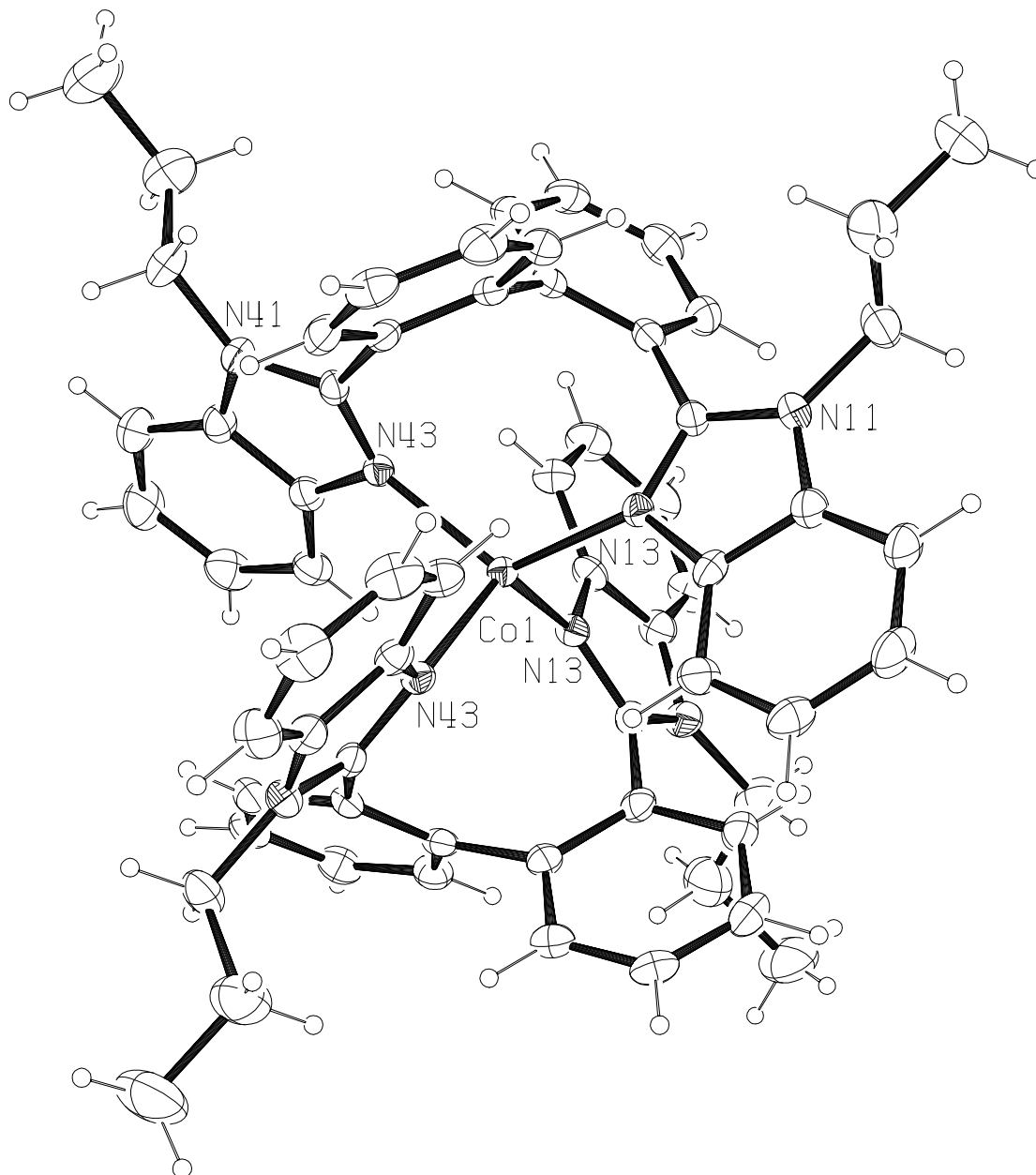
The cation of *rac*-bis-[2,2'-bis[2-(1-propylbenzimidazol-2-yl)]biphenyl)]cobalt(II) bis(perchlorate), *rac*-Co(II)(**9b**)₂·(ClO₄)₂. (**2-5**)
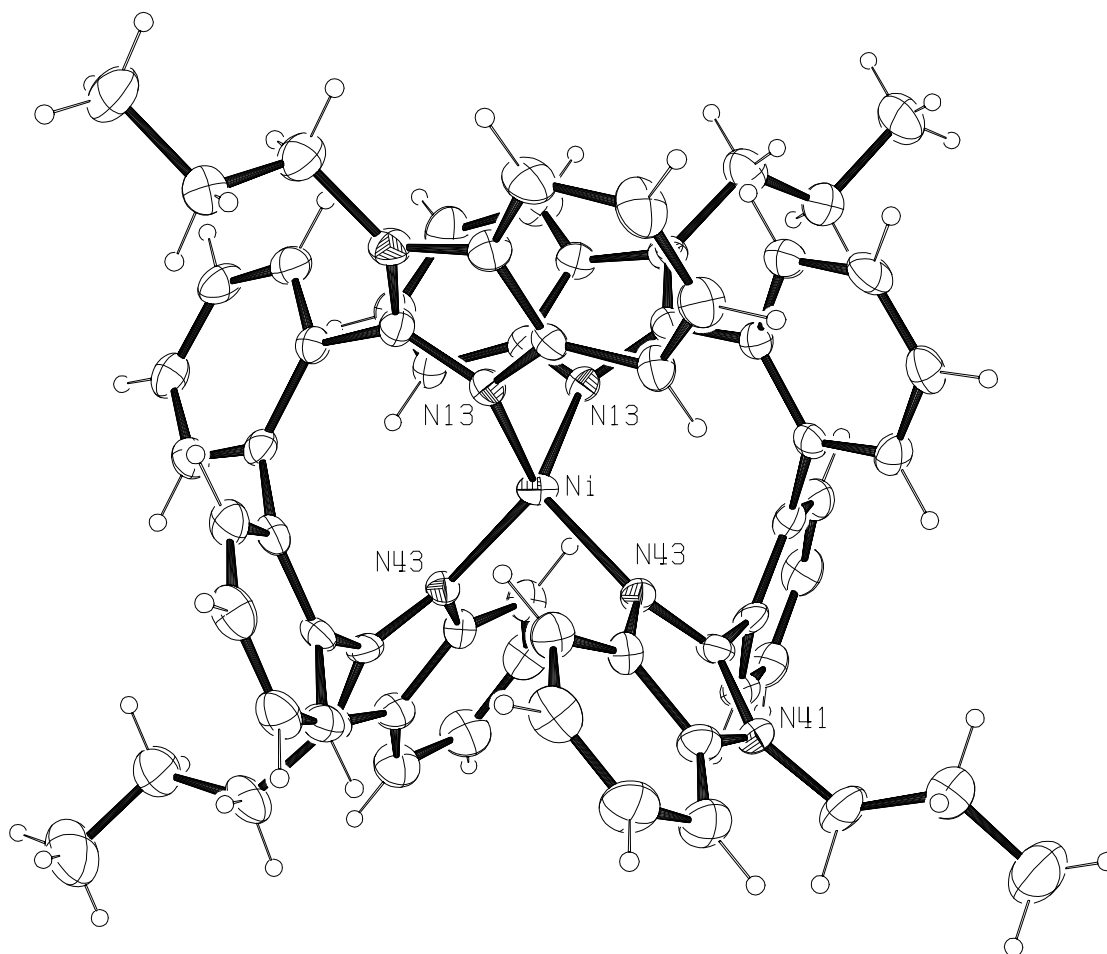
The cation of *rac*-bis-[2,2'-bis[2-(1-propylbenzimidazol-2-yl)]biphenyl)]nickel(II) bis(perchlorate), *rac*-Ni(II)(**9b**)$_2$·(ClO$_4$)$_2$. (**2-6**)
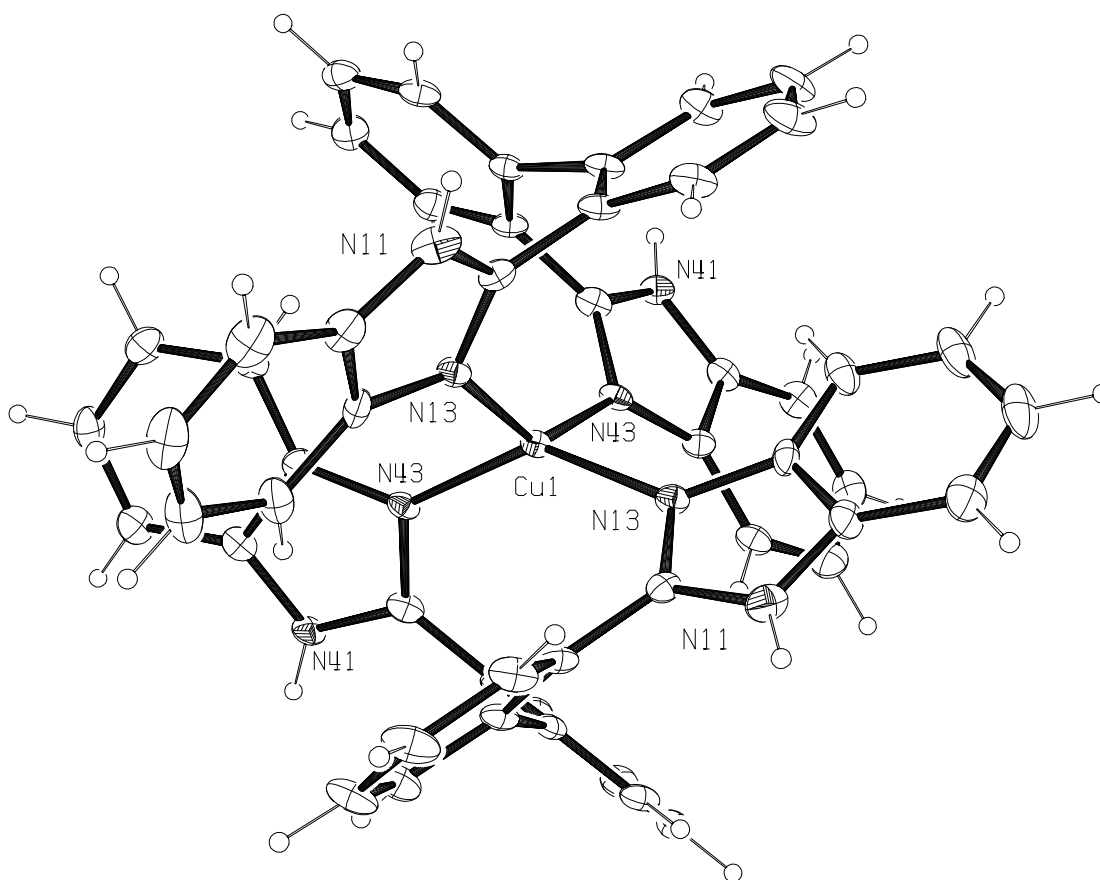
The cation of *rac*-bis-[2,2'-bis[2-(1-hydrobenzimidazol-2-yl)]biphenyl)]copper(II) bis(perchlorate), *rac*-Cu(II)(**1e**)$_2$·(ClO$_4$)$_2$. (**2-7**)
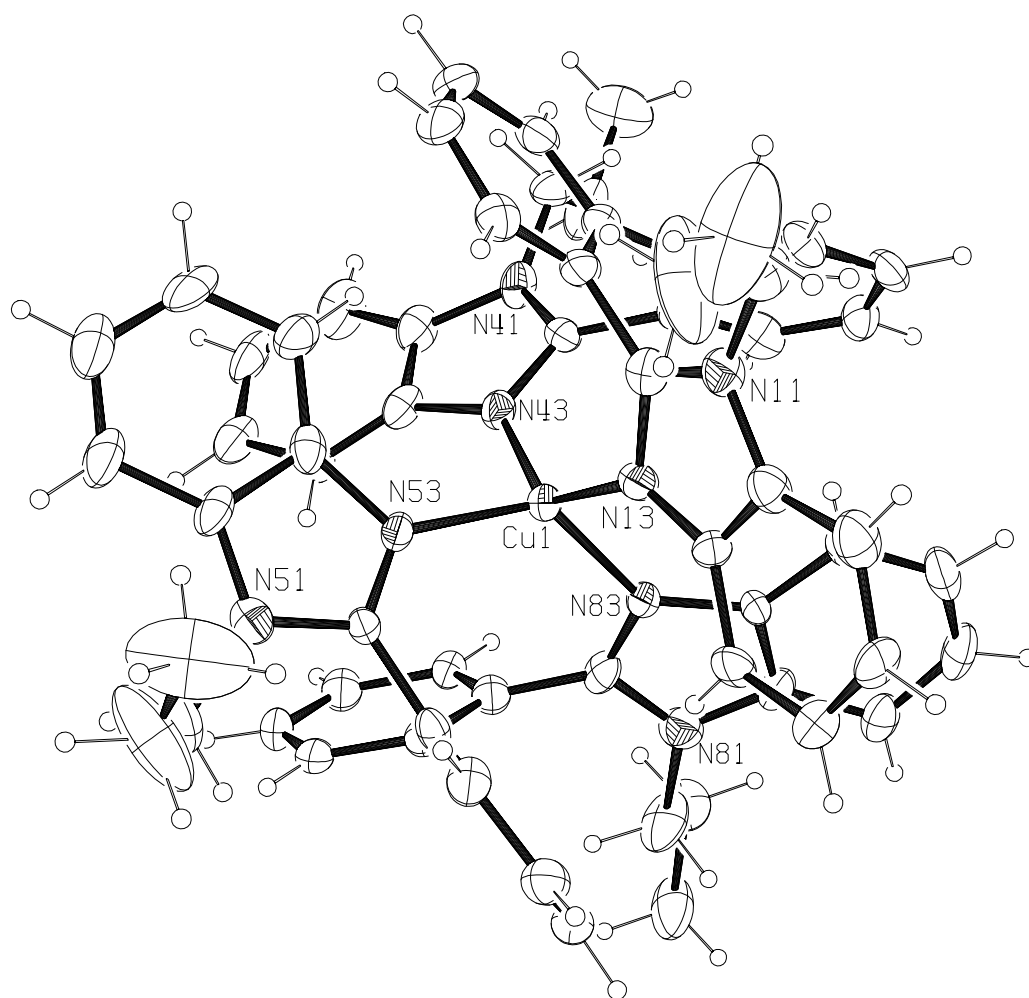
The cation of *rac*- bis- [2,2'-bis [2-(1-propylbenzimidazol-2-yl)] biphenyl)] copper(II) bis(perchlorate), *rac*-Cu(II)(**9b**)$_2$·(ClO$_4$)$_2$. (**2-8**)
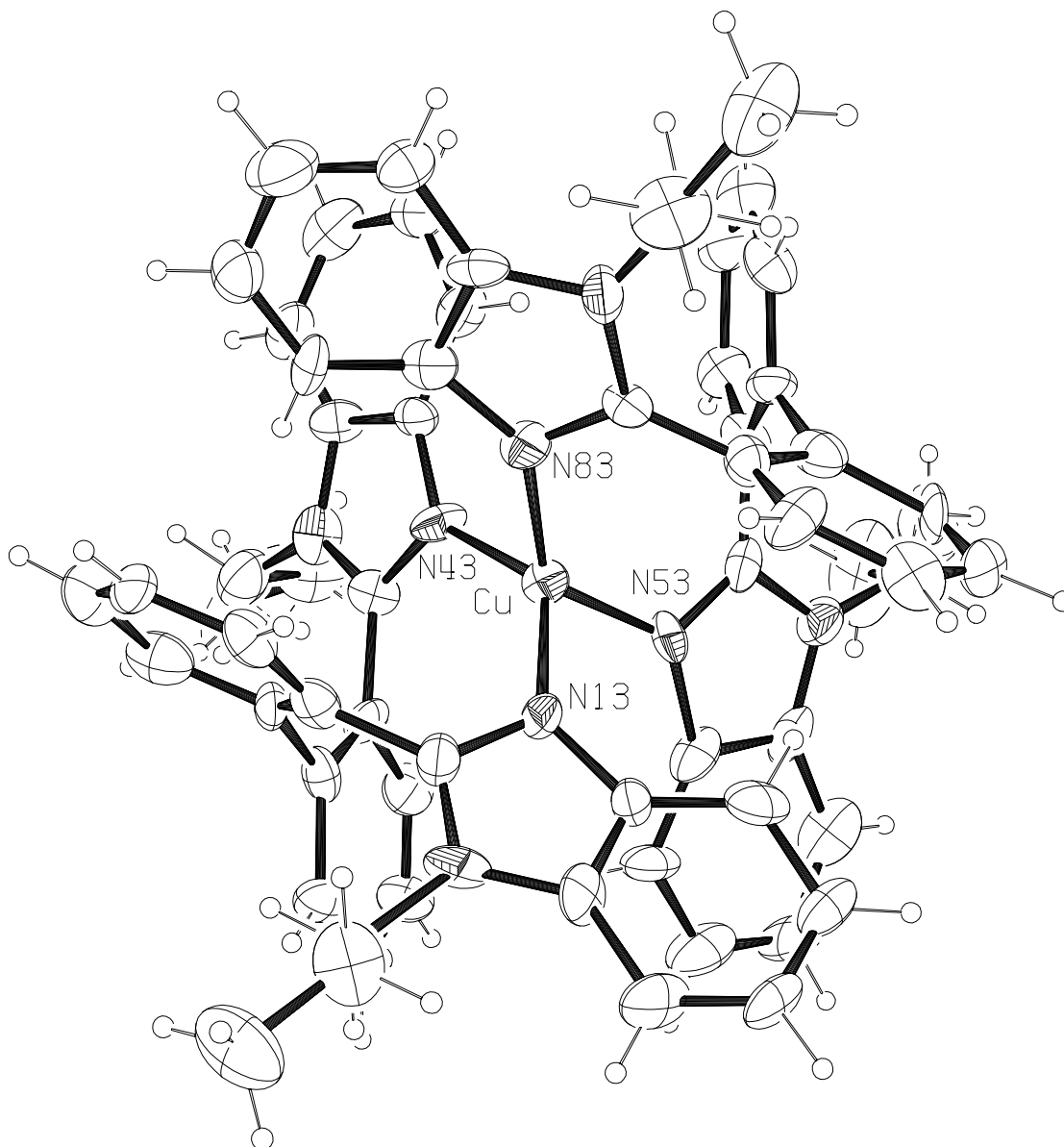
The cation of *rac*- bis-[2,2'-bis [2-(1-propylbenzimidazol-2-yl)] biphenyl)] copper(II) bis(trifluoromethanesulfonate), *rac*-Cu(II)(**9b**)₂·(CF₃SO₃)₂. (**2-9**)
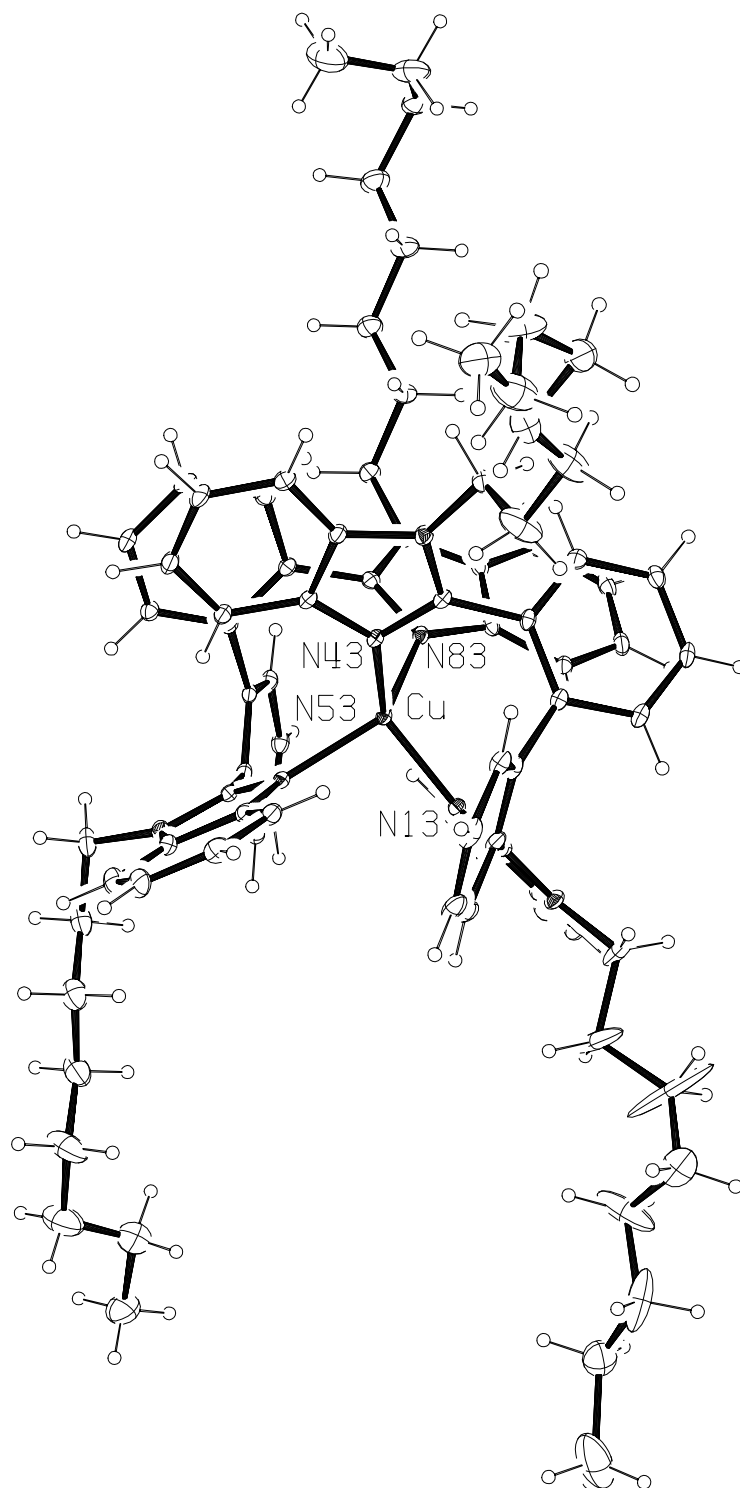
The cation of *rac*- bis-[2,2'-bis [2-(1-octylbenzimidazol-2-yl)] biphenyl)] copper(II) bis (trifluoromethanesulfonate) · ethanol, *rac*-Cu(II)(**9c**)$_2$·(CF$_3$SO$_3$)$_2$·CH$_3$CH$_2$OH. (**2-10**)
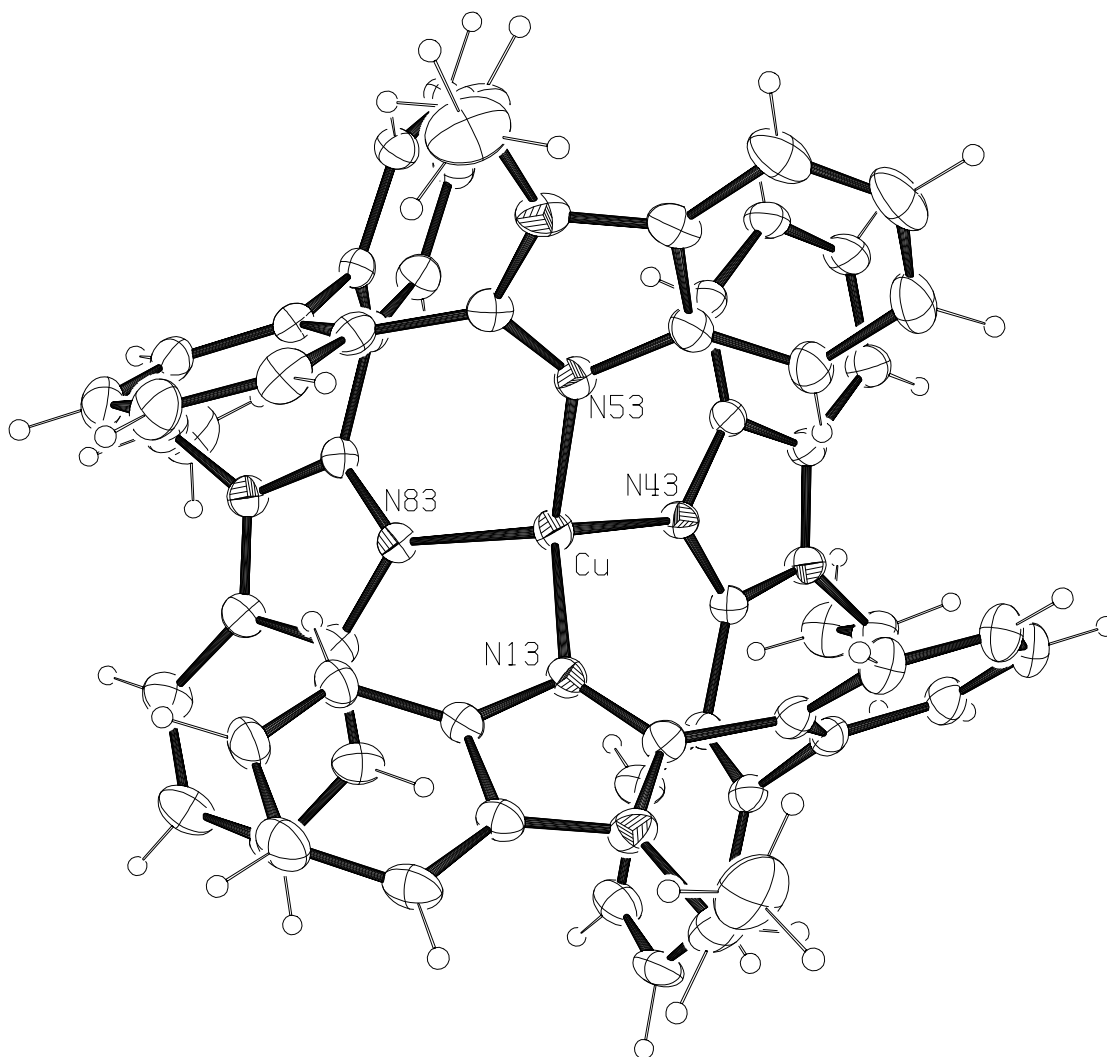
The cation of *rac*-bis-[2,2′-bis(1-ethylbenzimidazol-2-yl)biphenyl)] copper(I) trfluoromethanesulfonate toluene solvate dihydrate, *rac*-Cu(I)(**9a**)$_2$ ·(CF$_3$SO$_3$)·(C$_7$H$_8$)·(H$_2$O). (**2-11**)
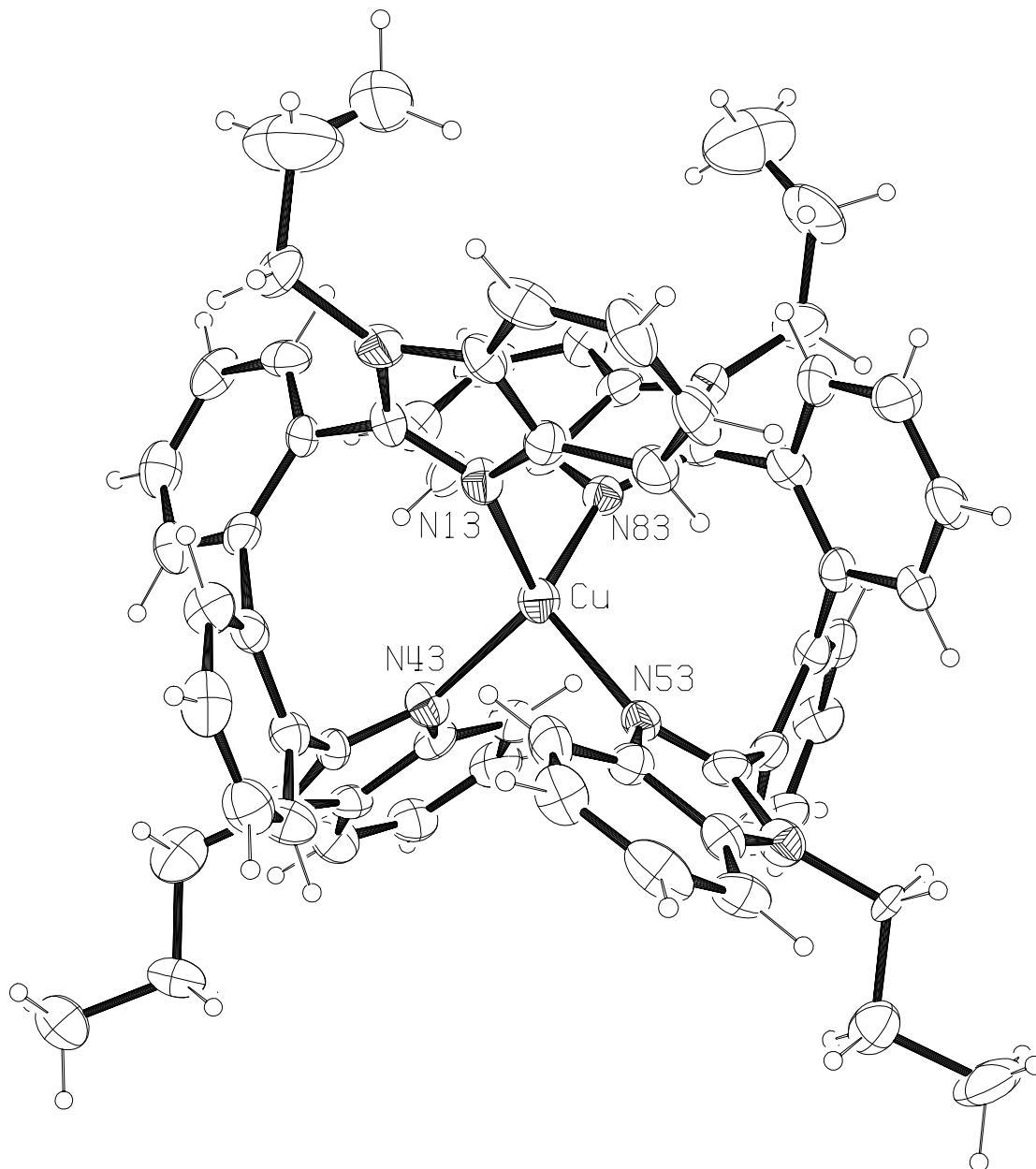
The cation of *rac*- bis-[2,2′-bis [2-(1-propylbenzimidazol-2-yl)] biphenyl)] copper(I) (perchlorate)·(CH₃CH₂OCH₂CH₃), *rac*-Cu(I)(**9b**)₂·(ClO₄)·(CH₃CH₂OCH₂CH₃). (**2-12**)
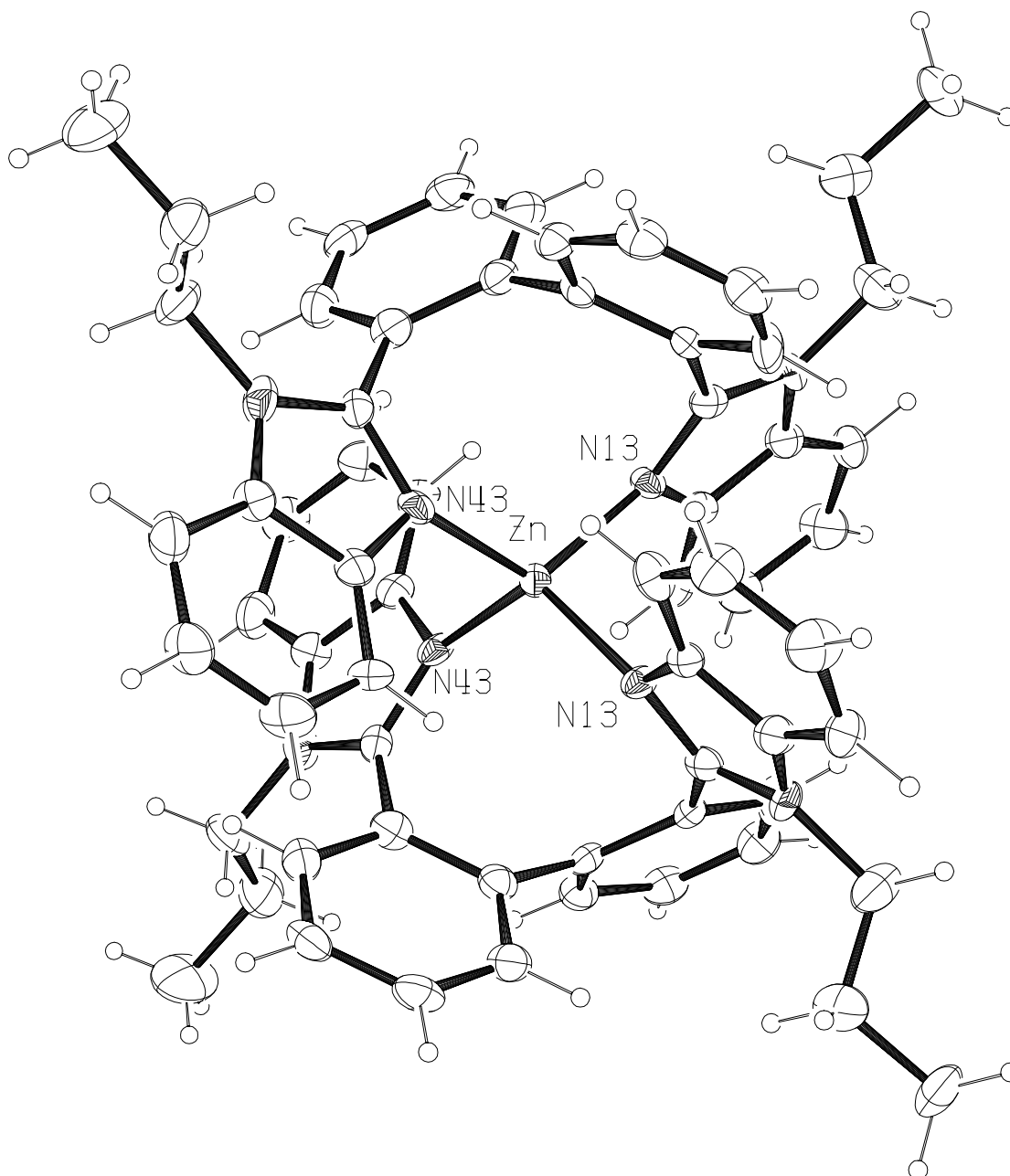
The cation of *rac*-bis-[2,2'-bis[2-(1-propylbenzimidazol-2-yl)]biphenyl)]zinc(II) bis(perchlorate), *rac*-Zn(II)(**9b**)$_2$·(ClO$_4$)$_2$. **(2-13)**
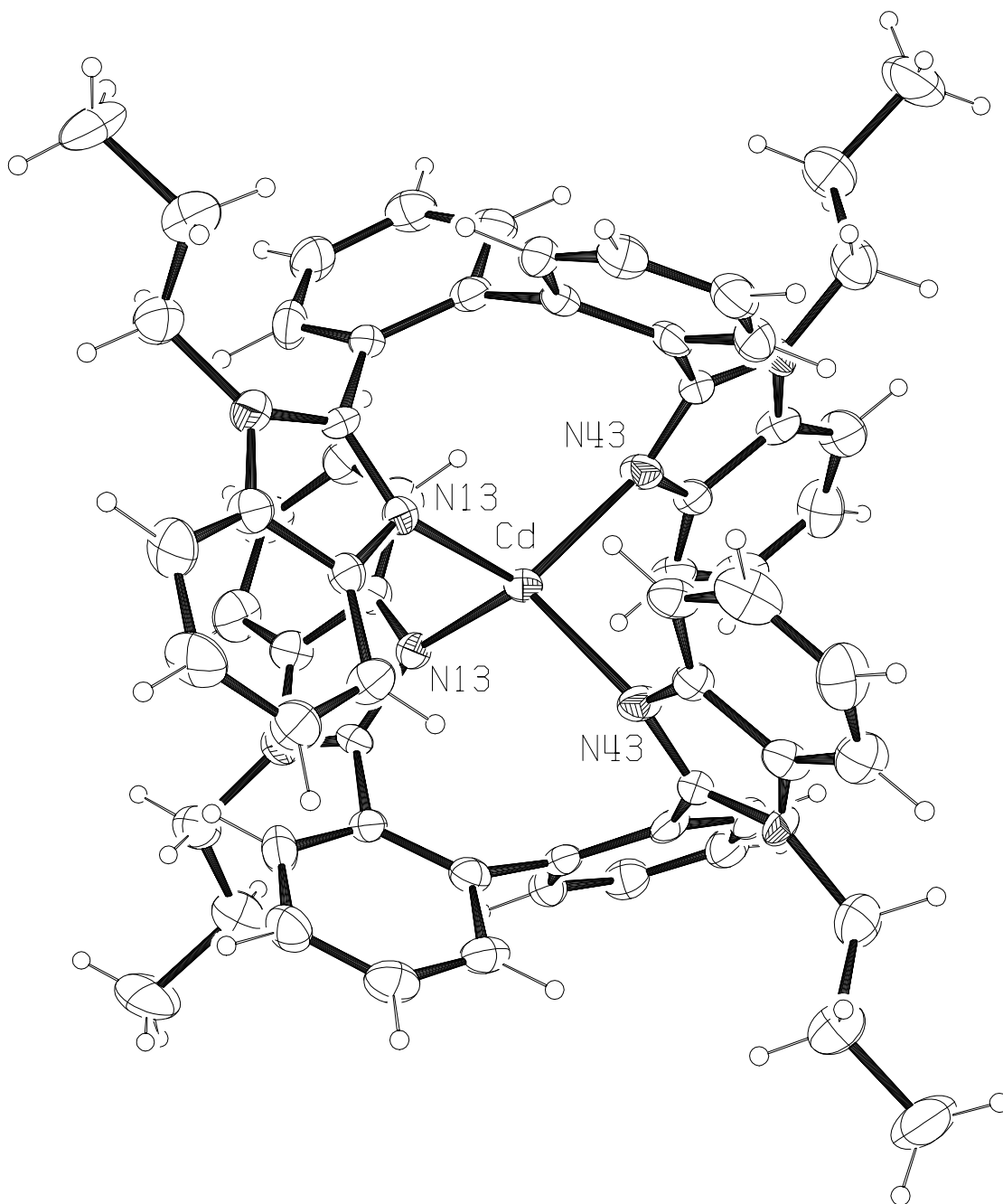
The cation of *rac*- bis-[2,2'-bis [2-(1-propylbenzimidazol-2-yl)] biphenyl)] cadmium(II) bis(perchlorate), *rac*-Cd(II)(**9b**)$_2$·(ClO$_4$)$_2$. (**2-14**)
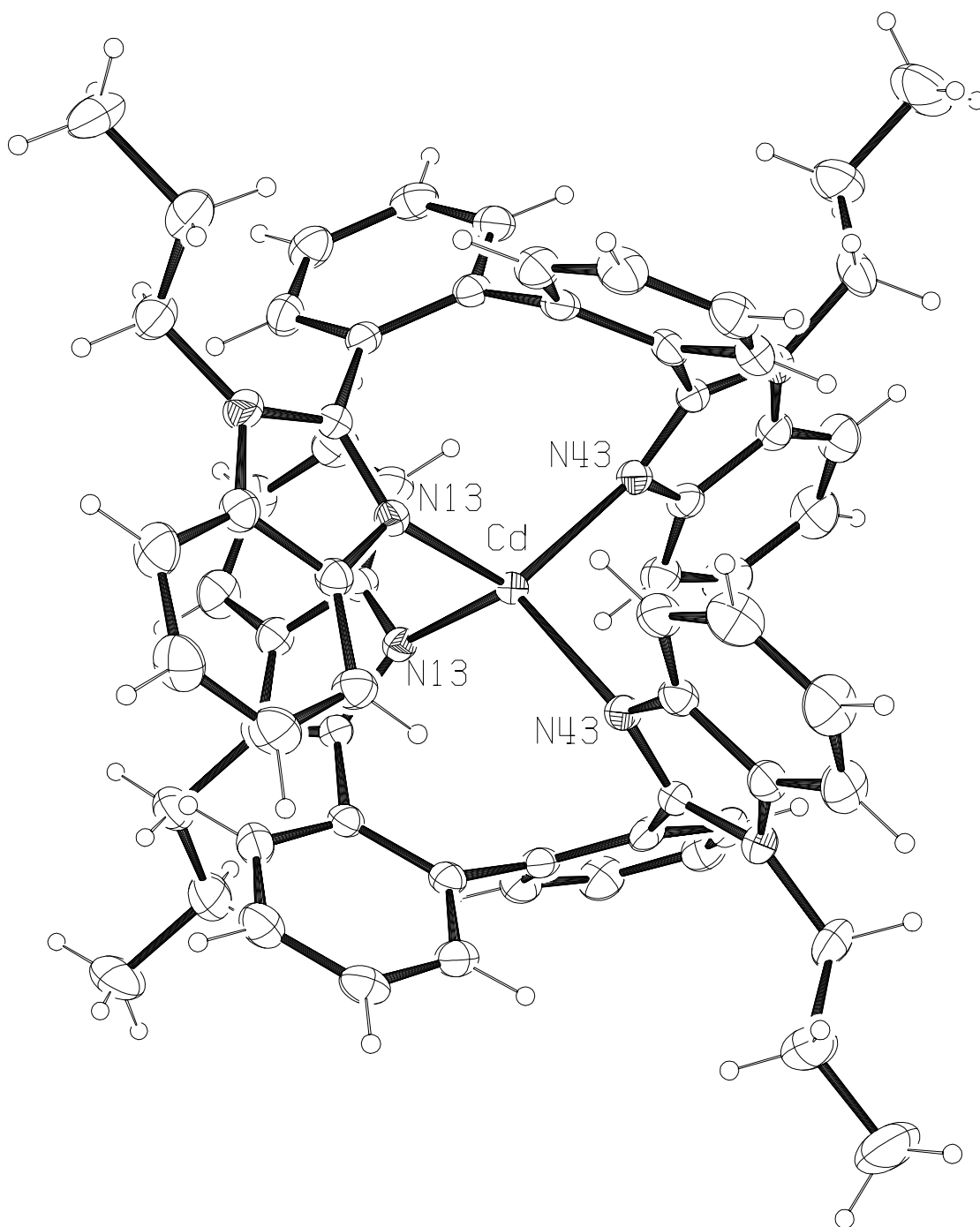
rac-   bis-[2,2'-bis   [2-(1-propylbenzimidazol-2-yl)]   biphenyl)]   copper(II)$_{0.03}$ cadmium$_{0.97}$(II) bis(perchlorate), *rac*-Cu(II)$_{0.03}$Cd$_{0.97}$(II)(**9b**)$_2$·(ClO$_4$)$_2$. (**2-15**)
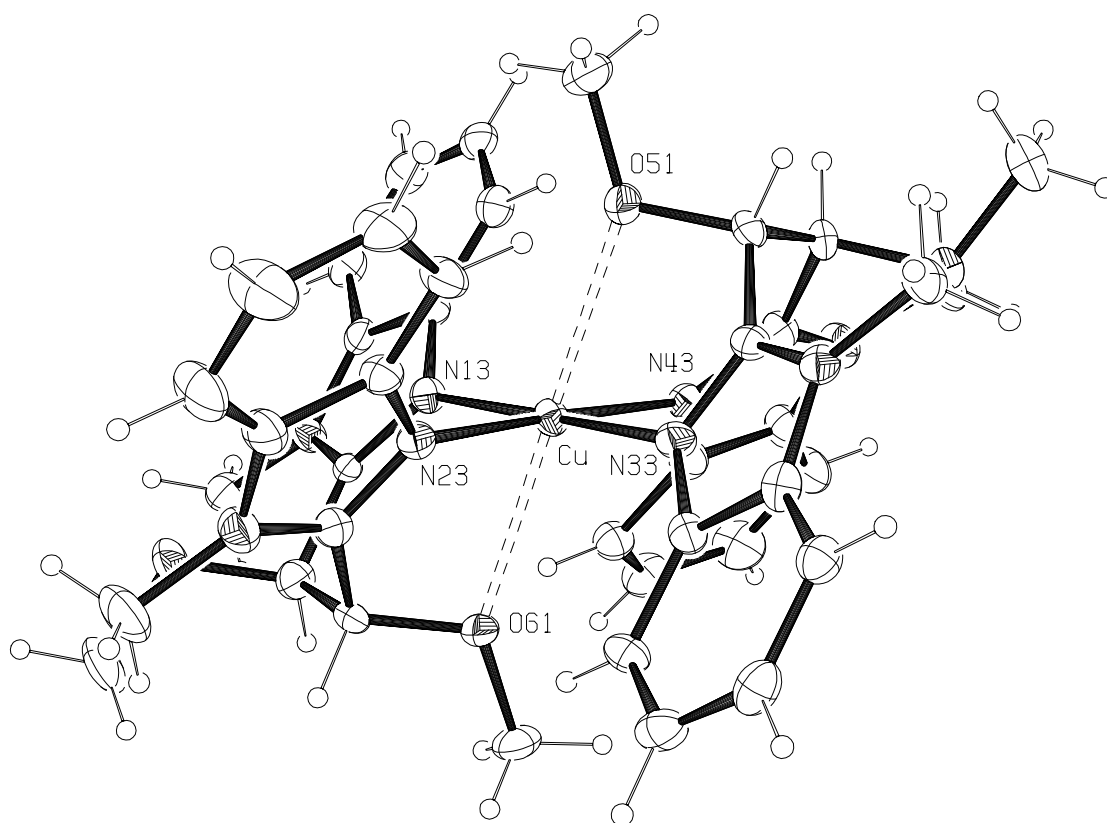
The cation of (*OC*-6-12)-bis[(*S*,*S*)-1,2-bis(1-methylbenzimidazol-2-yl)-1′,2′-bis(methoxy)ethane]copper(II) bis(tetrafluoroborate) acetonitrile disolvate, Cu(II)(**15a**)$_2$·(BF$_4$)$_2$ · (acetonitrile)$_2$. (**2-16**)
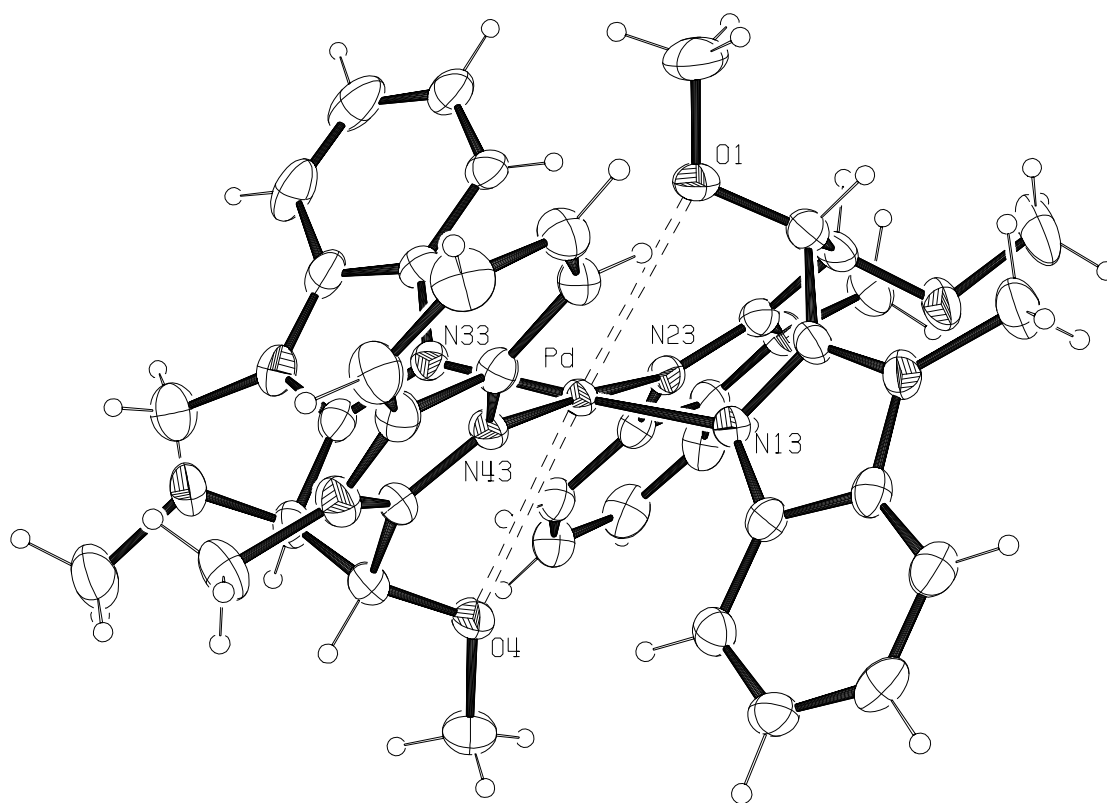
The cation of (*OC*-6-12)-bis[(*S*,*S*)-1,2-bis(1-methylbenzimidazol-2-yl)-1′,2′-bis(methoxy)ethane]palladium(II) dichloride, Pd(II)(**15a**)₂·Cl₂. (**2-17**)
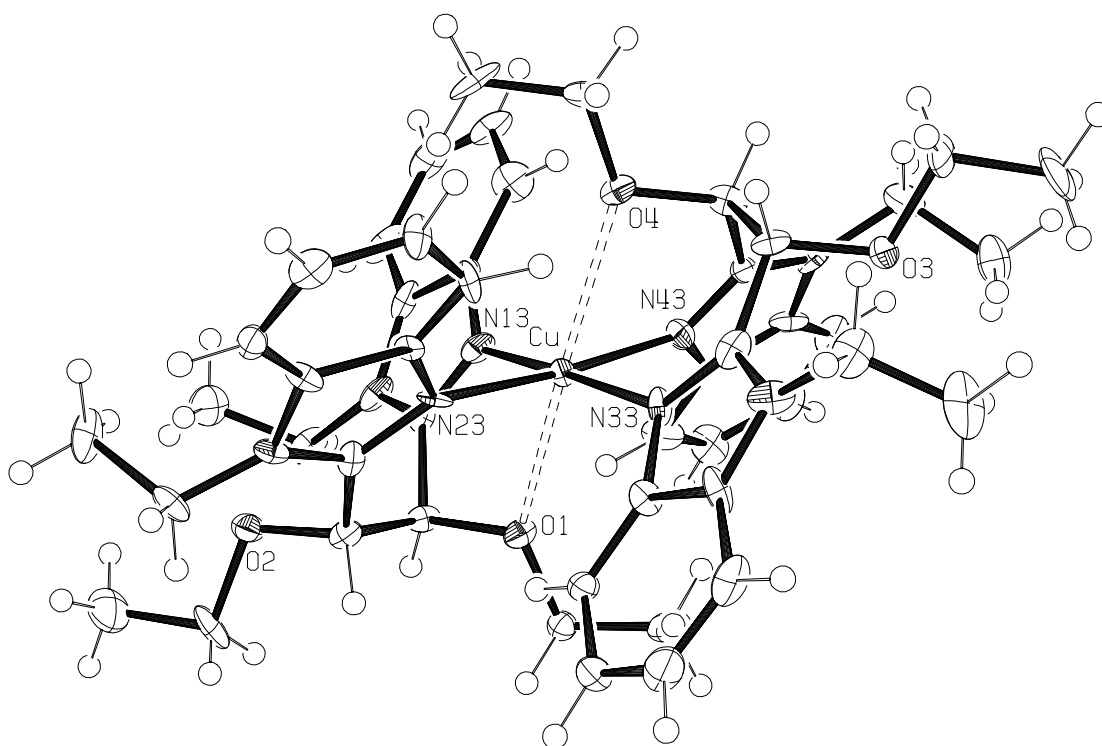
The cation of (*OC*-6-12) - bis[(*R*,*R*)-1,2-bis(1-ethylbenzimidazol-2-yl)-1′,2′-diethoxy-ethane] copper(II) bis(perchlorate), Cu(II)(**15d**)₂·(ClO₄)₂. (**2-18**)
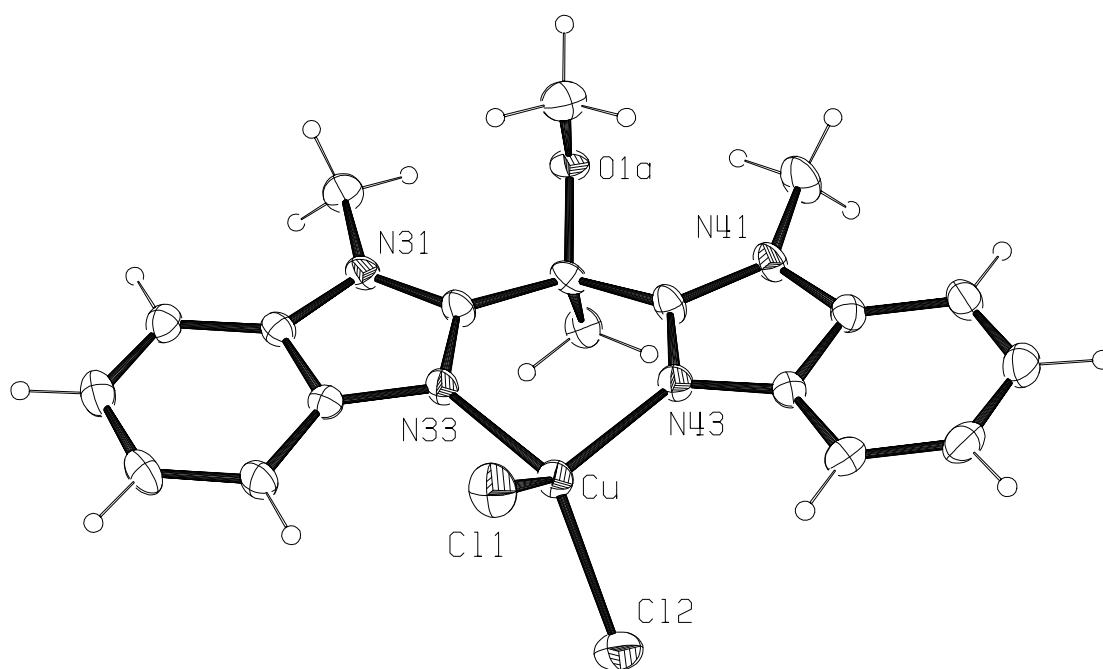
(1,1′-bis(1-methylbenzimidazol-2-yl)-1″-(methoxy)ethane)copper(II)   dichloride,

Cu(II)(**7**)Cl₂. (**3-7**)

Curriculum Vitae

Robert T. Stibrany

Education

	Houghton College, Houghton, NY September 1981 – May 1983
B.S., Chemistry	Cook College, Rutgers University October 1985
	Pennsylvania State University Graduate School, University Park, PA September 1985 – May 1986
Ph. D., Chemistry	Rutgers University Graduate School, New Brunswick, NJ January 2004 – August 2007

"Exploration of Benzimidazole Chemistry"

Work Experience

Teaching Assistant	Teaching Chemistry 11, 14, 15 Pennsylvania State University September 1985 – May 1986
Senior Laboratory Technician	Allied-Signal Corporation Morristown, NJ August 1986 – May 1989
Associate Chemist	Exxon Research and Engineering Company Annandale, NJ June 1989 – August 1992
Associate Research Chemist	Exxon Research and Engineering Company Annandale, NJ August 1992 – June 1998

Senior Associate Research Chemist   ExxonMobil Research and Engineering Company
Annandale, NJ
June 1998 – January 2002

Senior Research Chemist   ExxonMobil Research and Engineering Company
Annandale, NJ
January 2002 – December 2005

Publications

1.   R. T. Stibrany and S. M. Gorun, <u>Angewandte</u> <u>Chemie</u> <u>Int.</u> <u>Ed.</u> <u>Engl.</u> *29*, (1990) 1156- 1158.   "Synthesis, Srtucture, and Catalase-Type Activity of a Novel Oxo-Bridged Tetranuclear Manganese Aggregate Exhibiting Short O···O Interactions".

2.   R. T. Stibrany and S. M. Gorun, In <u>Dioxygen</u> <u>Activation</u> <u>and</u> <u>Homogeneous</u> <u>Catalytic</u>   <u>Oxidation.</u> "Synthesis and Molecular Structure of a Novel Biomimetic Tetranuclear Manganese Aggregate" L. I. Simándi, Ed., Elsevier: Amsterdam, 1991, 681-687.

3.   M. N. Potenza, R. T. Stibrany, J. A. Potenza and H. J. Schugar, <u>Acta</u> <u>Cryst.</u> *C48,* (1992)   454-457. "Structures of Zinc(II) with Tetradentate N_2S_2 Ligation".

4.   R. T. Stibrany, J. A. Potenza and H. J. Schugar, <u>Acta</u> <u>Cryst.</u> *C49,* (1993) 1561-1564. "Isostructural Trigonal-Bipyramidal Cu(II) and Nominally 1% Cu(II)-Doped Zn(II) Complexes with N_5 Ligation".

5.   S. M. Gorun, G. W. Schriver, T. H. Vanderspurt, R. T. Stibrany and J. E. Bond, In <u>The</u>   <u>Activation</u> <u>of</u> <u>Dioxygen</u> <u>and</u> <u>Homogeneous</u> <u>Catalytic</u> <u>Oxidation</u>. "Bioinspired Catalysis: Hydroperoxidation of Alkylaromatics" D. H. R. Barton, Ed., Plenum Press: New York, 1993, 199-208.

6.   S. Vepachedu, R. T. Stibrany, S. Knapp, J. A. Potenza and H. J. Schugar, <u>Acta</u> <u>Cryst.</u> *C51*, (1995) 423-426. "Structure of Tris(3,5-dimethylpyrazol-1-yl)methylsilane".

7.   R. T. Stibrany, J. A. Potenza and H. J. Schugar, <u>Inorg.</u> <u>Chimica</u> <u>Acta</u> *243*, (1996) 33-37. "Synthesis, Structure, and Spectroscopic Properties of (Nitrito-O-O')$_2$[Tris[2-(1- methyl)imidazoyl]methoxymethane]copper(II), Cu(II)(TIMM)(NO$_2$)$_2$".

8.   S. M. Gorun, R. T. Stibrany, A. R. Katritzky, J. J. Slawinski, H. Faid-Allah and F.

Brunner, <u>Inorg. Chem.</u> *35*, (1996) 3-4. "Benzimidazol-2-yl Carbinols and Ketones : Bifunctional Chelating Ligands for Copper".

9. M. M. Grush, J. Chen, T. L. Stemmler, S. J. George, C. Y. Ralston, R. T. Stibrany, A. Gelasco, G. Christou, S. M. Gorun, J. E. Penner-Hahn, and S. P. Cramer, <u>J.</u> <u>Am.</u> <u>Chem.</u> <u>Soc.</u> *118*, (1996) 65-69. "Manganese L-Edge X-ray Absorption Spectroscopy of Manganese Catalase from *Lactobacillus plantarum* and Mixed Valence Manganese Complexes".

10. S. Fox, R. T. Stibrany, J. A. Potenza, and H. J. Schugar, <u>Acta</u> <u>Cryst.</u> *C52*, (1996) 2731- 2734. "A Mixed-Metal Pentanuclear Complex Containing Linked Ni(II) N_2S_2 and Cu(I)I Units".

11. R. T. Stibrany, J. Vasudevan, S. Knapp, J. A. Potenza, T. Emge, and H. J. Schugar, <u>J.</u> <u>Am.</u> <u>Chem.</u> <u>Soc.</u> *118*, (1996) 3980-3981. "Two Modes of Self-Coordinating Edge-over-Edge Zn(II) Porphyrin Dimerization: A Structural and Spectroscopic Comparison".

12. J. Vasudevan, R. T. Stibrany, J. Bumby, S. Knapp, J. A. Potenza, T. Emge, and H. J. Schugar, <u>J.</u> <u>Am.</u> <u>Chem.</u> <u>Soc.</u> *118*, (1996) 11676-11677. "An Edge-over-edge Zn(II) Bacteriochlorin Dimer Having an Unshifted Q_y Band. The Importance of π-Overlap".

13. S. M. Gorun, R. T. Stibrany and A. Lillo, <u>Inorg.</u> <u>Chem.</u> *37*, (1998) 836-837. "Supramolecular Mn-Ca Aggregates as Models for the Photosynthetic Water Oxidation Complex".

14. R. T. Stibrany, S. Knapp, J. A. Potenza, and H. J. Schugar, <u>Inorg.</u> <u>Chem.</u> *38*, (1999) 132- 135. "Product of a DMF Aminalization, Bis[bis(3,5-dimethylpyrazol-1-yl)(dimethylamino)methane]copper(II)Perchlorate-Bis(dichloromethane)".

15. R. T. Stibrany, and S. M. Gorun, <u>J.</u> <u>Organomet.</u> <u>Chem.</u> *579*, (1999), 217-221. "Complexes Exhibiting Non-Conventional Solubility: Synthesis and Characterization of *trans*- $Pt[(CF_3(CF_2)_5(CH_2)_2)_3P]_2Cl_2$".

16. S. M. Gorun, Z. Hu, R. T. Stibrany and G. Carpenter, <u>Inorg.</u> <u>Chimica</u> <u>Acta</u> *297*, (2000), 383-388. "Synthesis and Molecular Structures and Oxidation Catalysis of Mixed Alkyl, Fluoroalkyl Pyrazolylborate Metal Complexes".

17. S. Fox, R. T. Stibrany, J. A. Potenza, S. Knapp, and H. J. Schugar, <u>Inorg.</u> <u>Chem.</u> *39*, (2000), 4950-4961. "Copper (II) and Nickel (II) Complexes of Binucleating Macrocyclic Bis(disulfide)tetramine Ligands".

18. R. T. Stibrany and P. Brant, <u>Acta</u> <u>Cryst.</u> *C57* (2001), 644-645. "Dimethyl(2-methylphenyl)ammonium hydroxotris(pentafluorophenyl)borate".

19. S. Fox, R. T. Stibrany, J. A. Potenza, and H. J. Schugar, <u>Inorg.</u> <u>Chimica</u> <u>Acta</u> *316*, (2001), 122-126. "Novel Mixed-Valence Trinuclear Complex Containing Nickel(I), Nickel(II) and Iodonium Moieties".

20. R. C. Prince, R. T. Stibrany, J. Hardenstine, G. S. Douglas, and E. H. Owens, <u>Environ.</u> <u>Sci.</u> <u>&</u> <u>Tech.</u> *36*, (2002) 2822-2825. "Aqueous Vapor Extraction; A Previously Unrecognized Weathering Process for Oil Spills in Vigorously Aerated Water".

21. R. T. Stibrany, A. O. Patil, and S. Zushma, <u>Poly.</u> <u>Mat.</u> <u>Sci.</u> <u>&</u> <u>Eng.</u> *86*, (2002) 323-324. "Copper Based Olefin Polymerization Catalysts".

22. R. T. Stibrany, D. N. Schulz, S. Kacker, A. O. Patil, L. S. Baugh, S. Zushma, E. Berluche, and J. A. Sissano, <u>Poly.</u> <u>Mat.</u> <u>Sci.</u> <u>&</u> <u>Eng.</u> *86*, (2002) 325. "Copper Catalysts for Homo- and Copolymerization of Olefins and Acrylates".

23. A. O. Patil, S. Zushma, R. T. Stibrany, and M. G. Matturro, <u>Poly.</u> <u>Mat.</u> <u>Sci.</u> <u>&</u> <u>Eng.</u> *86*, (2002) 335-336. "Vinyl-Type Polymerization of Norbornene by Nickel(II) Bis-Benzimidazole Catalysts".

24. R. T. Stibrany, J. A. Potenza and H. J. Schugar, <u>Acta</u> <u>Cryst.</u> *E58,* (2002) o848-o850. "1-Benzyl-4,5-diphenyl-3-vinylimidazolium bromide".

25. R. T. Stibrany, H. J. Schugar, and J. A. Potenza <u>Acta</u> <u>Cryst.</u> *E58,* (2002) o1142-o1144. "$\kappa^2 N^{13}, N^{13'}$-Hydro-*rac*-2,2′-bis[2-(1-propylbenzimidazol-2yl)]biphenyl trifluoromethanesulfonate, The Salt of a Novel Proton Sponge".

26. R. T. Stibrany, R. Fikar, M. Brader, M. N. Potenza, J. A. Potenza, and H. J. Schugar, <u>Inorg.</u> <u>Chem.</u> *41,* (2002) 5203-5215. "Charge-Transfer Spectra of Structurally Characterized Mixed-Valence Thiolate-Bridged Cu(I)/Cu(II) Cluster Complexes".

27. A. O. Patil, S. Zushma, R. T. Stibrany, S. P. Rucker, and L. M. Wheeler, In <u>Beyond</u> <u>Metallocenes</u>, <u>Next-Generation</u> <u>Polymerization</u> <u>Catalysts</u>. "Vinyl-Type Polymerization of Norbornene by Nickel(II) bis-Benzimidazole Catalysts" A. O. Patil and G. G. Hlatky, Eds.; ACS Symp. Ser. 857; Am. Chem. Soc.: Washington, DC, 2003, 173-191.

28. R. T. Stibrany, A. O. Patil, and S. Zushma, In <u>Beyond</u> <u>Metallocenes</u>, <u>Next-Generation</u> <u>Polymerization</u> <u>Catalysts</u>. "Copper-Based Olefin Polymerization Catalysts" A. O. Patil and G. G. Hlatky, Eds.; ACS Symp. Ser. 857; Am. Chem. Soc.: Washington, DC, 2003, 194-209.

29. R. T. Stibrany, In <u>Beyond</u> <u>Metallocenes</u>, <u>Next-Generation</u> <u>Polymerization</u> <u>Catalysts</u>. "Copper-Based Olefin Polymerization Catalysts: High-Pressure [19]F

NMR Catalyst Probe" A. O. Patil and G. G. Hlatky, Eds.; ACS Symp. Ser. 857; Am. Chem. Soc.: Washington, DC, 2003, 210-221.

30.   R. T. Stibrany, D. N. Schulz, S. Kacker, A. O. Patil, L. S. Baugh, S. P. Rucker, S. Zushma, E. Berluche, and J. A. Sissano, In <u>Beyond</u> <u>Metallocenes</u>, <u>Next-Generation</u> <u>Polymerization</u> <u>Catalysts</u>. "Cu Catalysts for Homo- and Copolymerization of Olefins and Acrylates" A. O. Patil and G. G. Hlatky, Eds.; ACS Symp. Ser. 857; Am. Chem. Soc.: Washington, DC, 2003, 222-230.

31.   R. T. Stibrany, D. N. Schulz, S. Kacker, A. O. Patil, L. S. Baugh, S. P. Rucker, S. Zushma, E. Berluche, and J. A. Sissano, <u>Macromolecules</u>. *36*, (2003) 8584-8586. "Polymerization and Copolymerization of Olefins and Acrylates by Bis(benzimidazole) Copper Catalysts".

32.   A. O. Patil, S. Zushma, R. T. Stibrany, S. P. Rucker, and L. M. Wheeler, <u>J</u>. <u>Polym</u>. <u>Sci</u>.: <u>Part</u> <u>A</u>: <u>Polymer</u> <u>Chem</u>. *41*, (2003) 2095-2106. "Vinyl-Type Polymerization of Norbornene by Nickel(II) bis-Benzimidazole Catalysts".

33.   R. T. Stibrany, H. J. Schugar and J. A. Potenza, <u>Acta</u> <u>Cryst</u>. *E59*, (2003) m630-m632. "A Pentanuclear Complex Exhibiting Two Short Ni-Cu Distances".

34.   R. T. Stibrany, H. J. Schugar and J. A. Potenza, <u>Acta</u> <u>Cryst</u>. *E59*, (2003) o693-o695. "2,2'-Bis(1-ethylbenzimidazol-2-yl)biphenyl".

35.   R. T. Stibrany, H. J. Schugar and J. A. Potenza, <u>Acta</u> <u>Cryst</u>. *E59*, (2003) o1448-o1450. "(*S,S*)-1,2-Bis(1-methylbenzimidazol-2-yl)-1',2'-bis(methoxy)ethane".

36.   R. T. Stibrany, H. J. Schugar and J. A. Potenza, <u>Acta</u> <u>Cryst</u>. *E60*, (2004) o28-o30. "1,3-Diethylbenzimidazolium Iodide".

37.   R. T. Stibrany, M. G. Matturro, S. Zushma, and A. O. Patil, <u>Acta</u> <u>Cryst</u>. *E60*, (2004) m188-m189. "*rac*-(2,2'-bis(1-ethylbenzimidazol-2-yl)biphenyl)nickel(II) dichloride".

38.   R. T. Stibrany, M. V. Lobanov, H. J. Schugar and J. A. Potenza, <u>Inorg</u>. <u>Chem</u>. *43*, (2004) 1472-1480. "A Geometrically-Constraining Bis(benzimidazole) Ligand and its Near-Tetrahedral Complexes with Fe(II) and Mn(II)".

39.   R. T. Stibrany, H. J. Schugar and J. A. Potenza, <u>Acta</u> <u>Cryst</u>. *E60*, (2004) o527-o529. "Hydrogen Bonding in 2-Phenylimidazoline".

40.   A. A. Holder, R. T. Stibrany, N. Bolotina, M. Hall, V. C. R. Payne, K. Kirschbaum, A. A. Pinkerton and A. A. Newton. <u>J</u>. <u>Chem</u>. <u>Cryst</u>. *34*, (2004) 383-386. "Synthesis and structure of [(nitrito-O,O′)bis(di-2-pyridylamine)copper(II)] nitrite".

41.   R. T. Stibrany, H. J. Schugar and J. A. Potenza, <u>Acta</u> <u>Cryst</u>. *E60*, (2004) o1012-o1014. "The Hydrogen-bonding Network in *rac*-ammonium-*trans*-2-carboxycylohexanecarboxylate)".

42.   R. T. Stibrany, H. J. Schugar and J. A. Potenza, <u>Acta</u> <u>Cryst</u>. *E60*, (2004) o1182-o1184. "A Second Polymorph of 1-hydro-4,5-diphenylimidazole".

43.   R. T. Stibrany, H. J. Schugar and J. A. Potenza, <u>Acta</u> <u>Cryst</u>. *E60*, (2004) m1147-m1150. "A chiral, facially coordinated copper(II) complex derived from a tridentate bis(benzimidazole) ligand: bis[(*S,S*)-1,2-dimethoxy-1,2-bis(1-methylbenzimidazol-2-yl)ethane]copper(II) bis(tetrafluoroborate) acetonitrile disolvate".

44.   R. T. Stibrany, H. J. Schugar and J. A. Potenza, <u>Acta</u> <u>Cryst</u>. *E60*, (2004) o1603-o1605. "5,6-dichloro-1-propylbenzimidazole".

45.   R. T. Stibrany, H. J. Schugar and J. A. Potenza, <u>Acta</u> <u>Cryst</u>. *E60*, (2004) o1648-o1651. "1-*H*-napth[2,3-d]imidazole".

46.   R. T. Stibrany, H. J. Schugar and J. A. Potenza, <u>Acta</u> <u>Cryst</u>. *E60*, (2004) m1836-m1840. "A Sterically Crowded Four-coordinate Copper(I) complex, *rac*-[bis(2,2'-bis[2-(1-ethylbenzimidazol-2-yl)]biphenyl)copper(I)] trifluoromethanesulfonate toluene 2 water solvate".

47.   R. T. Stibrany, H. J. Schugar and J. A. Potenza, <u>Acta</u> <u>Cryst</u>. *C61*, (2005) o354-o357. "The Structures of three species containing (*E*)-1,2-bis(benzimidazol-2-yl)ethene groups".

48.   R. T. Stibrany, H. J. Schugar and J. A. Potenza, <u>Acta</u> <u>Cryst</u>. *E61*, (2005) m1904-m1906. "A copper(II)-oxalate compound resulting from the fixation of carbon dioxide: μ-oxalato-bis[bis(1-benzyl-1H-pyrazole)(trifluoromethanesulfonato)copper(II)]".

49.   R. T. Stibrany, H. J. Schugar and J. A. Potenza, <u>Acta</u> <u>Cryst</u>. *E61*, (2005) m1991-m1994. "[Bis[(*S,S*)-1,2-bis (1-methylbenzimidazol-2-yl) -1′,2′-bis (methoxy) ethane]palladium(II)] dichloride".

50.   R. T. Stibrany, S. Fox, P. K. Bharadwaj, H. J. Schugar, and J. A. Potenza, <u>Inorg.</u> <u>Chem.</u> *44*, (2005), 8234-8242. "Structural and Spectroscopic Features of Mono- and Binuclear Nickel(II) Complexes with Tetradentate N(amine)$_2$S(thiolate)$_2$ Ligation".

51.   R. T. Stibrany, H. J. Schugar and J. A. Potenza, <u>Acta</u> <u>Cryst</u>. *E62*, (2006) o140-o142. "*trans*-1,2-Bis(1-methylbenzimidazol-2-yl)cyclohexane monohydrate".

52. R. T. Stibrany and J. A. Potenza, <u>Acta</u> <u>Cryst</u>. *E62*, (2006) o828-o830. "The hydrogen-bonding network in (*E*)-1,2-bis-(1-ethylbenzimidazol-2-yl)ethene dihydrate".

53. L. S. Baugh, J. A. Sissano, S. Kacker, E. Berluche, R. T. Stibrany, D. N. Schulz, and S. P. Rucker, <u>J.</u> <u>Polym.</u> <u>Sci.</u> <u>Part</u> <u>A:</u> <u>Polym.</u> <u>Chem.</u> *44*, (2006) 1817-1840. "Fluorinated and Ring-Substituted Bisbenzimidazole Copper Complexes for Ethylene/Acrylate Copolymerization".

54. R. T. Stibrany, C. Zhang, T. J. Emge, H. J. Schugar, J. A. Potenza, and S. Knapp, <u>Inorg.</u> <u>Chem.</u> *45*, (2006) 9713-9720. "A Tris(pyrazolyl) η^6-arene Ligand with Convergent Pyrazoles that Selects Cu(I) over Cu(II)".

55. R. T. Stibrany and J. A. Potenza, <u>Acta</u> <u>Cryst</u>. *E62*, (2006) m3425-m3428. "A Structure with Trigonally and Tetrahedrally Coordinated Cu(I) cations, *Rac*-[[[2,2′-(1-propylbenzimidazol-2-yl)biphenyl)(acetonitrile)copper(I)](perchlorate)] [[2,2′-(1-propylbenzimidazol-2-yl)biphenyl)bis(acetonitrile)copper(I)](perchlorate)]]".

56. V. C. R. Payne, O. St. C. Headley, R. T. Stibrany, P. T. Maragh, T. P. Dasgupta, A. M. Newton, and A. A. Holder, <u>J.</u> <u>Chem.</u> <u>Cryst</u>. *37*, (2007) 309-314. "The Crystal Structure of a Bis(2,6-pyridinedicarboxylato)chromate(III) Anion with an Elaborate Network of Hydrogen Bonding and π Stacking".

57. V. C. R. Payne, R. T. Stibrany, and A. A. Holder, <u>Analytical</u> <u>Sciences</u> *23*, (2007) x169-x170. "Synthesis and Crystal Structure of Tris(1,10-phenanthroline)iron(II) perchlorate ethanol monosolvate hemihydrate".

Patents

1. U. S. Patent 5,025,101
   Issued June 18, 1991
   R. T. Stibrany and S. M. Gorun
   "Novel Tetranuclear Manganese Complexes"

2. JP Patent 04305589
   R. T. Stibrany and S. M. Gorun
   "Novel Tetranuclear Manganese Complexes"

3. U. S. Patent 5,041,575
   Issued August 20, 1991

R. T. Stibrany and S. M. Gorun
"Manganese Oligomer Containing Main Group Elements"

4. U. S. Patent 5,099,045
Issued March 24, 1992
R. T. Stibrany and S. M. Gorun
"Manganese Oligomer Containing Main Group Elements"

5. JP Patent 04305590
R. T. Stibrany and S. M. Gorun
"Manganese Oligomer Containing Main Group Elements"

6. U. S. Patent 5,183,945
Issued February 2, 1993
R. T. Stibrany and S. M. Gorun
"Catalytic Production of Aryl Alkyl Hydroperoxides by Manganese Complexes"

7. JP Patent 05194375
R. T. Stibrany and S. M. Gorun
"Catalytic Production of Aryl Alkyl Hydroperoxide by Manganese Complex"

8. EP Patent 0466341
Issued March 8, 1995
R. T. Stibrany and S. M. Gorun
"Tetranuclear Manganese Complexes"

9. EP Patent 0475695
Issued March 29, 1995
S. M. Gorun and R. T. Stibrany
"Manganese Oligomer Containing Main Group Elements"

10. EP Patent 0512765
Issued June 21, 1995
S. M. Gorun and R. T. Stibrany
"Manganese Oligomer Containing Main Group Elements"

11. JP Patent 05239001
S. M. Gorun and R. T. Stibrany
"Manganese Oligomer Containing Main Group Elements"

12. EP Patent 0543619
Issued March 27, 1996

R. T. Stibrany and S. M. Gorun
"Catalytic Production of Aryl Alkyl Hydroperoxides by Manganese Complexes"

13. U. S. Patent 5,504,256
Issued April 2, 1996
J. E. Bond, S. M. Gorun, G. W. Schriver, R. T. Stibrany and T. H. Vanderspurt
"Catalytic Production of Aryl Alkyl Hydroperoxides by Polynuclear Transition Metal Aggregates"

14. U. S. Patent 5,627,164
Issued May 6, 1997
S. M. Gorun and R. T. Stibrany
"Fluorinated Pyrazolyl Borate Metal Complexes"

15. WO Patent 97/36910
Issued October 9, 1997
J. E. Bond, S. M. Gorun, G. W. Schriver, R. T. Stibrany, T. H. Vanderspurt, G. H. Via, B. Zhang, and J. M. Dakka
"Catalytic Production of Aryl Alkyl Hydroperoxides by Polynuclear Transition Metal Aggregates"

16. WO Patent 99/30822
Issued June 24,1999
R. T. Stibrany, D. N. Schulz, S. Kacker, and A. O. Patil
"Group 11 Transition Metal Amine Catalysts for Olefin Polymerization"

17. U. S. Patent 5,922,920
Issued July 13, 1999
J. E. Bond, S. M. Gorun, G. W. Schriver, R. T. Stibrany, T. H. Vanderspurt, G. H. Via, B. Zhang, and J. M. Dakka
"Catalytic Production of Aryl Alkyl Hydroperoxides by Polynuclear Transition Metal Aggregates"

18. U. S. Patent 6,037,297
Issued March 14, 2000
R. T. Stibrany, D. N. Schulz, S. Kacker, and A. O. Patil
"Catalyst Complexes and Polymers Therefrom"

19. EP Patent 0891368
Issued August 9, 2000
J. E. Bond, S. M. Gorun, G. W. Schriver, R. T. Stibrany, T. H. Vanderspurt, G. H. Via, B. Zhang, and J. M. Dakka
"Catalytic Production of Aryl Alkyl Hydroperoxides by Polynuclear Transition Metal Aggregates"

20. U. S. Patent 6,180,788
Issued January 30, 2001
R. T. Stibrany
"Catalyst Compositions"

21. WO Patent 01/74743
Issued October 11, 2001
R. T. Stibrany, M. G. Matturo, S. Zushma, and A. O. Patil
"Novel Late Transition Metal Catalyst Complexes and Oligomers Therefrom"

22. WO Patent 02/16033
Issued February 28, 2002
A. O. Patil, R. T. Stibrany, S. Zushma, E. Berluche and D. N. Schulz
"Polymerization Using Late Transition Metal Catalyst Complexes Formed in situ"

23. WO Patent 02/16373
Issued February 28, 2002
R. T. Stibrany, and S. Kacker
"Late Transition Metal Catalyst Complexes, Their Use as Catalysts and Polymers Therefrom"

24. U. S. Patent Application 2002/0045790
Issued April 18, 2002
R. T. Stibrany, M. G. Matturo, S. Zushma, and A. O. Patil
"Transition Metal Complexes and Oligomers Therefrom"

25. U. S. Patent 6,417,303
Issued July 9, 2002
R. T. Stibrany, D. N. Schulz, S. Kacker, and A. O. Patil
"Substantially Linear Copolymers"

26. U. S. Patent 6,479,425
Issued November 12, 2002
R. T. Stibrany, and S. Kacker
"Late Transition Metal Catalyst Complexes, Their Use as Catalysts and Polymers Therefrom"

27. U. S. Patent 6,501,000
Issued December 31, 2002
R. T. Stibrany, M. G. Matturo, S. Zushma, and A. O. Patil
"Late Transition Metal Complexes and Oligomers Therefrom"

28. EP Patent 1268371
Issued December 31, 2002
R. T. Stibrany, M. G. Matturo, S. Zushma, and A. O. Patil
"Novel Late Transition Metal Catalyst Complexes and Oligomers Therefrom"

29. U. S. Patent 6,506,859
Issued January 14, 2003
A. O. Patil, R. T. Stibrany, S. Zushma, E. Berluche and D. N. Schulz
"Polymerization Using Late Transition Metal Catalyst Complexes Formed In Situ"

30. U. S. Patent Application 2003/0027714
Issued February 6, 2003
R. T. Stibrany and S. Kacker
"Late Transition Metal Complexes, Their Use As Catalysts And Polymers Therefrom".

31. WO Patent 03/020778
Issued March 13, 2003
L. S. Baugh, A. O. Patil, D. N. Schulz, R. T. Stibrany, J. A. Sissano, and S. Zushma
"Multi-Dentate Late Transition Metal Catalyst Complexes and Polymerization Methods Using Those Complexes"

32. WO Patent 03/027130
Issued April 3, 2003
R. T. Stibrany M. G. Matturro, S. Zushma and A. O. Patil
"Late Transition Metal Complexes And Oligomers Therefrom".

33. U. S. Patent Application 2003/0069128
Issued April 10, 2003
L. S. Baugh, A. O. Patil, D. N. Schulz, R. T. Stibrany, J. A. Sissano, and S. Zushma
"Multi-Dentate Late Transition Metal Catalyst Complexes and Polymerization Methods Using Those Complexes"

34. EP Patent 1311512
Issued May 21, 2003
R. T. Stibrany and S. Kacker
"Late Transition Metal Complexes, Their Use As Catalysts And Polymers Therefrom".

238

35.   EP Patent 1318867
        Issued June 18, 2003
        A. O. Patil, R. T. Stibrany, S. Zushma, E. Berluche and D. N. Schulz
        "Polymerization Using Late Transition Metal Catalyst Complexes Formed in situ"

36.   U. S. Patent 6,642,327
        Issued November 4, 2003
        R. T. Stibrany and S. Kacker
        "Late Transition Metal Complexes, Their Use As Catalysts And Polymers
        Therefrom".

37.   U. S. Patent 6,689,928
        Issued February 10, 2004
        R. T. Stibrany, M. G. Matturro, S. Zushma and A. O. Patil
        "Late Transition Metal Complexes And Oligomers Therefrom".

38.   U. S. Patent 6,809,058
        Issued October 26, 2004
        L. S. Boffa, A. O. Patil, D. N. Schulz, R. T. Stibrany, J. A. Sissano, and S.
        Zushma
        "Late Transition Metal Complexes And Oligomers Therefrom".

39.   U. S. Patent Application 2004/0254067
        Issued December 16, 2004
        L. S. Baugh, A. O. Patil, D. N. Schulz, R. T. Stibrany, J. A. Sissano, and S.
        Zushma
        "Multi-Dentate Late Transition Metal Catalyst Complexes and Polymerization
        Methods Using Those Complexes"

40.   U. S. Patent Application 2005/0004334
        Issued January 6, 2005
        L. S. Baugh, A. O. Patil, D. N. Schulz, R. T. Stibrany, J. A. Sissano, and S.
        Zushma
        "Multi-Dentate Late Transition Metal Catalyst Complexes and Polymerization
        Methods Using Those Complexes"

41.   U. S. Patent 6,864,334
        Issued March 8, 2005
        L. S. Baugh, A. O. Patil, D. N. Schulz, R. T. Stibrany, J. A. Sissano, and S.
        Zushma
        "Multi-Dentate Late Transition Metal Catalyst Complexes and Polymerization
        Methods Using Those Complexes"

42.   U. S. Patent Application 2005/0054868
       Issued March 10, 2005
       R. T. Stibrany, C. P. Mehnert, and M. G. Matturro
       "Use of a Ionic Halide Free Copper Catalyst for the Production of Dialkyl
       Carbonates"

43.   U. S. Patent Application 2005/0288464
       Issued December 29, 2005
       S. Kacker, E. Berluche, R. T. Stibrany, J. A Sissano, and L. S. Baugh
       "Chromium Trihalide Complexes having Bisbenzimidazole Ligands and their
       Olefin Polymerization"

44.   U. S. Patent 7,049,457
       Issued May 23, 2006
       R. T. Stibrany, C. P. Mehnert, and M. G. Matturro
       "Use of a Ionic Halide Free Copper Catalyst for the Production of Dialkyl
       Carbonates"

45.   U. S. Patent 7,297,805
       Issued November 20, 2007
       S. Kacker, E. Berluche, R. T. Stibrany, J. A. Sissano, and L. S. Baugh
       "Chromium Complexes and Their Use in Olefin Polymerization"

Non-Refereed Publications

1.   R. T. Stibrany, J. A. Potenza, and H. J. Schugar, Private Communication (1999)
      CCDC 133683. "Structure of tetrakis(1-methylimidazole)copper(II)ditriflate".

2.   R. T. Stibrany, J. A. Potenza, and H. J. Schugar, Private Communication (1999)
      CCDC 134170. "Structure of 3,5-diphenylpyrazole"

3.   R. T. Stibrany, J. A. Potenza, and H. J. Schugar, Private Communication (2001)
      CCDC 170707. "Structure of 1-hydrobenzimidazol-2-yl".

4.   R. T. Stibrany, J. A. Potenza, and H. J. Schugar, Private Communication (2001)
      CCDC 172587. "Structure of 6,7-dimethyl-1,4-dihydro-2,3-quinoxalinedione".

5.   R. T. Stibrany, J. A. Potenza, and H. J. Schugar, Private Communication (2001)
      CCDC 172750. "Structure of 1-hydro-4,5-diphenylimidazole".

6.   R. T. Stibrany, J. A. Potenza, and H. J. Schugar, Private Communication (2001)
      CCDC 172751. "Structure of 1-ethyl-4,5-diphenylimidazole".

7.   R. T. Stibrany, J. A. Potenza, and H. J. Schugar, Private Communication (2001)

CCDC 176707. "Structure of 1,2,3-indantrione monohydrate".

8. R. T. Stibrany, <u>Metallocene</u> and <u>Single-Site</u> <u>Catalyst</u> <u>Monitor</u> *10*, (2002) 4-7. "Cu-Based Catalysts at ExxonMobil".

9. R. T. Stibrany, H. J. Schugar, and J. A. Potenza, <u>International</u> <u>Union</u> <u>Crystallography</u> <u>Newsletter</u> *11*, 2, (2003) 7. "Structure of 2,2'-Bis(1-ethylbenzimidazol-2-yl)biphenyl".

10. R. T. Stibrany, M. G. Matturro, S. Zushma, and A. O. Patil, Private Communication (2003) CCDC 224191. "Structure of *R*-(2,2'-bis(1-ethylbenzimidazol-2-yl)biphenyl)nickel(II) dichloride".

11. R. T. Stibrany, J. A. Potenza, and H. J. Schugar, Private Communication (2005) CCDC 289132. "Structure of 1-hydro-5,6-dimethylbenzimidazole".

12. R. T. Stibrany, H. J. Schugar, and J. A. Potenza, Private Communication (2005) CCDC 293676. "Structure of 2,3,5,6-tetraphenylpyrazine".

13. R. T. Stibrany, H. J. Schugar, and J. A. Potenza, Private Communication (2006) CCDC 603057. "Structure of bis-μ-trifluoromethanesulfonate-κ^2O,O'-bis[bis((2-diphenylphosphinophenyl)ether)copper(I)] · toluene".

14. R. T. Stibrany and J. A. Potenza, Private Communication (2006) CCDC 604501. "Structure of $\kappa^2N^{13},N^{43'}$-Hydro-*rac*-2,2'-bis[2-(1-ethylbenzimidazol-2-yl)]biphenyl perchlorate".

15. R. T. Stibrany and J. A. Potenza, Private Communication (2006) CCDC 604806. "Structure of 1,1'-binaphthyl".

16. R. T. Stibrany and J. A. Potenza, Private Communication (2006) CCDC 604897. "Structure of $N^{13},N^{43'}$-dihydro-*rac*-2,2'-bis[2-(1-propylbenzimidazol-1-ium)]biphenyl bis(perchlorate)".

17. R. T. Stibrany and J. A. Potenza, Private Communication (2006) CCDC 609179. "Structure of κ^2N,N'-hydro-1,8-bis(dimethylamino)naphthalene trifluoromethanesulfonate".

18. R. T. Stibrany and J. A. Potenza, Private Communication (2006) CCDC 612691. "Structure of $\kappa^2N^{13},N^{13'}$-Hydro-*rac*-2,2'-bis[2-(1-propylbenzimidazol-2-yl)]biphenyl (hexafluorophosphate)".

19. R. T. Stibrany and J. A. Potenza, Private Communication (2006) CCDC 613440. "Structure of (*R,R*)-1,2-Bis(1-methylbenzimidazol-2-yl)-1',2'-bis(methoxy)ethane".

20. R. T. Stibrany and J. A. Potenza, Private Communication (2006) CCDC 617708. "Structure of (*R,S*)-1,2-Bis(1-methylbenzimidazol-2-yl)-1',2'-bis(methoxy)ethane".

21. R. T. Stibrany and J. A. Potenza, Private Communication (2006) CCDC 618562. "Structure of (Bis(1,1'-bis(1-methylbenzimidazol-2-yl)-1''-(methoxy)ethane)copper(II) chloride) · chloride · *x* methanol · *y* water".

22. R. T. Stibrany and J. A. Potenza, Private Communication (2006) CCDC 619068. "Structure of 5-Bromo-2-methoxybenzaldehyde".

23. R. T. Stibrany and J. A. Potenza, Private Communication (2006) CCDC 619078. "Structure of 1*H*-naphth[2,3-d]imidazole".

24. R. T. Stibrany and J. A. Potenza, Private Communication (2006) CCDC 619256. "Structure of (*Z*)-1,2-(1-methylbenzimidazol-2-yl)ethenol · 1.5 water".

25. R. T. Stibrany and J. A. Potenza, Private Communication (2006) CCDC 619678. "Structure of *N*-(2,6-diisopropylphenyl)formamide".

26. R. T. Stibrany and J. A. Potenza, Private Communication (2006) CCDC 619685. "Structure of *N*-(2,6-dimethylphenyl)acetamide".

27. R. T. Stibrany and J. A. Potenza, Private Communication (2006) CCDC 620503. "Structure of *N,N´*-bis(2,6-diisopropylphenyl)formamidine".

28. R. T. Stibrany, C. Zhang, T. J. Emge, H. J. Schugar, J. A. Potenza, and S. Knapp, Private Communication (2006) CCDC 620847. "Structure of 1,3,5-Tris[2′-((3,5-dimethylpyrazol-1-yl)methyl)phenyl]benzene · 0.5 methylene chloride".

29. R. T. Stibrany, C. Zhang, T. J. Emge, H. J. Schugar, J. A. Potenza, and S. Knapp, Private Communication (2006) CCDC 620864. "Structure of 1,3,5-Tris[2′-((3,5-dimethylpyrazol-1-yl)methyl)phenyl]benzene · 0.5 diethyl ether · 0.5 acetone".

30. R. T. Stibrany, C. Zhang, T. J. Emge, H. J. Schugar, J. A. Potenza, and S. Knapp, Private Communication (2006) CCDC 620866. "Structure of [(1,3,5-Tris[2′-((3,5-dimethylpyrazol-1-yl)methyl)phenyl]benzene)copper(I)](trifluoromethanesulfonate) · 0.5 acetone · 0.5 ethyl acetate".

31. R. T. Stibrany and J. A. Potenza, Private Communication (2006) CCDC 621178. "Structure of $N^{13},N^{43'}$-dihydro-[*rac*-2,2′-bis(2-(1-propyl-5,6-dimethylbenzimidazol-1-ium))biphenyl] di(trifluoromathanesulfonate) · hydrate".

32. R. T. Stibrany and J. A. Potenza, Private Communication (2006) CCDC 621180. "Structure of $N^{13},N^{43'}$-dihydro-[*rac*-2,2′-bis(2-(1-benzylbenzimidazol-1-

ium))biphenyl](trifluoromethanesulfonate)(bromide)".

33. R. T. Stibrany and J. A. Potenza, Private Communication (2006) CCDC 631444. "Structure of *rac*-(2,2'-bis(1-benzylbenzimidazol-2-yl)biphenyl)copper(II) dichloride".

34. R. T. Stibrany and J. A. Potenza, Private Communication (2006) CCDC 631445. "Structure of *rac*-(2,2'-bis(1-benzylbenzimidazol-2-yl)biphenyl)copper(II) dichloride · nitromethane".

35. R. T. Stibrany and J. A. Potenza, Private Communication (2006) CCDC 631853. "Structure of Tetrakis(3,5-dimethylpyrazole)copper(II) bis(trifluoromethanesulfonate)".

36. R. T. Stibrany and J. A. Potenza, Private Communication (2007) CCDC 634493. "Structure of [bis(N,N'-(butane-2,3-diylidene)bis(2,4,6-trimethylaniline))palladium(II)]di(trifluoromethanesulfonate)".

37. R. T. Stibrany, C. Zhang, and J. A. Potenza, Private Communication (2007) CCDC 634605. "Structure of 2′-((pyrazol-1-yl)methyl)benzamide".

38. R. T. Stibrany and J. A. Potenza, Private Communication (2007) CCDC 635590. "Structure of 1-hydro-2-methyl-5-nitrobenzimidazol-2-yl".

39. R. T. Stibrany and J. A. Potenza, Private Communication (2007) CCDC 639034. "Structure of bis-μ-trifluoromethanesulfonate-$\kappa^2 O,O'$-*rac*-bis[[2,2′-bis(1-ethylbenzimidazol-2-yl]copper(I)]".

40. R. T. Stibrany and J. A. Potenza, Private Communication (2007) CCDC 645792. "Structure of 6*R**,7*R**,16*R**,17*R**-3,3,10,10,13,13,20,20-octamethyl-diperhydrobenzo-[f,p]-1,2,10,12-tetrathia-5,8,15,18-tetraaza-cycloicosane di(hydrogen triiodide)".

41. R. T. Stibrany and J. A. Potenza, Private Communication (2007) CCDC 651959. "Structure of *rac*-(2,2'-bis(1-ethylbenzimidazol-2-yl)biphenyl)copper(II) dichloride".

42. R. T. Stibrany and J. A. Potenza, Private Communication (2007) CCDC 652811. "Structure of 3-(1-hydrobenzimidazol-2-yl)pentane".

43. R. T. Stibrany and J. A. Potenza, Private Communication (2007) CCDC 653352. "Structure of 2-benzyl-1-hydrobenzimidazol-2-yl".

44. R. T. Stibrany and J. A. Potenza, Private Communication (2007) CCDC 653762. "Structure of *rac*-(2,2'-bis(1-propylbenzimidazol-2-yl)biphenyl)copper(II) dichloride".

45. R. T. Stibrany and J. A. Potenza, Private Communication (2007) CCDC 654274. "Structure of N^1-(diaminomethylene)heptane-1,7-diaminium sulfate".

46. R. T. Stibrany and J. A. Potenza, Private Communication (2007) CCDC 654503. "Structure of *rac-trans*-cyclohexane-1,2-diol".

47. R. T. Stibrany and J. A. Potenza, Private Communication (2007) CCDC 656120. "Structure of [*rac*-(2,2'-bis(1-propylbenzimidazol-2-yl)biphenyl)copper(I)(acetonitrile)] perchlorate α-methylstyrene solvate".

48. R. T. Stibrany and J. A. Potenza, Private Communication (2007) CCDC 656384. "Structure of *rac*-(2,2'-bis(1-ethylbenzimidazol-2-yl)biphenyl)copper(II) diκ*N*-cyanate".

49. R. T. Stibrany and J. A. Potenza, Private Communication (2007) CCDC 657141. "Structure of [[*N,N*-bis(2-aminoethyl)-1,2-ethanediamine]copper(II)$_{0.50}$zinc(II)$_{0.50}$(azide)] perchlorate".

50. R. T. Stibrany and J. A. Potenza, Private Communication (2007) CCDC 659009. "Structure of (*E*)-*N*-(2,6-dimethylphenyl)-*N*′-naphthalene-1-yl)acetimidamide".

51. R. T. Stibrany and J. A. Potenza, Private Communication (2007) CCDC 660561. "Structure of 1,2-ethyl-bis(η^5-1-indenyl)dimethylzirconium(IV)".

52. R. T. Stibrany and J. A. Potenza, Private Communication (2007) CCDC 66562. "Structure of (*S,S*)-1,2-diethoxy-1,2-bis(3-ethylbenzimidazol-1-ium)ethane diperchlorate".

53. R. T. Stibrany and J. A. Potenza, Private Communication (2007) CCDC 662009. "Structure of *rac*-2,2'-bis(dibromomethyl)-1,1′binaphthyl".

54. R. T. Stibrany and J. A. Potenza, Private Communication (2007) CCDC 666757. "Structure of hexa-μ$_2$-chloro-tetrakis(3,5-dimethylpyrazole)-μ$_4$-oxo-tetracopper(II)".

55. R. T. Stibrany and J. A. Potenza, Private Communication (2007) CCDC 668695. "Structure of (*E*)-*N,N*′-bis(4-methoxylphenyl)formimidamide".

56. R. T. Stibrany and J. A. Potenza, Private Communication (2007) CCDC 668696. "Structure of [*rac*-(2,2'-bis(1-propylbenzimidazol-2-yl)biphenyl)copper(II)] bis(perchlorate) · solvate".

External Presentations

1. R. T. Stibrany, J. Vasudevan, S. Knapp, J. A. Potenza, T. Emge, and H. J. Schugar, 30th MARM, Philadelphia, PA (1996). "Two Modes of Self-Coordinating Edge-Over-Edge Zn(II) Porphyrin Dimerization".

2. J. Vasudevan, S. Knapp, R. T. Stibrany, J. Bumby, J. A. Potenza, T. Emge, and H. J. Schugar, 213th ACS Meeting, San Francisco, CA (1997). "Synthesis and Spectroscopy of Edge-Over-Edge Zn(II) Porphyrin and Bacteriochlorin Dimers".

3. R. T. Stibrany, A. O. Patil and S. Zushma, 223rd ACS Meeting, Orlando, FL (2002). "Copper Based Olefin Polymerization Catalysts".

4. R. T. Stibrany, D. N. Schulz, S. Kacker, A. O. Patil, L. S. Baugh, S. P. Rucker, S. Zushma, E. Berluche, and L. A. Sissano 223rd ACS Meeting, Orlando, FL (2002). "Cu Catalysts for Homo- and Copolymerization of Olefins and Acrylates".

5. A. O. Patil, S. Zushma, R. T. Stibrany, and M. G. Matturro 223rd ACS Meeting, Orlando, FL (2002). "Vinyl-type Polymerization of Norbornene by Nickel(II) Bis-benzimidazole Catalysts".

6. R. T. Stibrany, MetCon2002, Houston, TX (2002). "Copper Based Olefin Polymerization Catalysts".

7. V. C. R. Payne, A. M. Newton, T. P. Dasgupta, P. T. Maragh, M. A. Singh-Wilmot, R. T. Stibrany, K. Kirschbaum, M. R. J. Elsegood, and A. A. Holder, 230th ACS Meeting, Washington, DC (2005). "Synthesis and Characterization of Some Transition Metal Complexes Containing 2,6-Pyridinecarboxylic Acid and Various Amines".